University of Natural Resources and Life Sciences, Vienna

Department of Water, Atmosphere and Environment

Institute of Hydraulics and Rural Water Management

Master Thesis

MONITORING AND SIMULATION OF SOIL EROSION IN THE ETHIOPIAN HIGHLANDS ON A PLOT SCALE

for attainment of the academic degree of

Diplomingenieur

presented by

Claire Brenner

Supervisor: Ao.Univ.Prof. Dipl.-Ing. Dr.nat.techn. Andreas Klik

Co – supervisor: Dipl.-Ing. Stefan Strohmeier

October 2013

Acknowledgement

„In jede hohe Freude mischt sich eine Empfindung der Dankbarkeit.“
Marie Freifrau von Ebner-Eschenbach

I would like to express my gratitude to my supervisor Andreas Klik, for his support and effort through the whole work. Furthermore, I want to thank my co-supervisor Stefan Strohmeier for his constant help during the writing process.

I wrote my thesis in the framework of the project “Unlocking the potential of rain-fed agriculture in Ethiopia for improved rural livelihood”. I wish to express my sincere thanks to the cooperation partners, ICARDA and ARARI, as well as the Austrian Development Agency, who sponsored the project. I give my special gratitude to Feras Ziadat and Wondimu Bayu, who supported and advised me in the fieldwork.

This thesis would not have been possible without the help and collaboration of the local community in the study area. I thank Baye, who was an indispensable help during the stay in Ethiopia.

A special thank goes to my friends and family. I am especially grateful for the love and encouragement of my mother, grandmother, Kathi, Elke and David, who supported me across the years. “*Let us be grateful to people who make us happy, they are the charming gardeners who make our souls blossom*.” (Marcel Proust)

Abstract

Soil erosion is the main driving force for global land degradation. Soil erosion measurements are an important tool to assess soil loss under site-specific conditions and evaluate the impact of changes in land use on its magnitude. Based on this, adjusted management strategies can help to maintain or enhance the state of the soil. This work assessed soil loss rates on a plot scale in a 54 km² large agricultural catchment near Gondar, Ethiopia. At the experimental site, stone bunds were implemented in 2011 to prevent severe soil erosion. During the rainy season 2012 (July and August), three soil erosion plots with areas between 300 and 480 m² were installed and soil loss measurements were carried out. Soil loss from the three plots was 0.3, 3.0 and 4.7 kg m^{-2}, respectively. Additionally, canopy and rock fragment cover, hydraulic conductivity as well as other soil properties were determined. Based on the data obtained from the field, the Water Erosion Prediction Project (WEPP) model was adjusted and calibrated. Furthermore, the model will be calibrated with more field-measured data sets of runoff and soil loss in the investigated watershed. In the future, it will then be used as demonstration tool to evaluate the response of soil erosion to changes in management practices or the implementation of soil and water conservation measures in the Ethiopian Highlands.

Zusammenfassung

Erosion stellt eine der größten Bedrohungen bei der Erhaltung der natürlichen Ressource *Boden* dar. Bodenerosionsmessungen helfen bei der Abschätzung von Erosionsraten unter spezifischen Bewirtschaftungs- und anderen ortsbezogenen Bedingungen. Davon ausgehend können Strategien zur Erhaltung oder Verbesserung des Bodens geplant und entwickelt werden. Um einer fortschreitenden Bodenerosion entgegenzuwirken, wurden 2011 „Stone Bunds“ im Untersuchungsgebiet, einem 54 km² großen, landwirtschaftlich genutzten Einzugsgebiet nahe Gondar, Äthiopien, errichtet. In dieser Arbeit wurden Bodenerosionsmessungen auf Plot-Ebene an drei Versuchsflächen (300 – 480 m²) durchgeführt. In der Regenperiode 2012 wurden in den Monaten Juli und August Bodenerosionsraten von 0.3, 3.0 und 4.7 kg m^{-2} für die Versuchsflächen gemessen. Zusätzlich zu den Bodenerosionsmessungen wurden ergänzende Informationen zum Standort, wie Pflanzenbedeckungsgrad, Steinanteil des Bodens, Bodentextur und Durchlässigkeit aufgenommen. Mithilfe von diesen - vor Ort gewonnenen - Daten wurde ein Bodenerosionsmodell, das Water Erosion Prediction Project (WEPP) Modell, an lokale Bedingungen angepasst und kalibriert. In einem nächsten Schritt wird das Modell aufgrund weiterer Abfluss- und Erosionsmessungen im untersuchten Einzugsgebiet geprüft und gegebenenfalls adaptiert werden. Zukünftig kann das Modell dazu genutzt werden, Auswirkungen durch Änderungen der Bewirtschaftung, Niederschlagsverhältnisse oder den Einsatz von bodenverbessernden Maßnahmen im Äthiopischen Hochland zu simulieren und zu bewerten.

Table of Content

1. Introduction and Objectives

Extensive land degradation in the Ethiopian Highlands jeopardizes rural livelihood. Ongoing deforestation and increasing population pressure worsen the soil erosion problem.

The project “Unlocking the potential of rain-fed agriculture in Ethiopia for improved rural livelihood” investigates strategies to prevent further degradation of the soil and enhance productivity of rain-fed agriculture in the Ethiopian Highlands. The Austrian Development Agency (ADA) sponsors this project, which is conducted in international cooperation between the University of Natural Resources and Life Sciences, Vienna (BOKU), the International Centre for Agricultural Research in the Dry Areas (ICARDA) and the Amhara Regional Agricultural Research Institute (ARARI). Experimental site is the Gumara-Maksegnit watershed, Amhara Region.

The present master thesis was conducted within this project. It aimed to monitor soil loss on a plot scale in a watershed in the Ethiopian Highlands and assess soil loss rates due to water erosion from arable land. The experimental site was situated in a watershed, representative for cultivated land in this region. Soil loss monitoring on a plot scale provides physically comprehensible conditions, which allow monitoring of soil loss at a site with known climate, crop and soil properties.

Data acquisition was conducted in July and August 2012. Soil loss was measured at three experimental plots situated at the same hillslope. Sediments were collected in retention basins at the end of the plots and removed and weighed as often as possible. Canopy and rock fragment cover as well as soil properties were analysed in order to estimate their impact on the soil erosion process. Additionally, this work accounted for the hillslope intersection effect by stone bunds, implemented at the experimental site.

This site-specific knowledge has been applied to a soil loss prediction model. The Water Erosion Prediction Project (WEPP) model was adapted to local conditions and calibrated based on field observations. The idea of this work was to find a configuration of the model, which predicts soil loss adequately for the experimental site. Once calibrated, the model enables simulation of various scenarios concerning the effect of large storms, crop rotation and conservation practices within short time. Thus, the aim of soil loss predictions was not to carve out an exact value of soil loss, but evaluate the effect of these different management scenarios.

In a successive step, this local information can be integrated into a conceptual soil erosion model, which models soil loss processes on a bigger scale.

2. Land degradation - a threat to rural livelihood

Soil forms the top layer of the earth's crust. It is a complex and variable system of mineral particles, water, air, organic matter, and living organisms. Soil provides multiple functions, which are essential to human well-being. Soil is the basis for human activities and infrastructure, food and biomass production. Additionally, it enables storage, filtration and transformation of organic and mineral substances. Soil is a source of raw materials and acts as habitat and gene pool ("European Commission" 2013). As the process of soil formation is slow, soil has to be considered as a non-renewable resource. Thus, its protection is crucial in order to guarantee its ecosystem services in the future (Jones et al. 2012).

Land degradation is a global problem, concerning soils around the planet. Figure 1 shows a map of global soil degradation levels. Except for the northern part of the northern hemisphere, most soils in the world are degraded or very degraded.

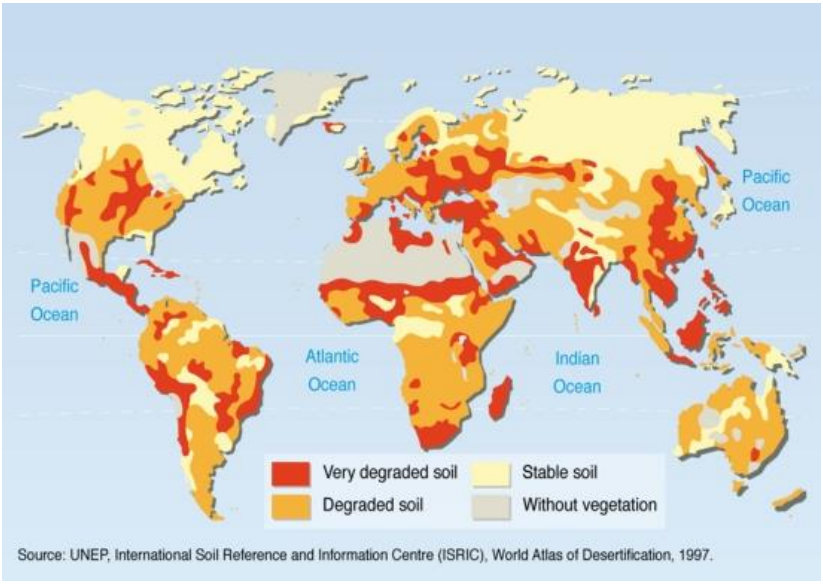

Figure 1: Global soil degradation map ("World Atlas of Desertification" 1997)

Soil degradation jeopardizes the land's capacity to provide ecosystem services and goods. ("Natural Resources and Environment: Land Degradation Assessment" 2013). It sums up the degradation effects of different processes including decline in biodiversity and organic matter, compaction, chemical contamination, wind and water erosion, salinisation, sealing and landslides (Jones et al. 2012).

According to the report *Global Environment Outlook 4: Environment for Development* (2007), increasing human demands on land resources are the main driving forces for ongoing land degradation. Changes in land use, such as forest cover and composition, cropland expansion and intensification, as well as urban development highly affect this process. Unsustainable agricultural land use - including poor soil and water conservation practices, poor crop rotation and irrigation schemes as well as overgrazing - put pressure on the environment and negatively influence soil and soil services.

Altogether, this leads to a reduction in productivity and biodiversity. Consequently socio-economic problems like uncertainty in food security and environmental problems as damage of ecosystems arise ("Natural Resources and Environment: Land Degradation Assessment"

2013). Land degradation and poverty accompany each other and end in a “poverty, food insecurity and natural resources degradation trap” (Dejene 2003).

The report “Ecosystems and Human Well-Being: Current State and Trends” stresses that the negative impacts of land degradation – even though it is a global problem – affect some regions more than others: the poorest people of the world are most exposed to negative effects of environmental change (Kasperson and Archer 2005).

Figure 2 maps types of degradation in Africa. 16 % of the total land area is affected by some kind of degradation. Among all types of degradation, water erosion is the key threat to soils in Africa and in the study area of this work, affecting about 8 % of the continent (Jones et al. 2013).

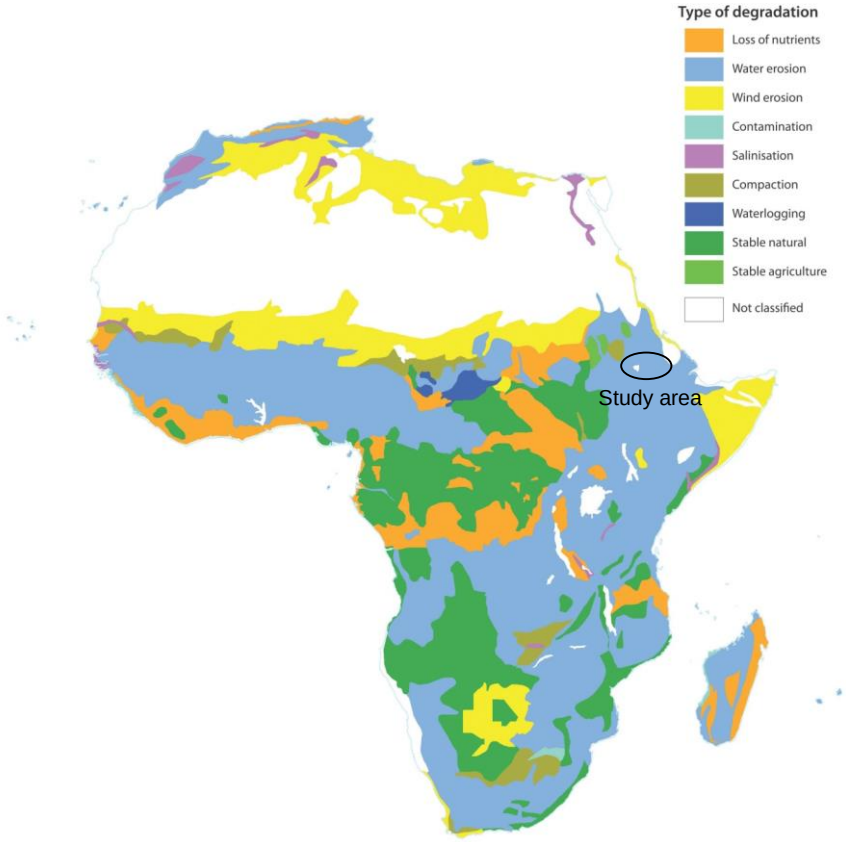

Figure 2: Map showing types of degradation across Africa (Jones et al. 2013)

3. Ethiopia – an overview

The study area is situated in Amhara Region, in the Ethiopia Highlands. The Ethiopian Highlands cover 44 % of the total area and are the largest continuous plateau of its altitude, above 1500 m a.s.l, in the African continent. 88 % of the country's population lives in the Ethiopian Highlands (Krüger, Gebremichael, and Kejela 1997).

Agriculture is the economic basis of the country, which accounts for almost half of the gross domestic product (GDP) of the country. 85 % of the population works in the agricultural sector. This goes along with a low urbanization level; More than 80 % of the whole population live in rural areas ("The World Factbook" 2013).

Soil erosion and loss of fertile topsoil jeopardize the livelihood of this rural population. The subsistence farming system leaves them highly vulnerable to decreases in production and crop yields.

Figure 1 shows a map of areas with most severe soil degradation in Africa. This classification in based on a combination of the degree and the relative extent of the process. The figure shows that big parts of Ethiopia are affected by most severe soil degradation.

Hurni (1988) estimated that soil loss from arable land in Ethiopia is about 42 t ha^{-1} yr^{-1}.

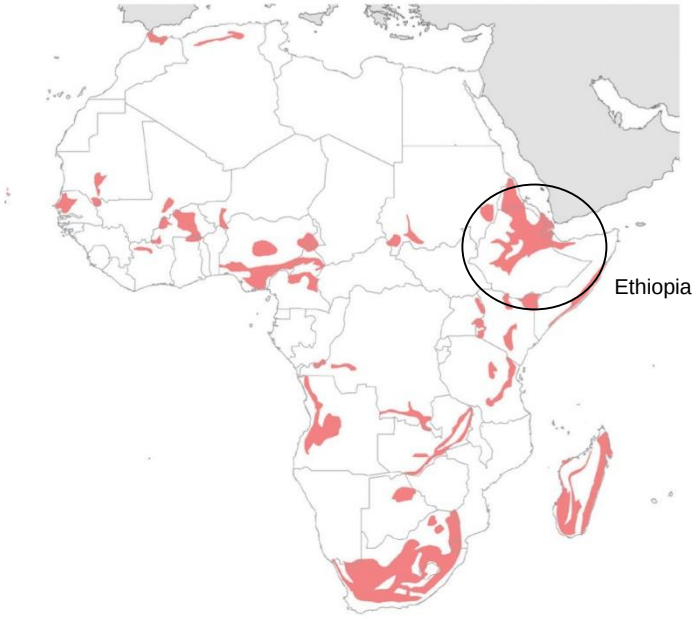

Figure 3: map showing areas with most severe soil degradation in Africa (L. R. Oldeman, Hakkeling, and Sombroek 1991).

Farmers mostly depend on subsistence rain-fed agriculture. In 2001, less than 3 % of the cultivated area was equipped for irrigation (aquastat 2005).

Ethiopia faced droughts and extreme famines in 1974 and 1975. This raised attention to the problem of soil erosion, as land degradation and loss of topsoil were linked to droughts. With the support of the "Food for Work" Program, the government started soil and water conservation and rehabilitation campaigns to combat further degradation of arable land. In 1981, in collaboration with the University of Bern, the Ministry of Agriculture founded the Soil Conservation Research Project (SCRP) (Dejene 2003).

The geographic location within the tropics characterizes the Ethiopian climate. Annual variation in temperature is low, while rainfall shows a pronounced bi-modal pattern with a main rainy season (*kiremt*) from June to September and a low rainy season (*belg*) from February to April.

4. Soil erosion

Erosion is a natural process intensified and accelerated by human action. Natural erosion rates increased due to anthropogenic influences up to irreversible levels, exceeding 1 t ha^{-1} yr^{-1} within a span of 50 – 100 years (Gentile and Jones 2013).Soil erosion is considered to be the most widespread and severest form of land degradation.

Soil erosion describes the process of detachment, entrainment, transport and deposition of soil particles either produced by water, wind, disturbance and translocation (e.g. tillage), landslides and floods. However, soil and wind erosion are the main drivers of soil degradation. 56 % of the total global degraded area is affected by water erosion; 28 % by wind erosion (L. Oldeman 1991).

Consequences of soil erosion are manifold and induce on-site as well as off-site effects. While on-site effects are mainly related to a reduction in topsoil and soil productivity, off-site effects occur due to deposition of transported sediments and chemicals causing sedimentation, silting of water resources, alteration of the landscape, reduction of habitats and infrastructure damages (Blanco-Canqui and Lal 2008).

Because of soil particle removal, the thickness of the nutrient-rich topsoil decreases. Thus, this decline in topsoil depth goes along with nutrient loss, reduction of rooting depth, reduction of water and nutrient storage capacity and, hence, plant productivity (Braimoh and Vlek 2008; Blanco-Canqui and Lal 2008). In Africa, 65 % of arable land faces loss of topsoil and nutrients due to erosion processes (Jones et al. 2013).

Referring to the causes of accelerated soil erosion, the leading drivers are deforestation, overgrazing and mismanagement of cultivated soil (Blanco-Canqui and Lal 2008). Soil texture and moisture, land use and vegetation cover, slope and climate are sensitive parameters influencing the intensity of soil erosion (Jones et al. 2013).

Arid and semi-arid regions with less than 600 mm precipitation per year and strong winds are especially prone to wind erosion. Low vegetation cover and poorly developed soils intensify wind erosion (Jones et al. 2013; Blanco-Canqui and Lal 2008). Saltation, soil creep and suspension are the forms of sediment transport due to wind erosion.

Contrary to wind erosion, water erosion is dominant in humid and sub-humid regions with intense rainfall events. It takes also an important role in arid and semiarid regions with distinctive seasonal rainfall pattern. Intense rainfall events occur after long dry periods when soils are bare and unprotected against the erosive power of the rainfall.

The following section outlines the mechanisms of erosion by water in more detail, as water erosion is the dominant form of erosion in this research study.

4.1 Water erosion

Soil erosion by water is the wearing away of topsoil as a result of the energy potential of rainfall and runoff. Detachment of soil particles initiates when shear stresses by raindrops and runoff exceed the resistance of the soil. Once in motion, sediments are transported by either saltation or surface runoff (Toy, Foster, and Renard 2002).

4.1.1 Processes

The kinematic energy of raindrops is the driving force for particle detachment. It depends on the falling velocity and the diameter of the raindrop (Roose 1996). It increases with rainfall intensity and raindrop size. Terminal velocity of the largest raindrops (6 mm) is about 10 m s^{-1} after falling more than 10 m (Gentile and Jones 2013; Roose 1996). Higher kinematic energy of the raindrops results in higher detachment rates.

Raindrops hitting the soil surface disperse and splash soil particles and eject them into the air (Blanco-Canqui and Lal 2008). Due to this splash effect of raindrops, particles distribute in all directions, but reach higher distances downhill than uphill. Consequently, particles move downslope. After particles are carried a short distance by this splash effect they are further transported by sheet runoff. Runoff starts when precipitation rates exceed infiltration rates and water starts to accumulate in puddles (Roose 1996). With increasing amount of water on the surface, a layer of flowing water forms and transports particles. This type of erosion is called interrill erosion.

Additionally, rain drops affecting the surface, break down soil aggregates and, thus, leave constituent particles. Those grains float into gaps, cracks or holes in the soil and plug soil pores, thus, form a crust on the top layer. After drying, these crusts enhance soil resistance and reduce infiltration. This leads to sealing of the surface and increasing runoff in storm rainfall events and increasing erosion rates downslope. Next to the crusting of the surface, the micro-topography and the sub-surface structure of the soil highly influence runoff and soil erosion. Micro-topography refers to the random roughness of the surface, which results from tillage and other management practices. Cracks and voids in the soil can build preferential flow paths, through which water infiltrates rapidly (Gentile and Jones 2013).

If runoff gains erosive power and entrains particles directly, small rills and channels of concentrated flow develop. Rills affect the heavily disturbed plough layer. As they do not deepen into layers beneath the ploughed layer, rills can be obliterated by tillage. Rills incising into deeper layers especially on steep slopes lead to the development of gullies, which cannot be undone by normal tillage operations (Gentile and Jones 2013). Rill erosion depends on the rill erodibility of the soil, runoff transport capacity and hydraulic shear of the runoff. Gully erosion is mainly controlled by the ratio of critical shear stress and shear stress induced on the channel bed by the runoff. If shear stress of the runoff exceeds the shear of the soil, new gullies form or extend (Blanco-Canqui and Lal 2008).

Table 1 lists types of soil erosion from initial splash erosion to gully erosion.

Table 1: Overview of soil erosion types (Blanco-Canqui and Lal 2008)

SPLASH EROSION	First stage of water erosion, when soil particles start moving due to the bombardment of the soil surface by raindrops.
SHEET/ INTERRILL EROSION	A shallow sheet of water flows over the surface and transports detached particles. It results in the removal of a thin, uniform layer of topsoil. Sheet erosion starts when rainfall intensity exceeds the infiltration capacity of the soil.
RILL EROSION	Sheet flow concentrates in channels. Due to higher flow velocity in the channel, concentrated flow not only transports but also detaches particles. Rills can be obliterated by tillage.
GULLY EROSION	Advanced stage of rill erosion, when rills deepen and widen until they form channels, which cannot be removed by tillage. Gullies account for severe sediment and nutrient loss, washout crops and expose plant roots, dissect cropland and cause alterations of the landscape.

4.1.2 Factors controlling water erosion

The main factors, which control the erosion process by water are PRECIPITATION, TOPOGRAPHY of the hillslope, SOIL PROPERTIES and VEGETATION COVER (Blanco-Canqui and Lal 2008). The Universal Soil Loss Equation (USLE) defines a fifth factor, the support practice factor, which determines the soil erosion process (Wischmeier and Smith 1965).

As already clear, PRECIPITATION is the main driving force for erosion. More intense storms lead to higher surface runoff and soil loss, thus intensity, amount and duration of the rainfall event strongly regulate the magnitude of soil loss.

The TOPOGRAPHY of a hillslope affects soil erosion, as steeper and longer slopes are more prone to surface runoff with high velocity. Additionally the transport capacity of the runoff increases with slope steepness.

VEGETATION intercepts rainfall water and thus protects the soil surface and minimizes the erosive force of the rainfall. Residues on the ground enhance the protection effect as they reduce the bouncing of the raindrops and increase surface roughness. In general, increase in vegetation cover leads to a decrease of soil detachment. Hereby, dense and short growing vegetation is more effective than scattered, taller vegetation. Perennial plants protect the soil better than annual crops, which leave the soil bare between to cropping seasons (Blanco-Canqui and Lal 2008).

Texture, macroporosity, infiltration capacity and organic matter content are SOIL PROPERTIES affecting the soil erosion process. Clay particles are easily transported by the runoff, but build strong aggregates, which hinders the detachment of the particles. The interaction of these factors defines the erodibility of the soil (Blanco-Canqui and Lal 2008).

4.1.3 Measuring soil erosion

Field experiments and soil erosion measurements are important tools to assess the degree of erosion at a specific area. The monitoring of soil loss under different management, soil and climatic conditions helps in the development and design of soil conservation measures and establishment of sustainable land management.

5. Stone bunds – a soil and water conservation measure

Stone bunds are a soil and water conservation measure. Its purpose is to control and diminish ongoing land degradation. An overview about soil and water conservation measures in general and stone bunds in particular is given in this chapter.

5.1 Soil and water conservation measures

Van Lynden et al. (2002) define soil and water conservation (SWC) measures as activities at a local level that maintain or enhance the productive capacity of the land in areas affected by, or prone to, degradation. SWC includes prevention or reduction in soil erosion, compaction, and salinity, conservation or drainage of surface and soil water, and maintenance or improvement of soil fertility. SWC technologies are agronomic, vegetative, structural, and management measures that control land degradation and enhance soil productivity (Liniger et al. 2002).

SWC includes measures on three different stages of degradation. Prevention intends to maintain and preserve soils, which are not affected by degradation yet. Mitigation takes place at an intermediate stage, when soils are already degraded, but land use is still possible. It aims to prevent further degradation and rebuild soil functions. If land degradation advanced to a stage, where previous land use cannot be continued, rehabilitation is the final stage for soil and water conservation measures. Of all three, the stage of rehabilitation needs the highest investment.

SWC measures can be classified into four groups (Braimoh and Vlek 2008).

1. Agronomic measures include mixed cropping, contour planting, mulching, direct planting and minimum/non-inversion tillage. They are not permanent but of short duration. As they are associated with annual crops, these measures recur every season. Agronomic measures do not alter the slope profile. An advantage of these measures is the little required input.

2. In contrary to agronomic measures, vegetative measures are associated with perennial plants, such as grasses, shrubs and trees. Thus, vegetative measures are of long duration. Grass strips, hedge barriers and windbreaks are often oriented along the contour, separating the fields. Commonly, they induce alteration of the slope profile.

3. Structural measures including terraces, banks, bunds, and palisades are constructions of wood, stone, concrete etc. Structural measures imply higher inputs of labour and money and are mostly of long duration or even permanent. Like vegetative measures, structural measures lead to changes in the slope profile. These structures are also applied along the contour or against wind direction.

4. Management measures involve a change in land use. This form of SWC is mainly applied to grazing land, where overgrazing led to severe degradation of the soil. Because of land use change, area closure or rotational grazing, vegetation cover improves.

Benefits from SWC measures are slowdown, retention and diversion of surface runoff, enhanced infiltration and surface cover, increased organic matter and soil fertility. Due to higher infiltration and reduced flow velocity, the soil is able to hold back more water. This effect is especially beneficiary in regions with longer dry seasons. Soil and water conservation measures can also help to disperse and interrupt concentrated flow (Braimoh and Vlek 2008).

5.2 Stone bunds

Stone bunds or stone lines are embankments set along the contours. They build barriers of stones, obstructing the surface runoff and reducing its velocity. Hence, these bunds reduce soil erosion on the field (Morgan 1995). Rows of stone bunds are placed at regular intervals and divide fields into segments of nearly the same length. Consequently, the effective slope length decreases. Sediments accumulate behind the bunds and backfill the bunds. Due to the deposition of sediments at the slope toe of each segment, terraces form and slope inclination declines.

In order to prevent further degradation of arable land, farmers in the study area applied graded stone bunds on their fields (February and April 2011). The implementation of this soil conservation measure was conducted in cooperation with the Government and within the framework of the project “Unlocking the potential of rain-fed agriculture in Ethiopia for improved rural livelihood”.

Stone bunds in the study area are slightly graded. This should guarantee that water, which accumulate behind the bunds, flows sidewise along the bund and leaves the field through a spillway. Figure 4 and Figure 5 show a stone bund at the experimental site and lines of stone bunds typical for the Ethiopian Highlands.

Figure 4: Stone bund at the experiment site. The area behind the bunds is not entirely filled

Figure 5: Stone bunds in the Ethiopian Highlands, Amhara Region

Bosshart (1997) divides the impacts of stone bunds into short- and long-term effects. While stone bunds reduce the slope length and retain runoff and sediments immediately after their construction, the effects of reduction in slope inclination, the formation of terraces and a change in land management are effects in the long-term.

In the Ethiopia Highlands, farmers take stones from their neighbouring fields for the construction of the bunds. Large stones (> 10 cm) build the skeletal structure of the wall. The medium stones are then used to backfill the bunds and small rock fragments top the backfill. Small stones with an average diameter of 2 cm act as filters and retain eroded sediments (Nyssen et al. 2001).

Gebremichael et al. (2005) showed that the introduction of stone bunds reduced annual soil loss due to water erosion by 68 %. This research was conducted in the Tigray Highlands, Ethiopia. Gebremichael et al. (2005) state that this positive effect due to accumulation behind the bunds, is highest for bunds in the first years after their construction, and declines with the age of the bunds, as they become more and more backfilled. Additionally, stone bunds enhance the storage of moisture in deeper horizons and lead to more productive arable land (Nyssen et al. 2007). In contrary, Hengsdijk et al. (2005) modelled the effect of stone bunds and concluded that the positive effect of this conservation measure is limited in the short run. (Herweg and Ludi 1999) also found no increase in yield but emphasize the effect of soil loss reduction due to stone bunds.

According to questionnaires and interviews by Nyssen et al. (2001), farmers in Ethiopia consider stone bunds to be the best way to deal with excess larger stones. However, farmers are aware of a positive effect on rock fragments on infiltration, retention of soil moisture and surface protection. Farmers are unwilling to remove especially the small stones, as they rate the beneficiary effects from this fraction as very positive. On the other hand, farmers often remove large stones with high surface cover.

6. WEPP – a soil erosion prediction model

EMPIRICAL, CONCEPTUAL and PHYSICALLY BASED models exist for different scales and available input parameters.

EMPIRICAL models have a simple structure, are user-friendly and allow rapid application. The empirical input coefficients are based on observations and measurements and thus do not simulate the erosion process as a physical process. Consequently, they are most suitable in regions with little input data. The Universal Soil Loss Equation (USLE) by Wischmeier and Smith (1965) is the most widely used empirical erosion model. It was originally developed from field observations in the U.S. and needs adjustments to local conditions in other regions of the world. In general, empirical models ignore the physical processes, the heterogeneity of rainfall, soil properties and other catchment characteristics.

CONCEPTUAL models are in between empirical and physically based models. They represent the processes in a catchment as a series of internal storages and include general process descriptions. They do not model interactions between processes and do not need extensive catchment information (Merritt, Letcher, and Jakeman 2003).

PHYSICALLY BASED models, in contrast, describe the physical processes behind soil erosion. They have a wider range of applicability as these models simulate the individual components of the entire erosion process by solving the corresponding equations. These models are more efficient in describing spatial and temporal variability of natural processes (Amore et al. 2004). Merritt et al. (2003) stress that measurement of all parameters is often not possible due to heterogeneities in the catchment, but parameters are estimated by calibrating simulated against observed data. Due to the vast amount of input needed for the model, uncertainties of the estimated parameters can lead to a “lack of identifiability of the parameters and a non-uniqueness of “best-fit” solutions”. Another problem of these kind of models is the upscaling of the governing processes, derived from small-scale observations, to much larger scales during the simulation process.

The Water Erosion Prediction Project (WEPP) (USDA-ARS 1989) is a distributed parameter, continuous simulation, erosion prediction model. It predicts soil loss and deposition as a function of its spatial and temporal distribution.

It is a physically based model, which needs input information on climate, slope, soil and management of the observed area. Each of these superior components consists of numerous parameters, as rainfall amounts and intensities, soil textural qualities, plant growth parameters, residue decomposition parameters, effects of tillage and tillage implements, slope shape and steepness and soil erodibility parameters. The input parameters, which change over time, such as surface roughness, canopy cover, canopy height, soil moisture and hydraulic conductivity are simulated on a daily basis. Based on this input, WEPP simulates runoff, soil detachment and deposition, sediment delivery off-site and sediment enrichment for each runoff event. The output holds information on on-site and off-site effects of soil loss separately. Runoff volume, soil loss, sediment yield and the characteristics of sediment size are predicted with temporal and spatial distribution. The application of the WEPP model is limited to areas with dominantly Hortonian overland flow, where rainfall rates exceed the infiltration capacity and subsurface flow is marginal.

Additionally to the soil erosion output, WEPP computes outputs on soil and plant parameters, water balance and crop yield.

By varying the input parameters and adapting them to different management and conservation scenarios, WEPP enables the evaluation of these scenarios according to multiple criteria.

The WEPP model can run in single storm or continuous mode. The present work is based on the monitoring of cumulative soil loss in the Gumara-Maksegnit watershed over the rainy period 2012 and thus WEPP ran in a continuous mode. Soil loss is predicted for a period of one year. Simulation starts on the first day of the year.

Zhang et al. (1996) evaluated the model using natural runoff plots. They contrasted measured and predicted soil loss and showed that WEPP slightly overestimated soil loss for small storms and for years with low runoff and soil loss rates and on the other hand underestimates soil loss for large events and for years with high runoff and soil loss rates. Nevertheless, average measured and predicted soil loss fit reasonably.

Even though the WEPP model is a physically based model Mahmoodabadi et al. (2013) stress that some empirical and/or statistical parameters are used in predicting model components. These dependencies can lead to reduced accuracy when these parameters do not suit to the conditions in the study area. The following section presents the model components and depicts their influence on soil loss.

6.1 Model components

The description of the main model components concentrates on those, which are essential to this work. This study was conducted on cropland and hence, this section outlines the model's approach to estimation of soil loss on cropland but does not consider solution methods, exclusively relevant for rangeland.

The description of the components is based on the WEPP Model Documentation (Flanagan and Nearing 1995).

a) Weather component

The WEPP model requires information on daily precipitation amount, storm duration, peak storm intensity, air temperature, solar radiation, dew point temperature and wind velocity and direction. For experimental sites in the United States, this information is available in high resolution from more than 1000 stations. In areas, where no long-time records are available, the user has to input breakpoint rainfall data and create the climate input file by hand.

b) Surface hydrology component

The surface hydrology component regulates the effect of the duration of rainfall excess and rainfall intensity, runoff volume and peak discharge rate. The amount of infiltrated water affects the water balance and crop growth, which then again affect infiltration and runoff rates.

The infiltration rate describes the change in cumulative infiltration depth over time. The Green-Ampt model modified by Mein-Larson is used with unsteady rainfall input for the computation of infiltration in the model.

Rainfall excess occurs when rainfall rates exceed the infiltration capacity of the soil and is the difference between cumulative rainfall and infiltration depth. Rainfall excess ponds the surface and depressions start to fill with water. After depression storage filled completely, runoff begins. The importance of depression storage depends mainly on the surface roughness and the slope of the surface.

If the amount of infiltrated water reaches the water storage capacity of the soil, all rainfall becomes rainfall excess.

In continuous simulation, peak discharge is calculated using an approximation of the kinematic wave model. Under constant rainfall excess, discharge increases up to the time to kinematic equilibrium. The time to kinematic equilibrium occurs when the equilibrium characteristic, which starts at the top of the hillslope at the beginning of the rainfall excess, reaches the bottom end of the slope. The time to kinematic equilibrium is

$$t_e = \left(\frac{L}{\alpha\, v^{m-1}}\right)^{1/m}$$

Equation 1

where t_e is the time to equilibrium (s), L is the length of the hillslope (m), v is the rainfall excess (m s^{-1}), α is the depth-discharge coefficient and m is the depth-discharge exponent.

Peak discharge rate is

$$q_p = v_c \left(\frac{D_v}{t_e}\right)^m$$

Equation 2

where q_p is the peak discharge (m s^{-1}) and D_v is the duration of rainfall excess (s) and vc is the constant rainfall excess rate (m s^{-1}).

When the duration of rainfall excess is greater than the time to kinematic equilibrium, the peak discharge rate is constant.

$$q_p = v_c$$

Equation 3

c) The water balance and subsurface hydrology

The water balance component predicts soil water content in the root zone as well as evapotranspiration losses with input from the climate, infiltration and crop growth components. Percolation and evapotranspiration is predicted on a daily basis. The continuous water balance describes the soil water content in the root zone Θ as:

$$\Theta = \Theta_{in} + (P - I) \pm S - Q - ET - D - Q_d$$

Equation 4

where Θ_{in} is the initial soil water in the root zone, P is the cumulative precipitation, I is the precipitation interception, S is the snow water content, Q is the cumulative amount of surface runoff, ET is the cumulative amount of evapotranspiration, D is the cumulative amount of percolation losses below the root zone and Q_d is subsurface lateral flow.

WEPP includes two options for the calculation of evapotranspiration. If wind information is available, the model uses the Penman equation for its calculation. If no wind data is available but only solar radiation and temperature data, the WEPP model uses the Priestly-Taylor method. In this work, no information on wind is available. Thus, the model uses the Priestly-Taylor method for evapotranspiration computation.

The soil evaporation and plant transpiration depend on solar radiation, albedo and air temperature as well as on input from the plant growth component (leaf area index, root depth,

total biomass and residue cover). If the water content in the soil depth influenced by evaporation is less than calculated soil evaporation, evaporation decreases accordingly.

During dry periods exists limiting soil moisture content, below which no water evaporates from the bare soil. This critical moisture content depends on bulk density, clay content and organic matter of the soil. In the study area, soil water content in the beginning of the simulation, in January, is low. As most of the rain falls during the rainy season in June to September, the soil is relatively dry in January. Until the first rainfall events of the year, when soil water content increases, there is no evaporation from the soil.

When the water content exceeds the field capacity of a layer, the water percolates to a deeper layer and leaves the root zone. Once below the root zone, the water is lost and will not be traced further. The WEPP model also includes a subsurface lateral flow model, which evaluates the effect of lateral drainage of the soil.

Water stress is an input to the plant growth component and water content of the upper soil layer influences the Green Ampt model for infiltration computation.

d) Soil component

Soil properties highly affect infiltration and surface runoff processes and thus soil erosion. Random roughness, ridge height, bulk density and effective hydraulic conductivity influence the hydrology of the erosion process.

Random roughness describes the irregularity in the micro-topography induced by soil disturbance, mainly tillage operations. Various models describe random roughness as the standard deviation of de-trended surface elevations (Van Wesemael et al. 1996). Random roughness is positively correlated with the surface hydraulic resistance and depression storage of rainfall excess. Random roughness is highest after tillage and decays over time due to the effect of rainfall. Ridge height is closely connected to the random roughness. It is an oriented roughness resulting from the use of tillage implements. Bulk density also influences infiltration into the soil. It is adjusted due to tillage operations and increases with the amount of cumulative rainfall after tillage and due to weathering and long-term consolidation.

Obviously, tillage causes alteration of soil properties and thus needs several input information as implement type, tillage date, depth and level of surface disturbance as well as the amount of buried residue.

As mentioned before, the Green-Ampt model describes the infiltration process. This model builds on two parameters, the effective hydraulic conductivity and the wetting front matric potential term. This term is not an input by the user but calculated internally by the program. It is a function of soil type, soil water content and bulk density.

The effective hydraulic conductivity can be an input by the user or might be estimated by the model. Depending on the clay content WEPP used two different equations.

$$K_b = -0.265 + 0.0086(100sand)^{1.8} + 11.46CEC^{-0.75}$$ for soil with clay content ≤ 40 %

$$K_b = 0.0066e^{\frac{2.44}{clay}}$$ for soil with clay content > 40 %

Equation 5

where K_b is the "baseline" effective conductivity (mm h^{-1}), sand and clay are the fractions of sand and clay and CEC is the cation exchange capacity (meq (100 g)$^{-1}$).

The WEPP model is capable of adjusting the effective hydraulic conductivity as a function of management and plant parameters. The user has two run options. "Baseline" effective conductivity will be adjusted internally by the model and is a function of the soil. The constant effective conductivity will not be adjusted by the model and thus has to account also for management practices. In field experiments the adjusted "baseline" effective conductivity led to better accordance of predicted and measured hydraulic conductivity (Albert et al. 1995).

The model uses fallow soil and crop specific adjustments. Adjustments to the fallow soil account for soil crusting and tillage effects. K_b describes maximum hydraulic conductivity of a freshly tilled soil for which conductivity will decrease as a function of the kinematic energy of the rainfall since last tillage until it reaches its minimum for a fully crusted soil. Sand and clay fractions and cation exchange capacity determine how stable the soil is against this process.

Surface cover from row crops increases effective hydraulic conductivity (K_e) as it reduces soil crusting. According to Wischmeier (1966), surface conditions and management have more influence on infiltration than the specific soil type. Furthermore, infiltration increases with larger storms. This effect reflects the adjustment of K_e due to canopy cover and height as well as residue cover. This leads to the final adjustment of the hydraulic conductivity to

$$K_e = K_{bare}\,(1 - scovef) + (0.0534 + 0.01179\,K_b)(rain)\,(scovef)$$

Equation 6

where K_e is the effective hydraulic conductivity (mm h^{-1}), K_{bare} is K_e of the bare area, K_b is the "baseline" effective conductivity, *scovef* is the effective surface cover and *rain* is the amount of storm rainfall (mm).

In a last step, K_e can be adapted due to bio-pores in the soil. Depending on the influence of bio-pores defined by abundance and size, the effective hydraulic conductivity increases by multiplying it with a ratio, which also depends on the input K_e. The increase of K_e due to biopores is highest for low hydraulic conductivity (ratio 12 to 18) and decreases for soil with already moderately high hydraulic conductivity (5 mm h^{-1}).

Adjustments for perennial crops and rangeland as well as time-invariant constant effective hydraulic conductivity are not discussed in detail, as they are not relevant to this work.

Baseline interrill and rill erodibility as well as critical shear stress are sensitive parameters to the model. All represent the parameter value of a freshly tilled soil. Depending on the sand content, the model uses two different equations for calculation of these parameters. "Baseline" interrill (K_{ib}) and rill erodibility (K_{rb}) for soil containing less than 30 % sand are calculated according to Equation 7 and Equation 8.

$$K_{ib} = 6054000 - 5513000\,clay \qquad \text{for soil with sand content} \leq 30\ \%$$

Equation 7

$$K_{rb} = 0.0069 + 0.134e^{-20clay} \qquad \text{for soil with sand content} \leq 30\ \%$$

Equation 8

The baseline values for interrill and rill erodibility are then adjusted to describe the effects of ground cover, roots, incorporated residues, crusting and sealing of the surface, slope and freeze and thaw. Adjustments to critical sheer stress consider the influence of random roughness, sealing and crusting and freezing and thaw.

e) Plant growth component

Plant growth influences many other model components. For example, the daily water use by the plants affects the water balance component and canopy height and cover affect interrill soil detachment in the erosion component. Assuming a potential growth, canopy cover and height, the model adjusts potential biomass production due to water and temperature stresses. Water stress occurs when the ratio between plant water use and potential plant evaporation is less than 1.0.

As a function of biomass production over the cropping season, the model generates a yield output.

f) Hydraulics of overland flow

The friction coefficient is an essential parameter for appropriate routing of the runoff. The WEPP model uses the Darcy-Weisbach equation under uniform flow conditions. The friction coefficient for rills is composed of friction coefficients for surface roughness, surface residue and living vegetation. The interrill friction coefficient also accounts for the friction coefficient of surface roughness and surface cover, living plants and bare soil. The total friction coefficient for cropland results from both, rill and interrill coefficients according to the ratio of rill and interrill area from the total area.

g) Hillslope erosion component

The hillslope component combines all the information given above and describes the processes of sediment continuity, detachment, deposition, shear stress and transport capacity. The constant of proportionality is the interrill erodibility.

Interrill erosion is a consequence of the impact of raindrops on the soil. It is proportional to the product of the intensity of the rainfall and interrill runoff rate. Interrill erosion delivers sediments to the rills, where sediments either are transported off the hillslope or deposit in the channel.

The steady-state sediment continuity equation describes the transport of sediments in the rills.

$$\frac{dG}{dx} = D_f + D_i$$

where G is the sediment load (kg s^{-1} m^{-1}), x is the distance downslope (m), D_f is the rill erosion rate (kg s^{-1} m^{-2}) and D_i is the interrill sediment delivery (kg s^{-1} m^{-2}).

Interrill sediment delivery is always positive, while a positive rill erosion rate indicates detachment and a negative rill erosion rate deposition, respectively. Net soil detachment in rills (D_f) occurs if the hydraulic shear stress by the flow exceeds the critical shear stress of the soil and the sediment load of the flow is less than the transport capacity. The detachment capacity is proportional to the difference between critical and actual shear stress. Rill erodibility is the constant of proportionality.

The WEPP model also considers particle size distribution. In deposition regions, the fraction of fine sediments increases as it comes to a selective deposition of coarser material. The model calculates a new particle size distribution for the flow leaving the deposition region.

The hydrologic input parameters (peak runoff, effective runoff duration, effective rainfall duration and effective rainfall intensity) are firstly dynamic but have to be transposed into steady-state values for the erosion equations. In order to keep the computational time low, parameters have to be normalized and computations are based on non-dimensional equations. In a later step, the parameters are re-transposed to the final solution.

7. Material and Methods

This work consists of a fieldwork and a subsequent step of computer-based modelling. Field data collection is the basis for the successive simulation of soil erosion by means of the Water Erosion Prediction Program (WEPP).

The idea of the fieldwork was the monitoring of soil loss from arable land on a plot scale. The soil loss monitoring aimed to assess the effect of parameters such as canopy and rock fragment cover and the impact of the slope reduction by stone bunds on the fields. Soil loss was recorded for the rainy season 2012 (end of June to end of August) at three soil erosion plots. In a successive step, the information of the fieldwork built the basis for the simulation of soil loss at the same site. The aim of the simulation process was to find a configuration of the model, which predicts soil loss adequately for this specific site. The following section presents the approach of the fieldwork and simulation consecutively.

The collection of the fieldwork data included a description of the study area, collection of precipitation data, a topographic survey, assessment of canopy and rock fragment cover, soil loss measurements, sampling and laboratory work.

7.1 Description of the study area

Study area is the Gumara-Maksegnit watershed in the North Gonder zone of Amhara Region. The watershed covers an area of 54 km². Altitudes range from 1933 m a.s.l to 2852 m a.s.l. About 75 % of the total area is arable land, used for subsistence farming (Hailu Kendie Addis unpublished). Most common crops are sorghum, tef, wheat, lentil and chickpea. The settlement is characterized by a scattered pattern of households, ranging from the low parts up to the fragile steep slopes in the upper part of the watershed.

The experimental plots were situated in the Ayaye sub-catchment of the Gumara-Maksegnit watershed. The Ayaye sub-catchment and the neighbouring sub-catchment Aba-Kaloye are involved in long-term soil erosion studies. Both sub-catchments show severe soil erosion problems, which become apparent in the formation of deep gullies. In the Ayaye sub-catchment, the gullies were treated by the construction of gabions. This measure should reduce the development and advancement of the gully system. The neighbouring Ayaye sub-catchment acts as a reference for gully development without measures. Additionally, stone bunds were applied at the field in the Ayaye sub-catchment, which retard the sheet erosion process.

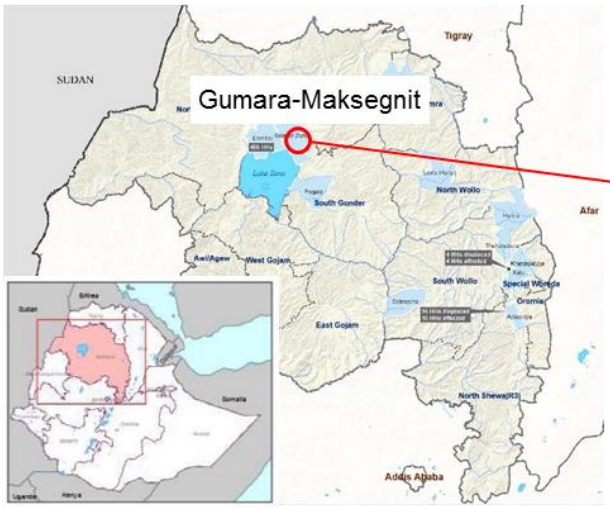

Figure 6: Amhara Region, the Gumara-Maksegnit watershed is located in the northeast of Lake Tana and is marked by the red circle. © ("OCHA" 2013)

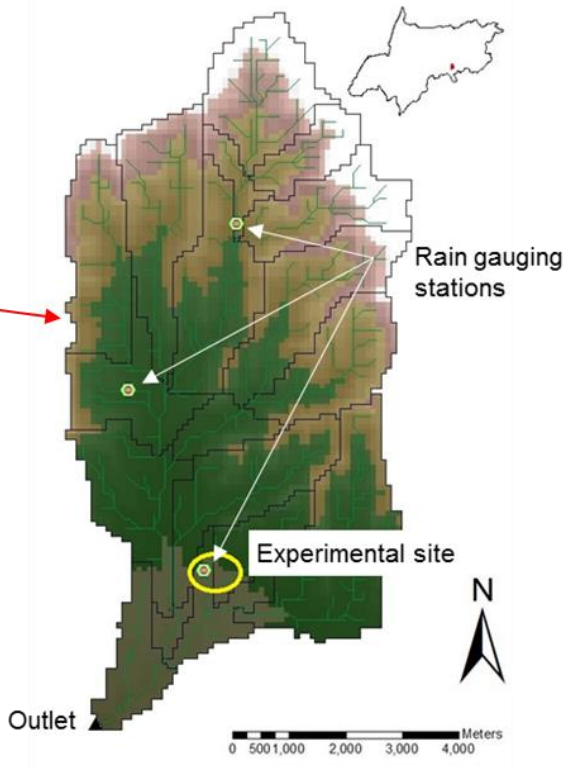

Figure 7: Gumara-Maksegnit watershed; the yellow circle indicates the experimental site (Kendie Addis unpublished)

Figure 6 shows a map of the Amhara Region with Lake Tana, the largest lake of Ethiopia. The Gumara-Maksegnit watershed, shown in Figure 7 is situated in the northeast of the Lake Tana basin and drainages into the Gumara River, which ultimately reaches Lake Tana. The yellow circle specifies the experimental site. The three smaller circles represent the three rain gauging stations within the watershed. The rain gauging station most to the south is located in the Aba-Kaloye sub-catchment. As the distance between experimental plots and rain gauging station is about one kilometre, the present work assumes that recorded precipitation in Aba-Kaloye is valid also for the Ayaye sub-catchment.

The Ayaye sub-catchment has a size of 24 ha. It is oriented north to south and is located in the lower part of the watershed. Altitudes range from 2012 m a.s.l to 2136 m a.s.l. The experimental plots are located in the lower gently sloped part, near the outlet of the sub-catchment.

In Ethiopia, with its wide altitude range, rainfall mainly correlates with elevation (FAO 2013). Depending on the altitude, five major agroclimatic zones can be distinguished. Table 2 shows range of altitude, rainfall, length of the growing period and average annual temperature for each region. The watershed is located in the Weyna Dega, cool and sub-humid agroclimate zone

Table 2: Agroclimatic Zones of Ethiopia after (Dejene 2003)

Zone	Altitude (m)	Rainfall (mm/year)	Length of growing period (days)	Average annual temperature (°C)
Wurch (cold and moist)	>3200	900 – 2200	211 – 365	>11.5
Dega (cool and humid)	2300 – 3200	900 – 1200	121 – 210	11.5 – 17.5
Weyna Dega (cool sub-humid)	1500 – 2300	800 – 1200	91 – 120	17.5 - 20
Kola (warm semi-arid)	500 – 1500	200 – 800	46 – 90	20 – 27.5
Berha (hot arid)	<500	<200	0 – 45	>27.5

According to precipitation records from 1987 to 2007 (GARC 2010), mean annual rainfall is 1052 mm varying from 641 mm to 1678 mm. About 600 mm rainfall occur in July and August. Information on temperature is available from records of the weather station in Maksegnit Town. Mean maximum and minimum temperature were recorded for 10 consecutive years. Mean maximum temperature is 28.5 °C; mean minimum temperature is 13.6 °C (GARC 2010).

Loam soils can be found in the higher parts of the watershed, while in the downstream clay soils occur. Soils in the upper stream are mainly shallow with rooting depth below 15 cm; whereas the clay soils are well developed with rooting depths exceeding 80 cm (Hailu Kendie Addis unpublished). Figure 9 shows a map of soil classes in the Gumara-Maksegnit watershed.

In the Ayaye sub-catchment, heavy soils predominate, characterized by its high clay content. In mixed samples, clay content was about 42 %. Silt content was high as well, and lay around 36 %. Correspondingly, sand content was about 22 %.

Figure 8 shows a soil texture triangle. With the percentages for clay, silt and sand, as described above, the soil of the experimental site is a clay soil.

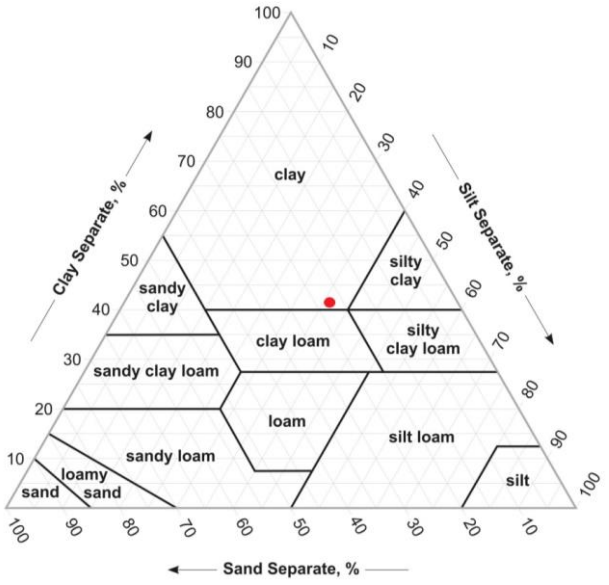

Figure 8: Soil texture triangle; the red dot represents the soil at the experimental site ("Guide to Texture by Feel | NRCS Soils" 2013){Citation}

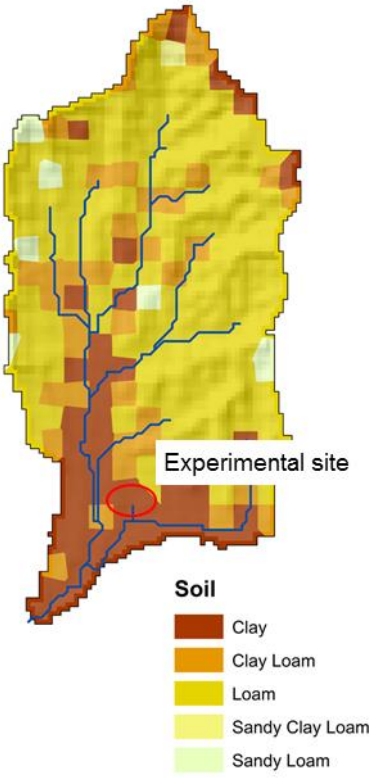

Figure 9: Soil map of the Gumara-Maksegnit watershed; the red circle indicates the experimental site (H. Kendie Addis et al. 2013)

At the west flake of the sub-catchment, all fields are treated with stone bunds except for the fields most to the south. Thus, fields with stone bunds and fields without measure directly adjoin each other. The distance between the stone bunds is about 25 m. In the Ayaye sub-catchment, steep slopes are used for grazing, while the gentile slopes are covered by different crops.

Due to the climate conditions in this region, there is only one cropping season per year. For tillage farmers use a traditional ox-drawn ard plough. In 2012, farmers mainly grew sorghum, tef and faba bean in the Ayaye sub-catchment. At the fields from the experimental plots famers sew sorghum in the beginning of June and harvested in mid-December. They tilled twice before planting sorghum (mid-February and mid-May).

7.2 Soil erosion measurement

The setup of the experimental plots should enable the evaluation of the impact of stone bunds on the soil erosion process by comparing soil loss under treated and untreated conditions. Moreover, soil loss monitoring under treated conditions included two different plot arrangements. First, one plot should investigate the effect of reduced slope length on soil erosion. Second, one plot should test the impact of stone bunds on soil erosion on entire hillslope length scale. Thus, one plot was situated between two subsequent stone bunds, while the other had a stone bund within the plot area. This setup resulted in the installation of three sediment retention plots.

a) Instillation of the sediment retention plots

The experimental site was selected due to its position, topography and management. The experimental plots were installed at a relatively uniform hillslope near the outlet of the sub-catchment.

Mean slope inclination is 6%; which is representative for the cultivated area in the sub-catchment. Lateral inclination at the plot area is low.

Figure 10 shows a scheme of the experimental site around the border between treated and untreated fields.

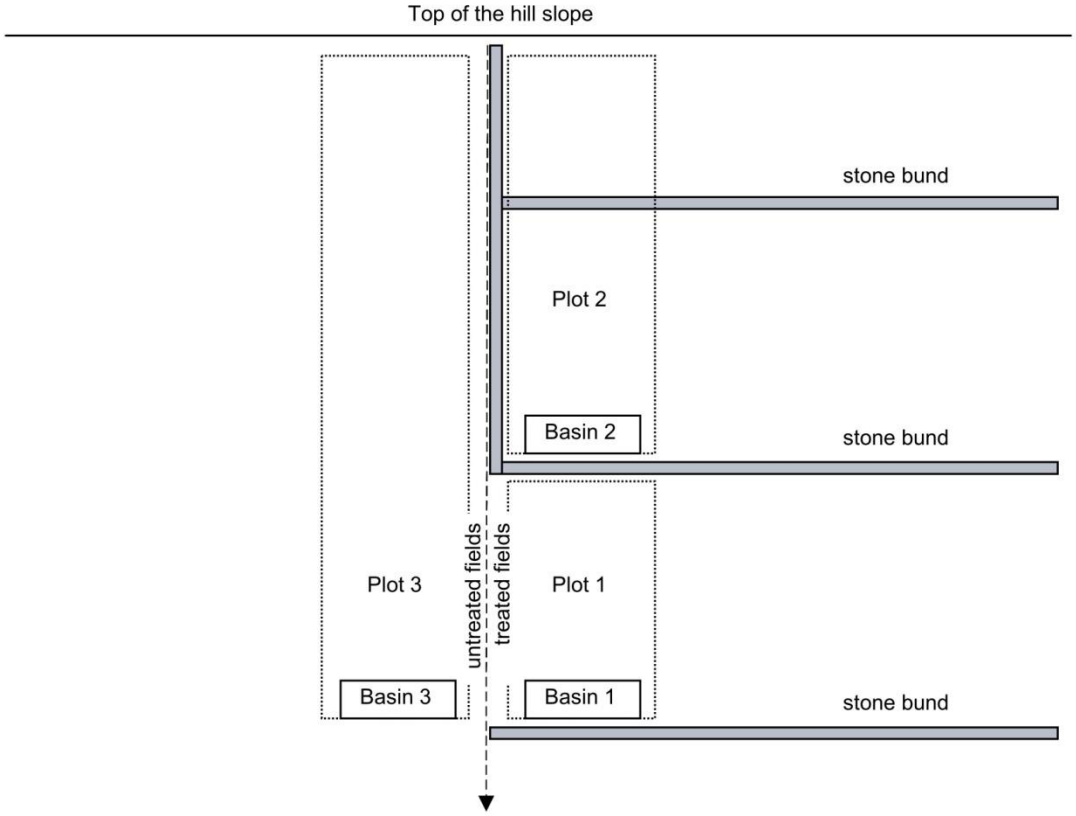

Figure 10: Scheme of the erosion plot setup

As shown in Figure 10, Plot 1 and Plot 2 were situated on farmland with stone bunds. Plot 3 was designed to be located next to both others on farmland without the influence of soil conservation measure. This setup should enable comparison of soil loss under treated and untreated conditions.

Plot 1 covered the area between two subsequent stone bunds. Thus, the stone bunds built the upper and lower limits of the plot. In this case, as already mentioned the upper stone bund reduced the effective slope length to the distance between the two bunds. As Plot 2 is located directly uphill of Plot 1 and, hence, sediments were prevented from entering Plot 1 from above, it can be assured that no additional sediments entered the plot from the uphill fields.

Plot 2 transcended the upper stone bund and extended to the top of the hillslope. Consequently, the plot was divided by the mid stone bund. This bund had a barrier effect to the soil detached from the upper part of the plot. It can be expected that sediments, which eroded uphill the mid stone bund, will at least partially deposit behind it and will not leave the plot at the outlet. If soil loss at Plot 2 is about the same as at Plot 1, it can be assumed that the

stone bund held back the material from above. Plot 2 was separated from the adjacent untreated land by a downhill-orientated stone bund.

Plot 3 had the same slope length as Plot 1 and Plot 2 together (around 50 m), but without any soil conservation measure in between. This plot acted as a reference plot for soil loss under untreated conditions.

The plots were naturally bordered. Thus, plot areas were defined by the topography of the hillslope. It was assumed, that by building sufficiently wide basins, the effect of surface water running sidewise could be kept low.

The width of the plots was defined by the width of the sediment retention basins, forming the lowest part of the plot. At the treated fields, the sediment retention basins were located directly uphill of the stone bunds.

b) Set-up of the sediment retention basins

The size of the retention basins, which formed the outlet of the plots, was 8 m by 1.5 m, with a depth of 0.75 m. We assumed that a width of 8 m is sufficient that the effect of lateral detachment is negligible.

The sediment retention basins were excavated and covered by a foil. Excavated basins instead of collection devices on the surface were considered to have several advantages. Firstly, the construction of excavated retention basins is simple. Additionally, little material is necessary in the construction, which makes them quiet theft proof.

In order to prevent the mixture of eroded material with the in situ soil, a perforated plastic foil was applied at the surface of the excavated basins. The perforated foil should enable infiltration of water, but detain sediments.

During heavy rainfall events with rainfall excess and surface runoff, soil particle were eroded and transported with the surface runoff. The sediments, which reached the bottom end of the plots, were trapped in the sediment retention basins and accumulated. By monitoring the amount of trapped sediments, one can draw conclusions about soil loss from the hillslope.

Construction of the basins was conducted on June 21th and June 22th, 2012. Figure 11 shows pictures of the construction process.

Figure 11: Construction of the sediment retention basins

c) Soil erosion measurement procedure

The soil loss measurements included the three steps: collection, removal and weighing of the trapped sediments.

The monitoring of soil loss was based on the collection of sediments, which deposited in the sediment retention basins from the three plots. The sediments, which would pass the lowest point of the plots and leave the plots at the bottom end due to rill and interrill erosion, accumulated in the sediment retention basins. Subsequently the sediments were removed and weighed.

Sediments were removed as often as possible. Nevertheless, it was not possible to collect sediments for single events separately, but sediments from more events accumulated between two days of removal. In total, accumulated sediments were collected, removed and weighed 13 times over the rainy season. Intervals between days of removal were not regular.

Percolation of collected surface runoff through the perforated plastic foil was low. We assumed that this due to the high clay content of the soil. The collected rainwater stayed in the basins, mixed with the fine sediment fraction (see Figure 12). The coarser material settled at the bottom of the basins. Thus, water content of the collected material was very high and additional action for the extraction of the water was necessary.

In a first step, the standing water in the basins was extracted using a hose (see Figure 13). The water ran freely due to a gradient in the water level. The hose was hold near the surface of the water table in order to avoid mixture with the coarse material. The volume of the extracted water was monitored. A sample (100 ml) for determination of the sediment concentration in the down pumped water was taken every 150 l. The 100 ml samples were put together and the sediment concentration of the mixed sample was determined in the laboratory using filters and oven drying of the particles. If sediment concentration varied strongly, two or more mixed samples were analysed separately and related to the water portion, which showed similar sediment content. The amount of sediments removed by the hose resulted from relating the volume of removed water to the sediment concentration.

Secondly, after removal of the liquid fraction, the coarser material, which stayed in the basins, was removed using buckets. The buckets were weighed by means of a spring balance with 0.5 kg accuracy (see Figure 14 and Figure 15). Mixed soil samples were retained for determination of the water content and dry weight. Water content of the material increased from the top to the bottom. Mixed samples were taken for different layers of the accumulated sediments. For each bucket, the representative mixed sample was noted.

Finally, water content of the mixed samples was determined by the difference between the weight of the immediately weighed samples and the weight of the samples after oven drying in the laboratory at 105°C.

Figure 12: Sediment retention basins filled with water after rainfall events

Figure 13: Extraction of standing water from the basins by free water levelling

Figure 14: Removal of sediments using buckets

Figure 15: Weighing of the removed sediment using a spring balance

The raw data of the soil loss monitoring is attached to the Annex.

7.3 Precipitation data collection

Three rain gauging stations are located within the Gumara-Maksegnit Watershed as shown in Figure 7, in 7.1.

The rain gauging station in the Aba-Kaloye sub-catchment is situated in about one kilometre distance from the experimental plots. Rainfall data from this station was used in this work.

Rainfall was monitored continuously using an ombrograph. Every tip is equivalent to 0.2 mm rainfall. Additionally the device measured air temperature every hour. Rainfall records were available from June 26th to December 31st 2012.

7.4 Topographic survey of the study area

In order to link soil loss from the three plots to the contributing areas, a topographic survey of the hillslope was conducted during the rainy season 2012. It was carried out by a local surveyor on August 22nd 2012 by means of a total station. As point measurements showed wrong values for the upper part of the hillslope, the survey partly had to be repeated on September 7th 2012.

An area of 2600 m² was surveyed by a raster of 1 x 1 m and 2 x 2 m on the first and second day of surveying, respectively.

A digital elevation model (DEM) of the experimental site was generated using Arc GIS 10. Based on the DEM and the position of the three retention basins within the hillslope, Arc GIS 10 confined the area, feeding each basin using the Watershed Tool in the Spatial Analyst Toolbox.

The Annex includes a detailed description of the procedure, used for delimiting the watersheds for the three plots.

7.5 Assessment of canopy and rock fragment cover

Determination of canopy and rock fragment cover is based on a photo image classification. On June 25th, photos were taken from 60 x 60 cm mini-plots, located along transacts at the treated and untreated fields. The mini-plots were evenly distributed over the length of the plots. Monitoring included 10 mini-plots at Plot 1 and Plot 2, respectively, and 20 mini plots at Plot 3. All photos for this work were taken from the same height and perpendicular to the ground.

The canopy and rock fragment cover was then evaluated using two different approaches: automatized analysis using Arc GIS and manual analysis using AutoCAD.

Arc GIS includes an Image Classification Tool, which was used in the first method. For each image, training samples for the categories *vegetation*, *soil* and *stones* were selected. By using these training samples as a reference, rock fragment and canopy cover were a result of an Interactive Supervised Classification by Arc GIS and a successive Maximum Likelihood Classification. The Arc GIS output is the number of pixels, which belong to each category. This information can then be related to the total pixel number and thus canopy and rock fragment cover is described as the particular percentage from the whole mini-plot area. It was assumed that this method would underestimate rock fragment cover as plant leafs overlap and hide stones.

A second method should help to evaluate this approach and verify its results. The second method for determining rock fragment cover only is based on a manual analysis using AutoCAD. This method was considered to be more correct, but time-consuming and difficult to exactly reproduce. Stones were encircled by polygons and the area of all polygons represented the portion of rock fragments at the mini-plots. This method has the advantage that stones are recorded separately. This would allow analysing the number and size of the rock fragments. Only rock fragments with an area exceeding 0.5 cm² were taken into account and classified as stone. In a field experiment in Tigray, Ethiopia, Nyssen et al. (2001) limited rock fragment size to fragments with an intermediate diameter exceeding 0.5 cm.

7.6 Sampling and laboratory work

The Gonder Laboratory undertook the analyses of the samples. The determined parameters were

- water content of the removed sediment
- sediment concentration of the down pumped surface runoff

Soil texture of the samples was determined for the first three days of removal.

7.7 Computer-based modelling (WEPP)

The WEPP model used results from the fieldwork as input information, to adapt soil loss prediction to local conditions. In general, the input parameters are excessive. For sites in the United States, for instance, the model accesses databases in order to get input parameter, which are valid to the study area. In the experimental site of this work, little information is available. This fact makes the modelling process difficult. The idea of this work was to find a configuration of the model, which depicts observed soil loss adequately.

The main WEPP output can be plotted as an annual, monthly or event-to-event based description of the erosion events. The output includes all days with surface runoff, even if no soil loss results from it. The hydrological output for each event includes the amount of rain and runoff, the rainfall duration and effective event duration (takes account of both, rainfall duration and runoff duration), the effective slope length and peak runoff rate.

For the analysis of the model's efficiency in simulating observed soil loss, the soil loss – the average net soil detachment rate – was the most important output. This value is the basis for the evaluation of the model's results. Surface runoff was not taken into account. The additional output as plant, water, soil and yield output discuss sections 8.6.5 and 8.6.7.

The sensitivity analysis gave information about the influence of selected parameters. The Latin Hypercube Sampling (LHS) method by McKay et al. (1979) built the basis of the parameter value selection. For each sensitive variable X, the parameter range was divided into intervals with equal probability. From each interval one value was selected and then paired randomly with the parameter values of the other variables X_i (Wyss and Jorgensen 1998). This method leads to the simulation of various scenarios.

To validate the model, the use of the 95 % confidence interval of the simulations led to the development of a range of soil loss prediction, which excludes outliers but still includes most of the parameter combinations. Where the measured value lies within the confidence interval, the model is capable of predicting soil loss adequately at least in one combination. The smaller the area between the two quintiles 2.5 % and 97.5 %, the better the models adaption to the problem and its calibration. It is obvious that the wider the range of predicted soil loss, the higher the likelihood that the observed value lies within this range.

7.7.1 Model sensitivity analysis

In a first step, sensitivity of the model to variation of single parameters was evaluated. For selected parameters, effective hydraulic conductivity, interrill and rill erodibility, random roughness, canopy cover coefficient, maximum leaf area index, rock fragments, cation exchange capacity and initial saturation level a sensitivity ratio was calculated using Equation 9 as proposed by Mahmoodabadi et al. (2013).

$$SR = \frac{[(O_{max} - O_{min})/O_{ave}]}{[(I_{max} - I_{min})/I_{ave}]}$$

Equation 9

where I_{max} and O_{max} are the maximum values of the input and output, I_{min} and O_{min} are the minimum values of the in- and output and I_{ave} and O_{ave} are the average values of maximum and minimum values.

Therefore, the parameters varied within a fixed range as shown in Table 3.

Table 3: List of parameters included in the sensitivity analysis and their tested ranges

Parameter	Tested range	Unit
rock fragments	5 - 55	%
rill erodibility	0.003 - 0.009	s m^{-1}
random roughness	4 - 15	cm
effective hydraulic conductivity	2 - 400	mm h^{-1}
cation exchange capacity	20 - 35	meq $(100g)^{-1}$
maximum leaf area index	4 -10	-
initial saturation level	0 - 100	%
canopy cover coefficient	6 - 18	-
interrill erodibility	2500000 - 5000000	kg s m^{-4}

7.7.2 Model validation

For the validation of the model, sensitive input parameters were altered leading to different scenarios. The root mean square error (RMSE), the model efficiency (NSE) and the coefficient of determination (^{2}) were calculated as objective functions, which indicate how well predicted and observed values fit together. The choice of the objective function affects the ranking of the scenario as not all objective functions result in the same order of the scenarios. In order to get the best model fit three separate objective functions should evaluate the model's capability to predict observed soil loss.

RMSE is calculated using Equation 10 (Thomann, (1982) cited by Mahmoodabadi and Cerdà, 2013):

$$RMSE = \sqrt{\frac{\sum_{i=1}^{n}(O_i - P_i)^2}{n}}$$

Equation 10

where O_i is the observed value at the point i, P_i is the predicted value at the point i and n is the number of paired O and P values. Smaller values indicate a better fit between observation and prediction.

The model efficiency after Nash and Sutcliffe (1970) is calculated according to Equation 11.

$$ME = 1 - \frac{\sum_{i=1}^{n}(O_i - P_i)^2}{\sum_{i=1}^{n}(O_i - O)^2}$$

Equation 11

where O is the mean of all measured values.

Possible values for the model efficiency parameter (NSE) are between -∞ to 1. The more the value converges to 1, the better the model's prediction. Negative values indicate that the mean of the observed values is the better predictor.

The coefficient of determination (R^2) describes the portion of the total variance of observations explained by the model. It is between 0 and 1 with better results converging to 1. It is calculated according to Equation 12.

$$R^2 = 1 - \frac{\sum_{i=1}^{n}(O_i - P_i)^2}{\left(\sum O_i^2\right) - \frac{(\sum O_i)^2}{n}}$$

Equation 12

The root mean square error (RMSE), model efficiency (NSE) and coefficient of determination (R^2) are three separate objective functions, which not necessarily coincide in one best result. All three parameters were calculated for each scenario.

7.7.3 Model input

The model input is partly based on results from the fieldwork, partly depends on WEPP integrated databases. The objective of the modelling process was to find a combination of input parameters, which allows an adequate simulation of observed soil loss. The definition of the input parameter reflects the information from the sensitivity analysis. Model input varied between the plots.

a) Climate input file

The climate input file is composed of information on time-related daily cumulative rainfall, minimum and maximum daily temperature, daily solar radiation, wind velocity, wind direction and dew point temperature.

First, the continuously logged daily rainfall was displayed as a cumulative graph. The breakpoint method was then used to create the climate file. A breakpoint file contains two columns with cumulative time from the beginning of the rainfall event and average rainfall intensity in the interval between two time steps in the second column. Breakpoints are inserted wherever the inclination of the hydrograph changes. All available rainfall data from the year 2012 - June 26th, 2012 to December 31th, 2012 - was embedded into the climate input file. Unfortunately, no precipitation data from January to June is available for any of the recording years.

Daily solar radiation and dew point temperature were derived from a default file from the region (Anjeni, Ethiopia). Wind velocity was set to zero, as no information is available. The lack of wind information is accounted for by using the Priestley-Taylor method for evapotranspiration computation.

b) Slope input file

The slope is an output of the Arc GIS computation. WEPP uses a list of segments of known length and slope as an input. The number of segments is limited to 9. Thus, the slope profile derived from Arc GIS has to be simplified and reproduced by at most 10 points, leading to 9 segments. The width of the hill slope in the computation is 1 m.

The slope files are attached to the Annex.

c) Soil input file

The soil input file holds information on soil texture, albedo, initial saturation level, soil depth, organic matter, cation exchange capacity and percentage of rock fragments.

The soil files are attached to the Annex.

d) Management input file

The plant and management file is the most extensive component, which contains all information on plant parameters, tillage sequences, tillage implement parameters, plant and residue management, initial conditions, contouring, subsurface drainage and crop rotation. The plant parameters specify plant growth and harvest parameters, temperature and radiation parameters, canopy, leaf area index, root parameters and senescence parameters.

For the simulation of the initial condition of the plots on January 1st, a second management input file was created with management operations from the previous year 2011.

The management files are attached to the Annex.

8. Results and Discussion

This section consists of two main parts, where the first presents the results from the fieldwork in the Ayaye sub-catchment in 2012 and the second part discusses the results from the successive soil loss prediction by the Water Erosion Prediction Project (WEPP).

8.1 Precipitation data

The rain gauging station in the Aba-Kaloye sub-catchment is the nearest and most significant gauging station for the experimental site. Figure 16 shows daily and cumulative rainfall for the year 2012.

Total rainfall in 2012 was 941 mm. According to records from 1987 to 2007 mean annual rainfall in the Gumara-Maksegnit watershed is 1052 mm (GARC 2010).

Compared to data from 2011, daily rainfall in 2012 was low. While in 2011 rainfall events with 90 and 130 mm per day occurred, daily rainfall did not pass over 40 mm during the rainy season 2012.

Although most rainfall events occurred, as expected, during the rainy season (July and August), the heaviest rainfall in 2012 is recorded at the end of October during off-season.

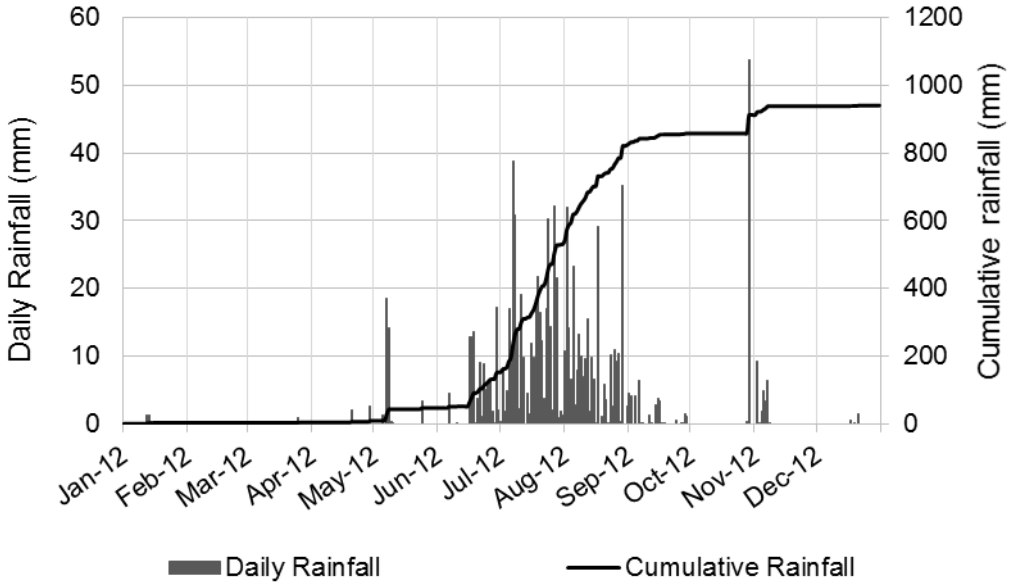

Figure 16: Daily precipitation and cumulative rainfall in the Aba-Kaloye sub-catchment in 2012

The sediment retention plots were installed on June 22nd 2012. Monitoring of the accumulated sediments ended on August 30th 2012. Total rainfall during this period was 697 mm. Within this time, the gauging station recorded two days without rainfall.

8.2 Topographic survey of the experimental site

a) Topography of the hillslope

The topographic survey was conducted on August 22nd 2012.

Figure 17 shows the digital elevation model of the hillslope derived from Arc GIS 10. Elevation ranges from 2023.3 m to 2036.7 m a.s.l. The length of the surveyed hillslope is around 75 m.

The lower part of the hillslope is arable land, in 2012 cultivated by sorghum. It extends up to an altitude of approximately 2031.3 m a.s.l. Bushes cover the hillslope above, so farmers use it for grazing of the cattle.

Furthermore, Figure 17 shows the position and orientation of the stone bunds, applied at the experimental site. Crest heights of the stone bunds were measured during the survey.

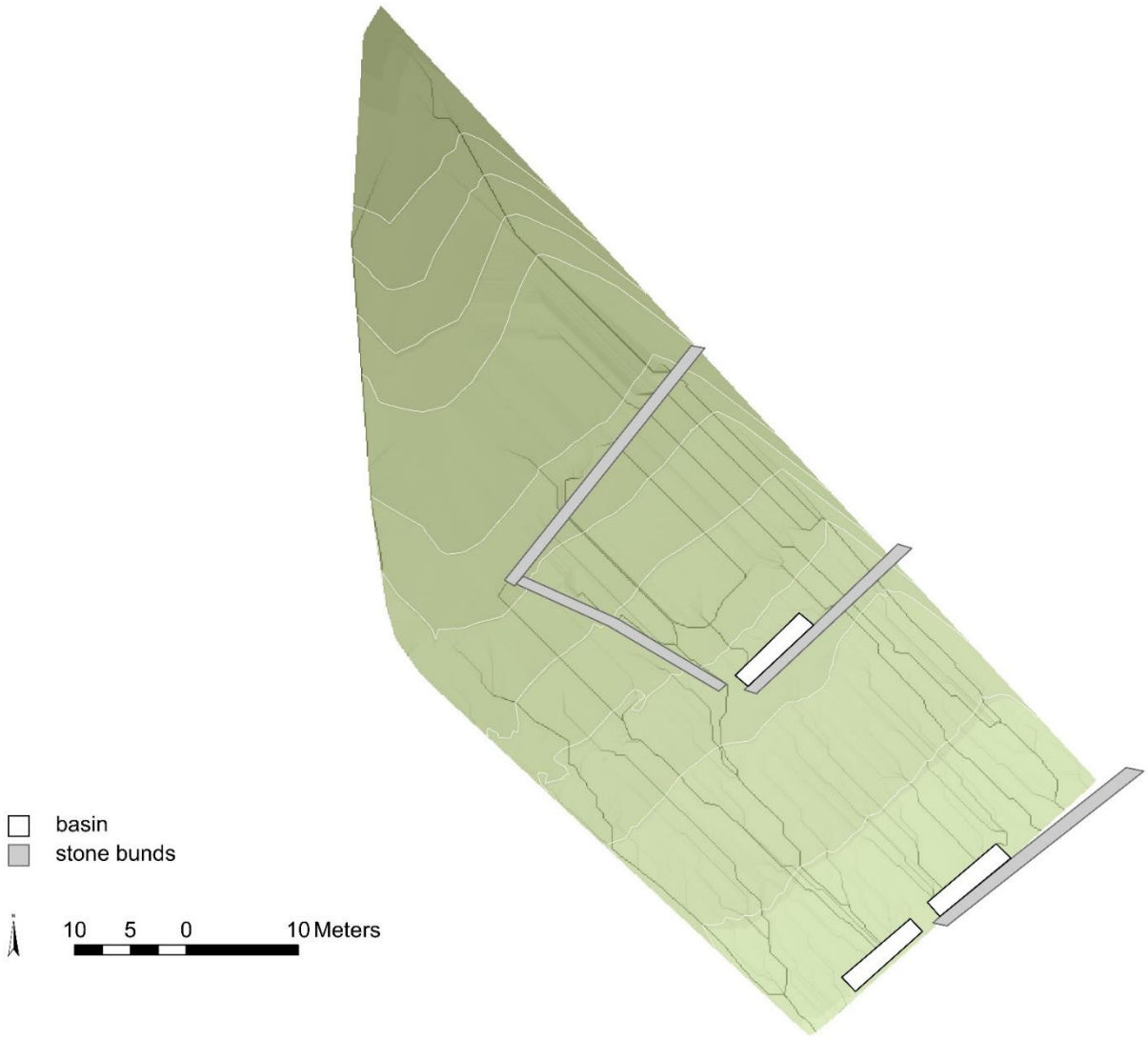

Figure 17: Digital Elevation Model and Flow Accumulation of the experimental site in the Ayaye sub-catchment (derived from Arc GIS 10)

The black lines in Figure 17 represent lines of flow accumulation. The line width is related to the amount of accumulated surface flow. Increased line width indicates increased cumulative surface runoff.

As already mentioned, the three soil erosion plots were constructed without artificial borders. The area of the plots is defined by the area with surface runoff flowing into the sediment retention basins at the outlet of the plots. Thus, plot areas represent areas with surface runoff flowing to the three retention basins. Knowing the plot area is essential in order to link the amount of collected sediments to its contributing area. As the soil loss rate (kg m^{-2}) describes the ratio between the amount of eroded soil and the influence area, it is highly sensitive to errors in area delineation.

b) Surface area of the soil erosion plot

Firstly, plot areas were derived from Arc GIS, using the Watershed Tool. Afterwards these plot areas were corrected and adapted as shown in the following.

According to the Arc GIS computation (see Figure 18), Plot 1 shows the least area with 297 m². A graded stone bund separated Plot 2 into an upper and lower section; it has an area of 323 m². The untreated Plot 3 is the biggest plot with 604 m².

Plot areas shown in Figure 18 do not account for land cover and land use. As the soil at the upper hillslope is covered entirely by grass and bushes (bush land), it is assumed that this area did not contribute to soil loss from the plots. The area of Plot 2 and Plot 3 was reduced by this section. Consequently, the area of Plot 2 decreased to 299 m². The reduced area of Plot 3 is 584 m².

Plot 3 acted as a reference area, which shows soil loss under untreated conditions. However, according to Figure 17 the influence area of this plot partly spreads into the treated fields. Surface runoff flows along the downhill-orientated stone bund and then into the basin of Plot 3. This would imply that all surface runoff and sediments from this treated area pass for a narrow run-through between the downhill-orientated stone bund and the basin of Plot 2. In site inspections, no signs of this excessive transport were visible. Furthermore, the resolution of the survey grid was too low for modelling micro-topography.

Due to the information from field observations, the plot areas by Arc GIS were altered. Concerning Plot 3, it is assumed that sediments from the treated field behind the downhill-orientated stone bund will not flow into the retention basin of this plot. The area of Plot 3 was reduced by the portion of Plot 3 situated on treated land. The area was added to Plot 2.

Figure 19 shows the final plot areas, used in the following.

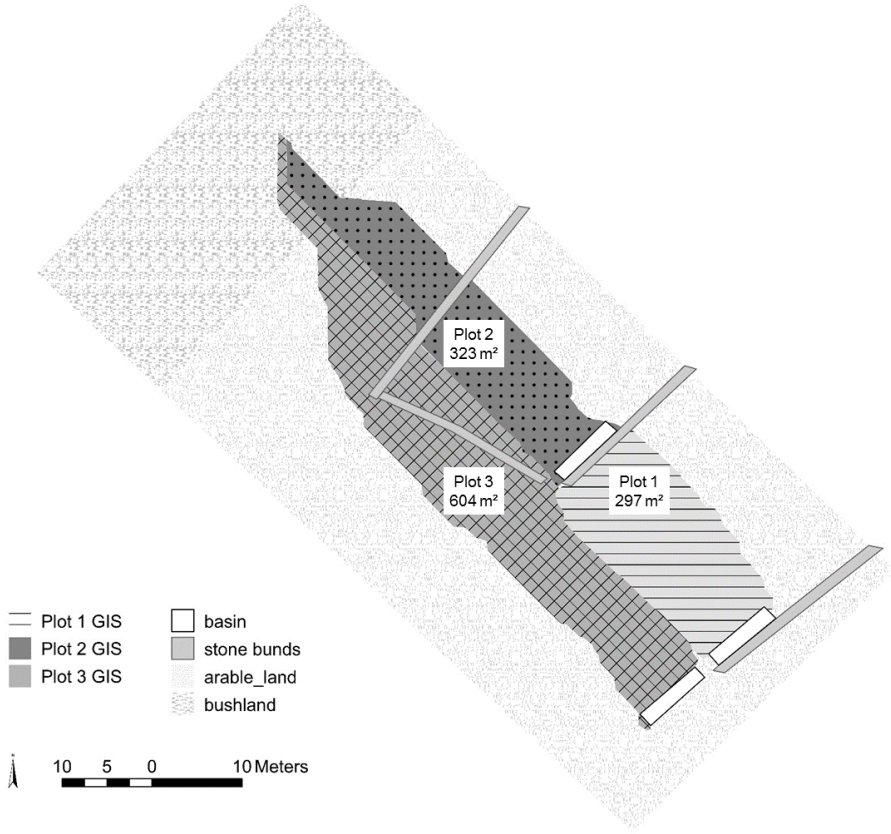

Figure 18: Plots areas derived from GIS

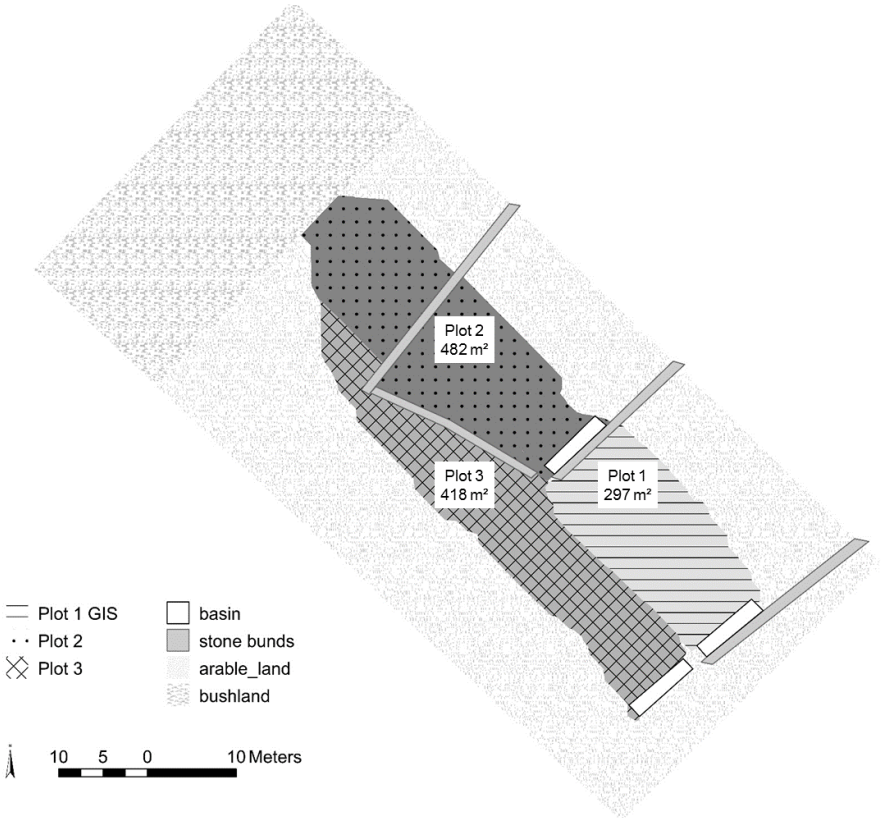

Figure 19: Plot areas: Area of Plot 3 reduced by the area behind the downhill-orientated stone bund and the bush land area. Plot 2 increased by the section of Plot 3 situated on treated fields and reduced by the bush land area

Plot 1 did not change in the post-processing of the data and kept a plot area of 297 m². Plot 2 increased in size and has an area of 482 m². The remaining plot area of Plot 3 is 418 m².

Even though the three sediment retention basins had the same size (8.0 x 1.5 x 0.75 m), the plot areas differed not just in length but also in width. While the width of Plot 1 and Plot 2 is 12.1 m and 12.7 m respectively, Plot 3 is the narrowest plot with a width of 9.4 m.

c) Slope profiles of the soil erosion plots

Figure 20, Figure 21 and Figure 22 show the profiles of the three plots. To get the average slope of the plots, Arc GIS computed profiles, evenly distributed over the plot width, and a mean slope was calculated.

Plot 1 is the shortest plot and measures 24.5 m. Figure 20 shows the length profile of this plot. At the upper border of the plot follows a stone bund and directly behind this stone bund follows the sediment retention basin of Plot 2. The steep slope in the first meters of Plot 1 is due to an earth bank behind the stone bund. This earth bank already existed before the start of the experiment.

The stone bund, which dissects Plot 2, is notable in Figure 21. It shows that the area behind the stone bund already filled up with sediments. The length of Plot 2 is about 38 m. The figure also shows a slight elevation at the end of the slope (at 33 m) and thus in front of sediment retention basin, which follows at the end of the profile.

Plot 3 is the longest plot. It has a length of up to 55 m and a uniform slope. Figure 22 shows the profile of this plot.

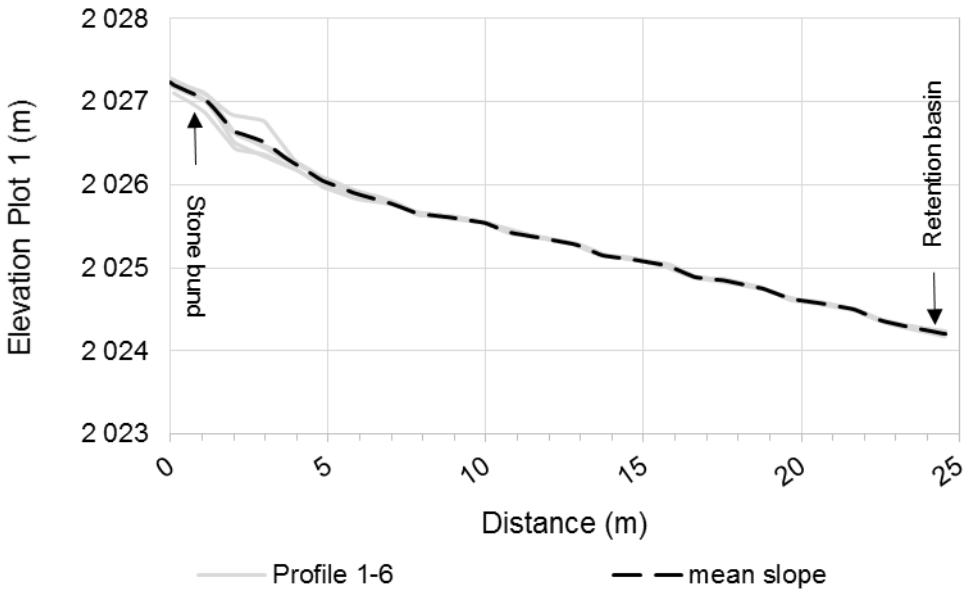

Figure 20: Slope profile of Plot 1

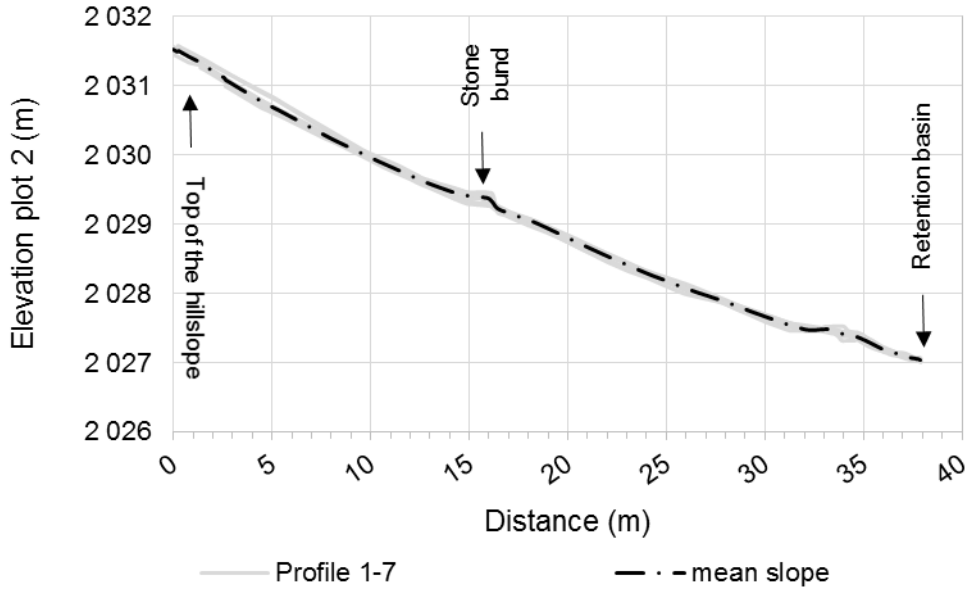

Figure 21: Slope profile of Plot 2

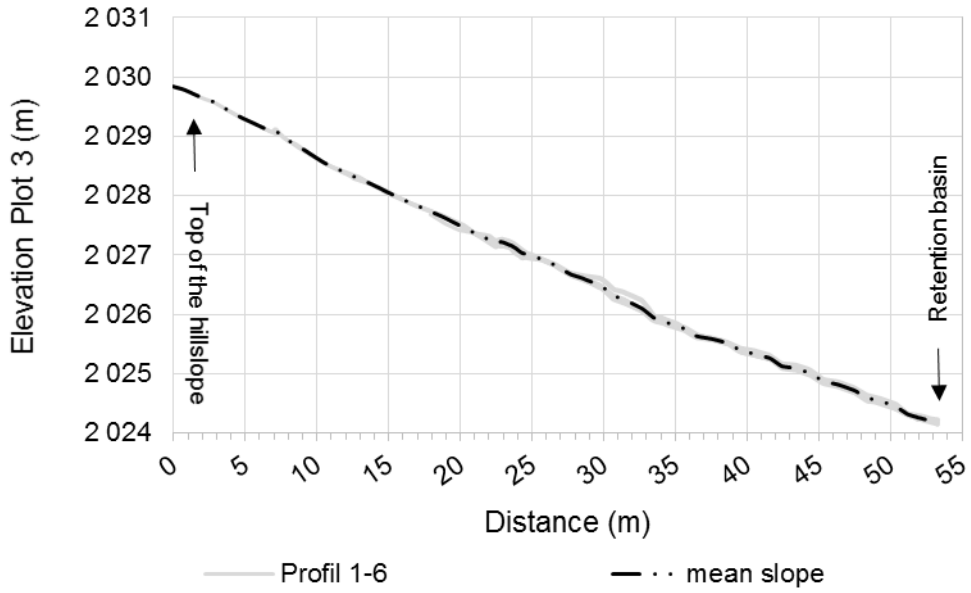

Figure 22: Slope profile of Plot 3

8.3 Assessment of canopy and rock fragment cover

The GIS and AutoCAD based image classifications show similar results and are consistent with each other.

The following compares canopy and rock fragment cover of the three soil erosion plots and additionally compares results from the manual and automatized analysis.

Table 4 and Table 5 show canopy and rock fragment cover derived from Arc GIS classification and manual analyse of rock fragment cover, respectively.

Table 4: Canopy and rock fragment cover derived from the Arc GIS Image Classification Tool.

	rock fragments [%]		**vegetation [%]**	
	mean	standard deviation	mean	standard deviation
Plot 1 (with SWC)	0.14	0.08	0.16	**0.15**
Plot 2 (with SWC)	0.17	0.09	**0.33**	0.12
Plot 3 (no SWC)	**0.24**	**0.11**	0.14	0.07

Table 5: Rock fragment cover derived from manual analyse.

	rock fragments [%]	
	mean	standard deviation
Plot 1 (with SWC)	0.13	0.07
Plot 2 (with SWC)	0.17	0.08
Plot 3 (no SWC)	**0.26**	**0.14**

Vegetation cover is in the same range for Plot 1 and Plot 3 and significantly higher on Plot 2. As surface cover has a high impact on surface runoff, this variation might influence the results from the soil erosion plots.

Figure 23 shows vegetation cover for each mini-plot at the three soil erosion plots. As Plot 3 is nearly double as long as Plot 1 and Plot 2, 20 mini-plots were distributed over Plot 3 while 10 mini-plots were installed at Plot 1 and Plot 2. The mini-plots of Plot 2 are in the same level as mini-plots 1 – 10 from Plot 3 and the mini-plots of Plot 1 on the other hand have the same level as the mini-plots 11 – 20 from Plot 3.

Focusing at the distribution of vegetation cover over the plot profiles, Figure 23 shows that vegetation cover increases at the bottom end of Plot 2 in front of the sediment retention basin. At the two other plots, there so no such effect noticeable. In contrary, vegetation cover at Plot 1 is highest directly behind the upper stone bund, which builds the top end of the plot. Vegetation cover has a slightly decreasing tendency from top to bottom.

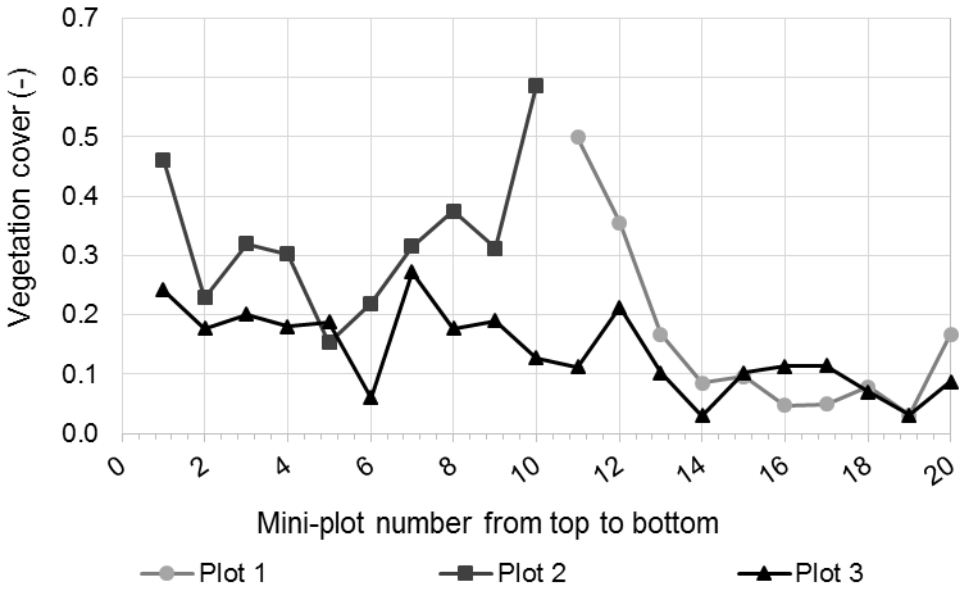

Figure 23: Vegetation cover for the mini-plots at Plot 1, 2 & 3 derived from the automatized Arc GIS analysis.

Concerning the rock fragment cover, Plot 3 shows higher values for this parameter than both treated plots. Figure 24 shows rock fragment cover for each mini-plot at the three soil erosion plots.

It is obvious, that the variation of rock fragment cover between mini-plots is high. At Plot 3 rock fragment cover varied from 7 % to 55 % (standard deviation of 0.14 %). Rock fragment cover of Plot 1 and Plot 2 ranged from 3 % - 25 % and 5 % - 28 %, respectively. Especially the long plot shows a systematic decline of rock fragment cover from top to bottom. The detailed list including rock fragment cover for all mini-plots separately is attached to the Annex.

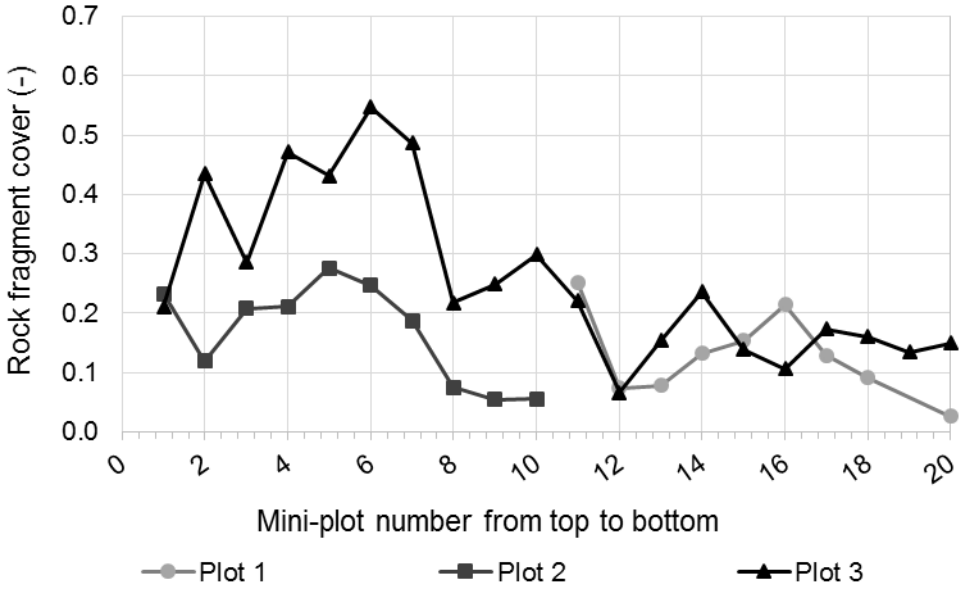

Figure 24: Rock fragment cover for the mini-plots at Plot 1, 2 & 3 derived from the manual analyse using AutoCAD.

8.4 Soil loss measurement

Sediments, which eroded during rainfall events, were collected in three retention basins located at the outlets of the plots. Next to the sediments, water accumulated in the basins. We assumed that this water results from surface runoff. As the clay content of the soil is high, the infiltration of the stored water is low and thus the water stays in the basins. The monitoring of removed water showed that this was not the case. Even if no rainfall occurred, the basins filled with water again after the removal. This indicates that the basins acted as a drainage of the fields and water infiltrated from the soil into the basins. Consequently, the amount of stored and measured water in the basins after rainfall events is not related to surface runoff and cannot be evaluated or used for the successive model calibration. A second effect, which supports this assumption, is that the basins mostly filled to the same level and never overtopped the basins. Because of this, solely information of the soil loss monitoring was used for the entire WEPP model calibration.

Figure 25 shows the amount of collected sediments per day of removal and daily rainfall during this period. It is noticeable, that the amount of accumulated sediments in the basin of Plot 2 was very low compared to the other basins. The highest amount of sediments was removed on August 1st, 2012. More than 450 kg accumulated in the sediment retention basins of Plot 1 and Plot 3.

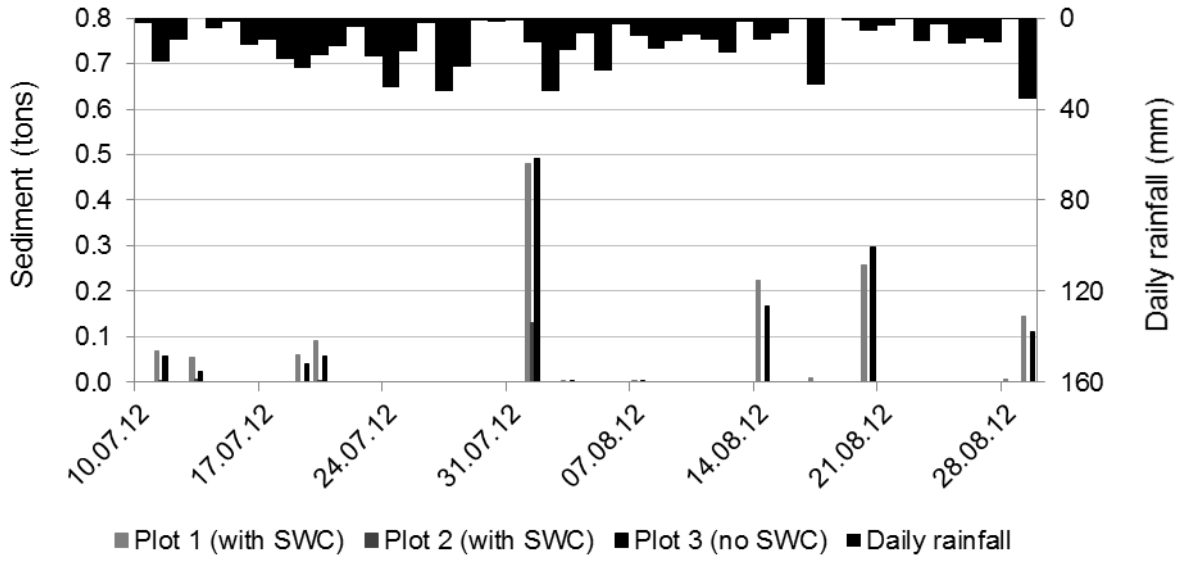

Figure 25: Mass of sediments in the retention basins for all days of monitoring

Figure 25 shows that on five days collected sediments were very low. On these five days water, which accumulated in the basins was removed and the sediment concentration of the water led to the recorded soil loss. Especially measurements on the last day of sediment removal emphasize the assumption that collected water did not result from surface runoff. Between the removal on August 29th and the following day no rainfall occurred. However, all water was removed from the basins on the first day and the basins were full with water again on August 30th; more than 2000 litres accumulated in the basins.

In the following, these five events were not considered as single events, but added to the next event with visible soil loss. Soil loss rates arise from relating the dry weight of the collected material to the contributing areas derived from the Arc GIS analysis of the surveying data (see Figure 19). Figure 26 shows soil loss rates from the three plots for the remaining eight days of soil loss monitoring.

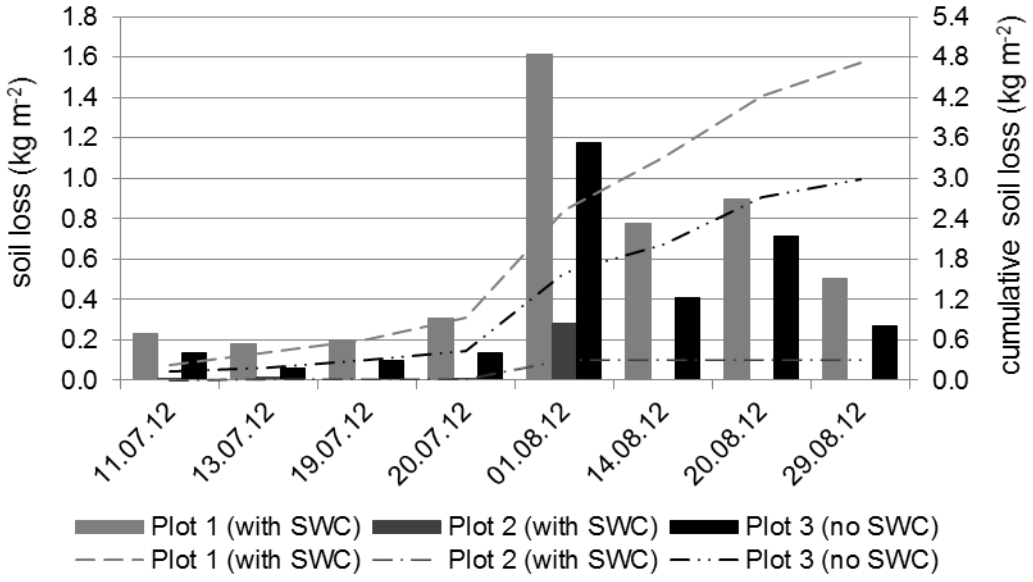

Figure 26: Comparison of soil loss rates from the three experimental plots

Figure 26 clearly shows that highest soil loss occurred at Plot 1 (with SWC). At Plot 2, the second plot with soil conservation measure, nearly no soil loss occurred. While at Plot 1 cumulative soil loss over the rainy season was 4.7 kg m^{-2}, only 0.3 kg m^{-2} sediments accumulated in the retention basin at Plot 2. Only on August 1st, 2012 considerable amount of sediments were removed from this basin (0.28 kg m^{-2}).

Soil loss from Plot 3 is lower than soil loss from the treated Plot 1, even though it is in the same range. Over the rainy period, cumulative soil loss from Plot 3 is about 3.0 kg m^{-2}.

The length of Plot 3 equals the length of Plot 1 and Plot 2 together. In this sense, Plot 3 and the combination of Plot 1 and Plot 2 can be seen as two transacts as shows Figure 27. Soil loss is in the same range for both transacts. However, most soil loss from the transact with stone bunds comes from Plot 1 (116 kg m^{-1}). Sediment delivery from Plot 2 is low (11 kg m^{-1}). Thus, this result for the weighted average soil loss has to be handled with care.

Plot 2, having the same length as Plot 1, shows much lower soil loss. The soil loss of 0.3 kg m^{-2} and 11 kg m^{-1} over the rainy season 2012 is extremely low compared to 4.7 kg m^{-2} and 116 kg m^{-1} and 3.0 kg m^{-2} and 133 kg m^{-1} for Plot 1 and Plot 3, respectively.

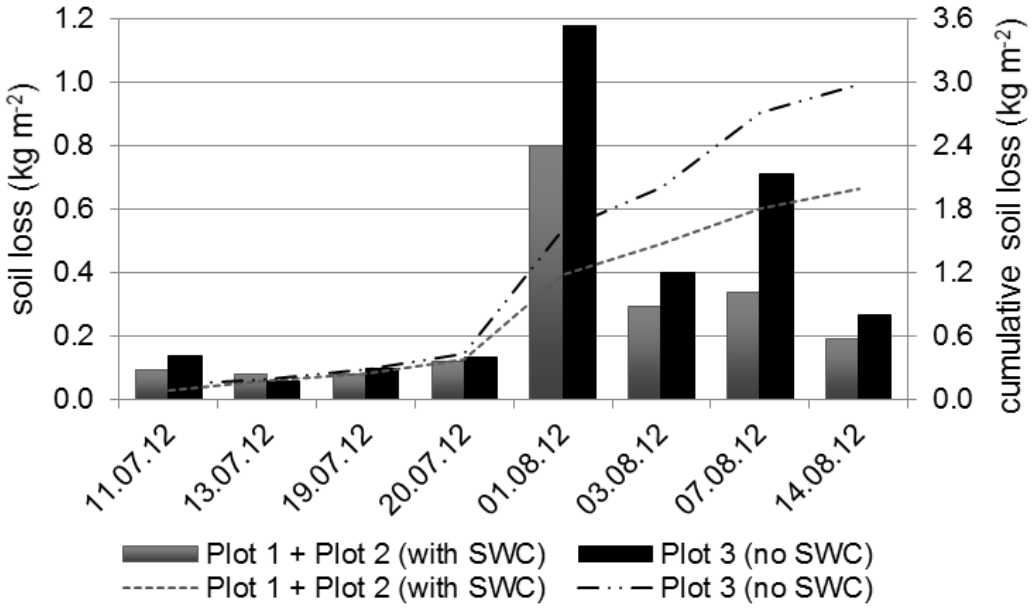

Figure 27: Weighted average soil loss of the two treated plots and Plot 3, separately.

8.5 Discussion of the field work results

Hurni (1988) estimated a mean soil loss rate from arable land of 4.2 kg m^{-2} for the Ethiopian Highlands. However, this value is an average for a bigger scale. Locally soil erosion rates might be significantly higher or lower. For Ethiopia, Gebreyesus and Kirubel (2009) defined a maximum tolerable soil loss of 1.8 kg m^{-2} per year. Thus, observed soil loss is more than twice this maximum tolerable value. However, it can be expected that parts of the eroded soil would deposit in depressions within the sub-catchment and would not leave the watershed. Concerning soil loss monitoring from 2012 it has to be mentioned that monitoring started in the end of June. Sometimes, intensive events occur in the beginning of the rainy season when soils are bare. These events were not monitored during the fieldwork. Additionally, the intensity of rainfall events was low compared to 2011 and 2013. Both facts make ongoing research necessary.

Soil loss measurements showed high variation at the three experimental plots. Comparing the two plots at fields with stone bunds, Plot 1 showed the highest and Plot 2 the lowest soil loss. Soil loss at Plot 1 was 15 times higher than at Plot 2. Plot 1 lay between two subsequent stone bunds and studied the effect of slope reduction by the bunds. An intersecting stone bund divided Plot 2 into an upper and lower part. Considering only the lower part of Plot 2 with a length of approximately 20 m, soil loss still is very low, compared to the second plot under treated conditions.

This significant difference in soil loss rates between Plot 1 and Plot 2 is only explicable by combination of several influencing parameters. One reason for this considerably smaller soil loss of Plot 2 is the higher canopy cover. As shown in 8.3 canopy cover on Plot 2 was double as high as on the other two plots. Figure 28 and Figure 29 show canopy cover at Plot 1 and Plot 2, respectively. Pictures were taken on August 14th 2012. Even though farmers cultivated sorghum and sow in the same time, the development of vegetation cover is completely different at the two plots.

Figure 28: Vegetation cover at Plot 1.

Figure 29: Vegetation cover at Plot 2.

However, the measurements imply that another reason for the low soil loss rate is the deposition of detached material from Plot 2 in the plot area in front of the retention basin. Thus, not all sediments moved downslope to the retention basin. The slope profile of this plot shows a slight elevation at the bottom end, which indicates that sediments deposited in this section. As the survey of the site was conducted only at the end of the rainy season, it is not possible to know if this deposition is due to the construction of the basins or already existed before. This aggravates the evaluation of soil loss from Plot 2.

Plot 3 was the longest plot, situated on fields without soil conservation measure. Soil loss from this plot was in the same range as for Plot 1, but still lower. In the case of Plot 3 the relatively higher rock fragment cover (mean 26 %) compared to the treated plots (mean 14 % and 17 %), might had have a positive effect on the soil erosion process. Especially the heterogeneous distribution of rock fragment cover of Plot 3 with higher fraction at the upper than at the bottom end, affects the soil erosion process. In the upper part, rock fragment cover was high with a mean value of 41 % for the first 15 m. Also for the rest of the slope length, rock fragment cover was higher (18 %) than at Plot 1 (13 %).

a) Effect of rock fragment cover

Stone fragment cover has a retardant effect on soil erosion. This positive effect is a result of several sub-processes, which are affected by rock fragment cover and lead to a reduction of soil erosion. Rock fragments protect the soil surface against raindrop impact and overland flow. Additionally, rock fragments reduce the effect of surface sealing (Poesen and Lavee 1994). Rock fragments retard ponding and slow down surface runoff and thus reduce its detachment and transport capacity (Cerdà 2001; Martínez-Zavala and Jordán 2008).

Especially at the untreated Plot 3, which is the longest soil erosion plot, rock fragment cover was high in the upper part and decreased towards the bottom. This can be reasoned by the fact that soil erodes from the upper part of the hillslope, exposing rock fragments. The selective erosion of fine particles by tillage erosion enforces this effect. While at the bottom part deposited sediments fill up the space between rock fragments and cover them. This second effect is apparent in in the slope profile (see Figure 24), as for all three soil erosion plots the lowest mini-plots showed relatively low rock fragment cover.

Another reason for the higher rock fragment cover at Plot 3 can be that farmers use rock fragments for the construction of the stone bunds from their fields. The higher rock fragment cover on the field without measure might reflect this fact. The lower rock fragment cover on the plots with stone bunds can be explained by the removal of stones for the construction of the bunds (Nyssen et al. 2001).

Nyssen et al. (2001) and Nyssen et al. (2007) showed that removal of rock fragments results in increased erosion rates and hence there exists a negative relationship between soil loss by water erosion and rock fragment cover. On the other hand, high rock fragment cover aggravates tillage and reduces the area available for plants. Hereby, farmers evaluate big stones as particularly disturbing.

b) Effect of infiltration rate

In general, Figure 26 shows that soil loss in the first half of the rainy season is low compared to the second half of the season. This is interesting, as one would expect that highest soil losses occur in the beginning when soils are bare and exposed to the erosive force of the rainfall and surface runoff.

The distribution of soil loss over the rainy season shows a heterogeneous pattern with lower soil erosion in the beginning of the rainy season and higher erosion rates towards the end (see Figure 26). This might be reasoned by the incidence of cracks in the soil. Over the dry season, shrinkage cracks develop due to very low soil moisture content. The cracks close during the first rainfall events as a consequence of swelling effects. It was assumed that these cracks cause a higher infiltration rate in the beginning of the rainy season, which will go down as the cracks start to close. Figure 30 shows cracks at the experimental site, on June 20th. After the first rainfall events, these cracks were not apparent at the soil surface. Nevertheless, these cracks might have a long-lasting effect on the subsurface structure of the soil. Nyssen et al. (2009) observed similar trends. They observed considerable surface runoff one month after the beginning of the main rainy season and not in the beginning of the rainy season when soils are bare and freshly tilled.

Figure 30: Cracks in the soil at the beginning of the rainy season

After the cracks close, infiltration should decrease drastically leading to important runoff. Due to the soil texture at the experimental site (clay 42 %, silt 36 %, sand 22 %), one would expect low hydraulic conductivity and infiltration capacity, which result in high surface runoff. Surprisingly, field measurements by Schürz (2012) showed high hydraulic conductivity at the plots (10^{-4} – 10^{-5} m s^{-1}) over the whole rainy season. Another fact, which supports the assumption of high hydraulic conductivity at the fields, is the filling of the sediment retention basins due to soil water. After rainfall events, when the soil was very wet, the sediment retention basins filled with water. The soil drained into the basins and filled them from bottom to the top.

c) Effect of slope length

As mentioned before, Plot 3 was the longest plot, with a longest distance of 55 m. In comparison, Plot 1 and Plot 2 had a length of 24.5 m and 38 m, respectively (see 8.2 c).

The length of the slope is positively correlated with soil erosion. Longer slopes lead to more accumulated runoff with increased velocity and kinetic energy. Finally, rill erosion starts and ends in the formation of gullies (Roose 1996). In the Universal Soil Loss Equation erosion increases exponentially with the length of the slope with an exponent of 0.5 (Wischmeier and Smith 1965). However, experiments showed that the influence of slope length is not consistent nor particularly strong (Roose 1996).

The theoretical basis of increased soil erosion due to longer hillslope is the ongoing accumulation of surface runoff, which leads to the initiation of rills. Rill erosion can contribute a big part to total soil erosion. Thus, the influence of slope length is linked to the soils sensitivity to rill erosion. In contrast, the increase in sheet erosion is little as the surface roughness controls the velocity of the sheet runoff and keeps it low (Roose 1996).

Surface roughness at the experimental plots was high (see 8.6.7). Signs that indicate the formation of rills at the fields were not visible over the rainy season. Additionally, the analysis of canopy and rock fragment cover (see 8.3) showed that especially in the upper part, rock fragment cover was high at Plot 3. This also might influence soil loss from this plot in the way that the high rock fragment cover in the upper part slowed down the runoff, enhanced infiltration

and reduced the erodibility in this section; hence, compensated the negative effect of the longer slope. This suggests that the impact of the slope length is not very strong at the plots.

d) Effect of the stone bunds

Even though soil loss was highest at the plot with stone bunds, the effect of stone bunds on the retention of sediments has to be stressed. Eroded soil within sections between two stone bunds accumulates behind the bunds and thus sediments are not delivered to the runoff channel and stay in the field. Gebremichael et al. (2005) conducted measurements in Tigray Region, in the Ethiopian Highlands, to assess the effectiveness of stone bunds in controlling soil erosion. He stresses that the introduction of stone bunds reduced annual soil loss by 68 %. Sediments accumulated behind the bunds until they filled up. After some years, the effect decreases if stone bunds are not maintained regularly. Additionally, stone bunds increase the number of boundaries between fields and hinder tillage erosion, which contributes a big part of the downslope movement of the soil. This effect was not measureable with the design in this work. The sediment retention basins of the plots were situated above the stone bunds. Soil loss from Plot 2, with a stone bund intersecting the plot in the middle, was 15 times smaller than soil loss from the two other plots. This cannot be attributed to the effect of the stone bunds. Considering that the intersecting stone bund hold back all sediments coming from above, soil loss at this plot was still one decade below soil loss from Plot 1. However, on-site observations showed that sediments accumulated in the area behind the stone bunds, but sediments also overtopped the bunds as show Figure 31 and Figure 32.

Figure 31: Sediments overtopping the stone bund

Figure 32: Stone bund; the area behind the bund did not fill entirely with sediments yet.

8.6 Results and Discussion of the computer-based modelling

8.6.1 Model sensitivity analysis

The sensitivity analysis describes the model's output response to variation of single parameters. Table 6 shows the sensitivity ratio (SR) for the analysed parameters. It shows that WEPP was sensitive to changes of rock fragment content, rill erodibility, random roughness and hydraulic conductivity and less sensitive to alteration of cation exchange capacity, maximum leaf area index, initial saturation level, canopy cover coefficient and interrill erodibility.

Table 6: Sensitivity analysis for selected parameters

Parameter	Unit	Tested range	Sensitivity Ratio (SR)
rock fragments	%	5 - 55	1.09
rill erodibility	s m^{-1}	0.003 - 0.009	0.82
random roughness	cm	4 - 15	0.68
effective hydraulic conductivity	mm h^{-1}	2 - 400	0.54
cation exchange capacity	meq $(100g)^{-1}$	20 - 35	0.14
maximum leaf area index	-	4 -10	0.07
initial saturation level	%	0 - 100	0.04
canopy cover coefficient	-	6 - 18	0.04
interrill erodibility	kg s m^{-4}	2500000 - 5000000	0.02

Rock fragment cover varied from 5 to 55 % in the field assessment. In these limits rock fragment cover was the most sensitive parameter of all.

If interrill and rill erodibility are known parameters the user can enter them as input parameters. In case of missing information on these parameters, the WEPP model calculates them according to dependencies from other input parameters (see 6.1, d). K_i ranged from 2500000 to 5000000 kg s m^{-4}, with the calculated value of 3740000 kg s m^{-4}. K_r varied between the limits 0.003 and 0.009 s m^{-1} with a calculated value 0.7 s m^{-1}. In this range, the sensitivity ratio was 0.82.

Concerning the random roughness of the surface, Zeleke (2001) used a value of 5 cm for the ox-drawn ard plough. Random roughness was tested in the range of 4 cm to 15 cm and showed a sensitivity ratio of 0.68.

"Baseline" hydraulic conductivity varied from 2 mm h^{-1} to 400 mm h^{-1}. The lower end of the range represents the value suggested by the WEPP model. The very high value of 400 mm h^{-1} on the other side results from measurements by Schürz (2012). Schürz conducted measurements of hydraulic conductivity at the experimental site during the period of observation and found that hydraulic conductivity is unexpectedly high for the given soil texture. He measured values of 300 mm h^{-1}. This range resulted in a sensitivity ratio of 0.54.

This information is the basis for defining the range of variation of the variable parameters rock fragment cover, rill erodibility coefficient, random roughness and "baseline" hydraulic conductivity. It was assumed that all other parameters are either known or not sensitive.

8.6.2 Analysis and definition of the model input

The objective of the modelling was to find a configuration of the model, which is calibrated to local conditions and enables simulation of various scenarios.

Soil loss was simulated for Plot 1 and Plot 3 using the WEPP model. Concerning Plot 2, soil loss was not simulated by the model. The results from the fieldwork showed that high uncertainty lies in the results of this plot. Preliminary tests to model the soil loss process at this plot showed that too little data is available to draw accurate conclusions from a simulation of this plot. In the following, this work concentrated on the configuration of a model setup, which predicts soil loss from the two other plots – without intersecting stone bund – adequately. Information from this work can contribute to the simulation of stone bunds in successive works.

a) Soil input

The soil is built from one layer with a soil depth of 1.5 m. Soil texture was determined from mixed samples for each plot. Variation in soil texture from one plot to the other was negligible and thus soil texture was set to a single value representative for all three plots. Table 7 shows fractions of clay, silt and sand. For the given composition of soil fractions, the soil is defined as a clay soil.

Table 7: Soil texture of the three plots used in the WEPP soil file

Soil texture	Clay [%]	Silt [%]	Sand [%]
Plot 1,2 & 3	42	36	22

Albedo was set to 0.3 as a function of organic matter, which is 1.5 %. According to Flanagan and Livingston (1995) cation exchange capacity (CEC) for clay soils is between 30 – 150 meq $(100g)^{-1}$. Alternatively CEC can be estimated by Equation 13 and results in 24 meq $(100g)^{-1}$.

$$CEC = 0.5 * clay + 2 * organic\ matter$$

Equation 13

Preliminary tests showed that soil loss prediction is slightly better using a CEC value of 24 meq $(100g)^{-1}$.

For soils with clay contents exceeding 40 %, WEPP estimates “baseline” hydraulic conductivity using Equation 5 (see 6.1 d).

Determined clay content at Plot 1 and Plot 2 was about 42 %. Applying Equation 5 to this soil, estimated hydraulic conductivity is 2.2 mm h^{-1}. At Plot 1 Schürz (2012) measured mean hydraulic conductivity of 296 mm h^{-1}, ranging from 204 – 419 mm h^{-1}. Mean hydraulic conductivity at Plot 2 averaged 291 mm h^{-1}, ranging from 194 – 362 mm h^{-1}. These values are high for a loamy clay soil, but measurements were stable over the rainy season. Huge cracks and the fissured structure of the soil affect the infiltration of surface water. To account for this enormous range of hydraulic conductivity and the fact that the model is sensitive to the variation of this parameter, the model ran scenarios with different K_b values. Four different scenarios accounted for the effect of “baseline” effective hydraulic conductivity.

For Plot 1 and 3 K_b was set to 2 mm h^{-1}, 100 mm h^{-1}, 200 mm h^{-1} and 300 mm h^{-1} for sets of simulations, respectively.

Another soil specific factor, which is a sensitive parameter in the model, is the rill erodibility factor. At Plot 1, one set of scenarios used the internally calculated K_r value of 0.007 s m^{-1},

while the other two scenarios used an increased value of 0.009 s m^{-1} and a reduced value of 0.005 s m^{-1}. For Plot 3, a different combination of rill erodibility coefficients was tested. The value of 0.007 s m^{-1} built the upper limit. Two other sets of scenarios included coefficients of 0.003 and 0.005 s m^{-1}.

The initial saturation level represents the saturation level of the soil on January 1st. Due to the precipitation pattern in the study area, saturation level is low in the beginning of the year. In the model, soil water stays at a constant level until the first rainfall occurs, as the model simulates no evaporation from bare soils below a residual moisture content (see 6.1 c). As mentioned before, there was no rainfall data available for the first months of 2012. The rainfall, which occurred in this period, infiltrated into the soil and increased the moisture content of the soil. Due to measurements by Schürz (2012) soil water content in the beginning of precipitation records is known. In order to compensate the lack of rainfall data from January to mid of June, the initial saturation level was adjusted to fit the field measurements and was set to 75 %.

At Plot 1, the mean of all rock fragment cover measurements (13%) was used for the whole hillslope. Due to high variation of rock fragment cover within the mini-plots at Plot 3 with a decrease from top to bottom of the hillslope, two rock fragment cover values were implemented in the model. The soil input interface allows the input of more than one Overland Flow Elements (OFE's). This means, that the hillslope can be divided into more sections with different soil properties. Thus, for the upper 15 m rock fragment cover was set to 41 % and to 18 % for the rest of the hillslope (30 m). 41 % and 18 % are the mean values for mini-plot 1 -7 and 8 – 20, respectively. Rock fragment cover is also a sensitive parameter for the model. Thus, the measured values varied in different scenarios with an increase and decrease of 3 % for each plot.

b) Management input

Over the period of one year, the management input file lists management operations chronologically. Table 8 gives an overview on the management in 2012. Starting point is the initial condition of the fields on January 1st.

Table 8: Chronology of Operation Types

MANAGEMENT
Rotation

Date	Operation Type
01.01.2012	Initial Conditions
10.02.2012	Primary Tillage
10.05.2012	Secondary Tillage
01.06.2012	Plant – Annual (Sorghum)
15.12.2012	Harvest – Annual (Sorghum)

Each operation type is specified in a separate file. The detailed list of input parameters for all management steps are given in the Annex.

The initial condition file describes the actual situation on January 1st, before the beginning of the experiment. Initial plant is tef, a traditional crop, which farmers cultivated during the

cropping season 2011. Tef was harvested in the end of November 2011. Last tillage operation was before sowing tef in June. Initial rill and interrill cover was set to zero.

Farmers tilled their fields twice before planting sorghum in 2012. Primary tillage was in February, while secondary tillage was in May. Tillage implement is a tradition ox-drawn ard plough, called *maresha*, which is used for both, primary and secondary tillage (see Figure 33 and Figure 34). Tillage depths were set to 12 cm and 10 cm for primary and secondary tillage, respectively. Ridge height (12 cm) and ridge interval (35 cm) were higher in primary tillage, which leaves 70 % of the surface area disturbed. Ridge height after secondary tillage was 10 cm. The ridge interval reduced to 25 cm. After secondary tillage, 100 % of the area is disturbed. Zeleke (2001) analysed the applicability of WEPP for runoff and soil loss prediction in the Ethiopian Highlands. In this work, similar values were used for tillage depth, ridge height and ridge interval and surface disturbance. In this work Zeleke (2001) used random roughness values for the ox-drawn ard plough between 4.5 and 5.5 cm. The simulation included four sets of scenarios with random roughness values of 5 cm, 8 cm, 11 cm and 14 cm.

Figure 33: Farmer in the study area ploughing his field using the *maresha* plough

Figure 34: wedge-shaped metal share of the *maresha* plough © (Nyssen et al. 2000)

In 2012 farmers cultivated sorghum at the plots. Sowing is in the beginning of June. WEPP contains plant files for sorghum under different fertilization levels. The file Sorghum – Low

Fertilization Level was used as draft and was adapted to local conditions. According to the farmers, maximum canopy height is 1.8 m. In the study area, sorghum is not planted in-row, but in an irregular pattern. Hence, the default row width was reduced to 15 cm, while the in-row plant spacing was slightly increased (15 cm).

The canopy cover coefficient (BBB), a crop-dependent parameter, describes the relationship between canopy cover and vegetative biomass. By increasing the parameter, the canopy cover will increase as a function of biomass. As second plant specific parameter, which influences the evolution of canopy cover over the cropping season is the maximum leaf area index (XMXLAI). It exist canopy cover records from July 25th, 2012, as described in 7.5. By running the model with different canopy cover coefficients and maximum leaf area indices, canopy cover can be altered until observed and simulated values coincide. Two ratios between canopy cover coefficient and maximum leaf area index are leading to the same canopy cover on the observation day. Preliminary tests showed that the ratio with lower BBB and higher XMXLAI leads to higher erosion rates in the end of the rainy season. This coincides better with field observations. As both parameters are not sensitive for the soil loss prediction, only one scenario with a BBB of 12 and the corresponding XMXLAI of 8 ran in the simulation of Plot 1. For Plot 3 this ratio was slightly different, with BBB 11 and XMXLAI 8.

8.6.3 Model scenarios

a) Plot 1 (plot with stone bunds at the upper and lower limits):

According to the variation of input parameters described in the previous section 8.6.2, soil loss for Plot 1 was calculated for 144 scenarios. Table 9 shows the variable input parameters in short.

Table 9: Overview of variable input parameters for Plot 1

Rill erodibility coefficient (RE)	0.005, 0.007, 0.009 s m^{-1}
Rock fragment cover (RO)	10, 13, 16 %
Random roughness (RR)	5, 8, 11, 14 cm
Baseline hydraulic conductivity (K_b)	2, 100, 200, 300 mm h^{-1}

b) Plot 3 (plot without stone bunds)

Soil loss simulation of Plot 3 included 144 scenarios. Values of the variable parameters shows Table 10.

Table 10: Overview of variable input parameters for Plot 3. * The first values stands for rock fragment cover in the upper 15 m, the second value for rock fragment cover at the rest of the plot.

Rill erodibility coefficient (RE)	0.003, 0.005, 0.007 s m^{-1}
Rock fragment cover (RO)	38/15, 41/18, 44/21* %
Random roughness (RR)	5, 8, 11, 14 cm
Baseline hydraulic conductivity (K_b)	2, 100, 200, 300 mm h^{-1}

8.6.4 WEPP soil loss prediction: Plot 1

Three objective functions, the root mean square error (RMSE), model efficiency function (NSE) and the coefficient of determination (R^2) proved the goodness of fit of each simulation scenario.

a) Objective functions

In the simulation of Plot 1, the development of all three functions was identical, which means that the ranking due to each function resulted in the same order of the scenarios. Out of all 144 scenarios, 14 had a model efficiency of zero or more. This means, that the model is the better predictor than the mean of the observed data. For the same 14 scenarios, the coefficient of determination was 0.90 or more and the mean root square error was below 0.5. Within these scenarios, 12 of 14 had a rill erodibility coefficient of 0.005 s m^{-1}, which is the lowest of the three tested values. The three other parameters occurred in more variations. Concerning random roughness, values of 8, 11 and 14 cm led to good objective functions; only the lowest value of 5 cm did not occur within the best simulation runs. Rock fragment cover existed in all its variations 10, 13 and 16 % within these 14 scenarios. Hydraulic conductivity ranged from 100 – 300 mm h^{-1}. Figure 35 shows the frequency of each parameter value graphically.

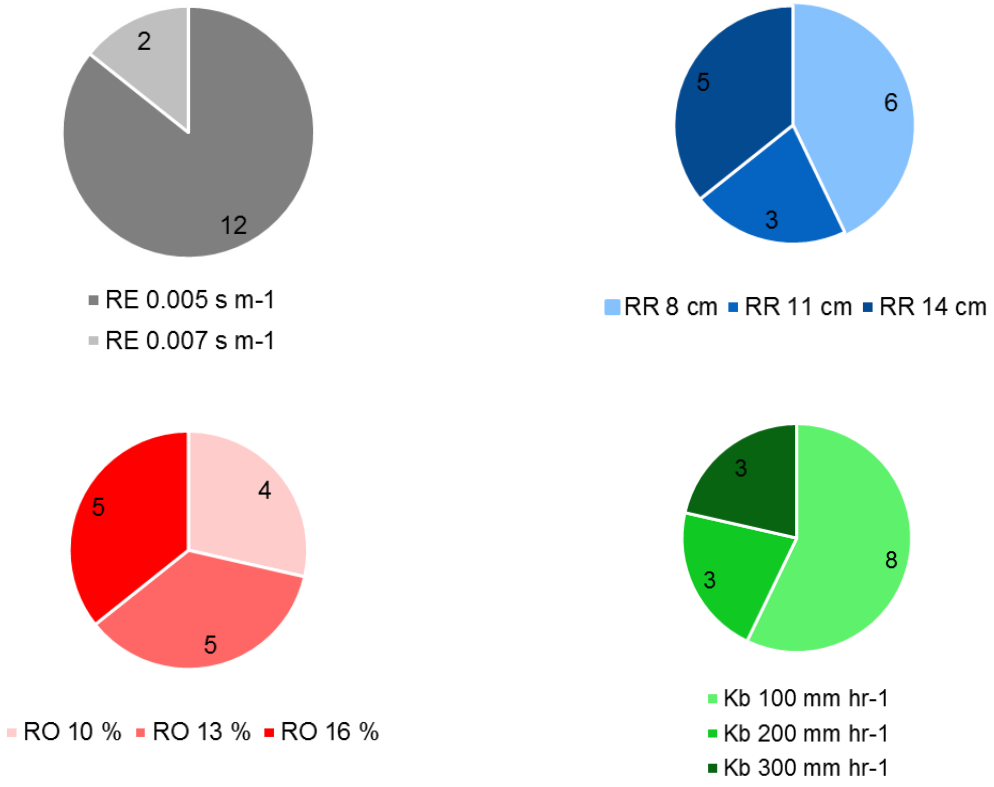

Figure 35: Frequency of each parameter value among the simulations with the best objective function results for Plot 1 (low RMSE, high NSE and R^2). RE = rill erodibility, RR = random roughness of the surface, RO = rock fragment cover, K_b = "baseline" hydraulic conductivity.

On the other hand, the scenarios with the poorest fit between observed and predicted soil loss had low hydraulic conductivity values in common. From the 14 simulation (10 %) with the worst objective function values (high RMSE, low NSE and R^2) 13 simulations ran with a hydraulic conductivity of 2 mm h^{-1}. Rock fragment cover again occurred in all combinations. While rill erodibility showed a tendency to higher values (0.007 and 0.009 s m^{-1}), random roughness

showed a reverse tendency to lower values (5 and 8 cm). This distribution of the parameters shows Figure 36.

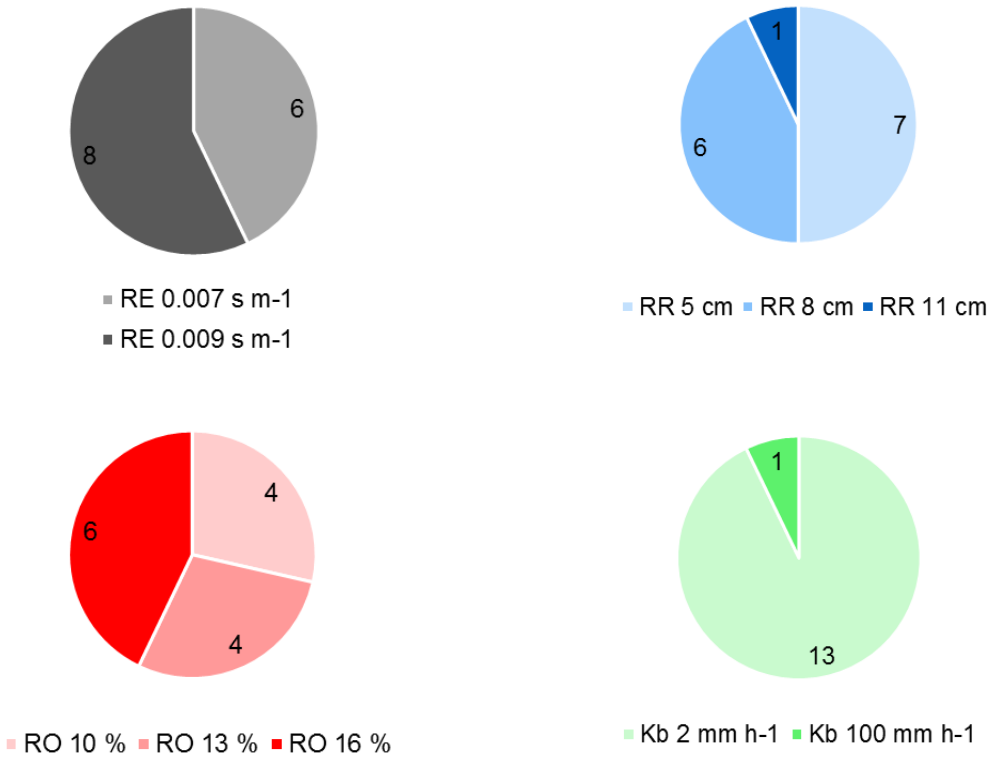

Figure 36: Frequency of each parameter values among the simulations with the worst objective function results for Plot 1 (high RMSE, low NSE and R^2). RE = rill erodibility, RR = random roughness of the surface, RO = rock fragment cover, K_b = "baseline" hydraulic conductivity.

The analysis of the objective functions shows that low values of hydraulic conductivity coincide with poor accordance of predicted and observed soil loss, while the low rill erodibility coefficient leads to the best results concerning the quality of fit between observed and predicted data.

b) Confidence interval

Predicted soil loss ranged from 2.0 kg m^{-2} to 18.6 kg m^{-2} for all simulation runs. These two boundary values result from the superposition of extreme parameter values for all variable parameters, which have the same effect on soil erosion. For the analysed parameters, all combinations were tested. Thus, scenarios with low hydraulic conductivity, rock fragment cover, and random roughness and high rill erodibility delivered very high soil loss rates. The vice versa case led to very low soil loss prediction. Histograms represent the distribution of data by showing the frequency of data classes. Using the statistic software "R", histograms showed the distribution of predicted soil loss for all observation days. Except for two days, soil loss is approximating a normal distribution, even though with pronounced skewness. The introduction of a confidence interval should help to eliminate the effect of superposition of parameter values, which lead to unlikely results as described above. The 2,5 % and 97,5 % quintile delimit the 95 % confidence interval. Figure 37 shows the area, which forms between the quintiles and observed soil loss for each day of removal.

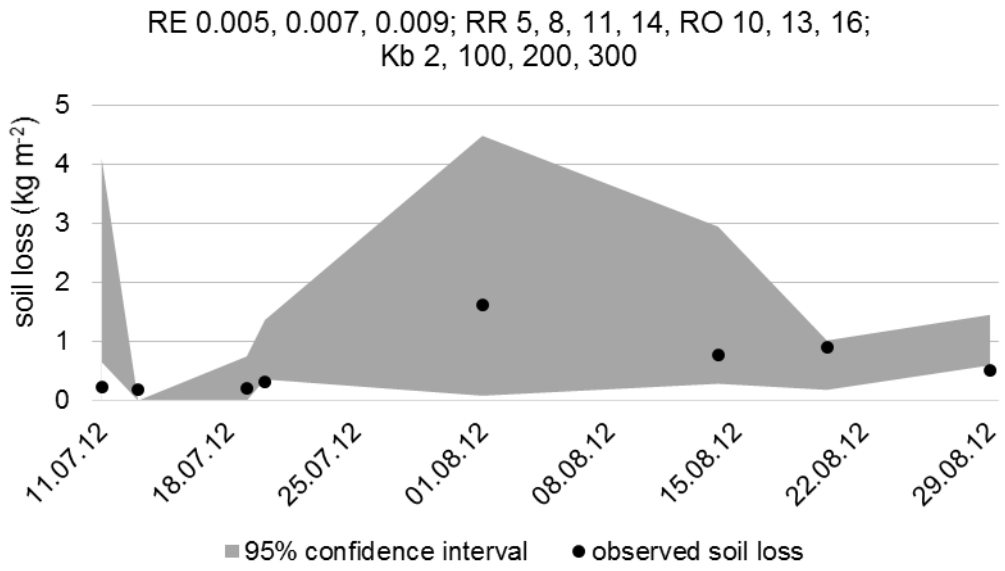

Figure 37: Simulated soil loss of Plot 1 with a 95 % confidence interval and measured values for all days of sediment removal and all combinations of parameters.

It was already clear from the analysis of the objective functions (8.6.2 a) that low agreement of measured and predicted soil loss is linked to low hydraulic conductivity and high rill erodibility coefficients. Two further bands of confidence intervals showed that the range in the confidence interval decreases by eliminating all scenarios with hydraulic conductivity of 2 mm h^{-1} and a rill erodibility coefficient of 0.009 s m^{-1}. The observed soil loss of 0.9 kg m^{-2} on 20th August 2012 left the confidence interval. For five days of removal, 13th, 19th, 20th July and 20th, 29th August 2012 the variance in the scenarios is low, which means that the confidence interval is narrow. On July 13th and 20th as well as August 29th the observed soil loss lies outside this interval but very close to it.

Still, the 95 % confidence interval built a wide band of simulation results. In further steps, the analysis of the development of the confidence interval intended to spot those parameters whose removal leads to a reduction of the area between the quintiles so that still the same amount of measurement points lies within the confidential range.

Random roughness of 5 cm did not appear in the best simulation results with positive model efficiency and a coefficient of determination above 0.9. Its removal led to a reduction of the confidential band. The elimination of the WEPP suggested value of the rill erodibility coefficient (0.007 s m^{-1}) narrowed the range of predictions even more. Then the only value of this parameter was 0.005 s m^{-1}. As all parameters, which result in too high soil loss by trend, were removed, the confidence interval shifted to lower values, as shows Figure 38.

In a last step, the removal of parameter combinations, which led to very low soil loss predictions, random roughness of 14 cm and hydraulic conductivity of 300 mm h^{-1}, led to the narrowest range of predicted soil loss for each day of removal. Even though, the area between the confidence interval decreased with every eliminated parameter value, the number of observations in this area stayed the same.

Figure 38 shows the change of the 95 % confidence interval due to a reduction of the parameter range of the four parameters rill erodibility, random roughness and hydraulic conductivity. The widest band of the confidence interval results from the analysis of all scenarios; the narrowest

band includes only those parameter values with the best accordance between observed and predicted soil loss (see Figure 39).

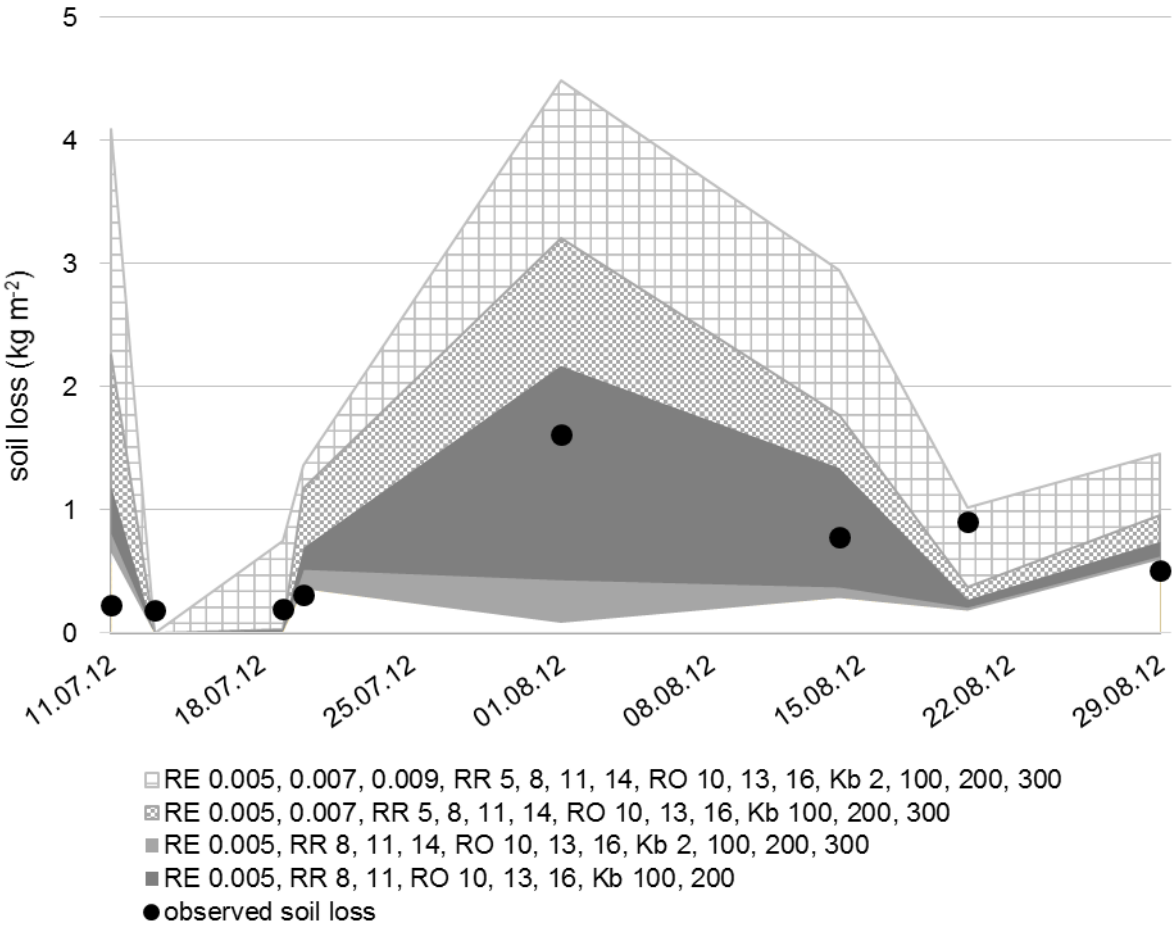

Figure 38: 95 % confidence interval of soil loss prediction and measured values for all days of sediment removal at Plot 1. Beginning from the combination of all scenarios, the interval decreases as some parameter values were eliminated from the analysis. Stepwise, scenarios that led to very high or low soil loss prediction were removed and thus the confidence interval narrowed. RE = rill erodibility, RR = random roughness of the surface, RO = rock fragment cover, K_b = "baseline" hydraulic conductivity

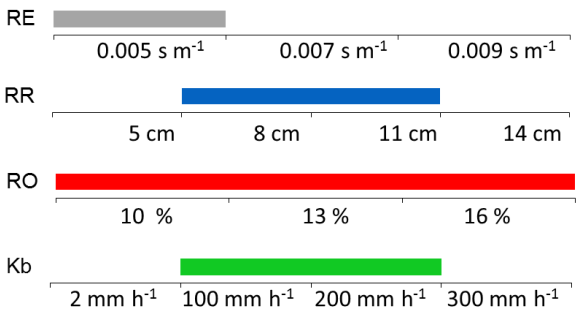

Figure 39: Range of parameter values, which remained in the set of scenarios leading to the narrowest confidence interval for Plot 1

The remaining parameter values are those, which performed best in simulating observed soil loss. The rill erodibility coefficient was lower than the value suggested by the model. Random roughness lay in the range of 8 to 11 cm. Rock fragment cover had little influence on the

simulation results; all three values led to good predictions. Hydraulic conductivity showed best results with values of 100 mm h^{-1} and 200 mm h^{-1}.

Twelve scenarios remained; six of these had positive model efficiency values. For all, the coefficient of determination ranged from 0.86 to 0.93, model efficiency from - 0.46 to 0.32 and the root mean square error from 0.38 to 0.56. Table 11 shows a list of the scenarios, which remained in the set of simulations.

Table 11: Measured and observed soil loss rates and objective functions of the remaining parameter value for the simulation of soil loss at Plot 1.

Scenario	Meas. soil loss (kg m^{-2})	obs. soil loss (kg m^{-2})	RMSE	ME	R^2
RE 0.005,RR 11,RO 16%,Kb 100	4.7	4.84	0.38	0.32	0.93
RE 0.005,RR 11,RO 13%,Kb 100	4.7	4.79	0.38	0.32	0.93
RE 0.005,RR 11,RO 10%,Kb 100	4.7	4.38	0.39	0.29	0.93
RE 0.005,RR 8,RO 10%,Kb 200	4.7	5.24	0.42	0.16	0.92
RE 0.005,RR 8,RO 13%,Kb 200	4.7	5.38	0.44	0.12	0.91
RE 0.005,RR 8,RO 16%,Kb 200	4.7	5.60	0.45	0.05	0.91
RE 0.005,RR 8,RO 10%,Kb 100	4.7	6.01	0.48	-0.08	0.89
RE 0.005,RR 8,RO 13%,Kb 100	4.7	6.25	0.51	-0.20	0.88
RE 0.005,RR 8,RO 16%,Kb 100	4.7	6.44	0.53	-0.29	0.87
RE 0.005,RR 11,RO 16%,Kb 200	4.7	3.09	0.55	-0.42	0.86
RE 0.005,RR 11,RO 13%,Kb 200	4.7	3.02	0.55	-0.43	0.86
RE 0.005,RR 11,RO 10%,Kb 200	4.7	2.95	0.56	-0.46	0.86

8.6.5 Best simulation scenario: Plot 1

Next to soil loss prediction, WEPP models additional output for each scenario. This additional information is presented for the scenario with a rill erodibility of 0.005 s m^{-1}, random roughness of 11 cm, rock fragment cover of 13 % and Kb of 100 mm h^{-1}.

a) Predicted surface runoff

In the time of observation, precipitation was 817 mm. Of this rainfall, the model calculated a surface runoff of 164 mm. This leads to a rainfall – runoff ration of 20 %, which is relatively low.

b) Predicted soil loss

Predicted soil loss is 4.8 kg m^{-2}, while measured soil loss was 4.7 kg m^{-2}. According to the simulation, there is no deposition zone along the whole hillslope profile but all net detached sediments leave the profile at the lowest point. Figure 40 shows the spatial distribution of soil loss over the profile. As shows Figure 20 in section 8.2 c, Plot 1 has a slightly undulating profile, with small local elevations and sinks. Between these two formations develop steeper slopes than the mean slope. The part with relatively high erosion rates (around 17 kg m^{-2}) is located in a transition between a high and low point and close to the end of the hillslope where runoff already gained considerable erosive forces. Besides this outlier, from a distance of about 8 m the erosion rate increases linearly with the slope length. The up and down of erosion rates in the first 8 m causes also the sequencing of sections with steeper and more gentle slope.

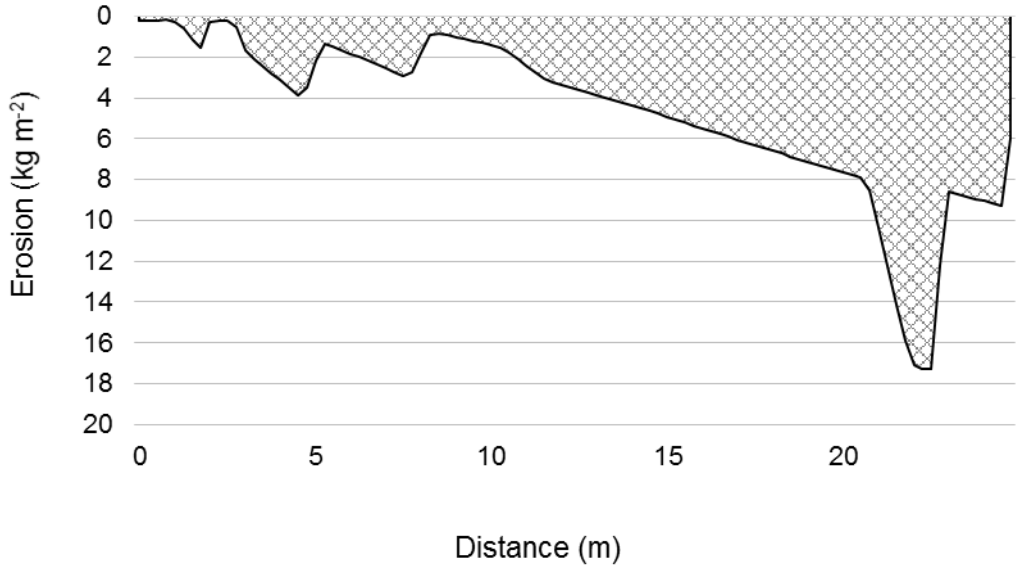

Figure 40: WEPP soil loss graph of Plot 1.

Figure 41 shows the direct comparison of measured and observed soil loss for every day of removal. No tested scenario was capable of predicting soil loss of the first event on July 11th 2012 adequately. The analysis of all events showed that there is a systematic error in the prediction of the first event. On July 13th 2012, sediments were removed for the second time. The sediments resulted from a rainfall event in the night from 11th to 12th of July. Due to a very low peak runoff rate and a rainfall duration, WEPP predicted runoff but no soil loss. The same situation occurred on July 19th. Beginning from this day, predicted and observed soil loss fit fairly well, with an exception of August 20th. The accumulated sediments eroded in a rainfall event on July 17th. WEPP under-predicted soil loss for this event.

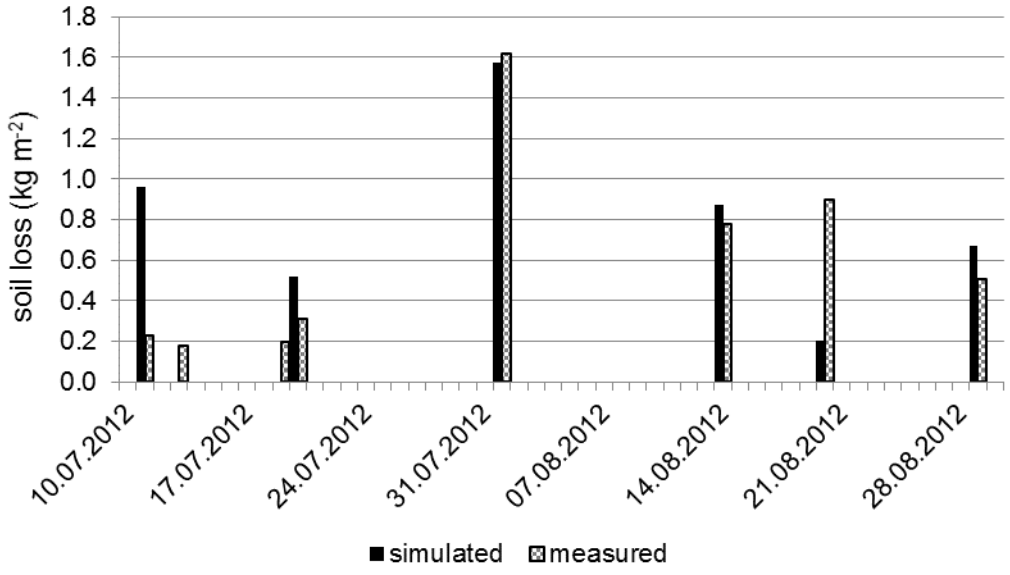

Figure 41: Comparison of observed and simulated soil loss of Plot 1 for all days of removal

c) Canopy cover and height

Sorghum seeding was on June 1st 2012. On June 28th 2012, crop height was 1 cm. Both parameters, canopy cover and height, then developed until they reached a maximum value before senescence of the plant starts and canopy cover decreases. At the end of the cropping season before harvesting at December 15th 2012, sorghum was around 1.25 m high and had a canopy cover of 0.83.

d) Predicted sorghum yield from the cropping season 2012

Predicted sorghum yield is 2.0 t ha^{-1}, which is too high in relation to the actual yield of 0.8 t ha^{-1} from 2012. Farmers reported that average sorghum yield at the experimental site reaches up to 2 t ha^{-1} but was low in the observed cropping season. The definition of the canopy cover coefficient and maximum leaf area index plays an important role for the development of the seasonal crop yield. As described in 7.7.3 d) two different ratios of these two parameters lead to the same canopy cover at the day of canopy cover determination at the field. Running the same model with all parameters as they are but changing this ratio from BBB 12 and XMXLAI 8 to BBB 17 and XMXLAI 5 the yield drops to 0.9 kg m^{-2}, while soil loss stays at a level of 4.5 kg m^{-2}. Too little information exists for these parameters at the experimental site, to exclude one of the two possible values. However, the effect on soil loss and runoff prediction is low (see 8.6.1).

e) Development of the parameters random roughness, rill erodibility, and hydraulic conductivity

The scenarios ran with four variable input parameters, of which three show a development over time – random roughness, rill erodibility coefficient, hydraulic conductivity. Rock fragment content of the soil does not change WEPP internally over time. For the other three input parameters the model uses the user input value and adapts it automatically as a function of cumulative rainfall, surface cover, roots and sealing and crusting.

As described in 6.1 d) random roughness is negatively correlated with the amount of cumulative rainfall and thus decreases while cumulative rainfall increases. This can cause problems with high rock fragment cover in the soil. Figure 42 shows this opposing trend of random roughness and rainfall accumulation.

The adjustment of the “baseline” hydraulic conductivity is a function of cumulative rainfall and of the development of canopy cover and residues. As shows Figure 43, hydraulic conductivity increased to its maximum value of 100 mm h^{-1} after the first tillage operation and stayed at this high value until July 8th 2012. At this day, hydraulic conductivity decreased drastically to only 2 mm h^{-1}. July 8th 2012 was the first day when surface runoff and soil erosion occurred. Hydraulic conductivity oscillated between 100 mm h^{-1} and 2 mm h^{-1} for the first runoff events and reached 100 mm h^{-1} at July 21st 2012 for the last time. After this, it ranged from 2 mm h^{-1} and 40 mm h^{-1} during the observation time.

Figure 44 shows the development of the rill erodibility factor, adjusted on a daily base due to ground cover, roots, incorporated residues, crusting and sealing of the surface.

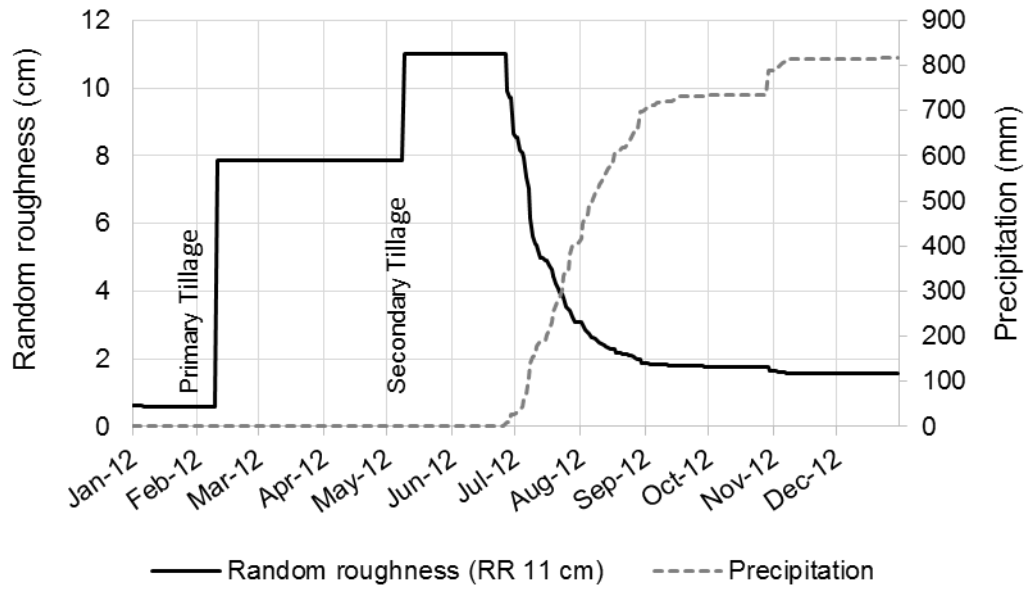

Figure 42: Development of random roughness and rainfall accumulation for Plot 1, where input random roughness is set to 11 cm.

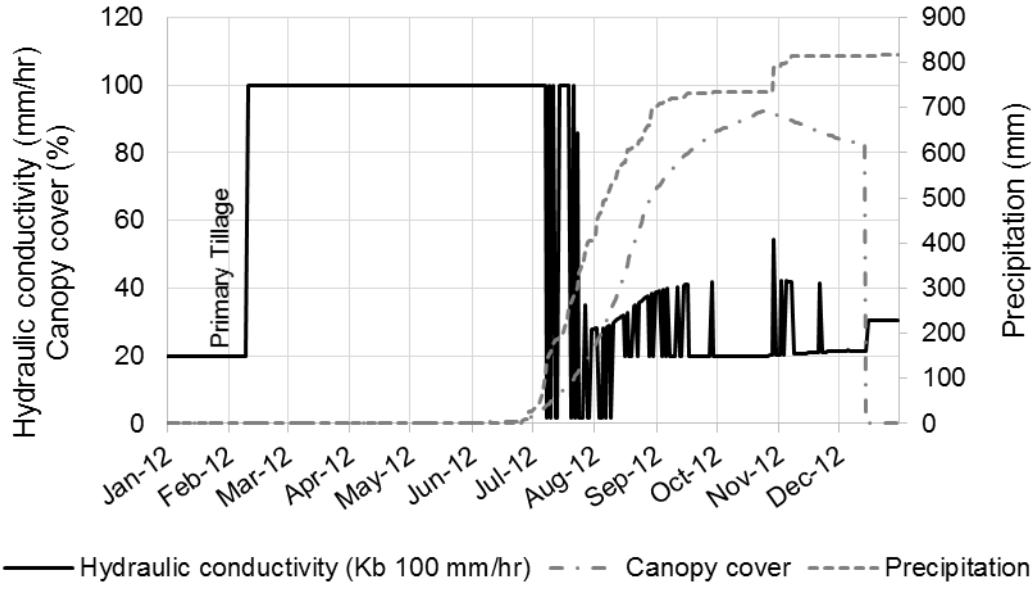

Figure 43: Development of hydraulic conductivity and opposing development of canopy cover and cumulative rainfall for Plot 1.

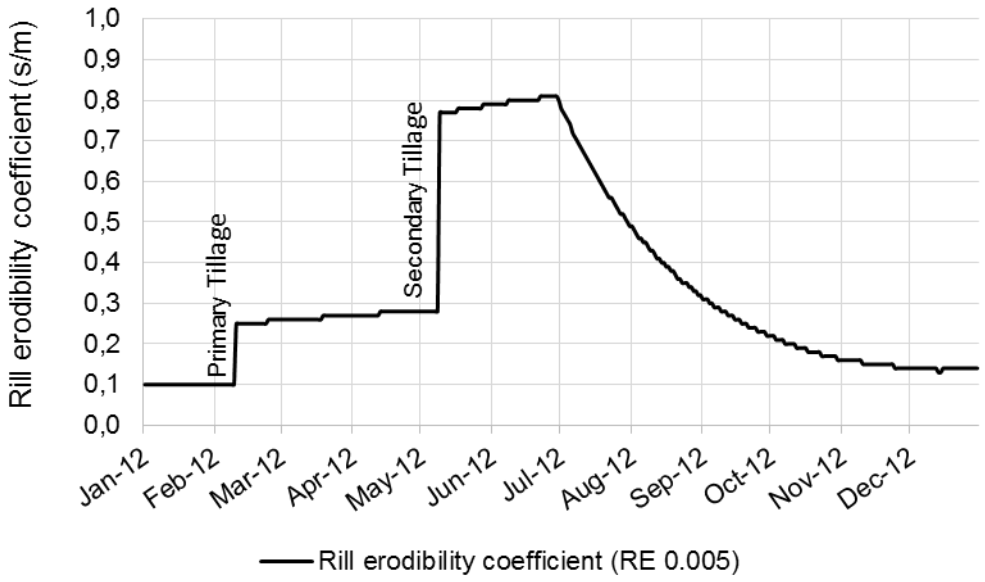

Figure 44: Development of rill erodibility coefficient over time.

8.6.6 WEPP soil loss prediction: Plot 3

In 144 scenarios the four sensitive input parameters varied within certain limits. Random roughness and hydraulic conductivity had the same range as for Plot 1 (RR 5, 8, 11, 14 cm and Kb 2, 100, 200, 300 mm h^{-1}). Rock fragment cover had two values, which represent the percentage of rock fragments in the upper and lower part of the plot separately according to field measurements (38/15, 41/18, 44/21 %). Rill erodibility had a lower range than at Plot 1 (0.003, 0.005, 0.007 s m^{-1}).

a) Objective functions

In the simulation of Plot 3 the development of all three functions was identical, which means that the ranking due to each function resulted in the same order of the scenarios. 10 of all 144 scenarios had a positive model efficiency (NSE), which means, that the model is the better predictor than the mean of the observed data. For the same 10 scenarios, the coefficient of determination ranged from 0.72 to 0.82 and the mean root square error was below 0.35. Within these scenarios, 9 of 10 had a rill erodibility coefficient of 0.003 s m^{-1}. Hydraulic conductivity values were 100 mm h^{-1} and 200 mm h^{-1}. Concerning random roughness, only the two high values, 11 cm and 14 cm, appeared in these 10 best results. Rock fragment cover occurred in all variations. Figure 45 shows the frequency of each parameter value graphically.

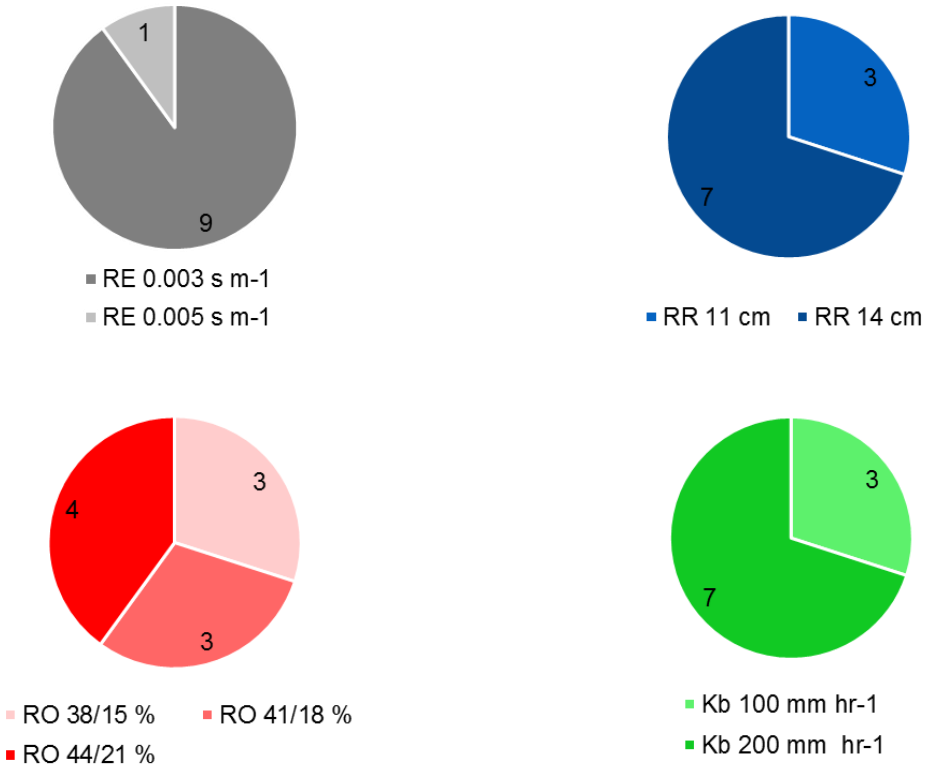

Figure 45: Frequency of each parameter value among the simulations with the best objective function results for Plot 3 (low RMSE, high NSE and R^2). RE = rill erodibility, RR = random roughness of the surface, RO = rock fragment cover, K_b = "baseline" hydraulic conductivity.

In contrast, low hydraulic conductivity had a dominant effect on the worst results of the three objective functions. All of the 14 simulation (10 % of all simulation runs) with the highest RMSE and lowest NSE and R^2 ran with a hydraulic conductivity of 2 mm h^{-1}. In trend, higher rill erodibility and lower random roughness led to less accordance of the prediction with the

observed data. Figure 46 shows for each parameter the number of parameter values occurring amongst the scenarios with the least accordance with observed soil loss.

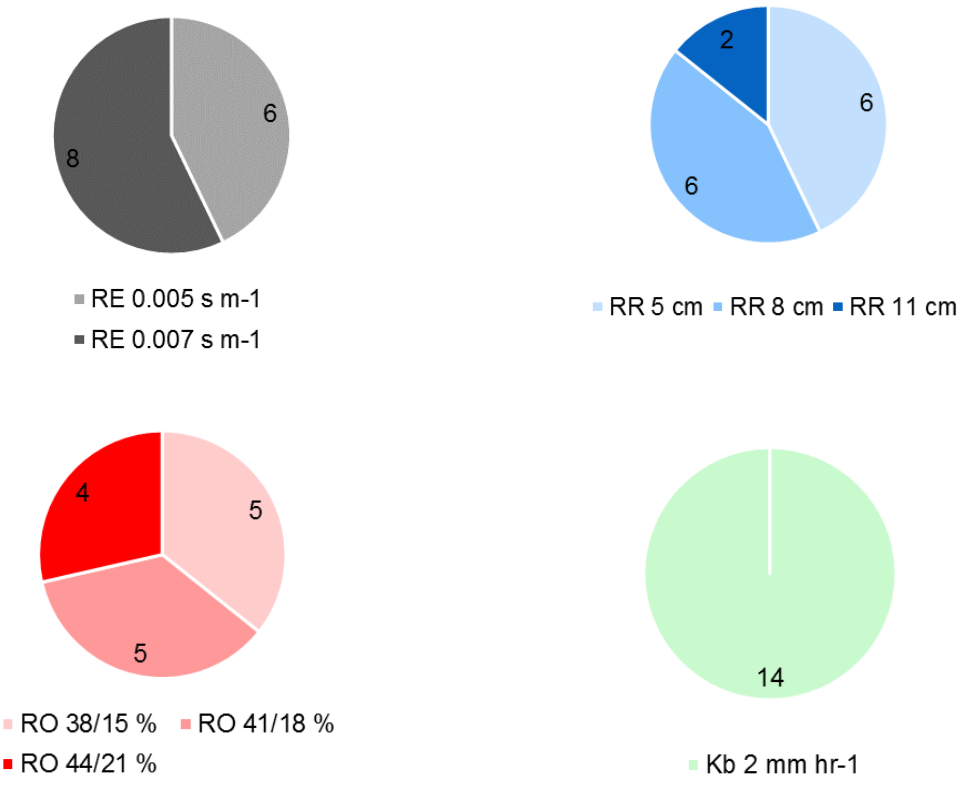

Figure 46: Frequency of each parameter value among the simulations with the worst objective function results for Plot 3 (high RMSE, low NSE and R^2). RE = rill erodibility, RR = random roughness of the surface, RO = rock fragment cover, K_b = "baseline" hydraulic conductivity.

b) Confidence interval

In general, soil loss in all simulations varied between 1.8 kg m^{-2} to 30.8 kg m^{-2}; thus, the variance in the results was high. The 95 % confidence interval shows the range of predicted soil loss for each day of removal of soil loss in the field without the influence of outliers on both sides. It shows that especially for August 1st 2012 the variation in prediction is high. This is because the time span from the previous field day, 20th July 2012, is relatively long and thus more events added up in between the two days of removal. The last observed event lies outside this confidence interval – all simulation runs over-estimated soil loss for this day. Using the statistic software "R", histograms showed the distribution of predicted soil loss for all observation days. Except for July 13th, soil loss is approximating a normal distribution. On July 13th, no scenario simulated soil loss. Figure 47 shows the 95 % confidence interval for all tested scenarios as well as observed soil loss.

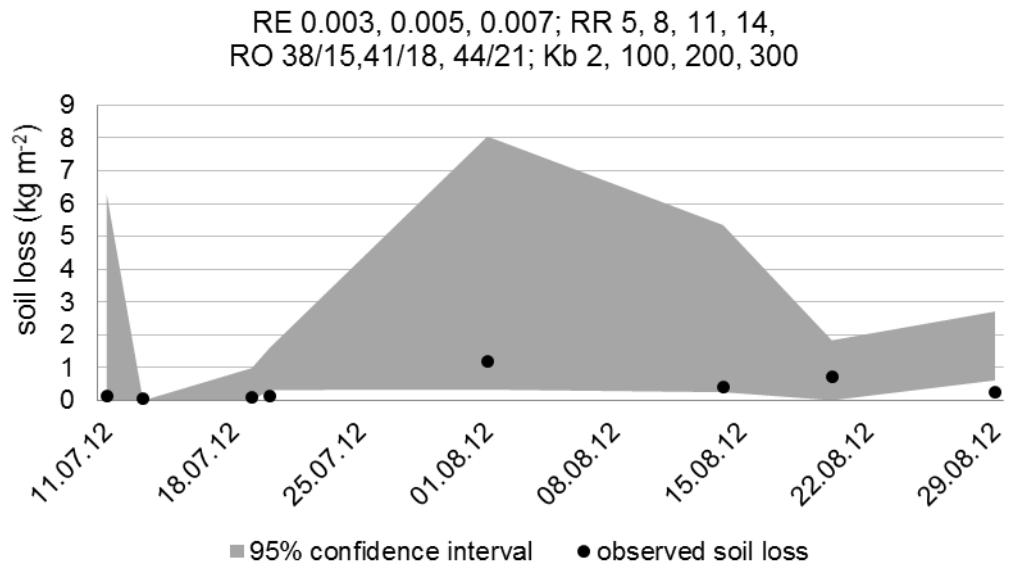

Figure 47: Simulated soil loss of Plot 3 with a 95 % confidence interval and measured values for all days of sediment removal and all combinations of parameters.

In a next step the parameter values, which did not occur in the best scenarios as described in 8.6.2 a), were removed from the simulation analysis. The confidence interval without a hydraulic conductivity of 2 mm h^{-1} and a rill erodibility coefficient of 0.007 s m^{-1} reduced drastically and narrowed the range of predicted soil loss. Removing the low random roughness values of 5 cm and 8 cm scaled down the range of the 95 % confidence interval even more. Consequently, soil loss from August 20th 2012 was under-estimated by the model and left the confidence interval. All the other days of removal stayed in the same relation to the confidence interval as for the interval considering all parameter combinations.

Hydraulic conductivity of 300 mm h^{-1} did not lead to good agreement between measured and simulated values and thus was eliminated from the input options. By removing the rill erodibility coefficient of 5 s m^{-1} the area between the 2.5 % and 97.5% quintiles further decreased. Figure 48 shows the decrease of the area between the 2.5 % and the 97.5 % quintile due to the reduction of possible input parameter values and scenarios. The narrowest band includes only those parameter value combinations (see Figure 49), which led to a good fit between observed and simulated soil loss.

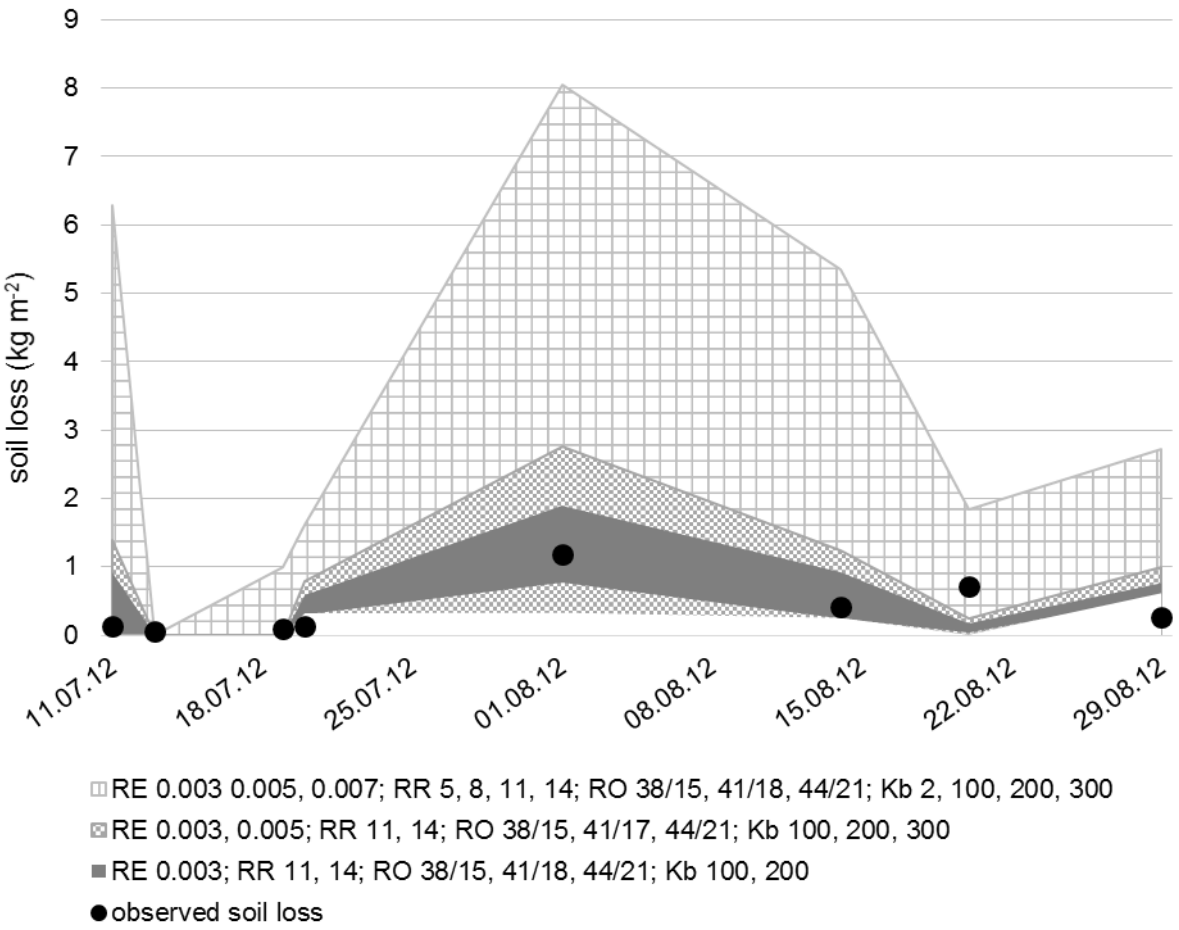

Figure 48: 95 % confidence interval of soil loss prediction and measured values for all days of sediment removal at Plot 3. Beginning from the combination of all scenarios, the interval decreases as some parameter values were eliminated from the analysis. Stepwise, scenarios that led to very high or low soil loss prediction were removed and thus the confidence interval narrowed. RE = rill erodibility, RR = random roughness of the surface, RO = rock fragment cover, K_b = "baseline" hydraulic conductivity

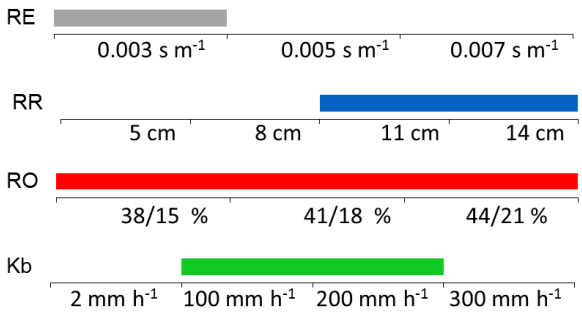

Figure 49: Range of parameter values, which remained in the set of scenarios leading to the narrowest confidence interval for Plot 3.

According to this analysis of influential parameters and their best fitting values of the tested range, best results coincide with a low rill erodibility coefficient (0.003 s m^{-1}), high random roughness (11 cm and 14 cm) and hydraulic conductivity of 100 mm h^{-1} and 200 mm h^{-1}. The effect of rock fragment cover is not significant. Table 12 shows a list of the scenarios, which remained in the set of simulations.

Table 12: Measured and observed soil loss rates and objective functions of the remaining parameter value for the simulation of soil loss at Plot 3.

Scenario	meas. soil loss (kg m^{-2})	obs. soil loss (kg m^{-2})	RMSE	ME	R^2
RE0.003,RR11,R4118,Kb200	3.0	2.86	0.28	0.40	0.82
RE0.003,RR11,R3815,Kb200	3.0	3.12	0.28	0.39	0.82
RE0.003,RR14,R4421,Kb100	3.0	2.79	0.29	0.38	0.82
RE0.003,RR14,R3815,Kb200	3.0	2.89	0.29	0.35	0.81
RE0.003,RR14,R4118,Kb100	3.0	3.03	0.29	0.35	0.81
RE0.003,RR14,R3815,Kb100	3.0	3.24	0.30	0.31	0.80
RE0.003,RR14,R4118,Kb200	3.0	2.80	0.31	0.29	0.79
RE0.003,RR11,R4421,Kb200	3.0	3.12	0.34	0.14	0.75
RE0.003,RR14,R4421,Kb200	3.0	1.76	0.35	0.06	0.72
RE0.003,RR11,R4421,Kb100	3.0	4.42	0.44	-0.46	0.57
RE0.003,RR11,R4118,Kb100	3.0	5.07	0.51	-0.94	0.43
RE0.003,RR11,R3815,Kb100	3.0	5.30	0.53	-1.10	0.39

8.6.7 Best simulation scenario: Plot 3

Next to soil loss prediction, WEPP models additional output for each scenario. This additional information is presented for the scenario with a rill erodibility of 0.003 s m^{-1}, random roughness of 11 cm, rock fragment cover of 41 % at the upper part and 18 % at the lower part. Hydraulic conductivity is 200 mm h^{-1}.

a) Predicted surface runoff

From 817 mm precipitation, the model calculates runoff of 126 mm. Thus, it results a rainfall – runoff ration of 15 %, which is most properly under-estimating actual runoff. High rock fragment mainly causes this low rainfall – runoff ratio.

b) Predicted soil loss

Predicted soil loss is 2.8 kg m^{-2}, while observed soil loss was 3.0 kg m^{-2}. As for Plot 1, no deposition zone developed. As shows Figure 50, in the upper section soil loss is relatively low as the rock fragment cover is high. At a 15 m distance from the top of the hillslope rock fragment cover drops from 41 % to only 18 % as the determination of rock fragment cover in the field showed.

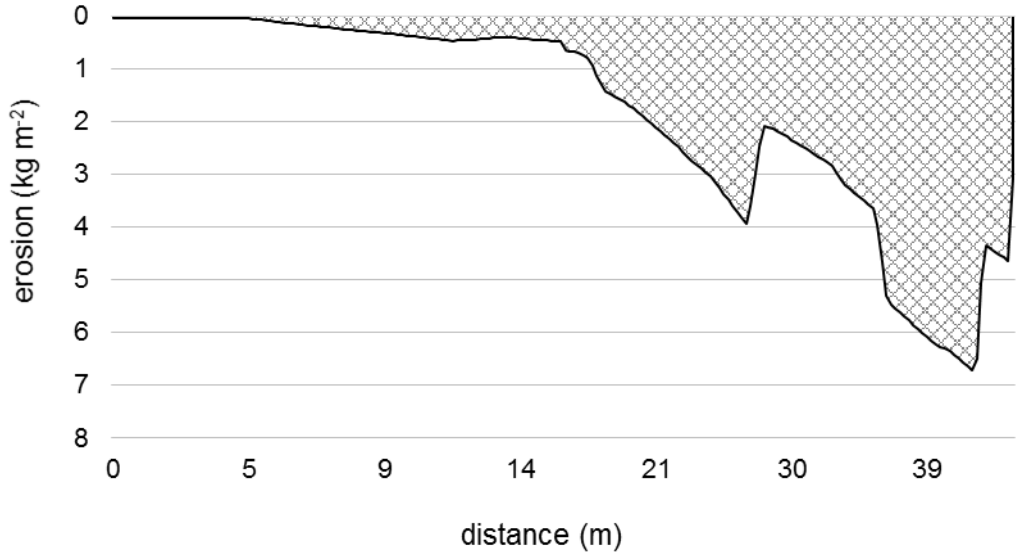

Figure 50: WEPP soil loss graph of Plot 3.

Figure 51 shows the comparison of measured and predicted soil loss for each day of sediment removal. Again, there is a systematic error in the simulation of the first event. However, with an opposing trend than at Plot 1. While all scenarios over-estimated soil loss for the first event at Plot 1, the model under-estimates soil loss at Plot 3.

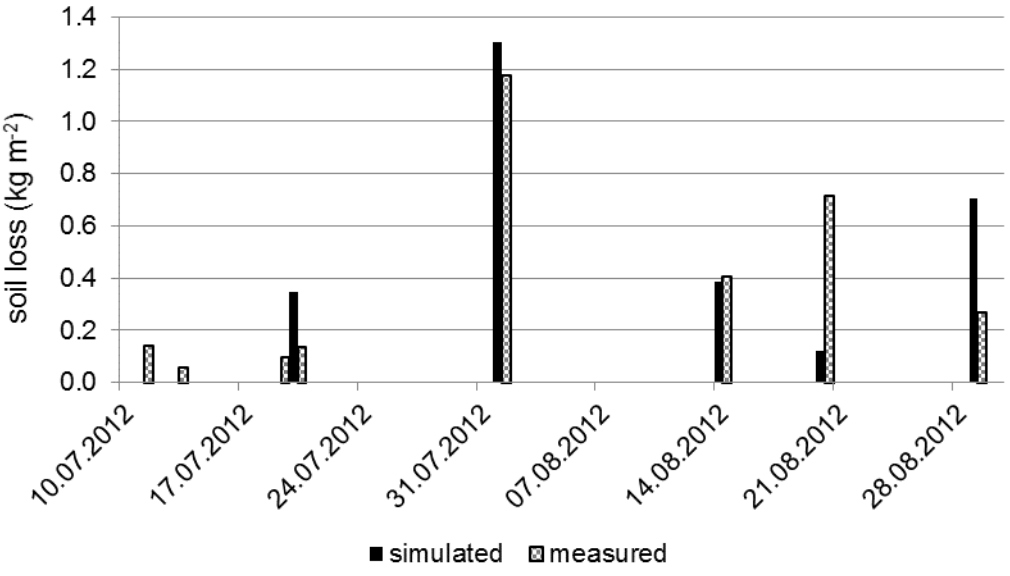

Figure 51: Comparison of observed and simulated soil loss of Plot 3 for all days of removal.

c) Canopy cover and height

Sorghum seeding was on June 1st 2012. On June 28th 2012, crop height was 1 cm. Both parameters, canopy height and cover, then developed until they reached a maximum value before senescence of the plant started and canopy cover decreased. At the end of the cropping season before harvesting at December 15th 2012, sorghum was around 1.26 m high and had a canopy cover of 0.82

d) Predicted yield from the cropping season 2012

The yield from Plot 3 reached the same value as for Plot 1 and was 2.0 t ha^{-1}. As described above this value exceeds the actual yield from 2012 with 0.8 t ha^{-1}. Again, the change of the ratio between canopy cover coefficient and maximum leaf area index leads to a predicted soil loss of 0.9 kg m^{-2}.

e) Development of the parameters random roughness, hydraulic conductivity and rill erodibility coefficient

Random roughness reached its maximum of 11 cm after second tillage and decreased as a function of cumulative rainfall. Figure 52 shows random roughness and cumulative rainfall over the year 2012.

"Baseline" hydraulic conductivity was 200 mm h^{-1} and stayed constant between first tillage operation and July 8th 2012. On this day, hydraulic conductivity dropped to 2 mm h^{-1} at the second surface runoff event – in contrary to Plot 1 at the event no soil loss occurred. Afterwards it increased again to 200 mm h^{-1} and then started decreasing on July 21st. From July 24th and the end of the period of observation it oscillated between 75 m/hr and 2 mm h^{-1}. Figure 53 shows hydraulic conductivity and cumulative rainfall and canopy cover, as those two are responsible for the WEPP internal adaption of this parameter.

The development of the rill erodibility coefficient varied for the two Overland Flow Elements (OFE) with different rock fragment content of the soil. WEPP calculates higher rill erodibility at the upper part with higher rock fragment cover. Figure 54 shows the difference in the development of the rill erodibility coefficient as a function of rock fragment cover.

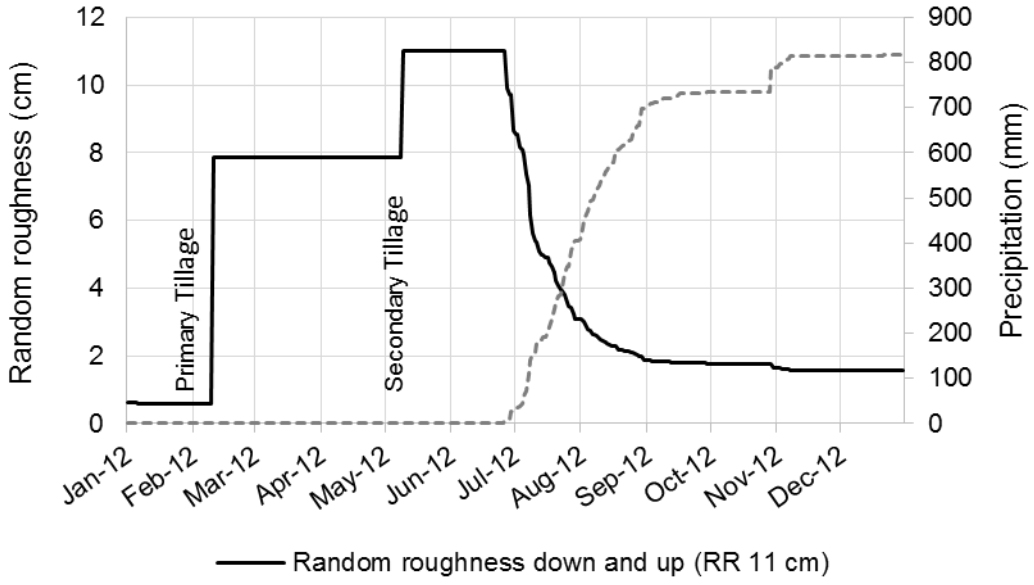

Figure 52: Development of random roughness and rainfall accumulation for Plot 3, where input random roughness is set to 11 cm

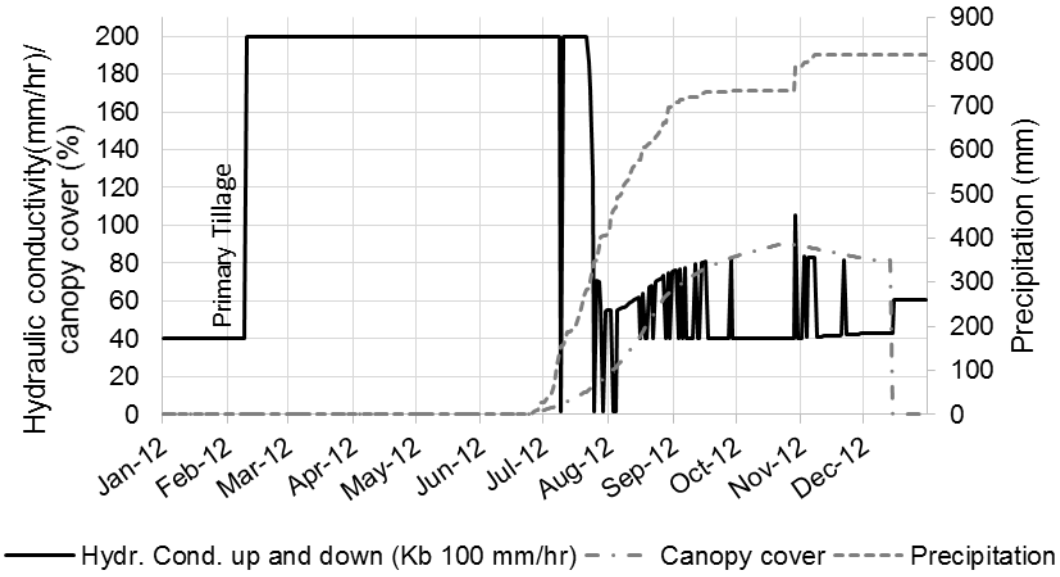

Figure 53: Development of hydraulic conductivity and opposing development of canopy cover and cumulative rainfall for Plot 3.

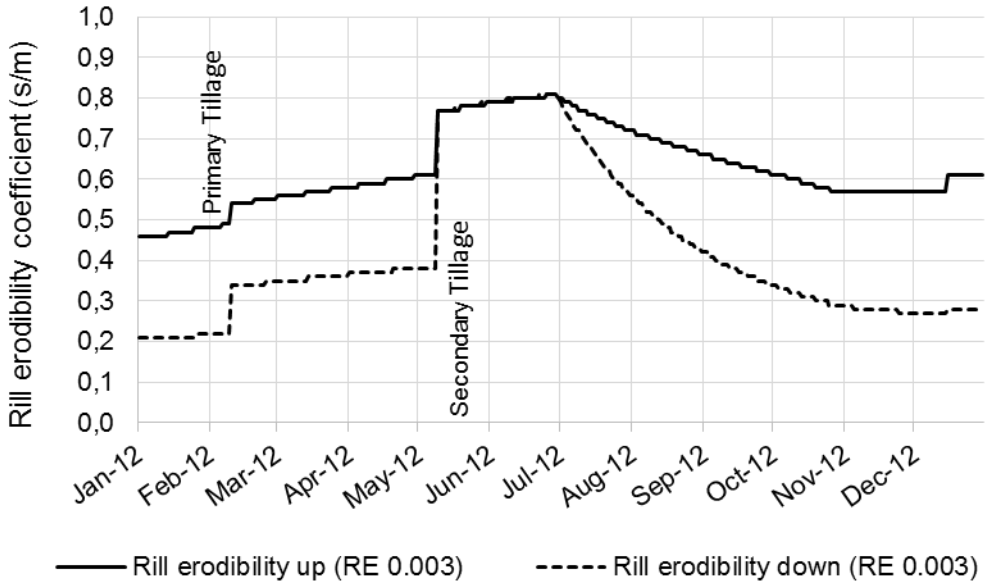

Figure 54: Development of rill erodibility coefficient at the two overland flow elements (OFE) with different rock fragment cover over time for Plot 3. Up and down stand for the OFE at the upper and lower part of the hillslope with a rock fragment content of 41 % and 18 %, respectively.

8.6.8 Discussion of the simulation results

The field experiment was the basis for the successive simulation of soil loss by the Water Erosion Prediction Project (WEPP). In this respect, the evaluation of the WEPP output depends on the results from the fieldwork. Measurement errors in the field would affect the model as well.

Field measurements are time-consuming and can monitor soil loss only under actual conditions. The simulation of the erosion process allows the evaluation of different management practices and conditions in short time.

For both plots, WEPP performed considerably well in predicting soil loss. The simulation ran 144 scenarios with varying input parameters for each plot. Best results went along with rill erodibility coefficients of 0.003 s m^{-1} and 0.005 s m^{-1}, hydraulic conductivity of 100 mm h^{-1} and 200 mm h^{-1} and random roughness of 8 cm, 11 cm, and 14 cm.

Concerning Plot 2, preliminary tests showed that soil loss simulation at this plot is difficult and involves important uncertainties. The profile of the hillslope implies that a considerable portion of detached sediments deposited within the plot. The topographic survey was too coarse to depict the irregular micro relief of this plot. As any conclusion would be difficult, the simulation process was limited to the two other plots.

a) Effect of rock fragment cover and random roughness

The scenario analysis showed that variation of rock fragment cover had little influence on the simulation result. This might be because variation of rock fragment cover was +/- 3 % of the determined cover (see 8.3). This variation might be too low to get a high response by the model.

Comparing the erosion profile of both plots (see Figure 40 and Figure 50), the reduction effect of high rock fragment cover on the soil erosion process is evident. While at Plot 1 soil loss starts from the top of the hillslope, considerable soil loss at Plot 3 starts at the transition from high (41 %) to lower (18 %) rock fragment cover. Beginning from this point, soil loss increases, with a section where the soil loss rate declines a little due to a flatter slope. This implies that the high rock fragment cover at the upper part of this plot kept soil loss from this section low. However, even though no soil detaches, surface runoff accumulates and gains flowing velocity. The sediment load of the accumulated surface flow is low and thus the capacity of the runoff to transport newly detached sediments is high. This explains the relatively strong increase of erosion beginning at 15 m from the top. Additionally, rock fragment cover also affects the development of the random roughness of the surface.

Concerning random roughness, higher values occurred at Plot 3, with high rock fragment cover especially in the upper part of the profile. Simulations performed best with random roughness of 8 cm and 11 cm at Plot 1 and random roughness values of 11 cm and 14 cm at Plot 3. Both showed bad soil loss prediction with random roughness of 5 cm.

Random roughness of the surface after tillage is an input of the tillage input file. The influence and integration of random roughness into the WEPP model is described in 6.1 d. The model assumes that random roughness is highest directly after tillage operations and decays with the amount of cumulative rainfall after tillage. Aggregates break down and sealing of the soil surface starts.

Van Wesemael et al. (1996) showed that this assumption is not valid for soils with high rock fragment cover. Random roughness of soils with small sized rock fragments decreased firstly

due to cumulative rainfall for the first 17.5 mm but then increases with cumulative rainfall. For soils with large rock fragments random roughness increased from the beginning. Van Wesemael et al. (1996) stress that rock fragments jut out of the soil and thus determine the roughness of the surface.

As stone cover at the plot was high and reached up to 55 % at the upper part of Plot 3, the model might misinterpret the evolution of random roughness. To account for the effect of the high rock fragment cover on the fields, the simulation included scenarios with higher random roughness values. This should compensate the effect of decreasing random roughness due to cumulative rainfall. Thus, even though Zeleke (2001) used random roughness values of 5 cm for the *maresha* ox-drawn ard plough in the Ethiopian Highlands, the higher random roughness value is justified by the incidence of high rock fragment cover.

From the high random roughness value after secondary tillage, the model adapts this parameter beginning from the first rainfall event. Random roughness decreases rapidly. On July 13th, it drops below 5 cm. In this sense, the high input value of random roughness might not represent this parameter correctly for the first rainfall events. However, it compensates the decrease due to cumulative rainfall. This fact might be the reason for the under-estimation of soil loss at the beginning of the rainy season for Plot 3, as high random roughness and rock fragment cover interact with each other.

Figure 55 shows the influence of rock fragment cover on soil loss as a function of random roughness. Starting from soil loss with a rock fragment cover of 0 %, the figure shows the variations of soil loss with the increase of rock fragment cover. With increasing random roughness, the effect of varying fragment cover gets more important.

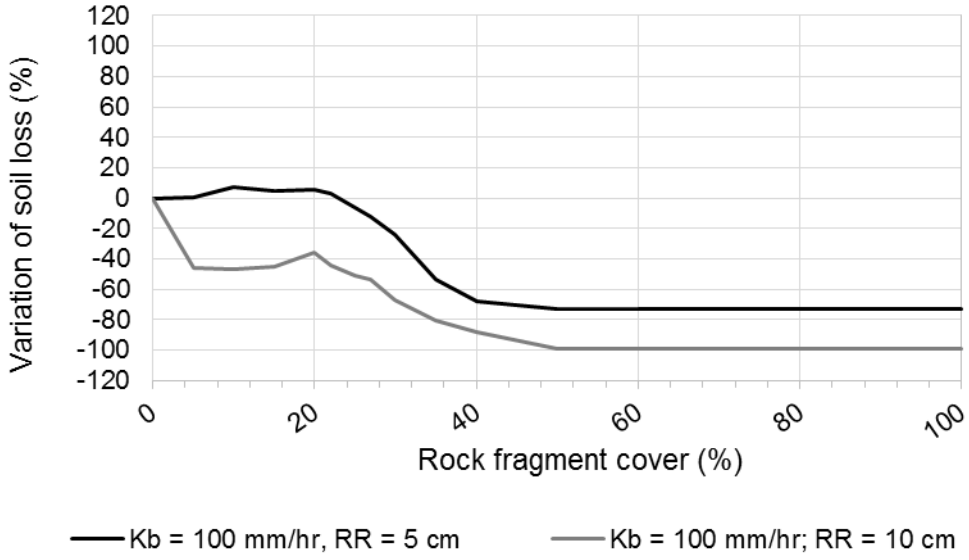

Figure 55: Variation of soil loss as function of rock fragment cover

b) Effect of hydraulic conductivity

In both simulations, the intermediate hydraulic conductivity values of 100 mm h^{-1} and 200 mm h^{-1} performed better than the lowest and highest parameter values (2 mm h^{-1} and 300 mm h^{-1}). Even if this seems high for the given soil texture, this hydraulic conductivity values give sense as firstly measurements by Schürz (2012) showed even higher values for the experimental site (300 mm h^{-1}) and secondly, the model internally reduces the high “baseline” value due to canopy cover and cumulative rainfall. Cracks in the soil lead to rapid infiltration of

surface water into the soil. Flanagan and Livingston (1995) suggest to adjust the effective hydraulic conductivity to account for the incidence of biopores, wormholes and cracks in the soil. The ratio, which is multiplied with the calculated or observed hydraulic conductivity, depends on size and abundance of biopores as well as the input hydraulic conductivity value. Thus, the high K_b input values also represents the effect of the cracks in the soil.

c) Effect of the rill erodibility coefficient

Best simulation results coincided with lower rill erodibility coefficients as the value suggested by WPP. The WEPP internal equation uses the clay fraction as only independent variable for the computation of rill erodibility. Nearing et al. (1990) found that rill erodibility is one of the most dominant factors related to the model response. According to measurements by Romero et al. (2007), the WEPP intern equations over-estimated the rill erodibility factor, while measurements by Reichert and Norton (2013) on a Vertisol soil resulted in the contrary. They showed that WEPP under-predicted the K_r factor. WEPP calculated a value of 0.007 s m^{-1} for this parameter. Best results at Plot 1 and Plot 3 came with a rill erodibility coefficient of 0.003 s m^{-1} and 0.005 s m^{-1}. It has to be mentioned that at Plot 1 no scenario ran with 0.003 s m^{-1} because information of the simulation of Plot 1 led to the adaption of the tested parameter range at Plot 3. Zeleke (2001) applied the WEPP model to an experimental site in the Ethiopian Highlands. The aim of this work was to adapt WEPP to tradition Ethiopian farming systems and site-specific factors. Amongst others, Zeleke (2001) changed the rill erodibility factor. Also from a suggested value of 0.007 s m^{-1} to 0.003 s m^{-1}. This coincides with findings in this work that lower rill erodibility values lead to better soil loss prediction.

d) Development of soil loss over the rainy season

For both plots, no tested scenario evaluated soil loss from the first event correctly. At Plot 1, the model over-predicted soil loss for the first surface runoff event. At Plot 3, the model under-predicted soil loss for the same event. This might be due to the high random roughness in combination with higher rock fragment content and lower rill erodibility. In all cases, predicted soil loss at Plot 1 was much higher than the observed value. The incidence of cracks in the soil might cause this poor accordance for the beginning of the rainy season. Even though hydraulic conductivity is high over the whole rainy season, the cracks in the soil might act as channels of preferential flow in the first rainfall events and reduce even more the development of the surface runoff.

Another reason for the poor quality of prediction in the first event might be the fact, that rainfall data was not available for the whole year but rainfall records started on June 26th, 2012. A high initial saturation level should compensate the missing data of rainfall from January to June.

In general, the fieldwork showed low soil loss rates in the beginning and higher rates in the end of the rainy season. In contrary, the simulation showed no such trend. Soil loss prediction gained accordance with measured soil loss as the rainy season advanced. As discussed in 8.5 b), various studies in the Ethiopian Highlands showed this similar trend of low soil loss in the beginning of the rainy season due to shrinking cracks in the soil. Hence, there is an inverse trend in the modelling and observation: While hydraulic conductivity declines in the WEPP model over time, observation shows increasing or at least constant hydraulic conductivity values. This emphasizes the assumption of a systematic error in soil loss prediction in the beginning of the rainy season.

The 95 % confidence interval of soil loss prediction of the simulation scenarios spans an area of possible model output with assumed parameter combinations. The analysis of this

confidence intervals showed that the range of predicted soil loss is little for several events; meaning that all scenarios lead to similar results. Observed soil loss lies outside this band for some events, but very close to it. In general, it has to be stressed that the use of more observed data points would strengthen the informative value of the model configuration. Thus ongoing research is necessary.

In soil erosion measurements in the Ethiopian Highlands Zeleke (2001) found that WEPP over-predicted runoff and slightly under-predicted soil loss and that prediction of soil loss is better than of runoff. However, he evaluated the WEPP model to perform fairly well under local conditions. This study did not include measurements of surface runoff, but only soil loss. With the found best fitting soil loss simulation, the model simulated rainfall – runoff ratios of 0.20 and 0.15 for Plot 1 and Plot 3, respectively. This implies that the model presumably under-estimated surface runoff. However, measurements in the study area from the following rainy season 2013 also indicate that the rainfall – runoff ratio is around 0.3. Considering that daily rainfall amount and intensities lay below those of 2013 and the average of long-term observations (see 8.1), this ratio is in a realistic range.

Information on the rainfall – runoff ration can improve the calibration of the WEPP model to observations at this site.

9. Summary and Conclusion

During the rainy season 2012 soil erosion measurements were carried out at three soil erosion plots. Additionally, canopy and rock fragment cover, hydraulic conductivity and soil texture were determined

Soil loss from these experimental plots was variable. Two plots showed comparable soil loss rates of 4.7 kg m^{-2} and 3.0 kg m^{-2}. Soil loss from the third plot was considerably lower (0.3 kg m^{-2}). For this plot, it is assumed that sediments deposited before entering the sediment retention basins. From the two other plots, one was situated on fields with stone bunds while the fields at the other plot were not treated with soil and water conservation measures.

Even if stone bunds reduce the effective length of the slope, highest soil loss occurred at the plot with stone bunds. The measurements imply that rock fragment cover determined the development of soil loss to a great extent. The untreated plot showed high rock fragment cover especially in the upper part. The high rock fragment cover and resulting high random roughness of the surface might have superposed the effect of the longer slope.

The distribution of soil loss over the rainy season showed a heterogeneous pattern with increasing soil loss rates from the beginning to the end of the rainy season. This might be attributed to the incidence of shrinkage cracks in the soil, which form during the dry period and close during the first rainfall events. Even though the cracks are invisible after the first days of rainfall, the constant high hydraulic conductivity (measured values from 200 to 400 mm h^{-1}) implies that the cracks affect the subsurface structure of the soil over the whole rainy season.

For the WEPP simulation of soil loss, the model's response to variation of several parameters was tested. The sensitivity analysis showed that the variation of random roughness, rock fragment cover, rill erodibility and hydraulic conductivity decisively affects the soil erosion prediction.

Good accordance between observed and simulated soil loss coincided with relatively high random roughness (8 – 14 cm), high hydraulic conductivity (100 – 200 mm h^{-1}) and a rill erodibility coefficient, which was lower than the value suggested by the model (0.003 – 0.005 s m^{-1}).

The hydraulic conductivity values are justified by the incidence of cracks in the soil, which act as paths of preferential flow and lead to rapid infiltration of surface water. According to Flanagan and Livingston (1995), the incidence of biopores or cracks can be accounted for by increasing the "baseline" hydraulic conductivity of the soil.

The high values of random roughness should compensate the effect of the WEPP internal adjustment of random roughness due to cumulative rainfall since last tillage. This decay of random roughness might lead to misinterpretation of this parameter in combination with high rock fragment cover. However, surface runoff with little sediment load accumulates in sections with high rock fragment cover and leads to increased soil erosion rates when rock fragments decline.

For the two simulated plots, soil loss prediction showed poor agreement with measurements at the beginning of the rainy season and improved as rainy season advanced.

Ongoing research and field measurements are necessary in order to validate the WEPP model in its presumed configuration. The implementation of data from soil erosion measurements of following years can help to further calibrate the model.

10. Outlook

For the WEPP model, little of the required input is known certainly for the experimental site. WEPP uses input databases for experimental sites in other regions, which hold long-term information on climate, cropping conditions etc. Thus, the validation of the model with the adapted parameter input needs on-site measurements to prove the goodness of simulation under different boundary conditions. During the rainy season 2013, again soil loss measurements were conducted at the same site. Comparison of soil loss prediction and observed soil loss can lead to further calibration of the model.

Additional measurements of the sensitive parameters in the WEPP model can help to prove if assumed parameters lie in a realistic range. Measurements of hydraulic conductivity, random roughness and rock fragment cover and content over depth contribute to the improvement of the model's prediction efficiency.

Further research is needed to assess the influence of stone bunds on the soil erosion process in the study area. Measurements behind the bunds might reveal the fraction of sediments depositing behind the bunds and lead to a quantitative assessment of the retention capacity of the stone bunds.

Improvements in the set-up of the experimental plots might be considered in ongoing research:

As mentioned before the setup in this work did not allow monitoring of surface runoff. The idea was to keep the material input in the field low and conduct soil loss measurements without the installation of dividers and storage tanks. Due to the same reason, plots were naturally delineated without the installation of artificial borders. Even though this setup has the advantage that there are no additional obstacles for the farmers managing the fields (e.g. tillage), this aggravated the delineation of the contributing areas and holds uncertainty in the soil erosion measurement.

During the design of the setup, much attention was paid to the fact that little material has to be left in the field. The perception was, that especially metal might be removed during the run-time of the project. After the first year of monitoring, this perception changed. Agreements with local farmers work fine. In return to some expenses, farmers oversee the installed equipment. The introduction of metal borders to the plots in future soil erosion monitoring plots could ease the delineation of the contributing areas and reduce uncertainty in the soil loss monitoring.

The collection of surface runoff can contribute to further validate the soil loss measurement. The installation of rain collectors distributed above the sub-catchment can validate if precipitation of the neighbouring Aba-Kaloye sub-catchment describes the rainfall pattern in the experimental site correctly.

Bibliography

Albert, E.E., M.A. Nearing, M.A. Weltz, L.M. Risse, F.B. Pierson, X.C. Zhang, J.M. Laflen, and J.R. Simanton. 1995. “Chapter 7. Soil Component.” NSERL Report. West Lafayette, Indiana: USDA-ARS National Soil Erosion Research Laboratory.

Amore, Elena, Carlo Modica, Mark A Nearing, and Vincenza C Santoro. 2004. “Scale Effect in USLE and WEPP Application for Soil Erosion Computation from Three Sicilian Basins.” *Journal of Hydrology* 293 (1–4) (June): 100–114. doi:10.1016/j.jhydrol.2004.01.018.

aquastat. 2005. “Country Fact Sheet Ethiopia”. 29. FAO Water Report. aquastat.

Blanco-Canqui, Humberto, and Rattan Lal. 2008. *Principles of Soil Conservation and Management*. Springer.

Bosshart, U. 1997. “Catchment Discharge and Suspended Sediment Transport as Indicators of Physical Soil and Water Conservation in the Michet Catchment, Anjeni Research Unit.” 40. Soil Conservation Research Project. Research Report. Schwitzerland: Centre for Development and Environment University of Berne.

Braimoh, Ademola K., and Paul L.G. Vlek. 2008. *Land Use and Soil Resources*. Springer.

Cerdà, A. 2001. “Effects of Rock Fragment Cover on Soil Infiltration, Interrill Runoff and Erosion.” *European Journal of Soil Science* 52 (1): 59–68. doi:10.1046/j.1365-2389.2001.00354.x.

Dejene, Alemneh. 2003. *Integrated Natural Resources Management to Enhance Food Security*. Organisation des Nations Unies pour l’alimentation et l’agriculture. ftp://ftp.fao.org/docrep../FAO/005/Y4818E/Y4818E00.pdf.

“European Commission.” 2013. Accessed July 15. http://ec.europa.eu/environment/soil/index_en.htm.

FAO. 2013. “Country Pasture/ Forage Resource Profiles, Ethiopia.” Accessed July 15. http://www.fao.org/ag/AGP/AGPC/doc/Counprof/Ethiopia/Ethiopia.htm#3.%20CLIMATE%20AND%20AGRO%20ECOLOGICAL.

Flanagan, D.C., and Stanley J. Livingston. 1995. “WEPP User Summary.” *NSERL Report* 11 (July). http://www.ars.usda.gov/SP2UserFiles/ad_hoc/36021500WEPP/usersum.pdf.

Flanagan, D.C., and M.A. Nearing. 1995. “USDA-Water Erosion Prediction Project - Hillslope Profile and Watershed Model Documentation.” NSERL Report. West Lafayette, Indiana: USDA-ARS National Soil Erosion Research Laboratory.

GARC. 2010. “Socio-economic Survey of Gumara-Maksegnit Watershed”. Gonder, Ethiopia: ICARDA, ARARI, EIAR, BOKU, SASAKAWA.

Gebremichael, D., J. Nyssen, J. Poesen, J. Deckers, M. Haile, G. Govers, and J. Moeyersons. 2005. “Effectiveness of Stone Bunds in Controlling Soil Erosion on Cropland in the Tigray Highlands, Northern Ethiopia.” *Soil Use and Management* 21 (3): 287–297. doi:10.1079/SUM2005321.

Gebreyesus, B, and M Kirubel. 2009. “Estimating Soil Loss Using Universal Soil Loss Equation (USLE) for Soil Conservation Planning at Medego Watershed, Northern Ethiopia.” *Journal of AMerican Science* 5 (1): 58–69.

Gentile, Anna Rita, and Robert JA Jones. 2013. “REPORTS OF THE TECHNICAL WORKING GROUPS.” Accessed July 15. http://citeseerx.ist.psu.edu/viewdoc/download?doi=10.1.1.130.5966&rep=rep1&type=pdf.

Global Environment Outlook 4: Environment for Development. 2007. Nairobi, Kenya: United Nations Environment Programme.

"Guide to Texture by Feel | NRCS Soils." 2013. Accessed July 21. http://soils.usda.gov/education/resources/lessons/texture/.

Hengsdijk, H., G.W. Meijerink, and M.E. Mosugu. 2005. "Modeling the Effect of Three Soil and Water Conservation Practices in Tigray, Ethiopia." *Agriculture, Ecosystems & Environment* 105 (1-2) (January): 29–40. doi:10.1016/j.agee.2004.06.002.

Herweg, Karl, and Eva Ludi. 1999. "The Performance of Selected Soil and Water Conservation Measures—case Studies from Ethiopia and Eritrea." *Catena* 36 (1): 99–114.

Hurni, H. 1988. "Degradation and Conservation of the Resources in the Ethiopian Highlands." *Mountain Research & Development* 8 (2-3): 123–130.

Jones, A., H Breuning-Madsen, M Brossard, and A Dampha. 2013. *Soil Atlas of Africa*. http://eusoils.jrc.ec.europa.eu/library/maps/Africa_Atlas/Documents/JRC_africa_soil_atlas_part1.pdf.

Jones, A., P. Panagos, S. Barcelo, F. Bourani, C. Bosco, O. Dewitte, C. Gardi, et al. 2012. "The State of Soil in Europe JRC Reference Report." http://ec.europa.eu/dgs/jrc/downloads/jrc_reference_report_2012_02_soil.pdf.

Kasperson, Roger E., and Emma RM Archer. 2005. "Vulnerable Peoples and Places." *Ecosystems and Human Well-Being: Current State and Trends: Findings of the Condition and Trends Working Group* 1: 143.

Kendie Addis, H., St. Strohmeier, R. Srinivasan, F. Ziadat, and A. Klik. 2013. "Using SWAT Model to Evaluate the Impact of Community-based Soil and Water Conservation Interventions for an Ethiopian Watershed." In *Proceedings of the 2013 International SWAT Conference, Paul Sabatier University, Toulouse, France July 17-19th, 2012*. Toulouse.

Kendie Addis, Hailu. unpublished. "Assessment of the Impact of Rainwater Harvesting and Soil Conservation Structures on Surface Runoff and Sediment Yield From an Agricultural Watershed in Ethiopia.pdf."

Krüger, H. J., Berhanu Fantew Yohannes Gebremichael, and Kefeni Kejela. 1997. "Inventory of Indigenious Soil and Water Conservation Measures on Selected Sites in the Ethiopia Highlands". 34. Soil Conservation Research Project. Research Report. Centre for Development and Environment University of Berne.

Liniger, H. P., Dennis Cahill, D. B. Thomas, G. W. J. van Lynden, and Gudrun Schwilch. 2002. "Categorization of SWC Technologies and Approaches–a Global Need." In *Proceedings of ISCO Conference 2002*, 3:6–12. http://www.wocat.net/fileadmin/user_upload/documents/Articles/ISCOSWC2002.PDF.

Mahmoodabadi, Majid, and Artemi Cerdà. 2013. "WEPP Calibration for Improved Predictions of Interrill Erosion in Semi-arid to Arid Environments." *Geoderma* 204–205 (August): 75–83. doi:10.1016/j.geoderma.2013.04.013.

Martínez-Zavala, L., and A. Jordán. 2008. "Effect of Rock Fragment Cover on Interrill Soil Erosion from Bare Soils in Western Andalusia, Spain." *Soil Use and Management* 24 (1): 108–117. doi:10.1111/j.1475-2743.2007.00139.x.

McKay, M.D., R.J. Beckman, and W.J. Conover. 1979. "A Comparison of Three Methods for Selecting Values of Input Variables in the Analysis of Output from a Computer Code." *Technometrics* 21 (2) (May).

Merritt, W.S., R.A. Letcher, and A.J. Jakeman. 2003. "A Review of Erosion and Sediment Transport Models." *Environmental Modelling & Software* 18 (8-9) (October): 761–799. doi:10.1016/S1364-8152(03)00078-1.

Morgan, R. P. C. 1995. *Soil Erosion and Conservation*. London and New York: Longman.

Nash, J.E., and J.V. Sutcliffe. 1970. “River Flow Forecasting through Conceptual Mmodels. Part 1. A Discussion of Principles.” *Journal of Hydrology* 10: 282 – 290.

“Natural Resources and Environment: Land Degradation Assessment.” 2013. Accessed July 15. http://www.fao.org/nr/land/degradation/en/.

Nearing, M.A., L. Deer-Ascough, and J.M. Laflen. 1990. “Sensitivity Analysis of the WEPP Hillslope Profile Erosion Model.” *Transactions of the ASAE* 33 (3): 839–849.

Nyssen, J, Jean Poesen, Desta Gebremichael, Karen Vancampenhout, Margo D’aes, Gebremedhin Yihdego, Gerard Govers, et al. 2007. “Interdisciplinary On-site Evaluation of Stone Bunds to Control Soil Erosion on Cropland in Northern Ethiopia.” *Soil and Tillage Research* 94 (1) (May): 151–163. doi:10.1016/j.still.2006.07.011.

Nyssen, J., J. Nyssen, Mitiku Haile, J. Poesen, J. Deckers, and J. Moeyersons. 2001. “Removal of Rock Fragments and Its Effect on Soil Loss and Crop Yield, Tigray, Ethiopia.” *Soil Use and Management* 17 (3) (September 1): 179–187. doi:10.1079/SUM200173.

Nyssen, J., J. Poesen, M. Haile, J. Moeyersons, and J. Deckers. 2000. “Tillage Erosion on Slopes with Soil Conservation Structures in the Ethiopian Highlands.” *Soil and Tillage Research* 57 (3): 115–127.

Nyssen, J., J. Poesen, M. Haile, J. Moeyersons, and H. Hurni. 2009. “Effects of Land Use and Land Cover on Sheet and Rill Erosion Rates in the Tigray Highlands, Ethiopia.” *Zeitschrift Für GEomorphologie* 53 (2) (June): 171–197.

Oldeman, L.R., R.T.A. Hakkeling, and W.G. Sombroek. 1991. *Global Assessment of Soil Degradation (GLASOD). World Map of the Status of Human-Induced Soil Degradation*. Wageningen: Internation Soil Reference and Information Centre, United Nations Environment Programme.

Oldeman, LR. 1991. “The Global Extent of Soil Degradation.” ISRIC Bi-Annuan Rport. Wageningen, Netherlands.

Poesen, J., and H Lavee. 1994. “Rock Fragments in Top Soils: Significance and Processes” 23 (1-2) (September): 1–28. doi:10.1016/0341-8162(94)90050-7.

Reichert, José Miguel, and L. Darrell Norton. 2013. “Rill and Interrill Erodibility and Sediment Characteristics of Clayey Australian Vertosols and a Ferrosol.” *Soil Research* 51 (1): 1. doi:10.1071/SR12243.

Romero, Consuelo C., Leo Stroosnijder, and Guillermo A. Baigorria. 2007. “Interrill and Rill Erodibility in the Northern Andean Highlands.” *CATENA* 70 (2) (July): 105–113. doi:10.1016/j.catena.2006.07.005.

Roose, Eric. 1996. *Land Husbandry: Components and Strategy*. Vol. 70. FAO Rome. http://www.betuco.be/CA/Land%20husbandry%20-%20Components%20and%20strategy%20erosion%20FAO.pdf.

Schürz, Christoph. 2012. “Field Measurements in the Framework of Data Acquisition for the Master Thesis.”

“The World Factbook.” 2013. Accessed July 15. https://www.cia.gov/library/publications/the-world-factbook/geos/et.html.

Thomann, R.V. 1982. “Verification of Water Quality Models.” *Journal of the Environmental Enineering Division* 108 (5): 923 – 940.

Toy, T. J., G. R. Foster, and K. G. Renard. 2002. *Soil Erosion: Processes, Prediction, Measurement, and Control*. 1st ed. John Wiley & Sons.

USDA-ARS. 1989. *Water Erosion Prediction Project (WEPP)*. Fortran. West Lafayette, Indiana: USDA-ARS, United States Department of Agriculture - Agricultural Research Service.

Van Lynden, G. W. J., H. P. Liniger, and Gudrun Schwilch. 2002. “The WOCAT Map Methodology, a Standardized Tool for Mapping Degradation and Conservation.” In *Proceedings of ISCO Conference*, 4:11–16. http://www.tucson.ars.ag.gov/isco/isco12/VolumeIV/TheWOCATMap.pdf.

Van Wesemael, Bas, Jean Poesen, Tomás de Figueiredo, and Gérard Govers. 1996. “Surface Roughness Evolution of Soils Containing Rock Fragments.” http://bibliotecadigital.ipb.pt/handle/10198/6480.

Wischmeier, W.H. 1966. “Surface Runoff in Relation to Physical and Management Factors.” In , 237–244. San Paulo, Brazil.

Wischmeier, W.H., and D.D. Smith. 1965. “Predicting Rainfall-erosion Losses from Cropland East of the Rocky Mountains: Guide for Selection of Practices for Soil and Water Conservation.”

“World Atlas of Desertification.” 1997. UNEP, International Soil Reference and Information Centre (ISRIC).

Wyss, G.D., and K.H. Jorgensen. 1998. “A User’s Guide to LHS: Sandia’s Latin Hypercube Sampling Software”. Albuquerque: Risk Assessment and Systems Modeling Department, Sandia National Laboratories.

Zeleke, Gete. 2001. “Application and Adaptation of WEPP to Traditional Farming Systems of the Ethiopian Highlands.” In *Sustaining the Global Farm. Selected Papers from the 10th International Soil Conservation Organization Meeting Held May 24-29, 1999*, edited by D.E. Stott, R.H Mohtar, and G.C. Steinhardt, 903–912. Purdue University and USDA-ARS National Soil Erosion Research Laboratory.

Zhang, X.C., M.A. Nearing, L.M. Risse, and K.C. McGregor. 1996. “Evaluation of WEPP Runoff and Soil Loss Predictions Using Natural Runoff Plot Data.” *Transactions of ASAE* 39 (3): 855–863.

12. Tables

12.1 Table of figures

12.2 Table directory

13. Annex

13.1 Survey: Delimiting watersheds with Arc GIS 10

Arc GIS 10 was used for post-processing of the survey data.

1)	Insert XYZ measurement points from spreadsheet	Add XY Data	
2)	Create TIN (Triangulated Irregular Network)	Create TIN	3D Analyst Tool
3)	Create DEM (Digital Elevation Model)	TIN to Raster Resolution: 0.1 x 0.1 m	3D Analyst Tool
4)	Insert retention basins 1,2,3	Draw polygon Convert Graphics to Features - Insert field "Elevation = 1"	Draw Tool
		Polygon to raster - Resolution: 0.1 x 0.1 m - Extent same as layer DEM	Conversion Tool
5)	Insert downhill stone bund	Draw polygon Convert Graphics to Features - Insert field "Elevation = 1"	Draw Tool
		Polygon to raster - Resolution: 0.1 x 0.1 m - Extent same as layer DEM	Conversion Tool
6)	Define basins and vertical stone bund as areas with no elevation information	Reclassify - basins 1,2,3: Elevation noData --> 1 Elevation 1 --> 0 - vertical stone bund: Elevation NoData --> 1 Elevation 1 --> 2	3D Analyst Tool
7)	Modify DEM	Raster Calculator - DEM * reclassified basins * vertical stone bund	Spatial Analyst Tool
8)	Eliminate sinks from DEM	Fill	Spatial Analyst Tool
9)	Compute flow direction	Flow Direction	Spatial Analyst Tool
10)	Compute flow accumulation	Flow Accumulation	Spatial Analyst Tool
11)	Compute watersheds for the three basins	Watershed	Spatial Analyst Tool
		Raster to Polygon	Conversion Tool

The first column refers to the purpose of each step, the second and third columns refer to the Arc GIS tool name and Arc GIS toolbox name, respectively.

The downhill-orientated stone bund, which builds the border between treated and untreated fields, influences the direction of the surface runoff and the area which drainages to each basin. To account for this effect, the digital elevation model was modified by inserting a linear structure with raised elevation along the vertical stone bund. Thus, the vertical stone bund acts as drainage divide.

13.2 Canopy and rock fragment cover

13.2.1 Automatized assessment of canopy and rock fragment cover

a) Plot 1 (treated):

Vegetation (-)	Rock fragments (-)	Soil (-)
0.50	0.18	0.32
0.36	0.05	0.60
0.17	0.10	0.70
0.08	0.19	0.71
0.10	0.19	0.71
0.05	0.21	0.74
0.05	0.14	0.80
0.08	0.10	0.82
0.03	0.00	0.95
0.17	0.24	0.59
0.16 (mean)	**0.14 (mean)**	**0.69 (mean)**
0.15 (standard deviation)	**0.08 (standard deviation)**	**0.17 (standard deviation)**

b) Plot 2 (treated)

Vegetation (-)	Rock fragments (-)	Soil (-)
0.50	0.18	0.32
0.36	0.05	0.60
0.17	0.10	0.70
0.08	0.19	0.71
0.10	0.19	0.71
0.05	0.21	0.74
0.05	0.14	0.80
0.08	0.10	0.82
0.03	0.00	0.95
0.17	0.24	0.59
0.16 (mean)	**0.14 (mean)**	**0.69 (mean)**
0.15 (standard deviation)	**0.08 (standard deviation)**	**0.17 (standard deviation)**

c) Plot 3 (untreated)

Vegetation (-)	Rock fragments (-)	Soil (-)
0.24	0.14	0.62
0.18	0.37	0.45
0.20	0.41	0.38
0.18	0.44	0.38
0.19	0.32	0.49

0.06	0.43	0.51
0.27	0.38	0.34
0.18	0.18	0.64
0.19	0.18	0.63
0.13	0.26	0.61
0.11	0.18	0.71
0.21	0.09	0.70
0.10	0.13	0.77
0.03	0.22	0.75
0.10	0.16	0.74
0.11	0.17	0.72
0.11	0.20	0.69
0.07	0.19	0.74
0.03	0.21	0.76
0.09	0.18	0.73
0.07	0.17	0.74
0.07	0.11	0.81
0.06	0.15	0.80
0.14	0.18	0.67
0.08	0.09	0.83
0.10	0.10	0.79
0.08	0.14	0.77
0.13	0.12	0.75
0.10	0.15	0.74
0.14 (mean)	**0.24 (mean)**	**0.62 (mean)**
0.07 (standard deviation)	**0.11 (standard deviation)**	**0.14 (standard deviation)**

13.2.2 Manual assessment of rock fragment cover

rock fragment cover (-)		
Plot 1 (treated)	Plot 2 (treated)	Plot 3 (untreated)
0.23	0.25	0.21
0.12	0.07	0.43
0.21	0.08	0.29
0.21	0.13	0.47
0.28	0.15	0.43
0.25	0.21	0.55
0.19	0.13	0.49
0.08	0.09	0.22
0.05	-	0.25

0.06	0.03	0.30
-	-	0.22
-	-	0.07
-	-	0.15
-	-	0.24
-	-	0.14
-	-	0.11
-	-	0.17
-	-	0.16
-	-	0.13
-	-	0.15
0.13 (mean)	**0.17 (mean)**	**0.26 (mean)**
0.07 (standard deviation)	**0.08 (standard deviation)**	**0.14 (standard deviation)**

13.3 Sediment amounts

Date	Precipitation	Plot 1 (treated) A = 297 m²		Plot 2 (treated) A = 482 m²		Plot 3 (treated) A = 418 m²	
	between days of removal	sediment	water	sediment	water	sediment	water
	(mm)	(kg)	(l)	(kg)	(l)	(kg)	(l)
11.07.12	-	68	-	1	-	58	250
13.07.12	28.8	54	1946	8	-	24	563
19.07.12	67.2	60	2827	-	-	41	1504
20.07.12	16.4	92	2085	1	-	57	862
01.08.12	148	480	1759	129	-	491	491
03.08.12	46.2	4	3095	-	-	1	2570
07.08.12	40.6	4	2250	-	-	3	1260
14.08.12	57	224	2441	-	-	256	1440
17.08.12	16.6	9	3065	-	-	-	-
20.08.12	36.0	258	2439	-	-	298	1305
28.08.12	47.6	5	2640	-	-	-	-
29.08.12	35.2	145	1965	-	-	111	2160
30.08.12	0	7	2355	-	-	7	2370

13.4 WEPP model input

13.4.1 Slope input file

Plot 1		Plot 3	
Length (m)	Slope (%)	Length (m)	Slope (%)
0.999	18.3	12.62	11.8
0.998	39.66	4.5	9.3
0.799	14.04	5.7	11.9
2.097	24.08	4.7	12.2
3.095	12.67	5.5	7.8
2.396	6.96	2.6	8.2
11.183	8.69	4.2	10
0.799	15.04	2.3	9.9
2.19	8.39	2.3	7.3
Mean	10.84	mean	10.78

13.4.2 Soil input file

SOIL Plot 1			
Number	Parameter	Value	Unit
1	Soil File Name	Maksegnit Plot 1 Soil	-
2	Soil Texture	Clay	-
3	Albedo	0.3	-
4	Initial Saturation Level	75	%
5	Interrill erodibility		kg s m^{-4}
6	Rill erodibility*	0.005, 0.007, 0.009*	s m^{-1}
7	Critical Shear		Pa
8	Eff. Hydr. Conductivity*	2, 100, 200, 300*	mm h^{-1}
9	Layer	1	-
10	Depth	1500	mm
11	Sand	22	%
12	Clay	42	%
13	Organic matter	1.5	%
14	CEC	24	meq $(100g)^{-1}$
15	Rock*	10, 13, 16*	%
* Variable parameters; changed in the scenarios			

SOIL Plot 3			
Number	Parameter	Value	Unit
1	Soil File Name	Maksegnit Plot 3 Soil	-
2	Soil Texture	Clay	-
3	Albedo	0.3	-
4	Initial Saturation Level	75	%
5	Interrill erodibility		kg s m^{-4}
6	Rill erodibility*	0.003, 0.005, 0.007*	s m^{-1}
7	Critical Shear		Pa
8	Eff. Hydr. Conductivity*	2, 100, 200, 300*	mm h^{-1}
9	Layer	1	-
10	Depth	1500	mm
11	Sand	22	%
12	Clay	42	%
13	Organic matter	1.5	%
14	CEC	24	meq $(100g)^{-1}$
15	Rock*	38/15, 41/18, 44/21*	%
* Variable parameters; changed in the scenarios			

13.4.3 Management input file

MANAGEMENT
Initial Condition

Number	Parameter	Value	Units
1	Initial Plant	Teff	-
2	Bulk density after last tillage	1.1	(g/cub. cm)
3	Initial canopy cover (0-100%)	0	%
4	Days since last tillage	180	days
5	Days since last harvest	35	days
6	Initial frost depth	0	cm
7	Initial interrill cover (0-100%)	0	%
8	Initial residue cropping system	Annual	-
9	Cumulative rainfall since last tillage	1000	mm
10	Initial ridge height after last tillage	4	cm
11	Initial rill cover (0-100%)	0	%
12	Initial roughness after last tillage	4	cm
13	Rill spacing	0	cm
14	Rill width type	Temporary	-
15	Initial snow depth	0	cm

16	Initial depth of thaw	0	cm
17	Depth of secondary tillage layer	10	cm
18	Depth of primary tillage layer	15	cm
19	Initial rill width	2.54	cm
20	Initial total dead root mass	0.2	kg/sq.m
21	Initial total submerged residue mass	0.1	kg/sq.m

MANAGEMENT
Tillage

Number	Parameter	Value	Value	Units
1	Percent residue buried on interrill areas for fragile crops	98		%
2	Percent residue buried on interrill areas for non-fragile crops	95		%
3	Number of rows of tillage implement	1		-
4	Implement Code	Other		-
5	Cultivator Position	Rear mounted		-
6	Ridge height value after tillage	12	6	cm
7	Ridge interval	35	20	cm
8	Percent residue buried on rill areas for fragile crops	98		%
9	Percent residue buried on rill areas for non-fragile crops	95		%
10	Random roughness value after tillage*	5/8/11/14*	5/8/11/14*	cm
11	Surface area disturbed (0-100%)	70	100	%
12	Mean tillage depth	12.5	10	cm
	Tillage Depth:	15	10	cm
	Tillage Type:	Primary	Secondary	
	* Variable parameters; changed in the scenarios			

MANAGEMENT
Plant - Annual
Sorghum, Plot 1

Number	Parameter	Value	Units
1	**Plant Growth and Harvest Parameters**		
2	Biomass energy ratio	12	kg/MJ
3	Growing degree days to emergence	60	Degrees C.days
4	Growing degree days for growing season	1450	Degrees C.days
5	In-row plant spacing	15	cm
6	Plant stem diameter at maturity	3.2	cm
7	Height of post-harvest standing residue; cutting height	60.9	cm
8	Harvest index (dry crop yield/total above ground dry biomass)	50	%
9	**Temperature and Radiation Parameters**		
10	Base daily air temperature	10	Degrees C
11	Optimal temperature for plant growth	27.5	Degrees C
12	Maximum temperature that stops the growth of a perennial crop	0	Degrees C
13	Critical freezing temperature for a perennial crop	0	Degrees C
14	Radiation extinction coefficient	0.6	
15	**Canopy, LAI and Root Parameters**		
16	Canopy cover coefficient	12	
17	Parameter value for canopy height equation	3	
18	Maximum canopy height	180	cm
19	Maximum leaf area index	8	
20	Maximum root depth	150	cm
21	Root to shoot ratio (% root growth/% above ground growth)	25	%
22	Maximum root mass for a perennial crop	0	kg/sq.m
23	**Senescence Parameters**		
24	Percent of growing season when leaf area index starts to decline (0-100%)	85	%
25	Period over which senescence occurs	40	days
26	Percent canopy remaining after senescence (0-100%)	90	%
27	Percent of biomass remaining after senescence (0-100%)	90	%
28	**Residue Parameters**		
29	Parameter for flat residue cover equation	2.9	sq.m/kg

30	Standing to flat residue adjustment factor (wind, snow, etc.)	99	%
31	Decomposition constant to calculate mass change of above-ground biomass	0.0074	
32	Decomposition constant to calculate mass change of root-biomass	0.0074	
33	Use fragile or non-fragile mfo values	Non-Fragile	
34	**Other Parameters**		
35	Plant specific drought tolerance (% of soil porosity)	0	%
36	Critical live biomass value below which grazing is not allowed	0	kg/sq.m
37	Maximum Darcy Weisbach friction factor for living plant	0	
38	Harvest Units	WeppWillSet	
39	Optimum yield under no stress conditions	0	kg/sq.m
	Row Width	20	cm

MANAGEMENT
Plant - Annual
Sorghum, Plot 3

Number	Parameter	Value	Units
1	**Plant Growth and Harvest Parameters**		
2	Biomass energy ratio	12	kg/MJ
3	Growing degree days to emergence	60	Degrees C.days
4	Growing degree days for growing season	1450	Degrees C.days
5	In-row plant spacing	15	cm
6	Plant stem diameter at maturity	3.2	cm
7	Height of post-harvest standing residue; cutting height	60.9	cm
8	Harvest index (dry crop yield/total above ground dry biomass)	50	%
9	**Temperature and Radiation Parameters**		
10	Base daily air temperature	10	Degrees C
11	Optimal temperature for plant growth	27.5	Degrees C
12	Maximum temperature that stops the growth of a perennial crop	0	Degrees C
13	Critical freezing temperature for a perennial crop	0	Degrees C
14	Radiation extinction coefficient	0.6	
15	**Canopy, LAI and Root Parameters**		
16	Canopy cover coefficient	11	

17	Parameter value for canopy height equation	3	
18	Maximum canopy height	180	Cm
19	Maximum leaf area index	8	
20	Maximum root depth	150	cm
21	Root to shoot ratio (% root growth/% above ground growth)	25	%
22	Maximum root mass for a perennial crop	0	kg/sq.m
23	**Senescence Parameters**		
24	Percent of growing season when leaf area index starts to decline (0-100%)	85	%
25	Period over which senescence occurs	40	days
26	Percent canopy remaining after senescence (0-100%)	90	%
27	Percent of biomass remaining after senescence (0-100%)	90	%
28	**Residue Parameters**		
29	Parameter for flat residue cover equation	2.9	sq.m/kg
30	Standing to flat residue adjustment factor (wind, snow, etc.)	99	%
31	Decomposition constant to calculate mass change of above-ground biomass	0.0074	
32	Decomposition constant to calculate mass change of root-biomass	0.0074	
33	Use fragile or non-fragile mfo values	Non-Fragile	
34	**Other Parameters**		
35	Plant specific drought tolerance (% of soil porosity)	0	%
36	Critical live biomass value below which grazing is not allowed	0	kg/sq.m
37	Maximum Darcy Weisbach friction factor for living plant	0	
38	Harvest Units	WeppWillSet	
39	Optimum yield under no stress conditions	0	kg/sq.m
	Row Width	20	cm

13.5 Simulation results: soil loss and objective functions for all scenarios

a) Plot 1 (treated)

Scenario	Soil loss (kg/m²)	RMSE	ME	R²
RE 0.003,RR 8,RO 10%,Kb 100	4.06	0.34	0.47	0.95
RE 0.003,RR 8,RO 10%,Kb 200	3.54	0.38	0.33	0.93
RE 0.005,RR 11,RO 16%,Kb 100	4.84	0.38	0.32	0.93
RE 0.005,RR 11,RO 13%,Kb 100	4.79	0.38	0.32	0.93
RE 0.005,RR 11,RO 10%,Kb 100	4.38	0.39	0.29	0.93
RE 0.005,RR 8,RO 10%,Kb 200	5.24	0.42	0.16	0.92
RE 0.005,RR 14,RO 16%,Kb 100	3.48	0.43	0.15	0.92
RE 0.005,RR 14,RO 13%,Kb 100	3.42	0.43	0.14	0.91
RE 0.005,RR 8,RO 13%,Kb 200	5.38	0.44	0.12	0.91
RE 0.005,RR 14,RO 10%,Kb 100	3.35	0.44	0.11	0.91
RE 0.007,RR 14,RO 16%,Kb 100	4.56	0.44	0.10	0.91
RE 0.007,RR 14,RO 13%,Kb 100	4.51	0.44	0.08	0.91
RE 0.005,RR 8,RO 10%,Kb 300	4.52	0.45	0.07	0.91
RE 0.003,RR 8,RO 10%,Kb 300	3.07	0.45	0.06	0.91
RE 0.005,RR 8,RO 13%,Kb 300	4.67	0.45	0.05	0.91
RE 0.005,RR 8,RO 16%,Kb 200	5.60	0.45	0.05	0.91
RE 0.005,RR 8,RO 16%,Kb 300	4.83	0.46	0.02	0.90
RE 0.005,RR 8,RO 10%,Kb 100	6.01	0.48	-0.08	0.89
RE 0.007,RR 11,RO 10%,Kb 200	5.79	0.51	-0.19	0.88
RE 0.007,RR 11,RO 10%,Kb 100	5.79	0.51	-0.19	0.88
RE 0.005,RR 8,RO 13%,Kb 100	6.25	0.51	-0.20	0.88
RE 0.009,RR 14,RO 16%,Kb 100	5.60	0.51	-0.22	0.88
RE 0.009,RR 14,RO 13%,Kb 100	5.56	0.51	-0.23	0.88
RE 0.009,RR 14,RO 10%,Kb 100	5.50	0.52	-0.25	0.88
RE 0.007,RR 11,RO 16%,Kb 100	6.31	0.52	-0.27	0.87
RE 0.007,RR 11,RO 13%,Kb 200	6.29	0.52	-0.28	0.87
RE 0.007,RR 11,RO 13%,Kb 100	6.29	0.52	-0.28	0.87
RE 0.005,RR 8,RO 16%,Kb 100	6.44	0.53	-0.29	0.87
RE 0.003,RR 8,RO 10%,Kb 2	6.37	0.55	-0.39	0.86
RE 0.007,RR 8,RO 10%,Kb 300	5.90	0.55	-0.40	0.86
RE 0.005,RR 5,RO 10%,Kb 300	5.80	0.55	-0.41	0.86
RE 0.005,RR 11,RO 16%,Kb 200	3.09	0.55	-0.42	0.86
RE 0.005,RR 11,RO 13%,Kb 200	3.02	0.55	-0.43	0.86
RE 0.005,RR 11,RO 10%,Kb 200	2.95	0.56	-0.46	0.86
RE 0.005,RR 5,RO 13%,Kb 300	5.92	0.56	-0.47	0.86
RE 0.007,RR 8,RO 13%,Kb 300	6.06	0.56	-0.47	0.85

RE 0.007,RR 11,RO 16%,Kb 200	4.02	0.56	-0.48	0.85
RE 0.005,RR 14,RO 10%,Kb 2	6.67	0.57	-0.49	0.85
RE 0.005,RR 5,RO 16%,Kb 300	6.09	0.58	-0.56	0.85
RE 0.005,RR 14,RO 13%,Kb 2	6.83	0.58	-0.57	0.85
RE 0.007,RR 8,RO 16%,Kb 300	6.23	0.58	-0.57	0.85
RE 0.005,RR 14,RO 16%,Kb 2	6.95	0.59	-0.60	0.84
RE 0.005,RR 11,RO 10%,Kb 2	7.20	0.59	-0.63	0.84
RE 0.007,RR 8,RO 10%,Kb 200	6.86	0.60	-0.68	0.83
RE 0.009,RR 11,RO 13%,Kb 200	4.85	0.60	-0.69	0.83
RE 0.009,RR 11,RO 16%,Kb 200	4.92	0.60	-0.70	0.83
RE 0.009,RR 11,RO 10%,Kb 200	4.79	0.61	-0.72	0.83
RE 0.005,RR 11,RO 13%,Kb 2	7.37	0.61	-0.73	0.83
RE 0.007,RR 8,RO 13%,Kb 200	7.01	0.62	-0.79	0.82
RE 0.005,RR 14,RO 16%,Kb 200	2.32	0.63	-0.87	0.82
RE 0.005,RR 14,RO 13%,Kb 200	2.28	0.63	-0.87	0.82
RE 0.005,RR 14,RO 10%,Kb 200	2.25	0.64	-0.88	0.81
RE 0.005,RR 5,RO 10%,Kb 200	6.62	0.64	-0.89	0.81
RE 0.005,RR 11,RO 16%,Kb 300	2.78	0.64	-0.90	0.81
RE 0.007,RR 14,RO 16%,Kb 200	3.03	0.64	-0.92	0.81
RE 0.007,RR 14,RO 13%,Kb 200	3.00	0.64	-0.92	0.81
RE 0.007,RR 14,RO 10%,Kb 200	2.97	0.64	-0.93	0.81
RE 0.005,RR 14,RO 16%,Kb 300	2.10	0.64	-0.93	0.81
RE 0.005,RR 11,RO 13%,Kb 300	2.65	0.64	-0.93	0.81
RE 0.007,RR 14,RO 13%,Kb 2	2.06	0.65	-0.94	0.81
RE 0.005,RR 14,RO 13%,Kb 300	2.06	0.65	-0.94	0.81
RE 0.005,RR 11,RO 10%,Kb 300	2.55	0.65	-0.95	0.81
RE 0.007,RR 8,RO 16%,Kb 200	7.25	0.65	-0.95	0.81
RE 0.007,RR 14,RO 16%,Kb 300	2.73	0.65	-0.95	0.81
RE 0.005,RR 14,RO 10%,Kb 300	2.01	0.65	-0.96	0.81
RE 0.007,RR 14,RO 13%,Kb 300	2.70	0.65	-0.96	0.81
RE 0.007,RR 14,RO 10%,Kb 300	2.66	0.65	-0.97	0.81
RE 0.005,RR 11,RO 16%,Kb 2	7.71	0.65	-0.99	0.80
RE 0.009,RR 14,RO 16%,Kb 300	3.34	0.66	-1.06	0.80
RE 0.009,RR 14,RO 13%,Kb 300	3.31	0.67	-1.07	0.80
RE 0.007,RR 11,RO 16%,Kb 300	3.61	0.67	-1.07	0.80
RE 0.009,RR 14,RO 10%,Kb 300	3.28	0.67	-1.07	0.80
RE 0.009,RR 14,RO 13%,Kb 200	3.69	0.67	-1.08	0.80
RE 0.009,RR 14,RO 16%,Kb 200	3.71	0.67	-1.08	0.80
RE 0.007,RR 11,RO 10%,Kb 300	3.34	0.67	-1.08	0.80

RE 0.009,RR 14,RO 10%,Kb 200	3.67	0.67	-1.09	0.79
RE 0.007,RR 11,RO 13%,Kb 300	3.47	0.67	-1.09	0.79
RE 0.005,RR 5,RO 16%,Kb 200	7.02	0.68	-1.13	0.79
RE 0.009,RR 8,RO 10%,Kb 300	7.20	0.70	-1.26	0.78
RE 0.005,RR 5,RO 10%,Kb 100	7.29	0.70	-1.31	0.77
RE 0.009,RR 11,RO 16%,Kb 100	7.72	0.71	-1.35	0.77
RE 0.009,RR 11,RO 10%,Kb 300	4.11	0.71	-1.35	0.77
RE 0.009,RR 11,RO 13%,Kb 100	7.70	0.71	-1.37	0.77
RE 0.009,RR 11,RO 13%,Kb 300	4.24	0.72	-1.39	0.77
RE 0.009,RR 11,RO 16%,Kb 300	4.41	0.72	-1.39	0.77
RE 0.005,RR 5,RO 13%,Kb 200	7.51	0.72	-1.44	0.76
RE 0.005,RR 5,RO 13%,Kb 100	7.51	0.72	-1.44	0.76
RE 0.007,RR 8,RO 10%,Kb 100	7.86	0.74	-1.56	0.75
RE 0.007,RR 5,RO 10%,Kb 300	7.43	0.74	-1.57	0.75
RE 0.009,RR 8,RO 16%,Kb 300	7.56	0.74	-1.58	0.75
RE 0.005,RR 5,RO 16%,Kb 100	7.71	0.75	-1.59	0.75
RE 0.007,RR 5,RO 13%,Kb 300	7.57	0.76	-1.69	0.73
RE 0.007,RR 8,RO 13%,Kb 100	8.14	0.78	-1.81	0.72
RE 0.007,RR 5,RO 16%,Kb 300	7.75	0.78	-1.86	0.72
RE 0.007,RR 8,RO 16%,Kb 100	8.34	0.80	-1.96	0.71
RE 0.009,RR 8,RO 10%,Kb 200	8.39	0.82	-2.09	0.70
RE 0.009,RR 8,RO 13%,Kb 300	8.55	0.84	-2.26	0.68
RE 0.009,RR 8,RO 13%,Kb 200	8.55	0.84	-2.26	0.68
RE 0.009,RR 8,RO 16%,Kb 200	8.82	0.87	-2.52	0.65
RE 0.007,RR 5,RO 10%,Kb 200	8.52	0.90	-2.80	0.63
RE 0.007,RR 14,RO 10%,Kb 100	8.84	0.91	-2.89	0.62
RE 0.007,RR 14,RO 10%,Kb 2	8.84	0.91	-2.89	0.62
RE 0.007,RR 5,RO 13%,Kb 200	8.67	0.92	-2.94	0.61
RE 0.007,RR 14,RO 16%,Kb 2	9.10	0.94	-3.07	0.60
RE 0.007,RR 11,RO 10%,Kb 2	9.47	0.95	-3.24	0.58
RE 0.007,RR 5,RO 16%,Kb 200	8.95	0.96	-3.25	0.58
RE 0.009,RR 5,RO 10%,Kb 300	8.97	0.96	-3.26	0.58
RE 0.005,RR 8,RO 10%,Kb 2	9.40	0.98	-3.44	0.56
RE 0.007,RR 11,RO 13%,Kb 2	9.65	0.98	-3.44	0.56
RE 0.009,RR 5,RO 13%,Kb 300	9.12	0.98	-3.45	0.56
RE 0.005,RR 8,RO 16%,Kb 2	9.72	0.99	-3.54	0.55
RE 0.005,RR 8,RO 13%,Kb 2	9.60	0.99	-3.54	0.55
RE 0.009,RR 5,RO 16%,Kb 300	9.30	1.00	-3.70	0.54
RE 0.009,RR 8,RO 10%,Kb 100	9.63	1.02	-3.83	0.52

RE 0.007,RR 11,RO 16%,Kb 2	10.05	1.02	-3.84	0.52
RE 0.007,RR 5,RO 10%,Kb 100	9.38	1.02	-3.85	0.52
RE 0.007,RR 5,RO 13%,Kb 100	9.64	1.05	-4.09	0.50
RE 0.009,RR 8,RO 13%,Kb 100	9.93	1.06	-4.22	0.49
RE 0.007,RR 5,RO 16%,Kb 100	9.83	1.07	-4.31	0.48
RE 0.009,RR 8,RO 16%,Kb 100	10.15	1.08	-4.43	0.47
RE 0.009,RR 5,RO 10%,Kb 200	10.32	1.18	-5.44	0.37
RE 0.009,RR 5,RO 16%,Kb 200	10.78	1.24	-6.13	0.30
RE 0.009,RR 14,RO 10%,Kb 2	10.91	1.27	-6.46	0.27
RE 0.005,RR 5,RO 10%,Kb 2	11.44	1.28	-6.61	0.25
RE 0.009,RR 14,RO 13%,Kb 2	11.06	1.28	-6.63	0.25
RE 0.009,RR 14,RO 16%,Kb 2	11.16	1.28	-6.67	0.24
RE 0.005,RR 5,RO 13%,Kb 2	11.70	1.30	-6.91	0.22
RE 0.009,RR 11,RO 10%,Kb 100	11.65	1.31	-7.04	0.21
RE 0.009,RR 11,RO 10%,Kb 2	11.65	1.31	-7.04	0.21
RE 0.009,RR 5,RO 10%,Kb 100	11.36	1.34	-7.31	0.18
RE 0.009,RR 11,RO 13%,Kb 2	11.82	1.34	-7.34	0.18
RE 0.005,RR 5,RO 16%,Kb 2	12.05	1.35	-7.48	0.17
RE 0.009,RR 5,RO 13%,Kb 200	11.64	1.37	-7.68	0.15
RE 0.009,RR 5,RO 13%,Kb 100	11.64	1.37	-7.68	0.15
RE 0.009,RR 11,RO 16%,Kb 2	12.28	1.38	-7.88	0.13
RE 0.009,RR 5,RO 16%,Kb 100	11.85	1.39	-7.96	0.12
RE 0.007,RR 8,RO 10%,Kb 2	12.27	1.43	-8.48	0.07
RE 0.007,RR 8,RO 16%,Kb 2	12.58	1.44	-8.60	0.06
RE 0.007,RR 8,RO 13%,Kb 2	12.47	1.44	-8.63	0.05
RE 0.007,RR 5,RO 10%,Kb 2	14.72	1.80	-14.07	-0.48
RE 0.007,RR 5,RO 13%,Kb 2	14.99	1.83	-14.53	-0.53
RE 0.009,RR 8,RO 10%,Kb 2	15.00	1.86	-15.18	-0.59
RE 0.009,RR 8,RO 16%,Kb 2	15.29	1.87	-15.28	-0.60
RE 0.009,RR 8,RO 13%,Kb 2	15.20	1.88	-15.38	-0.61
RE 0.007,RR 5,RO 16%,Kb 2	15.39	1.88	-15.48	-0.62
RE 0.009,RR 5,RO 10%,Kb 2	17.81	2.30	-23.54	-1.41
RE 0.009,RR 5,RO 13%,Kb 2	18.11	2.33	-24.17	-1.48
RE 0.009,RR 5,RO 16%,Kb 2	18.55	2.39	-25.54	-1.61

b) Plot 3 (untreated)

Scenario	Soil loss (kg/m²)	RMSE	ME	R²
RE0.003,RR11,R4118,Kb200	2.857	0.28	0.40	0.82
RE0.003,RR11,R3815,Kb200	3.115	0.28	0.39	0.82
RE0.003,RR14,R4421,Kb100	2.788	0.29	0.38	0.82
RE0.003,RR14,R3815,Kb200	2.89	0.29	0.35	0.81
RE0.003,RR14,R4118,Kb100	3.031	0.29	0.35	0.81
RE0.003,RR14,R3815,Kb100	3.24	0.30	0.31	0.80
RE0.003,RR14,R4118,Kb200	2.804	0.31	0.29	0.79
RE0.003,RR11,R4421,Kb200	3.12	0.34	0.14	0.75
RE0.005,RR14,R4421,Kb200	2.479	0.34	0.13	0.75
RE0.003,RR14,R4421,Kb200	1.761	0.35	0.06	0.72
RE0.007,RR14,R4421,Kb200	3.153	0.37	-0.03	0.70
RE0.003,RR11,R4118,Kb300	3.059	0.39	-0.18	0.65
RE0.003,RR11,R3815,Kb300	3.054	0.40	-0.22	0.64
RE0.003,RR8,R4421,Kb300	3.84	0.40	-0.24	0.64
RE0.003,RR14,R4118,Kb300	2.619	0.41	-0.27	0.63
RE0.003,RR8,R3815,Kb200	4.45	0.42	-0.33	0.61
RE0.005,RR11,R4118,Kb200	4.08	0.43	-0.42	0.58
RE0.005,RR14,R4421,Kb100	3.961	0.43	-0.43	0.58
RE0.003,RR11,R4421,Kb100	4.419	0.44	-0.46	0.57
RE0.003,RR8,R4421,Kb200	4.305	0.45	-0.52	0.55
RE0.003,RR14,R3815,Kb300	2.44	0.46	-0.60	0.53
RE0.003,RR8,R4118,Kb300	4.64	0.48	-0.74	0.49
RE0.005,RR11,R3815,Kb200	4.493	0.48	-0.74	0.49
RE0.003,RR14,R4421,Kb300	2.024	0.48	-0.77	0.48
RE0.005,RR14,R3815,Kb200	4.20	0.49	-0.82	0.47
RE0.005,RR14,R4118,Kb100	4.344	0.49	-0.83	0.47
RE0.003,RR8,R3815,Kb300	4.91	0.49	-0.84	0.46
RE0.005,RR14,R4118,Kb300	3.81	0.49	-0.84	0.46
RE0.005,RR14,R4118,Kb200	4.04	0.50	-0.91	0.44
RE0.003,RR11,R4118,Kb100	5.068	0.51	-0.94	0.43
RE0.003,RR11,R4421,Kb300	2.286	0.51	-0.96	0.43
RE0.005,RR11,R4118,Kb300	4.426	0.52	-1.02	0.41
RE0.005,RR11,R3815,Kb300	4.47	0.52	-1.06	0.40
RE0.005,RR14,R3815,Kb100	4.68	0.52	-1.06	0.40
RE0.003,RR11,R3815,Kb100	5.303	0.53	-1.10	0.39
RE0.003,RR8,R4118,Kb200	4.715	0.53	-1.15	0.37
RE0.005,RR14,R3815,Kb300	3.58	0.55	-1.25	0.34

RE0.005,RR14,R4421,Kb300	2.931	0.55	-1.27	0.33
RE0.005,RR11,R4421,Kb200	4.433	0.57	-1.42	0.29
RE0.005,RR11,R4421,Kb300	3.286	0.60	-1.74	0.20
RE0.005,RR8,R4421,Kb300	5.434	0.61	-1.78	0.19
RE0.007,RR14,R4118,Kb300	4.918	0.62	-1.89	0.15
RE0.007,RR14,R4421,Kb100	5.046	0.63	-1.96	0.13
RE0.007,RR11,R4118,Kb200	5.223	0.63	-2.03	0.11
RE0.007,RR14,R4421,Kb300	3.78	0.64	-2.09	0.10
RE0.007,RR14,R3815,Kb300	4.66	0.67	-2.36	0.02
RE0.007,RR11,R4118,Kb300	5.69	0.68	-2.47	-0.02
RE0.003,RR5,R4421,Kb200	6.008	0.68	-2.52	-0.03
RE0.003,RR8,R4421,Kb100	5.966	0.69	-2.55	-0.04
RE0.007,RR11,R3815,Kb300	5.792	0.69	-2.55	-0.04
RE0.007,RR11,R3815,Kb200	5.773	0.71	-2.85	-0.13
RE0.003,RR5,R4118,Kb300	6.344	0.71	-2.86	-0.13
RE0.007,RR14,R4118,Kb100	5.55	0.72	-2.89	-0.14
RE0.007,RR11,R4421,Kb300	4.216	0.72	-2.89	-0.14
RE0.005,RR11,R4421,Kb100	6.321	0.72	-2.93	-0.15
RE0.007,RR14,R3815,Kb200	5.40	0.72	-2.95	-0.16
RE0.003,RR5,R3815,Kb300	6.513	0.73	-3.02	-0.18
RE0.007,RR14,R4118,Kb200	5.188	0.73	-3.05	-0.19
RE0.005,RR8,R3815,Kb200	6.359	0.74	-3.12	-0.21
RE0.005,RR8,R4421,Kb200	6.057	0.76	-3.34	-0.27
RE0.007,RR14,R3815,Kb100	6.01	0.77	-3.45	-0.30
RE0.003,RR8,R4118,Kb100	6.654	0.78	-3.65	-0.36
RE0.003,RR5,R4118,Kb200	7.082	0.80	-3.83	-0.41
RE0.007,RR11,R4421,Kb200	5.651	0.81	-4.01	-0.47
RE0.005,RR8,R4118,Kb300	6.635	0.82	-4.09	-0.49
RE0.007,RR8,R4421,Kb300	6.889	0.83	-4.18	-0.52
RE0.003,RR8,R3815,Kb100	6.896	0.83	-4.20	-0.52
RE0.003,RR5,R4421,Kb300	6.953	0.84	-4.39	-0.58
RE0.003,RR5,R3815,Kb200	7.194	0.85	-4.45	-0.60
RE0.005,RR8,R3815,Kb300	7.073	0.86	-4.54	-0.62
RE0.005,RR11,R4118,Kb100	7.296	0.86	-4.61	-0.64
RE0.005,RR11,R3815,Kb100	7.703	0.91	-5.20	-0.82
RE0.005,RR8,R4118,Kb200	6.696	0.92	-5.38	-0.87
RE0.003,RR5,R3815,Kb100	7.62	0.95	-5.85	-1.01
RE0.007,RR11,R4421,Kb100	8.049	1.00	-6.63	-1.23
RE0.003,RR14,R4421,Kb2	9.129	1.04	-7.24	-1.42

RE0.007,RR8,R3815,Kb200	8.087	1.05	-7.34	-1.44
RE0.007,RR8,R4421,Kb200	7.648	1.06	-7.51	-1.49
RE0.003,RR5,R4421,Kb100	8.223	1.06	-7.53	-1.50
RE0.005,RR5,R4421,Kb200	8.325	1.07	-7.60	-1.52
RE0.005,RR8,R4421,Kb100	8.449	1.11	-8.36	-1.74
RE0.003,RR14,R3815,Kb2	9.317	1.12	-8.53	-1.79
RE0.003,RR14,R4118,Kb2	9.465	1.13	-8.62	-1.82
RE0.007,RR8,R4118,Kb300	8.455	1.15	-8.98	-1.92
RE0.005,RR5,R4118,Kb300	8.942	1.16	-9.17	-1.98
RE0.003,RR5,R4118,Kb100	8.797	1.17	-9.41	-2.05
RE0.005,RR5,R4421,Kb300	9.191	1.20	-9.87	-2.18
RE0.007,RR11,R4118,Kb100	9.316	1.20	-9.95	-2.21
RE0.005,RR5,R3815,Kb300	9.266	1.20	-9.95	-2.21
RE0.007,RR8,R3815,Kb300	9.043	1.20	-9.95	-2.21
RE0.005,RR5,R4118,Kb200	9.877	1.26	-11.04	-2.53
RE0.007,RR11,R3815,Kb100	9.881	1.27	-11.17	-2.56
RE0.005,RR8,R4118,Kb100	9.517	1.28	-11.36	-2.62
RE0.007,RR8,R4118,Kb200	8.498	1.28	-11.48	-2.66
RE0.003,RR11,R3815,Kb2	10.609	1.32	-12.21	-2.87
RE0.003,RR11,R4118,Kb2	10.803	1.34	-12.52	-2.96
RE0.003,RR11,R4421,Kb2	11.021	1.35	-12.83	-3.05
RE0.005,RR8,R3815,Kb100	9.93	1.36	-12.96	-3.09
RE0.005,RR5,R3815,Kb200	10.166	1.36	-12.98	-3.10
RE0.007,RR5,R4421,Kb200	10.406	1.42	-14.31	-3.49
RE0.005,RR5,R3815,Kb100	10.69	1.50	-16.04	-3.99
RE0.007,RR8,R4421,Kb100	10.685	1.51	-16.26	-4.06
RE0.005,RR5,R4421,Kb100	11.022	1.52	-16.54	-4.14
RE0.007,RR5,R4421,Kb300	11.201	1.54	-16.92	-4.25
RE0.007,RR5,R4118,Kb300	11.281	1.57	-17.58	-4.44
RE0.007,RR5,R3815,Kb300	11.756	1.64	-19.31	-4.95
RE0.005,RR14,R4421,Kb2	12.831	1.65	-19.56	-5.02
RE0.005,RR5,R4118,Kb100	11.732	1.66	-19.89	-5.12
RE0.007,RR5,R4118,Kb200	12.389	1.68	-20.42	-5.28
RE0.007,RR8,R4118,Kb100	12.088	1.73	-21.72	-5.66
RE0.005,RR14,R4118,Kb2	13.476	1.80	-23.49	-6.17
RE0.003,RR8,R3815,Kb2	14.113	1.81	-23.89	-6.29
RE0.005,RR14,R3815,Kb2	13.43	1.82	-24.17	-6.37
RE0.007,RR5,R3815,Kb200	12.843	1.83	-24.21	-6.39
RE0.007,RR8,R3815,Kb100	12.647	1.85	-24.74	-6.54

RE0.003,RR8,R4118,Kb2	14.521	1.87	-25.39	-6.73
RE0.003,RR8,R4421,Kb2	14.524	1.88	-25.72	-6.83
RE0.007,RR5,R4421,Kb100	13.514	1.95	-27.65	-7.39
RE0.007,RR5,R3815,Kb100	13.427	2.00	-29.26	-7.87
RE0.005,RR11,R4421,Kb2	15.436	2.08	-31.69	-8.58
RE0.005,RR11,R4118,Kb2	15.293	2.09	-32.05	-8.68
RE0.005,RR11,R3815,Kb2	15.198	2.10	-32.29	-8.75
RE0.007,RR5,R4118,Kb100	14.355	2.12	-32.97	-8.95
RE0.007,RR14,R4421,Kb2	16.175	2.20	-35.70	-9.75
RE0.003,RR5,R3815,Kb2	16.883	2.28	-38.21	-10.49
RE0.003,RR5,R4118,Kb2	17.545	2.37	-41.58	-11.48
RE0.007,RR14,R4118,Kb2	17.095	2.41	-43.00	-11.89
RE0.003,RR5,R4421,Kb2	17.919	2.42	-43.26	-11.97
RE0.007,RR14,R3815,Kb2	17.14	2.46	-44.82	-12.42
RE0.007,RR11,R4421,Kb2	19.405	2.74	-55.72	-15.62
RE0.007,RR11,R4118,Kb2	19.323	2.77	-57.15	-16.04
RE0.005,RR8,R3815,Kb2	20.163	2.80	-58.07	-16.31
RE0.007,RR11,R3815,Kb2	19.316	2.80	-58.33	-16.38
RE0.005,RR8,R4421,Kb2	20.308	2.83	-59.36	-16.68
RE0.005,RR8,R4118,Kb2	20.537	2.84	-60.07	-16.89
RE0.005,RR5,R3815,Kb2	23.767	3.41	-86.79	-24.72
RE0.005,RR5,R4118,Kb2	24.488	3.51	-92.34	-26.35
RE0.005,RR5,R4421,Kb2	24.771	3.54	-93.93	-26.81
RE0.007,RR8,R3815,Kb2	25.533	3.67	-100.53	-28.75
RE0.007,RR8,R4421,Kb2	25.453	3.67	-100.64	-28.78
RE0.007,RR8,R4118,Kb2	25.886	3.71	-102.89	-29.44
RE0.007,RR5,R3815,Kb2	29.806	4.39	-144.94	-41.76
RE0.007,RR5,R4118,Kb2	30.578	4.51	-152.68	-44.02
RE0.007,RR5,R4421,Kb2	30.782	4.52	-153.74	-44.34

University of Natural Resources and Life Sciences, Vienna

Department of Water, Atmosphere and Environment

Institute of Hydraulics and Rural Water Management

Master Thesis

MONITORING AND SIMULATION OF SOIL EROSION IN THE ETHIOPIAN HIGHLANDS ON A PLOT SCALE

for attainment of the academic degree of

Diplomingenieur

presented by

Claire Brenner

Supervisor: Ao.Univ.Prof. Dipl.-Ing. Dr.nat.techn. Andreas Klik

Co – supervisor: Dipl.-Ing. Stefan Strohmeier

October 2013

Acknowledgement

„In jede hohe Freude mischt sich eine Empfindung der Dankbarkeit.“
Marie Freifrau von Ebner-Eschenbach

I would like to express my gratitude to my supervisor Andreas Klik, for his support and effort through the whole work. Furthermore, I want to thank my co-supervisor Stefan Strohmeier for his constant help during the writing process.

I wrote my thesis in the framework of the project “Unlocking the potential of rain-fed agriculture in Ethiopia for improved rural livelihood”. I wish to express my sincere thanks to the cooperation partners, ICARDA and ARARI, as well as the Austrian Development Agency, who sponsored the project. I give my special gratitude to Feras Ziadat and Wondimu Bayu, who supported and advised me in the fieldwork.

This thesis would not have been possible without the help and collaboration of the local community in the study area. I thank Baye, who was an indispensable help during the stay in Ethiopia.

A special thank goes to my friends and family. I am especially grateful for the love and encouragement of my mother, grandmother, Kathi, Elke and David, who supported me across the years. “*Let us be grateful to people who make us happy, they are the charming gardeners who make our souls blossom*.” (Marcel Proust)

Abstract

Soil erosion is the main driving force for global land degradation. Soil erosion measurements are an important tool to assess soil loss under site-specific conditions and evaluate the impact of changes in land use on its magnitude. Based on this, adjusted management strategies can help to maintain or enhance the state of the soil. This work assessed soil loss rates on a plot scale in a 54 km² large agricultural catchment near Gondar, Ethiopia. At the experimental site, stone bunds were implemented in 2011 to prevent severe soil erosion. During the rainy season 2012 (July and August), three soil erosion plots with areas between 300 and 480 m² were installed and soil loss measurements were carried out. Soil loss from the three plots was 0.3, 3.0 and 4.7 kg m^{-2}, respectively. Additionally, canopy and rock fragment cover, hydraulic conductivity as well as other soil properties were determined. Based on the data obtained from the field, the Water Erosion Prediction Project (WEPP) model was adjusted and calibrated. Furthermore, the model will be calibrated with more field-measured data sets of runoff and soil loss in the investigated watershed. In the future, it will then be used as demonstration tool to evaluate the response of soil erosion to changes in management practices or the implementation of soil and water conservation measures in the Ethiopian Highlands.

Zusammenfassung

Erosion stellt eine der größten Bedrohungen bei der Erhaltung der natürlichen Ressource *Boden* dar. Bodenerosionsmessungen helfen bei der Abschätzung von Erosionsraten unter spezifischen Bewirtschaftungs- und anderen ortsbezogenen Bedingungen. Davon ausgehend können Strategien zur Erhaltung oder Verbesserung des Bodens geplant und entwickelt werden. Um einer fortschreitenden Bodenerosion entgegenzuwirken, wurden 2011 „Stone Bunds“ im Untersuchungsgebiet, einem 54 km² großen, landwirtschaftlich genutzten Einzugsgebiet nahe Gondar, Äthiopien, errichtet. In dieser Arbeit wurden Bodenerosionsmessungen auf Plot-Ebene an drei Versuchsflächen (300 – 480 m²) durchgeführt. In der Regenperiode 2012 wurden in den Monaten Juli und August Bodenerosionsraten von 0.3, 3.0 und 4.7 kg m^{-2} für die Versuchsflächen gemessen. Zusätzlich zu den Bodenerosionsmessungen wurden ergänzende Informationen zum Standort, wie Pflanzenbedeckungsgrad, Steinanteil des Bodens, Bodentextur und Durchlässigkeit aufgenommen. Mithilfe von diesen - vor Ort gewonnenen - Daten wurde ein Bodenerosionsmodell, das Water Erosion Prediction Project (WEPP) Modell, an lokale Bedingungen angepasst und kalibriert. In einem nächsten Schritt wird das Modell aufgrund weiterer Abfluss- und Erosionsmessungen im untersuchten Einzugsgebiet geprüft und gegebenenfalls adaptiert werden. Zukünftig kann das Modell dazu genutzt werden, Auswirkungen durch Änderungen der Bewirtschaftung, Niederschlagsverhältnisse oder den Einsatz von bodenverbessernden Maßnahmen im Äthiopischen Hochland zu simulieren und zu bewerten.

Table of Content

1. Introduction and Objectives

Extensive land degradation in the Ethiopian Highlands jeopardizes rural livelihood. Ongoing deforestation and increasing population pressure worsen the soil erosion problem.

The project “Unlocking the potential of rain-fed agriculture in Ethiopia for improved rural livelihood” investigates strategies to prevent further degradation of the soil and enhance productivity of rain-fed agriculture in the Ethiopian Highlands. The Austrian Development Agency (ADA) sponsors this project, which is conducted in international cooperation between the University of Natural Resources and Life Sciences, Vienna (BOKU), the International Centre for Agricultural Research in the Dry Areas (ICARDA) and the Amhara Regional Agricultural Research Institute (ARARI). Experimental site is the Gumara-Maksegnit watershed, Amhara Region.

The present master thesis was conducted within this project. It aimed to monitor soil loss on a plot scale in a watershed in the Ethiopian Highlands and assess soil loss rates due to water erosion from arable land. The experimental site was situated in a watershed, representative for cultivated land in this region. Soil loss monitoring on a plot scale provides physically comprehensible conditions, which allow monitoring of soil loss at a site with known climate, crop and soil properties.

Data acquisition was conducted in July and August 2012. Soil loss was measured at three experimental plots situated at the same hillslope. Sediments were collected in retention basins at the end of the plots and removed and weighed as often as possible. Canopy and rock fragment cover as well as soil properties were analysed in order to estimate their impact on the soil erosion process. Additionally, this work accounted for the hillslope intersection effect by stone bunds, implemented at the experimental site.

This site-specific knowledge has been applied to a soil loss prediction model. The Water Erosion Prediction Project (WEPP) model was adapted to local conditions and calibrated based on field observations. The idea of this work was to find a configuration of the model, which predicts soil loss adequately for the experimental site. Once calibrated, the model enables simulation of various scenarios concerning the effect of large storms, crop rotation and conservation practices within short time. Thus, the aim of soil loss predictions was not to carve out an exact value of soil loss, but evaluate the effect of these different management scenarios.

In a successive step, this local information can be integrated into a conceptual soil erosion model, which models soil loss processes on a bigger scale.

2. Land degradation - a threat to rural livelihood

Soil forms the top layer of the earth's crust. It is a complex and variable system of mineral particles, water, air, organic matter, and living organisms. Soil provides multiple functions, which are essential to human well-being. Soil is the basis for human activities and infrastructure, food and biomass production. Additionally, it enables storage, filtration and transformation of organic and mineral substances. Soil is a source of raw materials and acts as habitat and gene pool ("European Commission" 2013). As the process of soil formation is slow, soil has to be considered as a non-renewable resource. Thus, its protection is crucial in order to guarantee its ecosystem services in the future (Jones et al. 2012).

Land degradation is a global problem, concerning soils around the planet. Figure 1 shows a map of global soil degradation levels. Except for the northern part of the northern hemisphere, most soils in the world are degraded or very degraded.

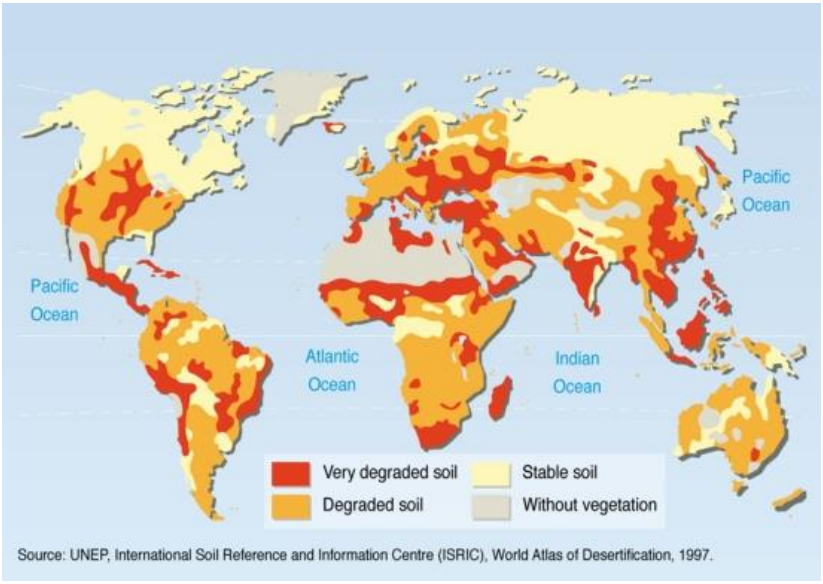

Figure 1: Global soil degradation map ("World Atlas of Desertification" 1997)

Soil degradation jeopardizes the land's capacity to provide ecosystem services and goods. ("Natural Resources and Environment: Land Degradation Assessment" 2013). It sums up the degradation effects of different processes including decline in biodiversity and organic matter, compaction, chemical contamination, wind and water erosion, salinisation, sealing and landslides (Jones et al. 2012).

According to the report *Global Environment Outlook 4: Environment for Development* (2007), increasing human demands on land resources are the main driving forces for ongoing land degradation. Changes in land use, such as forest cover and composition, cropland expansion and intensification, as well as urban development highly affect this process. Unsustainable agricultural land use - including poor soil and water conservation practices, poor crop rotation and irrigation schemes as well as overgrazing - put pressure on the environment and negatively influence soil and soil services.

Altogether, this leads to a reduction in productivity and biodiversity. Consequently socio-economic problems like uncertainty in food security and environmental problems as damage of ecosystems arise ("Natural Resources and Environment: Land Degradation Assessment"

2013). Land degradation and poverty accompany each other and end in a “poverty, food insecurity and natural resources degradation trap” (Dejene 2003).

The report “Ecosystems and Human Well-Being: Current State and Trends” stresses that the negative impacts of land degradation – even though it is a global problem – affect some regions more than others: the poorest people of the world are most exposed to negative effects of environmental change (Kasperson and Archer 2005).

Figure 2 maps types of degradation in Africa. 16 % of the total land area is affected by some kind of degradation. Among all types of degradation, water erosion is the key threat to soils in Africa and in the study area of this work, affecting about 8 % of the continent (Jones et al. 2013).

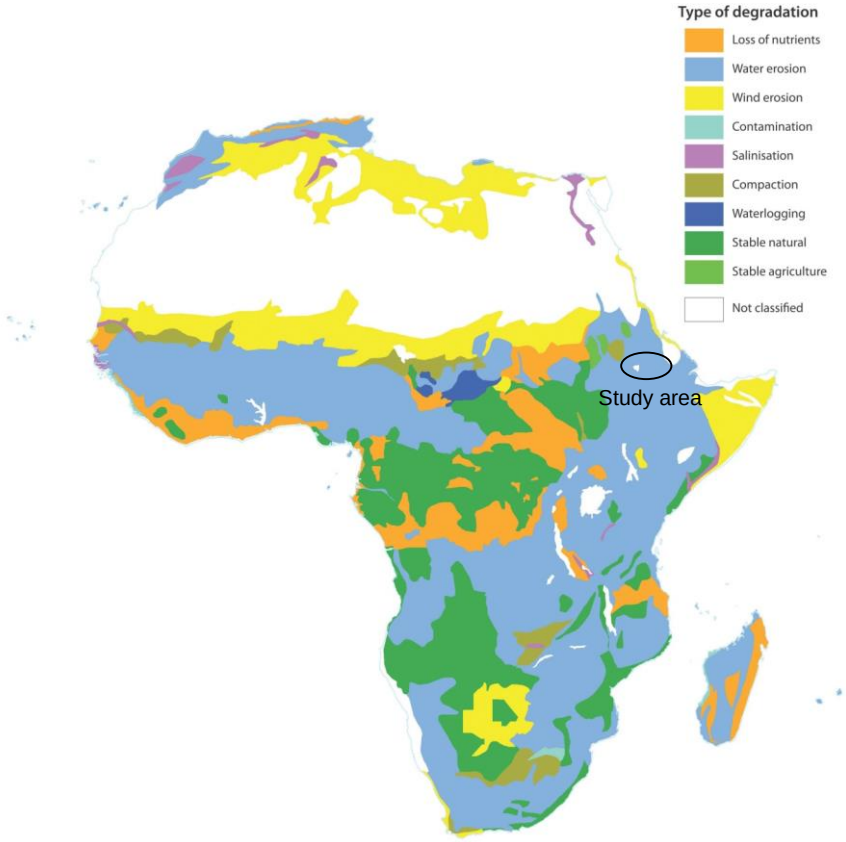

Figure 2: Map showing types of degradation across Africa (Jones et al. 2013)

3. Ethiopia – an overview

The study area is situated in Amhara Region, in the Ethiopia Highlands. The Ethiopian Highlands cover 44 % of the total area and are the largest continuous plateau of its altitude, above 1500 m a.s.l, in the African continent. 88 % of the country's population lives in the Ethiopian Highlands (Krüger, Gebremichael, and Kejela 1997).

Agriculture is the economic basis of the country, which accounts for almost half of the gross domestic product (GDP) of the country. 85 % of the population works in the agricultural sector. This goes along with a low urbanization level; More than 80 % of the whole population live in rural areas ("The World Factbook" 2013).

Soil erosion and loss of fertile topsoil jeopardize the livelihood of this rural population. The subsistence farming system leaves them highly vulnerable to decreases in production and crop yields.

Figure 1 shows a map of areas with most severe soil degradation in Africa. This classification in based on a combination of the degree and the relative extent of the process. The figure shows that big parts of Ethiopia are affected by most severe soil degradation.

Hurni (1988) estimated that soil loss from arable land in Ethiopia is about 42 t ha^{-1} yr^{-1}.

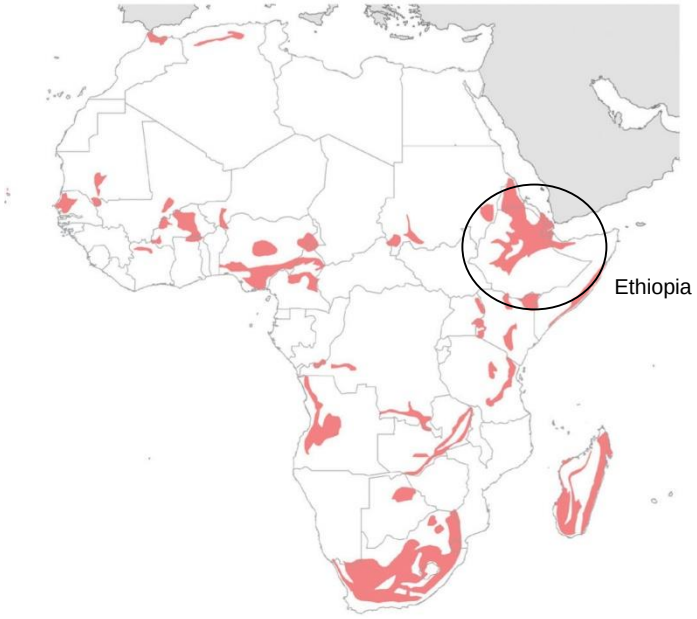

Figure 3: map showing areas with most severe soil degradation in Africa (L. R. Oldeman, Hakkeling, and Sombroek 1991).

Farmers mostly depend on subsistence rain-fed agriculture. In 2001, less than 3 % of the cultivated area was equipped for irrigation (aquastat 2005).

Ethiopia faced droughts and extreme famines in 1974 and 1975. This raised attention to the problem of soil erosion, as land degradation and loss of topsoil were linked to droughts. With the support of the "Food for Work" Program, the government started soil and water conservation and rehabilitation campaigns to combat further degradation of arable land. In 1981, in collaboration with the University of Bern, the Ministry of Agriculture founded the Soil Conservation Research Project (SCRP) (Dejene 2003).

The geographic location within the tropics characterizes the Ethiopian climate. Annual variation in temperature is low, while rainfall shows a pronounced bi-modal pattern with a main rainy season (*kiremt*) from June to September and a low rainy season (*belg*) from February to April.

4. Soil erosion

Erosion is a natural process intensified and accelerated by human action. Natural erosion rates increased due to anthropogenic influences up to irreversible levels, exceeding 1 t ha^{-1} yr^{-1} within a span of 50 – 100 years (Gentile and Jones 2013).Soil erosion is considered to be the most widespread and severest form of land degradation.

Soil erosion describes the process of detachment, entrainment, transport and deposition of soil particles either produced by water, wind, disturbance and translocation (e.g. tillage), landslides and floods. However, soil and wind erosion are the main drivers of soil degradation. 56 % of the total global degraded area is affected by water erosion; 28 % by wind erosion (L. Oldeman 1991).

Consequences of soil erosion are manifold and induce on-site as well as off-site effects. While on-site effects are mainly related to a reduction in topsoil and soil productivity, off-site effects occur due to deposition of transported sediments and chemicals causing sedimentation, silting of water resources, alteration of the landscape, reduction of habitats and infrastructure damages (Blanco-Canqui and Lal 2008).

Because of soil particle removal, the thickness of the nutrient-rich topsoil decreases. Thus, this decline in topsoil depth goes along with nutrient loss, reduction of rooting depth, reduction of water and nutrient storage capacity and, hence, plant productivity (Braimoh and Vlek 2008; Blanco-Canqui and Lal 2008). In Africa, 65 % of arable land faces loss of topsoil and nutrients due to erosion processes (Jones et al. 2013).

Referring to the causes of accelerated soil erosion, the leading drivers are deforestation, overgrazing and mismanagement of cultivated soil (Blanco-Canqui and Lal 2008). Soil texture and moisture, land use and vegetation cover, slope and climate are sensitive parameters influencing the intensity of soil erosion (Jones et al. 2013).

Arid and semi-arid regions with less than 600 mm precipitation per year and strong winds are especially prone to wind erosion. Low vegetation cover and poorly developed soils intensify wind erosion (Jones et al. 2013; Blanco-Canqui and Lal 2008). Saltation, soil creep and suspension are the forms of sediment transport due to wind erosion.

Contrary to wind erosion, water erosion is dominant in humid and sub-humid regions with intense rainfall events. It takes also an important role in arid and semiarid regions with distinctive seasonal rainfall pattern. Intense rainfall events occur after long dry periods when soils are bare and unprotected against the erosive power of the rainfall.

The following section outlines the mechanisms of erosion by water in more detail, as water erosion is the dominant form of erosion in this research study.

4.1 Water erosion

Soil erosion by water is the wearing away of topsoil as a result of the energy potential of rainfall and runoff. Detachment of soil particles initiates when shear stresses by raindrops and runoff exceed the resistance of the soil. Once in motion, sediments are transported by either saltation or surface runoff (Toy, Foster, and Renard 2002).

4.1.1 Processes

The kinematic energy of raindrops is the driving force for particle detachment. It depends on the falling velocity and the diameter of the raindrop (Roose 1996). It increases with rainfall intensity and raindrop size. Terminal velocity of the largest raindrops (6 mm) is about 10 m s^{-1} after falling more than 10 m (Gentile and Jones 2013; Roose 1996). Higher kinematic energy of the raindrops results in higher detachment rates.

Raindrops hitting the soil surface disperse and splash soil particles and eject them into the air (Blanco-Canqui and Lal 2008). Due to this splash effect of raindrops, particles distribute in all directions, but reach higher distances downhill than uphill. Consequently, particles move downslope. After particles are carried a short distance by this splash effect they are further transported by sheet runoff. Runoff starts when precipitation rates exceed infiltration rates and water starts to accumulate in puddles (Roose 1996). With increasing amount of water on the surface, a layer of flowing water forms and transports particles. This type of erosion is called interrill erosion.

Additionally, rain drops affecting the surface, break down soil aggregates and, thus, leave constituent particles. Those grains float into gaps, cracks or holes in the soil and plug soil pores, thus, form a crust on the top layer. After drying, these crusts enhance soil resistance and reduce infiltration. This leads to sealing of the surface and increasing runoff in storm rainfall events and increasing erosion rates downslope. Next to the crusting of the surface, the micro-topography and the sub-surface structure of the soil highly influence runoff and soil erosion. Micro-topography refers to the random roughness of the surface, which results from tillage and other management practices. Cracks and voids in the soil can build preferential flow paths, through which water infiltrates rapidly (Gentile and Jones 2013).

If runoff gains erosive power and entrains particles directly, small rills and channels of concentrated flow develop. Rills affect the heavily disturbed plough layer. As they do not deepen into layers beneath the ploughed layer, rills can be obliterated by tillage. Rills incising into deeper layers especially on steep slopes lead to the development of gullies, which cannot be undone by normal tillage operations (Gentile and Jones 2013). Rill erosion depends on the rill erodibility of the soil, runoff transport capacity and hydraulic shear of the runoff. Gully erosion is mainly controlled by the ratio of critical shear stress and shear stress induced on the channel bed by the runoff. If shear stress of the runoff exceeds the shear of the soil, new gullies form or extend (Blanco-Canqui and Lal 2008).

Table 1 lists types of soil erosion from initial splash erosion to gully erosion.

Table 1: Overview of soil erosion types (Blanco-Canqui and Lal 2008)

SPLASH EROSION	First stage of water erosion, when soil particles start moving due to the bombardment of the soil surface by raindrops.
SHEET/ INTERRILL EROSION	A shallow sheet of water flows over the surface and transports detached particles. It results in the removal of a thin, uniform layer of topsoil. Sheet erosion starts when rainfall intensity exceeds the infiltration capacity of the soil.
RILL EROSION	Sheet flow concentrates in channels. Due to higher flow velocity in the channel, concentrated flow not only transports but also detaches particles. Rills can be obliterated by tillage.
GULLY EROSION	Advanced stage of rill erosion, when rills deepen and widen until they form channels, which cannot be removed by tillage. Gullies account for severe sediment and nutrient loss, washout crops and expose plant roots, dissect cropland and cause alterations of the landscape.

4.1.2 Factors controlling water erosion

The main factors, which control the erosion process by water are PRECIPITATION, TOPOGRAPHY of the hillslope, SOIL PROPERTIES and VEGETATION COVER (Blanco-Canqui and Lal 2008). The Universal Soil Loss Equation (USLE) defines a fifth factor, the support practice factor, which determines the soil erosion process (Wischmeier and Smith 1965).

As already clear, PRECIPITATION is the main driving force for erosion. More intense storms lead to higher surface runoff and soil loss, thus intensity, amount and duration of the rainfall event strongly regulate the magnitude of soil loss.

The TOPOGRAPHY of a hillslope affects soil erosion, as steeper and longer slopes are more prone to surface runoff with high velocity. Additionally the transport capacity of the runoff increases with slope steepness.

VEGETATION intercepts rainfall water and thus protects the soil surface and minimizes the erosive force of the rainfall. Residues on the ground enhance the protection effect as they reduce the bouncing of the raindrops and increase surface roughness. In general, increase in vegetation cover leads to a decrease of soil detachment. Hereby, dense and short growing vegetation is more effective than scattered, taller vegetation. Perennial plants protect the soil better than annual crops, which leave the soil bare between to cropping seasons (Blanco-Canqui and Lal 2008).

Texture, macroporosity, infiltration capacity and organic matter content are SOIL PROPERTIES affecting the soil erosion process. Clay particles are easily transported by the runoff, but build strong aggregates, which hinders the detachment of the particles. The interaction of these factors defines the erodibility of the soil (Blanco-Canqui and Lal 2008).

4.1.3 Measuring soil erosion

Field experiments and soil erosion measurements are important tools to assess the degree of erosion at a specific area. The monitoring of soil loss under different management, soil and climatic conditions helps in the development and design of soil conservation measures and establishment of sustainable land management.

5. Stone bunds – a soil and water conservation measure

Stone bunds are a soil and water conservation measure. Its purpose is to control and diminish ongoing land degradation. An overview about soil and water conservation measures in general and stone bunds in particular is given in this chapter.

5.1 Soil and water conservation measures

Van Lynden et al. (2002) define soil and water conservation (SWC) measures as activities at a local level that maintain or enhance the productive capacity of the land in areas affected by, or prone to, degradation. SWC includes prevention or reduction in soil erosion, compaction, and salinity, conservation or drainage of surface and soil water, and maintenance or improvement of soil fertility. SWC technologies are agronomic, vegetative, structural, and management measures that control land degradation and enhance soil productivity (Liniger et al. 2002).

SWC includes measures on three different stages of degradation. Prevention intends to maintain and preserve soils, which are not affected by degradation yet. Mitigation takes place at an intermediate stage, when soils are already degraded, but land use is still possible. It aims to prevent further degradation and rebuild soil functions. If land degradation advanced to a stage, where previous land use cannot be continued, rehabilitation is the final stage for soil and water conservation measures. Of all three, the stage of rehabilitation needs the highest investment.

SWC measures can be classified into four groups (Braimoh and Vlek 2008).

1. Agronomic measures include mixed cropping, contour planting, mulching, direct planting and minimum/non-inversion tillage. They are not permanent but of short duration. As they are associated with annual crops, these measures recur every season. Agronomic measures do not alter the slope profile. An advantage of these measures is the little required input.

2. In contrary to agronomic measures, vegetative measures are associated with perennial plants, such as grasses, shrubs and trees. Thus, vegetative measures are of long duration. Grass strips, hedge barriers and windbreaks are often oriented along the contour, separating the fields. Commonly, they induce alteration of the slope profile.

3. Structural measures including terraces, banks, bunds, and palisades are constructions of wood, stone, concrete etc. Structural measures imply higher inputs of labour and money and are mostly of long duration or even permanent. Like vegetative measures, structural measures lead to changes in the slope profile. These structures are also applied along the contour or against wind direction.

4. Management measures involve a change in land use. This form of SWC is mainly applied to grazing land, where overgrazing led to severe degradation of the soil. Because of land use change, area closure or rotational grazing, vegetation cover improves.

Benefits from SWC measures are slowdown, retention and diversion of surface runoff, enhanced infiltration and surface cover, increased organic matter and soil fertility. Due to higher infiltration and reduced flow velocity, the soil is able to hold back more water. This effect is especially beneficiary in regions with longer dry seasons. Soil and water conservation measures can also help to disperse and interrupt concentrated flow (Braimoh and Vlek 2008).

5.2 Stone bunds

Stone bunds or stone lines are embankments set along the contours. They build barriers of stones, obstructing the surface runoff and reducing its velocity. Hence, these bunds reduce soil erosion on the field (Morgan 1995). Rows of stone bunds are placed at regular intervals and divide fields into segments of nearly the same length. Consequently, the effective slope length decreases. Sediments accumulate behind the bunds and backfill the bunds. Due to the deposition of sediments at the slope toe of each segment, terraces form and slope inclination declines.

In order to prevent further degradation of arable land, farmers in the study area applied graded stone bunds on their fields (February and April 2011). The implementation of this soil conservation measure was conducted in cooperation with the Government and within the framework of the project “Unlocking the potential of rain-fed agriculture in Ethiopia for improved rural livelihood”.

Stone bunds in the study area are slightly graded. This should guarantee that water, which accumulate behind the bunds, flows sidewise along the bund and leaves the field through a spillway. Figure 4 and Figure 5 show a stone bund at the experimental site and lines of stone bunds typical for the Ethiopian Highlands.

Figure 4: Stone bund at the experiment site. The area behind the bunds is not entirely filled

Figure 5: Stone bunds in the Ethiopian Highlands, Amhara Region

Bosshart (1997) divides the impacts of stone bunds into short- and long-term effects. While stone bunds reduce the slope length and retain runoff and sediments immediately after their construction, the effects of reduction in slope inclination, the formation of terraces and a change in land management are effects in the long-term.

In the Ethiopia Highlands, farmers take stones from their neighbouring fields for the construction of the bunds. Large stones (> 10 cm) build the skeletal structure of the wall. The medium stones are then used to backfill the bunds and small rock fragments top the backfill. Small stones with an average diameter of 2 cm act as filters and retain eroded sediments (Nyssen et al. 2001).

Gebremichael et al. (2005) showed that the introduction of stone bunds reduced annual soil loss due to water erosion by 68 %. This research was conducted in the Tigray Highlands, Ethiopia. Gebremichael et al. (2005) state that this positive effect due to accumulation behind the bunds, is highest for bunds in the first years after their construction, and declines with the age of the bunds, as they become more and more backfilled. Additionally, stone bunds enhance the storage of moisture in deeper horizons and lead to more productive arable land (Nyssen et al. 2007). In contrary, Hengsdijk et al. (2005) modelled the effect of stone bunds and concluded that the positive effect of this conservation measure is limited in the short run. (Herweg and Ludi 1999) also found no increase in yield but emphasize the effect of soil loss reduction due to stone bunds.

According to questionnaires and interviews by Nyssen et al. (2001), farmers in Ethiopia consider stone bunds to be the best way to deal with excess larger stones. However, farmers are aware of a positive effect on rock fragments on infiltration, retention of soil moisture and surface protection. Farmers are unwilling to remove especially the small stones, as they rate the beneficiary effects from this fraction as very positive. On the other hand, farmers often remove large stones with high surface cover.

6. WEPP – a soil erosion prediction model

EMPIRICAL, CONCEPTUAL and PHYSICALLY BASED models exist for different scales and available input parameters.

EMPIRICAL models have a simple structure, are user-friendly and allow rapid application. The empirical input coefficients are based on observations and measurements and thus do not simulate the erosion process as a physical process. Consequently, they are most suitable in regions with little input data. The Universal Soil Loss Equation (USLE) by Wischmeier and Smith (1965) is the most widely used empirical erosion model. It was originally developed from field observations in the U.S. and needs adjustments to local conditions in other regions of the world. In general, empirical models ignore the physical processes, the heterogeneity of rainfall, soil properties and other catchment characteristics.

CONCEPTUAL models are in between empirical and physically based models. They represent the processes in a catchment as a series of internal storages and include general process descriptions. They do not model interactions between processes and do not need extensive catchment information (Merritt, Letcher, and Jakeman 2003).

PHYSICALLY BASED models, in contrast, describe the physical processes behind soil erosion. They have a wider range of applicability as these models simulate the individual components of the entire erosion process by solving the corresponding equations. These models are more efficient in describing spatial and temporal variability of natural processes (Amore et al. 2004). Merritt et al. (2003) stress that measurement of all parameters is often not possible due to heterogeneities in the catchment, but parameters are estimated by calibrating simulated against observed data. Due to the vast amount of input needed for the model, uncertainties of the estimated parameters can lead to a “lack of identifiability of the parameters and a non-uniqueness of “best-fit” solutions”. Another problem of these kind of models is the upscaling of the governing processes, derived from small-scale observations, to much larger scales during the simulation process.

The Water Erosion Prediction Project (WEPP) (USDA-ARS 1989) is a distributed parameter, continuous simulation, erosion prediction model. It predicts soil loss and deposition as a function of its spatial and temporal distribution.

It is a physically based model, which needs input information on climate, slope, soil and management of the observed area. Each of these superior components consists of numerous parameters, as rainfall amounts and intensities, soil textural qualities, plant growth parameters, residue decomposition parameters, effects of tillage and tillage implements, slope shape and steepness and soil erodibility parameters. The input parameters, which change over time, such as surface roughness, canopy cover, canopy height, soil moisture and hydraulic conductivity are simulated on a daily basis. Based on this input, WEPP simulates runoff, soil detachment and deposition, sediment delivery off-site and sediment enrichment for each runoff event. The output holds information on on-site and off-site effects of soil loss separately. Runoff volume, soil loss, sediment yield and the characteristics of sediment size are predicted with temporal and spatial distribution. The application of the WEPP model is limited to areas with dominantly Hortonian overland flow, where rainfall rates exceed the infiltration capacity and subsurface flow is marginal.

Additionally to the soil erosion output, WEPP computes outputs on soil and plant parameters, water balance and crop yield.

By varying the input parameters and adapting them to different management and conservation scenarios, WEPP enables the evaluation of these scenarios according to multiple criteria.

The WEPP model can run in single storm or continuous mode. The present work is based on the monitoring of cumulative soil loss in the Gumara-Maksegnit watershed over the rainy period 2012 and thus WEPP ran in a continuous mode. Soil loss is predicted for a period of one year. Simulation starts on the first day of the year.

Zhang et al. (1996) evaluated the model using natural runoff plots. They contrasted measured and predicted soil loss and showed that WEPP slightly overestimated soil loss for small storms and for years with low runoff and soil loss rates and on the other hand underestimates soil loss for large events and for years with high runoff and soil loss rates. Nevertheless, average measured and predicted soil loss fit reasonably.

Even though the WEPP model is a physically based model Mahmoodabadi et al. (2013) stress that some empirical and/or statistical parameters are used in predicting model components. These dependencies can lead to reduced accuracy when these parameters do not suit to the conditions in the study area. The following section presents the model components and depicts their influence on soil loss.

6.1 Model components

The description of the main model components concentrates on those, which are essential to this work. This study was conducted on cropland and hence, this section outlines the model's approach to estimation of soil loss on cropland but does not consider solution methods, exclusively relevant for rangeland.

The description of the components is based on the WEPP Model Documentation (Flanagan and Nearing 1995).

a) Weather component

The WEPP model requires information on daily precipitation amount, storm duration, peak storm intensity, air temperature, solar radiation, dew point temperature and wind velocity and direction. For experimental sites in the United States, this information is available in high resolution from more than 1000 stations. In areas, where no long-time records are available, the user has to input breakpoint rainfall data and create the climate input file by hand.

b) Surface hydrology component

The surface hydrology component regulates the effect of the duration of rainfall excess and rainfall intensity, runoff volume and peak discharge rate. The amount of infiltrated water affects the water balance and crop growth, which then again affect infiltration and runoff rates.

The infiltration rate describes the change in cumulative infiltration depth over time. The Green-Ampt model modified by Mein-Larson is used with unsteady rainfall input for the computation of infiltration in the model.

Rainfall excess occurs when rainfall rates exceed the infiltration capacity of the soil and is the difference between cumulative rainfall and infiltration depth. Rainfall excess ponds the surface and depressions start to fill with water. After depression storage filled completely, runoff begins. The importance of depression storage depends mainly on the surface roughness and the slope of the surface.

If the amount of infiltrated water reaches the water storage capacity of the soil, all rainfall becomes rainfall excess.

In continuous simulation, peak discharge is calculated using an approximation of the kinematic wave model. Under constant rainfall excess, discharge increases up to the time to kinematic equilibrium. The time to kinematic equilibrium occurs when the equilibrium characteristic, which starts at the top of the hillslope at the beginning of the rainfall excess, reaches the bottom end of the slope. The time to kinematic equilibrium is

$$t_e = \left(\frac{L}{\alpha\, v^{m-1}}\right)^{1/m}$$

Equation 1

where t_e is the time to equilibrium (s), L is the length of the hillslope (m), v is the rainfall excess (m s^{-1}), α is the depth-discharge coefficient and m is the depth-discharge exponent.

Peak discharge rate is

$$q_p = v_c \left(\frac{D_v}{t_e}\right)^m$$

Equation 2

where q_p is the peak discharge (m s^{-1}) and D_v is the duration of rainfall excess (s) and vc is the constant rainfall excess rate (m s^{-1}).

When the duration of rainfall excess is greater than the time to kinematic equilibrium, the peak discharge rate is constant.

$$q_p = v_c$$

Equation 3

c) The water balance and subsurface hydrology

The water balance component predicts soil water content in the root zone as well as evapotranspiration losses with input from the climate, infiltration and crop growth components. Percolation and evapotranspiration is predicted on a daily basis. The continuous water balance describes the soil water content in the root zone Θ as:

$$\Theta = \Theta_{in} + (P - I) \pm S - Q - ET - D - Q_d$$

Equation 4

where Θ_{in} is the initial soil water in the root zone, P is the cumulative precipitation, I is the precipitation interception, S is the snow water content, Q is the cumulative amount of surface runoff, ET is the cumulative amount of evapotranspiration, D is the cumulative amount of percolation losses below the root zone and Q_d is subsurface lateral flow.

WEPP includes two options for the calculation of evapotranspiration. If wind information is available, the model uses the Penman equation for its calculation. If no wind data is available but only solar radiation and temperature data, the WEPP model uses the Priestly-Taylor method. In this work, no information on wind is available. Thus, the model uses the Priestly-Taylor method for evapotranspiration computation.

The soil evaporation and plant transpiration depend on solar radiation, albedo and air temperature as well as on input from the plant growth component (leaf area index, root depth,

total biomass and residue cover). If the water content in the soil depth influenced by evaporation is less than calculated soil evaporation, evaporation decreases accordingly.

During dry periods exists limiting soil moisture content, below which no water evaporates from the bare soil. This critical moisture content depends on bulk density, clay content and organic matter of the soil. In the study area, soil water content in the beginning of the simulation, in January, is low. As most of the rain falls during the rainy season in June to September, the soil is relatively dry in January. Until the first rainfall events of the year, when soil water content increases, there is no evaporation from the soil.

When the water content exceeds the field capacity of a layer, the water percolates to a deeper layer and leaves the root zone. Once below the root zone, the water is lost and will not be traced further. The WEPP model also includes a subsurface lateral flow model, which evaluates the effect of lateral drainage of the soil.

Water stress is an input to the plant growth component and water content of the upper soil layer influences the Green Ampt model for infiltration computation.

d) Soil component

Soil properties highly affect infiltration and surface runoff processes and thus soil erosion. Random roughness, ridge height, bulk density and effective hydraulic conductivity influence the hydrology of the erosion process.

Random roughness describes the irregularity in the micro-topography induced by soil disturbance, mainly tillage operations. Various models describe random roughness as the standard deviation of de-trended surface elevations (Van Wesemael et al. 1996). Random roughness is positively correlated with the surface hydraulic resistance and depression storage of rainfall excess. Random roughness is highest after tillage and decays over time due to the effect of rainfall. Ridge height is closely connected to the random roughness. It is an oriented roughness resulting from the use of tillage implements. Bulk density also influences infiltration into the soil. It is adjusted due to tillage operations and increases with the amount of cumulative rainfall after tillage and due to weathering and long-term consolidation.

Obviously, tillage causes alteration of soil properties and thus needs several input information as implement type, tillage date, depth and level of surface disturbance as well as the amount of buried residue.

As mentioned before, the Green-Ampt model describes the infiltration process. This model builds on two parameters, the effective hydraulic conductivity and the wetting front matric potential term. This term is not an input by the user but calculated internally by the program. It is a function of soil type, soil water content and bulk density.

The effective hydraulic conductivity can be an input by the user or might be estimated by the model. Depending on the clay content WEPP used two different equations.

$$K_b = -0.265 + 0.0086(100sand)^{1.8} + 11.46CEC^{-0.75}$$ for soil with clay content ≤ 40 %

$$K_b = 0.0066e^{\frac{2.44}{clay}}$$ for soil with clay content > 40 %

Equation 5

where K_b is the "baseline" effective conductivity (mm h^{-1}), sand and clay are the fractions of sand and clay and CEC is the cation exchange capacity (meq (100 g)$^{-1}$).

The WEPP model is capable of adjusting the effective hydraulic conductivity as a function of management and plant parameters. The user has two run options. "Baseline" effective conductivity will be adjusted internally by the model and is a function of the soil. The constant effective conductivity will not be adjusted by the model and thus has to account also for management practices. In field experiments the adjusted "baseline" effective conductivity led to better accordance of predicted and measured hydraulic conductivity (Albert et al. 1995).

The model uses fallow soil and crop specific adjustments. Adjustments to the fallow soil account for soil crusting and tillage effects. K_b describes maximum hydraulic conductivity of a freshly tilled soil for which conductivity will decrease as a function of the kinematic energy of the rainfall since last tillage until it reaches its minimum for a fully crusted soil. Sand and clay fractions and cation exchange capacity determine how stable the soil is against this process.

Surface cover from row crops increases effective hydraulic conductivity (K_e) as it reduces soil crusting. According to Wischmeier (1966), surface conditions and management have more influence on infiltration than the specific soil type. Furthermore, infiltration increases with larger storms. This effect reflects the adjustment of K_e due to canopy cover and height as well as residue cover. This leads to the final adjustment of the hydraulic conductivity to

$$K_e = K_{bare}\,(1 - scovef) + (0.0534 + 0.01179\,K_b)(rain)\,(scovef)$$

Equation 6

where K_e is the effective hydraulic conductivity (mm h^{-1}), K_{bare} is K_e of the bare area, K_b is the "baseline" effective conductivity, *scovef* is the effective surface cover and *rain* is the amount of storm rainfall (mm).

In a last step, K_e can be adapted due to bio-pores in the soil. Depending on the influence of bio-pores defined by abundance and size, the effective hydraulic conductivity increases by multiplying it with a ratio, which also depends on the input K_e. The increase of K_e due to biopores is highest for low hydraulic conductivity (ratio 12 to 18) and decreases for soil with already moderately high hydraulic conductivity (5 mm h^{-1}).

Adjustments for perennial crops and rangeland as well as time-invariant constant effective hydraulic conductivity are not discussed in detail, as they are not relevant to this work.

Baseline interrill and rill erodibility as well as critical shear stress are sensitive parameters to the model. All represent the parameter value of a freshly tilled soil. Depending on the sand content, the model uses two different equations for calculation of these parameters. "Baseline" interrill (K_{ib}) and rill erodibility (K_{rb}) for soil containing less than 30 % sand are calculated according to Equation 7 and Equation 8.

$$K_{ib} = 6054000 - 5513000\,clay \qquad \text{for soil with sand content} \leq 30\ \%$$

Equation 7

$$K_{rb} = 0.0069 + 0.134e^{-20clay} \qquad \text{for soil with sand content} \leq 30\ \%$$

Equation 8

The baseline values for interrill and rill erodibility are then adjusted to describe the effects of ground cover, roots, incorporated residues, crusting and sealing of the surface, slope and freeze and thaw. Adjustments to critical sheer stress consider the influence of random roughness, sealing and crusting and freezing and thaw.

e) Plant growth component

Plant growth influences many other model components. For example, the daily water use by the plants affects the water balance component and canopy height and cover affect interrill soil detachment in the erosion component. Assuming a potential growth, canopy cover and height, the model adjusts potential biomass production due to water and temperature stresses. Water stress occurs when the ratio between plant water use and potential plant evaporation is less than 1.0.

As a function of biomass production over the cropping season, the model generates a yield output.

f) Hydraulics of overland flow

The friction coefficient is an essential parameter for appropriate routing of the runoff. The WEPP model uses the Darcy-Weisbach equation under uniform flow conditions. The friction coefficient for rills is composed of friction coefficients for surface roughness, surface residue and living vegetation. The interrill friction coefficient also accounts for the friction coefficient of surface roughness and surface cover, living plants and bare soil. The total friction coefficient for cropland results from both, rill and interrill coefficients according to the ratio of rill and interrill area from the total area.

g) Hillslope erosion component

The hillslope component combines all the information given above and describes the processes of sediment continuity, detachment, deposition, shear stress and transport capacity. The constant of proportionality is the interrill erodibility.

Interrill erosion is a consequence of the impact of raindrops on the soil. It is proportional to the product of the intensity of the rainfall and interrill runoff rate. Interrill erosion delivers sediments to the rills, where sediments either are transported off the hillslope or deposit in the channel.

The steady-state sediment continuity equation describes the transport of sediments in the rills.

$$\frac{dG}{dx} = D_f + D_i$$

where G is the sediment load (kg s^{-1} m^{-1}), x is the distance downslope (m), D_f is the rill erosion rate (kg s^{-1} m^{-2}) and D_i is the interrill sediment delivery (kg s^{-1} m^{-2}).

Interrill sediment delivery is always positive, while a positive rill erosion rate indicates detachment and a negative rill erosion rate deposition, respectively. Net soil detachment in rills (D_f) occurs if the hydraulic shear stress by the flow exceeds the critical shear stress of the soil and the sediment load of the flow is less than the transport capacity. The detachment capacity is proportional to the difference between critical and actual shear stress. Rill erodibility is the constant of proportionality.

The WEPP model also considers particle size distribution. In deposition regions, the fraction of fine sediments increases as it comes to a selective deposition of coarser material. The model calculates a new particle size distribution for the flow leaving the deposition region.

The hydrologic input parameters (peak runoff, effective runoff duration, effective rainfall duration and effective rainfall intensity) are firstly dynamic but have to be transposed into steady-state values for the erosion equations. In order to keep the computational time low, parameters have to be normalized and computations are based on non-dimensional equations. In a later step, the parameters are re-transposed to the final solution.

7. Material and Methods

This work consists of a fieldwork and a subsequent step of computer-based modelling. Field data collection is the basis for the successive simulation of soil erosion by means of the Water Erosion Prediction Program (WEPP).

The idea of the fieldwork was the monitoring of soil loss from arable land on a plot scale. The soil loss monitoring aimed to assess the effect of parameters such as canopy and rock fragment cover and the impact of the slope reduction by stone bunds on the fields. Soil loss was recorded for the rainy season 2012 (end of June to end of August) at three soil erosion plots. In a successive step, the information of the fieldwork built the basis for the simulation of soil loss at the same site. The aim of the simulation process was to find a configuration of the model, which predicts soil loss adequately for this specific site. The following section presents the approach of the fieldwork and simulation consecutively.

The collection of the fieldwork data included a description of the study area, collection of precipitation data, a topographic survey, assessment of canopy and rock fragment cover, soil loss measurements, sampling and laboratory work.

7.1 Description of the study area

Study area is the Gumara-Maksegnit watershed in the North Gonder zone of Amhara Region. The watershed covers an area of 54 km². Altitudes range from 1933 m a.s.l to 2852 m a.s.l. About 75 % of the total area is arable land, used for subsistence farming (Hailu Kendie Addis unpublished). Most common crops are sorghum, tef, wheat, lentil and chickpea. The settlement is characterized by a scattered pattern of households, ranging from the low parts up to the fragile steep slopes in the upper part of the watershed.

The experimental plots were situated in the Ayaye sub-catchment of the Gumara-Maksegnit watershed. The Ayaye sub-catchment and the neighbouring sub-catchment Aba-Kaloye are involved in long-term soil erosion studies. Both sub-catchments show severe soil erosion problems, which become apparent in the formation of deep gullies. In the Ayaye sub-catchment, the gullies were treated by the construction of gabions. This measure should reduce the development and advancement of the gully system. The neighbouring Ayaye sub-catchment acts as a reference for gully development without measures. Additionally, stone bunds were applied at the field in the Ayaye sub-catchment, which retard the sheet erosion process.

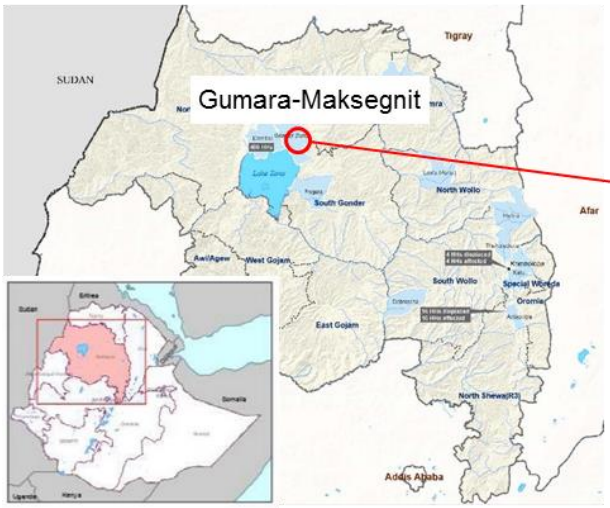

Figure 6: Amhara Region, the Gumara-Maksegnit watershed is located in the northeast of Lake Tana and is marked by the red circle. © ("OCHA" 2013)

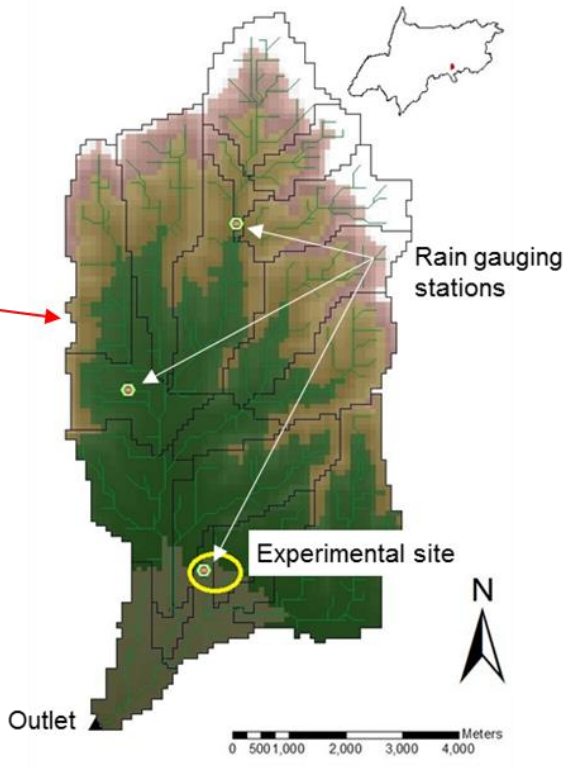

Figure 7: Gumara-Maksegnit watershed; the yellow circle indicates the experimental site (Kendie Addis unpublished)

Figure 6 shows a map of the Amhara Region with Lake Tana, the largest lake of Ethiopia. The Gumara-Maksegnit watershed, shown in Figure 7 is situated in the northeast of the Lake Tana basin and drainages into the Gumara River, which ultimately reaches Lake Tana. The yellow circle specifies the experimental site. The three smaller circles represent the three rain gauging stations within the watershed. The rain gauging station most to the south is located in the Aba-Kaloye sub-catchment. As the distance between experimental plots and rain gauging station is about one kilometre, the present work assumes that recorded precipitation in Aba-Kaloye is valid also for the Ayaye sub-catchment.

The Ayaye sub-catchment has a size of 24 ha. It is oriented north to south and is located in the lower part of the watershed. Altitudes range from 2012 m a.s.l to 2136 m a.s.l. The experimental plots are located in the lower gently sloped part, near the outlet of the sub-catchment.

In Ethiopia, with its wide altitude range, rainfall mainly correlates with elevation (FAO 2013). Depending on the altitude, five major agroclimatic zones can be distinguished. Table 2 shows range of altitude, rainfall, length of the growing period and average annual temperature for each region. The watershed is located in the Weyna Dega, cool and sub-humid agroclimate zone

Table 2: Agroclimatic Zones of Ethiopia after (Dejene 2003)

Zone	Altitude (m)	Rainfall (mm/year)	Length of growing period (days)	Average annual temperature (°C)
Wurch (cold and moist)	>3200	900 – 2200	211 – 365	>11.5
Dega (cool and humid)	2300 – 3200	900 – 1200	121 – 210	11.5 – 17.5
Weyna Dega (cool sub-humid)	1500 – 2300	800 – 1200	91 – 120	17.5 - 20
Kola (warm semi-arid)	500 – 1500	200 – 800	46 – 90	20 – 27.5
Berha (hot arid)	<500	<200	0 – 45	>27.5

According to precipitation records from 1987 to 2007 (GARC 2010), mean annual rainfall is 1052 mm varying from 641 mm to 1678 mm. About 600 mm rainfall occur in July and August. Information on temperature is available from records of the weather station in Maksegnit Town. Mean maximum and minimum temperature were recorded for 10 consecutive years. Mean maximum temperature is 28.5 °C; mean minimum temperature is 13.6 °C (GARC 2010).

Loam soils can be found in the higher parts of the watershed, while in the downstream clay soils occur. Soils in the upper stream are mainly shallow with rooting depth below 15 cm; whereas the clay soils are well developed with rooting depths exceeding 80 cm (Hailu Kendie Addis unpublished). Figure 9 shows a map of soil classes in the Gumara-Maksegnit watershed.

In the Ayaye sub-catchment, heavy soils predominate, characterized by its high clay content. In mixed samples, clay content was about 42 %. Silt content was high as well, and lay around 36 %. Correspondingly, sand content was about 22 %.

Figure 8 shows a soil texture triangle. With the percentages for clay, silt and sand, as described above, the soil of the experimental site is a clay soil.

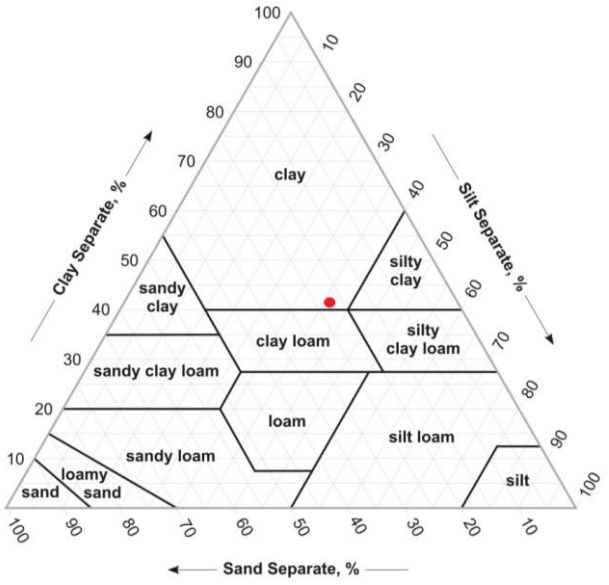

Figure 8: Soil texture triangle; the red dot represents the soil at the experimental site ("Guide to Texture by Feel | NRCS Soils" 2013){Citation}

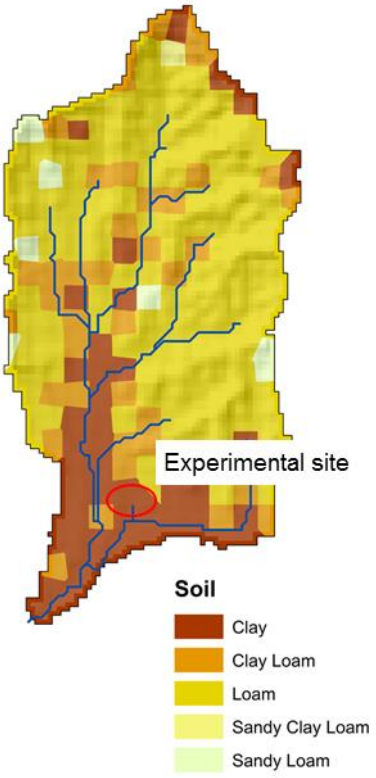

Figure 9: Soil map of the Gumara-Maksegnit watershed; the red circle indicates the experimental site (H. Kendie Addis et al. 2013)

At the west flake of the sub-catchment, all fields are treated with stone bunds except for the fields most to the south. Thus, fields with stone bunds and fields without measure directly adjoin each other. The distance between the stone bunds is about 25 m. In the Ayaye sub-catchment, steep slopes are used for grazing, while the gentile slopes are covered by different crops.

Due to the climate conditions in this region, there is only one cropping season per year. For tillage farmers use a traditional ox-drawn ard plough. In 2012, farmers mainly grew sorghum, tef and faba bean in the Ayaye sub-catchment. At the fields from the experimental plots famers sew sorghum in the beginning of June and harvested in mid-December. They tilled twice before planting sorghum (mid-February and mid-May).

7.2 Soil erosion measurement

The setup of the experimental plots should enable the evaluation of the impact of stone bunds on the soil erosion process by comparing soil loss under treated and untreated conditions. Moreover, soil loss monitoring under treated conditions included two different plot arrangements. First, one plot should investigate the effect of reduced slope length on soil erosion. Second, one plot should test the impact of stone bunds on soil erosion on entire hillslope length scale. Thus, one plot was situated between two subsequent stone bunds, while the other had a stone bund within the plot area. This setup resulted in the installation of three sediment retention plots.

a) Instillation of the sediment retention plots

The experimental site was selected due to its position, topography and management. The experimental plots were installed at a relatively uniform hillslope near the outlet of the sub-catchment.

Mean slope inclination is 6%; which is representative for the cultivated area in the sub-catchment. Lateral inclination at the plot area is low.

Figure 10 shows a scheme of the experimental site around the border between treated and untreated fields.

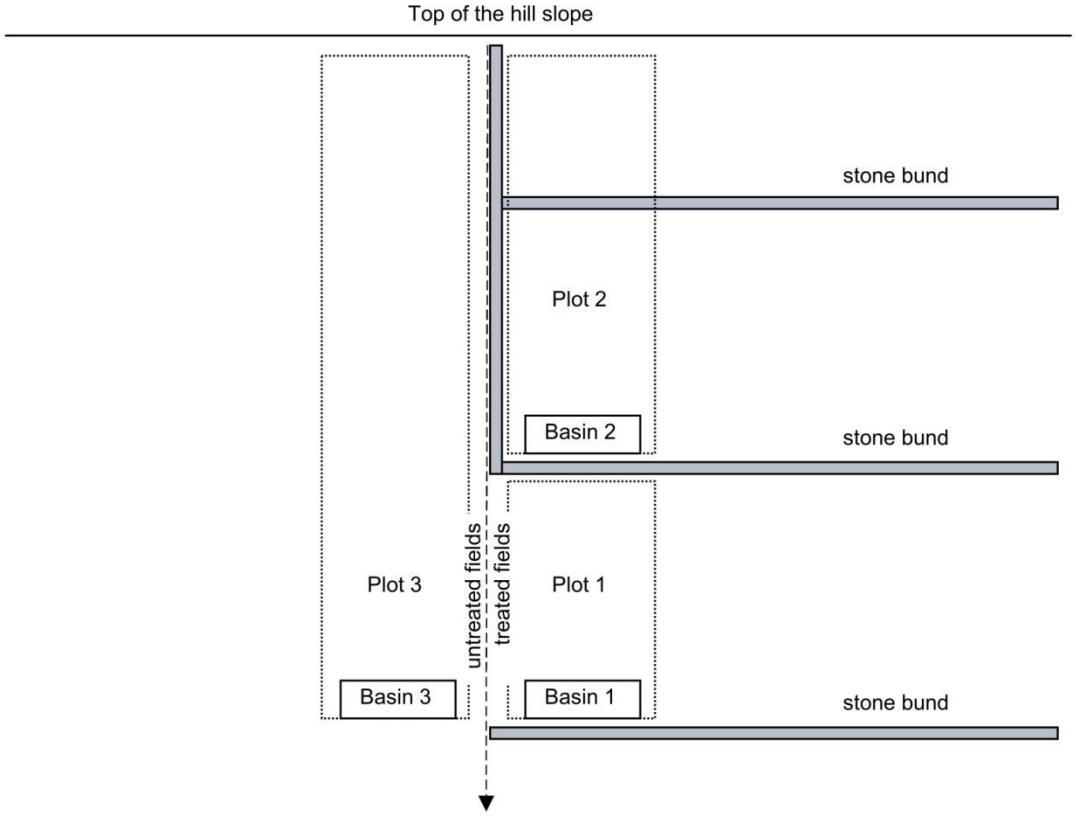

Figure 10: Scheme of the erosion plot setup

As shown in Figure 10, Plot 1 and Plot 2 were situated on farmland with stone bunds. Plot 3 was designed to be located next to both others on farmland without the influence of soil conservation measure. This setup should enable comparison of soil loss under treated and untreated conditions.

Plot 1 covered the area between two subsequent stone bunds. Thus, the stone bunds built the upper and lower limits of the plot. In this case, as already mentioned the upper stone bund reduced the effective slope length to the distance between the two bunds. As Plot 2 is located directly uphill of Plot 1 and, hence, sediments were prevented from entering Plot 1 from above, it can be assured that no additional sediments entered the plot from the uphill fields.

Plot 2 transcended the upper stone bund and extended to the top of the hillslope. Consequently, the plot was divided by the mid stone bund. This bund had a barrier effect to the soil detached from the upper part of the plot. It can be expected that sediments, which eroded uphill the mid stone bund, will at least partially deposit behind it and will not leave the plot at the outlet. If soil loss at Plot 2 is about the same as at Plot 1, it can be assumed that the

stone bund held back the material from above. Plot 2 was separated from the adjacent untreated land by a downhill-orientated stone bund.

Plot 3 had the same slope length as Plot 1 and Plot 2 together (around 50 m), but without any soil conservation measure in between. This plot acted as a reference plot for soil loss under untreated conditions.

The plots were naturally bordered. Thus, plot areas were defined by the topography of the hillslope. It was assumed, that by building sufficiently wide basins, the effect of surface water running sidewise could be kept low.

The width of the plots was defined by the width of the sediment retention basins, forming the lowest part of the plot. At the treated fields, the sediment retention basins were located directly uphill of the stone bunds.

b) Set-up of the sediment retention basins

The size of the retention basins, which formed the outlet of the plots, was 8 m by 1.5 m, with a depth of 0.75 m. We assumed that a width of 8 m is sufficient that the effect of lateral detachment is negligible.

The sediment retention basins were excavated and covered by a foil. Excavated basins instead of collection devices on the surface were considered to have several advantages. Firstly, the construction of excavated retention basins is simple. Additionally, little material is necessary in the construction, which makes them quiet theft proof.

In order to prevent the mixture of eroded material with the in situ soil, a perforated plastic foil was applied at the surface of the excavated basins. The perforated foil should enable infiltration of water, but detain sediments.

During heavy rainfall events with rainfall excess and surface runoff, soil particle were eroded and transported with the surface runoff. The sediments, which reached the bottom end of the plots, were trapped in the sediment retention basins and accumulated. By monitoring the amount of trapped sediments, one can draw conclusions about soil loss from the hillslope.

Construction of the basins was conducted on June 21th and June 22th, 2012. Figure 11 shows pictures of the construction process.

Figure 11: Construction of the sediment retention basins

c) Soil erosion measurement procedure

The soil loss measurements included the three steps: collection, removal and weighing of the trapped sediments.

The monitoring of soil loss was based on the collection of sediments, which deposited in the sediment retention basins from the three plots. The sediments, which would pass the lowest point of the plots and leave the plots at the bottom end due to rill and interrill erosion, accumulated in the sediment retention basins. Subsequently the sediments were removed and weighed.

Sediments were removed as often as possible. Nevertheless, it was not possible to collect sediments for single events separately, but sediments from more events accumulated between two days of removal. In total, accumulated sediments were collected, removed and weighed 13 times over the rainy season. Intervals between days of removal were not regular.

Percolation of collected surface runoff through the perforated plastic foil was low. We assumed that this due to the high clay content of the soil. The collected rainwater stayed in the basins, mixed with the fine sediment fraction (see Figure 12). The coarser material settled at the bottom of the basins. Thus, water content of the collected material was very high and additional action for the extraction of the water was necessary.

In a first step, the standing water in the basins was extracted using a hose (see Figure 13). The water ran freely due to a gradient in the water level. The hose was hold near the surface of the water table in order to avoid mixture with the coarse material. The volume of the extracted water was monitored. A sample (100 ml) for determination of the sediment concentration in the down pumped water was taken every 150 l. The 100 ml samples were put together and the sediment concentration of the mixed sample was determined in the laboratory using filters and oven drying of the particles. If sediment concentration varied strongly, two or more mixed samples were analysed separately and related to the water portion, which showed similar sediment content. The amount of sediments removed by the hose resulted from relating the volume of removed water to the sediment concentration.

Secondly, after removal of the liquid fraction, the coarser material, which stayed in the basins, was removed using buckets. The buckets were weighed by means of a spring balance with 0.5 kg accuracy (see Figure 14 and Figure 15). Mixed soil samples were retained for determination of the water content and dry weight. Water content of the material increased from the top to the bottom. Mixed samples were taken for different layers of the accumulated sediments. For each bucket, the representative mixed sample was noted.

Finally, water content of the mixed samples was determined by the difference between the weight of the immediately weighed samples and the weight of the samples after oven drying in the laboratory at 105°C.

Figure 12: Sediment retention basins filled with water after rainfall events

Figure 13: Extraction of standing water from the basins by free water levelling

Figure 14: Removal of sediments using buckets

Figure 15: Weighing of the removed sediment using a spring balance

The raw data of the soil loss monitoring is attached to the Annex.

7.3 Precipitation data collection

Three rain gauging stations are located within the Gumara-Maksegnit Watershed as shown in Figure 7, in 7.1.

The rain gauging station in the Aba-Kaloye sub-catchment is situated in about one kilometre distance from the experimental plots. Rainfall data from this station was used in this work.

Rainfall was monitored continuously using an ombrograph. Every tip is equivalent to 0.2 mm rainfall. Additionally the device measured air temperature every hour. Rainfall records were available from June 26th to December 31st 2012.

7.4 Topographic survey of the study area

In order to link soil loss from the three plots to the contributing areas, a topographic survey of the hillslope was conducted during the rainy season 2012. It was carried out by a local surveyor on August 22nd 2012 by means of a total station. As point measurements showed wrong values for the upper part of the hillslope, the survey partly had to be repeated on September 7th 2012.

An area of 2600 m² was surveyed by a raster of 1 x 1 m and 2 x 2 m on the first and second day of surveying, respectively.

A digital elevation model (DEM) of the experimental site was generated using Arc GIS 10. Based on the DEM and the position of the three retention basins within the hillslope, Arc GIS 10 confined the area, feeding each basin using the Watershed Tool in the Spatial Analyst Toolbox.

The Annex includes a detailed description of the procedure, used for delimiting the watersheds for the three plots.

7.5 Assessment of canopy and rock fragment cover

Determination of canopy and rock fragment cover is based on a photo image classification. On June 25th, photos were taken from 60 x 60 cm mini-plots, located along transacts at the treated and untreated fields. The mini-plots were evenly distributed over the length of the plots. Monitoring included 10 mini-plots at Plot 1 and Plot 2, respectively, and 20 mini plots at Plot 3. All photos for this work were taken from the same height and perpendicular to the ground.

The canopy and rock fragment cover was then evaluated using two different approaches: automatized analysis using Arc GIS and manual analysis using AutoCAD.

Arc GIS includes an Image Classification Tool, which was used in the first method. For each image, training samples for the categories *vegetation*, *soil* and *stones* were selected. By using these training samples as a reference, rock fragment and canopy cover were a result of an Interactive Supervised Classification by Arc GIS and a successive Maximum Likelihood Classification. The Arc GIS output is the number of pixels, which belong to each category. This information can then be related to the total pixel number and thus canopy and rock fragment cover is described as the particular percentage from the whole mini-plot area. It was assumed that this method would underestimate rock fragment cover as plant leafs overlap and hide stones.

A second method should help to evaluate this approach and verify its results. The second method for determining rock fragment cover only is based on a manual analysis using AutoCAD. This method was considered to be more correct, but time-consuming and difficult to exactly reproduce. Stones were encircled by polygons and the area of all polygons represented the portion of rock fragments at the mini-plots. This method has the advantage that stones are recorded separately. This would allow analysing the number and size of the rock fragments. Only rock fragments with an area exceeding 0.5 cm² were taken into account and classified as stone. In a field experiment in Tigray, Ethiopia, Nyssen et al. (2001) limited rock fragment size to fragments with an intermediate diameter exceeding 0.5 cm.

7.6 Sampling and laboratory work

The Gonder Laboratory undertook the analyses of the samples. The determined parameters were

- water content of the removed sediment
- sediment concentration of the down pumped surface runoff

Soil texture of the samples was determined for the first three days of removal.

7.7 Computer-based modelling (WEPP)

The WEPP model used results from the fieldwork as input information, to adapt soil loss prediction to local conditions. In general, the input parameters are excessive. For sites in the United States, for instance, the model accesses databases in order to get input parameter, which are valid to the study area. In the experimental site of this work, little information is available. This fact makes the modelling process difficult. The idea of this work was to find a configuration of the model, which depicts observed soil loss adequately.

The main WEPP output can be plotted as an annual, monthly or event-to-event based description of the erosion events. The output includes all days with surface runoff, even if no soil loss results from it. The hydrological output for each event includes the amount of rain and runoff, the rainfall duration and effective event duration (takes account of both, rainfall duration and runoff duration), the effective slope length and peak runoff rate.

For the analysis of the model's efficiency in simulating observed soil loss, the soil loss – the average net soil detachment rate – was the most important output. This value is the basis for the evaluation of the model's results. Surface runoff was not taken into account. The additional output as plant, water, soil and yield output discuss sections 8.6.5 and 8.6.7.

The sensitivity analysis gave information about the influence of selected parameters. The Latin Hypercube Sampling (LHS) method by McKay et al. (1979) built the basis of the parameter value selection. For each sensitive variable X, the parameter range was divided into intervals with equal probability. From each interval one value was selected and then paired randomly with the parameter values of the other variables X_i (Wyss and Jorgensen 1998). This method leads to the simulation of various scenarios.

To validate the model, the use of the 95 % confidence interval of the simulations led to the development of a range of soil loss prediction, which excludes outliers but still includes most of the parameter combinations. Where the measured value lies within the confidence interval, the model is capable of predicting soil loss adequately at least in one combination. The smaller the area between the two quintiles 2.5 % and 97.5 %, the better the models adaption to the problem and its calibration. It is obvious that the wider the range of predicted soil loss, the higher the likelihood that the observed value lies within this range.

7.7.1 Model sensitivity analysis

In a first step, sensitivity of the model to variation of single parameters was evaluated. For selected parameters, effective hydraulic conductivity, interrill and rill erodibility, random roughness, canopy cover coefficient, maximum leaf area index, rock fragments, cation exchange capacity and initial saturation level a sensitivity ratio was calculated using Equation 9 as proposed by Mahmoodabadi et al. (2013).

$$SR = \frac{[(O_{max} - O_{min})/O_{ave}]}{[(I_{max} - I_{min})/I_{ave}]}$$

Equation 9

where I_{max} and O_{max} are the maximum values of the input and output, I_{min} and O_{min} are the minimum values of the in- and output and I_{ave} and O_{ave} are the average values of maximum and minimum values.

Therefore, the parameters varied within a fixed range as shown in Table 3.

Table 3: List of parameters included in the sensitivity analysis and their tested ranges

Parameter	Tested range	Unit
rock fragments	5 - 55	%
rill erodibility	0.003 - 0.009	s m^{-1}
random roughness	4 - 15	cm
effective hydraulic conductivity	2 - 400	mm h^{-1}
cation exchange capacity	20 - 35	meq $(100g)^{-1}$
maximum leaf area index	4 -10	-
initial saturation level	0 - 100	%
canopy cover coefficient	6 - 18	-
interrill erodibility	2500000 - 5000000	kg s m^{-4}

7.7.2 Model validation

For the validation of the model, sensitive input parameters were altered leading to different scenarios. The root mean square error (RMSE), the model efficiency (NSE) and the coefficient of determination (^{2}) were calculated as objective functions, which indicate how well predicted and observed values fit together. The choice of the objective function affects the ranking of the scenario as not all objective functions result in the same order of the scenarios. In order to get the best model fit three separate objective functions should evaluate the model's capability to predict observed soil loss.

RMSE is calculated using Equation 10 (Thomann, (1982) cited by Mahmoodabadi and Cerdà, 2013):

$$RMSE = \sqrt{\frac{\sum_{i=1}^{n}(O_i - P_i)^2}{n}}$$

Equation 10

where O_i is the observed value at the point i, P_i is the predicted value at the point i and n is the number of paired O and P values. Smaller values indicate a better fit between observation and prediction.

The model efficiency after Nash and Sutcliffe (1970) is calculated according to Equation 11.

$$ME = 1 - \frac{\sum_{i=1}^{n}(O_i - P_i)^2}{\sum_{i=1}^{n}(O_i - O)^2}$$

Equation 11

where O is the mean of all measured values.

Possible values for the model efficiency parameter (NSE) are between -∞ to 1. The more the value converges to 1, the better the model's prediction. Negative values indicate that the mean of the observed values is the better predictor.

The coefficient of determination (R^2) describes the portion of the total variance of observations explained by the model. It is between 0 and 1 with better results converging to 1. It is calculated according to Equation 12.

$$R^2 = 1 - \frac{\sum_{i=1}^{n}(O_i - P_i)^2}{\left(\sum O_i^2\right) - \frac{(\sum O_i)^2}{n}}$$

Equation 12

The root mean square error (RMSE), model efficiency (NSE) and coefficient of determination (R^2) are three separate objective functions, which not necessarily coincide in one best result. All three parameters were calculated for each scenario.

7.7.3 Model input

The model input is partly based on results from the fieldwork, partly depends on WEPP integrated databases. The objective of the modelling process was to find a combination of input parameters, which allows an adequate simulation of observed soil loss. The definition of the input parameter reflects the information from the sensitivity analysis. Model input varied between the plots.

a) Climate input file

The climate input file is composed of information on time-related daily cumulative rainfall, minimum and maximum daily temperature, daily solar radiation, wind velocity, wind direction and dew point temperature.

First, the continuously logged daily rainfall was displayed as a cumulative graph. The breakpoint method was then used to create the climate file. A breakpoint file contains two columns with cumulative time from the beginning of the rainfall event and average rainfall intensity in the interval between two time steps in the second column. Breakpoints are inserted wherever the inclination of the hydrograph changes. All available rainfall data from the year 2012 - June 26th, 2012 to December 31th, 2012 - was embedded into the climate input file. Unfortunately, no precipitation data from January to June is available for any of the recording years.

Daily solar radiation and dew point temperature were derived from a default file from the region (Anjeni, Ethiopia). Wind velocity was set to zero, as no information is available. The lack of wind information is accounted for by using the Priestley-Taylor method for evapotranspiration computation.

b) Slope input file

The slope is an output of the Arc GIS computation. WEPP uses a list of segments of known length and slope as an input. The number of segments is limited to 9. Thus, the slope profile derived from Arc GIS has to be simplified and reproduced by at most 10 points, leading to 9 segments. The width of the hill slope in the computation is 1 m.

The slope files are attached to the Annex.

c) Soil input file

The soil input file holds information on soil texture, albedo, initial saturation level, soil depth, organic matter, cation exchange capacity and percentage of rock fragments.

The soil files are attached to the Annex.

d) Management input file

The plant and management file is the most extensive component, which contains all information on plant parameters, tillage sequences, tillage implement parameters, plant and residue management, initial conditions, contouring, subsurface drainage and crop rotation. The plant parameters specify plant growth and harvest parameters, temperature and radiation parameters, canopy, leaf area index, root parameters and senescence parameters.

For the simulation of the initial condition of the plots on January 1st, a second management input file was created with management operations from the previous year 2011.

The management files are attached to the Annex.

8. Results and Discussion

This section consists of two main parts, where the first presents the results from the fieldwork in the Ayaye sub-catchment in 2012 and the second part discusses the results from the successive soil loss prediction by the Water Erosion Prediction Project (WEPP).

8.1 Precipitation data

The rain gauging station in the Aba-Kaloye sub-catchment is the nearest and most significant gauging station for the experimental site. Figure 16 shows daily and cumulative rainfall for the year 2012.

Total rainfall in 2012 was 941 mm. According to records from 1987 to 2007 mean annual rainfall in the Gumara-Maksegnit watershed is 1052 mm (GARC 2010).

Compared to data from 2011, daily rainfall in 2012 was low. While in 2011 rainfall events with 90 and 130 mm per day occurred, daily rainfall did not pass over 40 mm during the rainy season 2012.

Although most rainfall events occurred, as expected, during the rainy season (July and August), the heaviest rainfall in 2012 is recorded at the end of October during off-season.

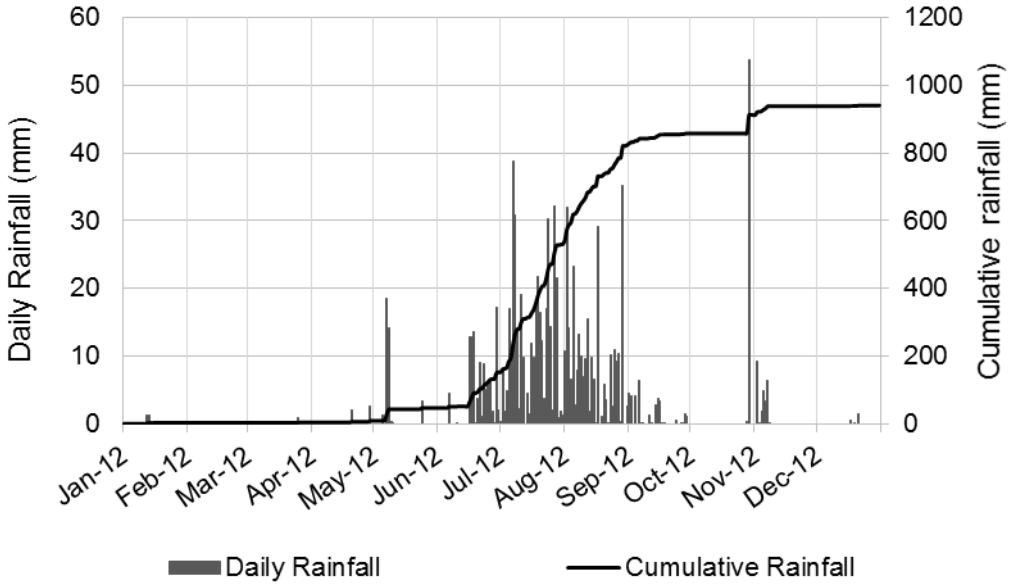

Figure 16: Daily precipitation and cumulative rainfall in the Aba-Kaloye sub-catchment in 2012

The sediment retention plots were installed on June 22nd 2012. Monitoring of the accumulated sediments ended on August 30th 2012. Total rainfall during this period was 697 mm. Within this time, the gauging station recorded two days without rainfall.

8.2 Topographic survey of the experimental site

a) Topography of the hillslope

The topographic survey was conducted on August 22nd 2012.

Figure 17 shows the digital elevation model of the hillslope derived from Arc GIS 10. Elevation ranges from 2023.3 m to 2036.7 m a.s.l. The length of the surveyed hillslope is around 75 m.

The lower part of the hillslope is arable land, in 2012 cultivated by sorghum. It extends up to an altitude of approximately 2031.3 m a.s.l. Bushes cover the hillslope above, so farmers use it for grazing of the cattle.

Furthermore, Figure 17 shows the position and orientation of the stone bunds, applied at the experimental site. Crest heights of the stone bunds were measured during the survey.

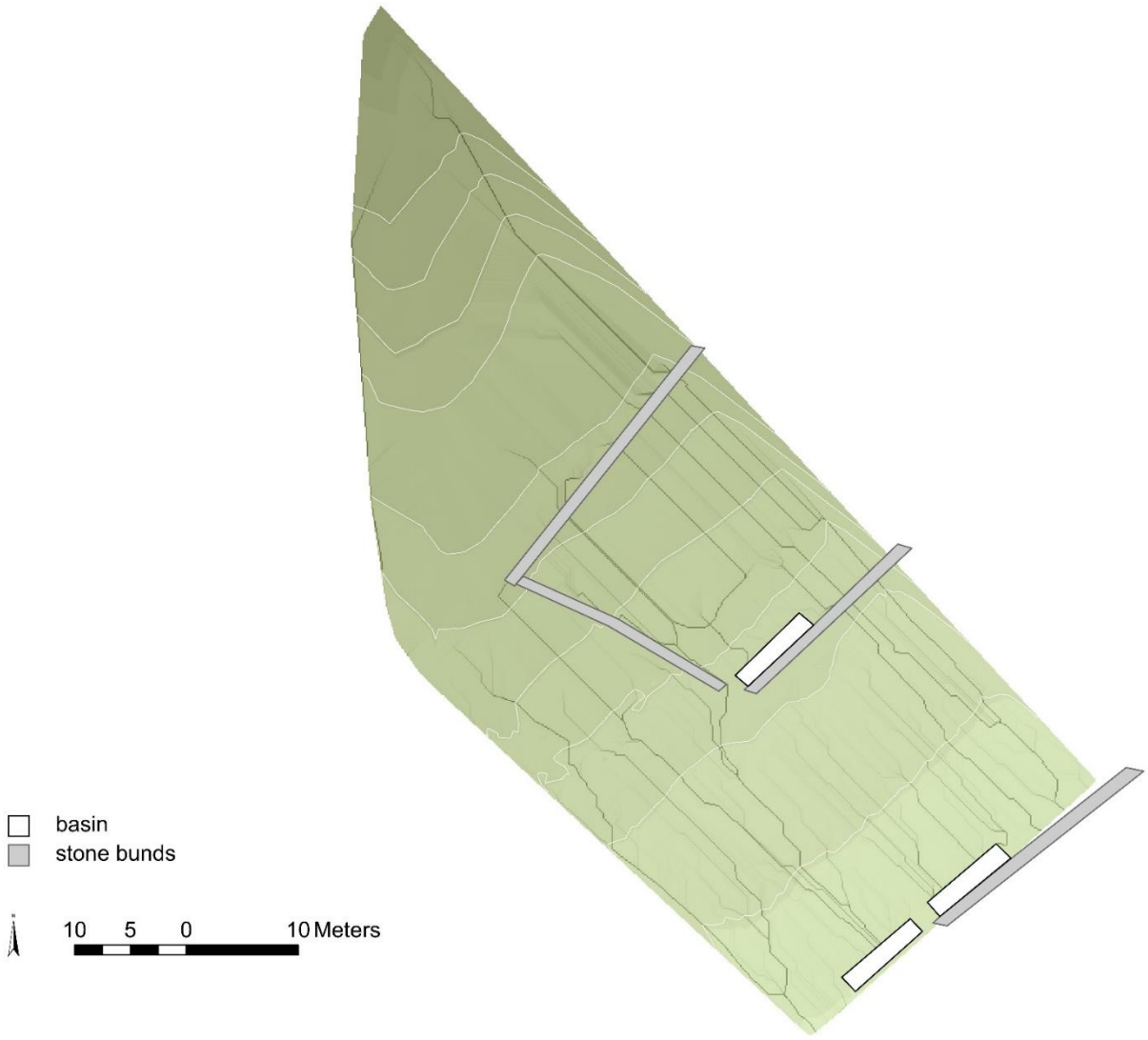

Figure 17: Digital Elevation Model and Flow Accumulation of the experimental site in the Ayaye sub-catchment (derived from Arc GIS 10)

The black lines in Figure 17 represent lines of flow accumulation. The line width is related to the amount of accumulated surface flow. Increased line width indicates increased cumulative surface runoff.

As already mentioned, the three soil erosion plots were constructed without artificial borders. The area of the plots is defined by the area with surface runoff flowing into the sediment retention basins at the outlet of the plots. Thus, plot areas represent areas with surface runoff flowing to the three retention basins. Knowing the plot area is essential in order to link the amount of collected sediments to its contributing area. As the soil loss rate (kg m^{-2}) describes the ratio between the amount of eroded soil and the influence area, it is highly sensitive to errors in area delineation.

b) Surface area of the soil erosion plot

Firstly, plot areas were derived from Arc GIS, using the Watershed Tool. Afterwards these plot areas were corrected and adapted as shown in the following.

According to the Arc GIS computation (see Figure 18), Plot 1 shows the least area with 297 m². A graded stone bund separated Plot 2 into an upper and lower section; it has an area of 323 m². The untreated Plot 3 is the biggest plot with 604 m².

Plot areas shown in Figure 18 do not account for land cover and land use. As the soil at the upper hillslope is covered entirely by grass and bushes (bush land), it is assumed that this area did not contribute to soil loss from the plots. The area of Plot 2 and Plot 3 was reduced by this section. Consequently, the area of Plot 2 decreased to 299 m². The reduced area of Plot 3 is 584 m².

Plot 3 acted as a reference area, which shows soil loss under untreated conditions. However, according to Figure 17 the influence area of this plot partly spreads into the treated fields. Surface runoff flows along the downhill-orientated stone bund and then into the basin of Plot 3. This would imply that all surface runoff and sediments from this treated area pass for a narrow run-through between the downhill-orientated stone bund and the basin of Plot 2. In site inspections, no signs of this excessive transport were visible. Furthermore, the resolution of the survey grid was too low for modelling micro-topography.

Due to the information from field observations, the plot areas by Arc GIS were altered. Concerning Plot 3, it is assumed that sediments from the treated field behind the downhill-orientated stone bund will not flow into the retention basin of this plot. The area of Plot 3 was reduced by the portion of Plot 3 situated on treated land. The area was added to Plot 2.

Figure 19 shows the final plot areas, used in the following.

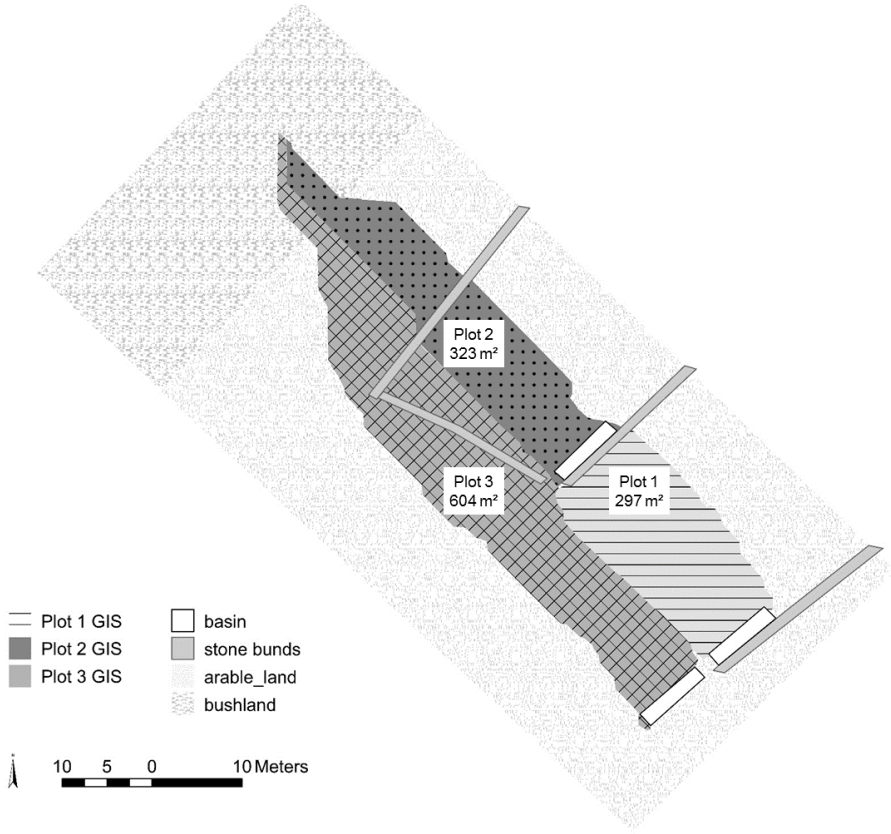

Figure 18: Plots areas derived from GIS

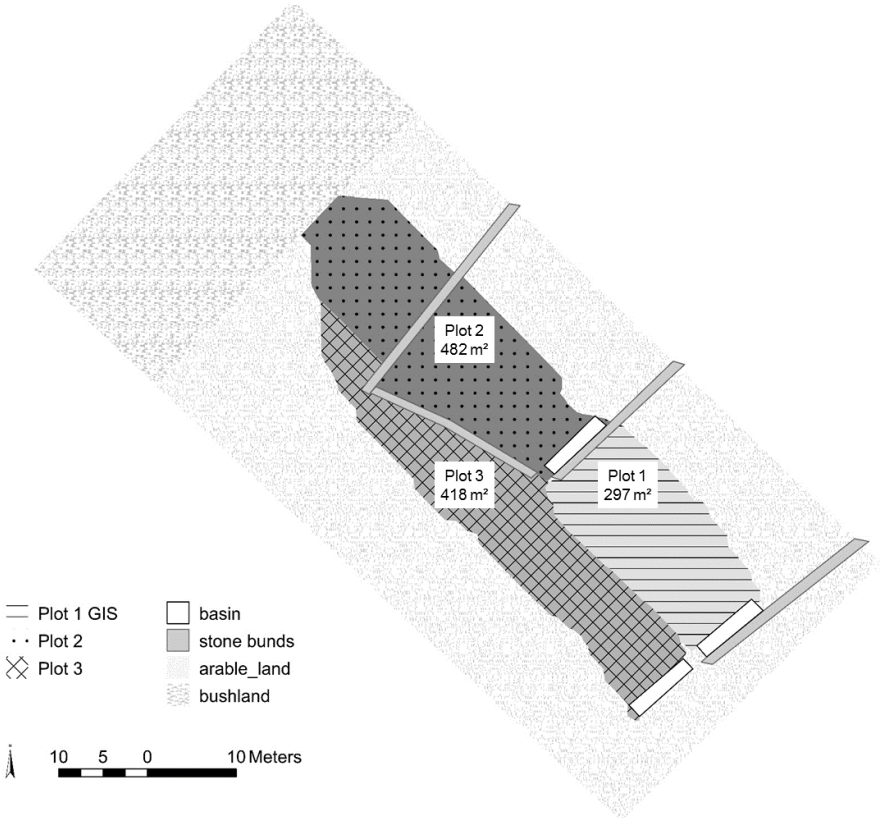

Figure 19: Plot areas: Area of Plot 3 reduced by the area behind the downhill-orientated stone bund and the bush land area. Plot 2 increased by the section of Plot 3 situated on treated fields and reduced by the bush land area

Plot 1 did not change in the post-processing of the data and kept a plot area of 297 m². Plot 2 increased in size and has an area of 482 m². The remaining plot area of Plot 3 is 418 m².

Even though the three sediment retention basins had the same size (8.0 x 1.5 x 0.75 m), the plot areas differed not just in length but also in width. While the width of Plot 1 and Plot 2 is 12.1 m and 12.7 m respectively, Plot 3 is the narrowest plot with a width of 9.4 m.

c) Slope profiles of the soil erosion plots

Figure 20, Figure 21 and Figure 22 show the profiles of the three plots. To get the average slope of the plots, Arc GIS computed profiles, evenly distributed over the plot width, and a mean slope was calculated.

Plot 1 is the shortest plot and measures 24.5 m. Figure 20 shows the length profile of this plot. At the upper border of the plot follows a stone bund and directly behind this stone bund follows the sediment retention basin of Plot 2. The steep slope in the first meters of Plot 1 is due to an earth bank behind the stone bund. This earth bank already existed before the start of the experiment.

The stone bund, which dissects Plot 2, is notable in Figure 21. It shows that the area behind the stone bund already filled up with sediments. The length of Plot 2 is about 38 m. The figure also shows a slight elevation at the end of the slope (at 33 m) and thus in front of sediment retention basin, which follows at the end of the profile.

Plot 3 is the longest plot. It has a length of up to 55 m and a uniform slope. Figure 22 shows the profile of this plot.

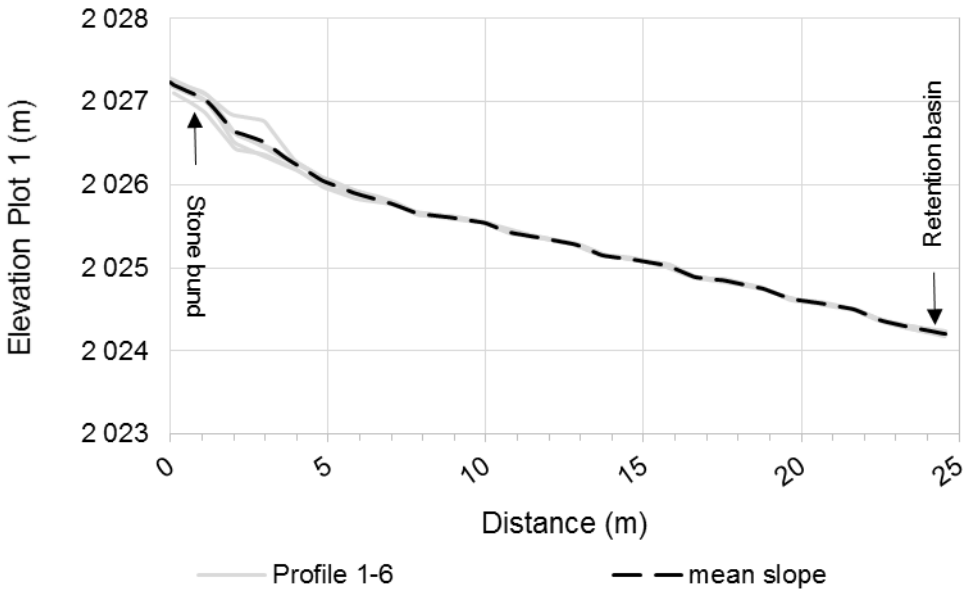

Figure 20: Slope profile of Plot 1

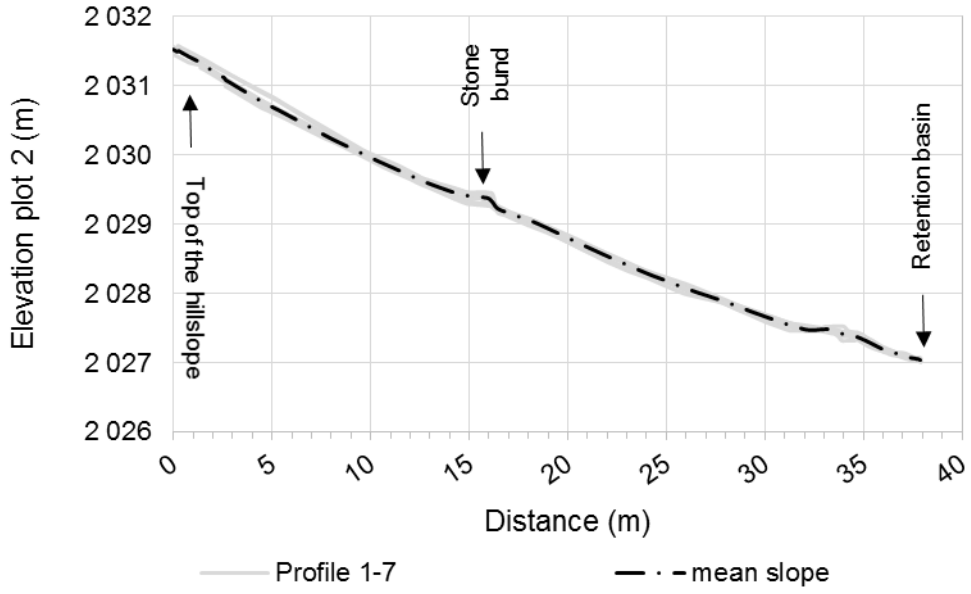

Figure 21: Slope profile of Plot 2

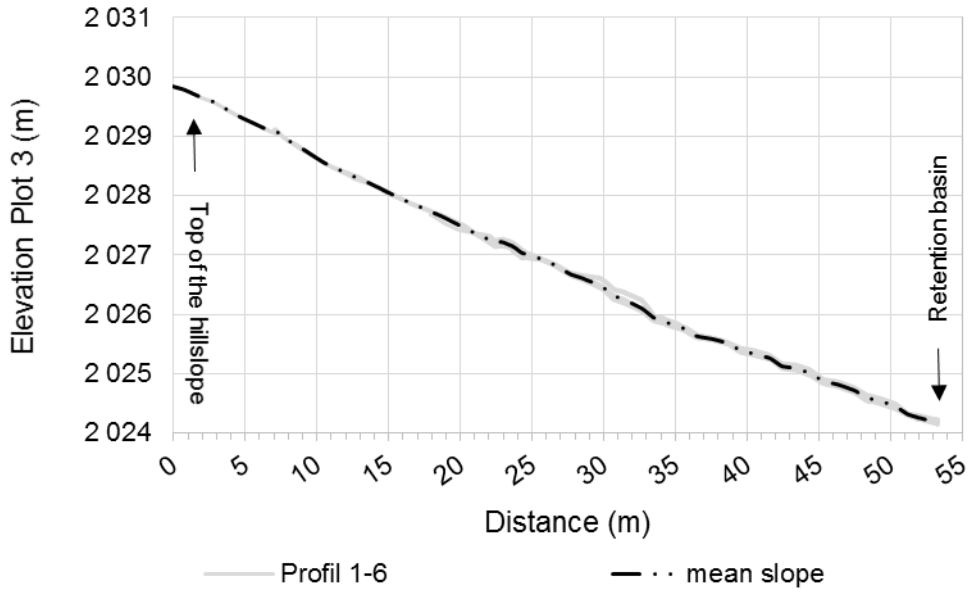

Figure 22: Slope profile of Plot 3

8.3 Assessment of canopy and rock fragment cover

The GIS and AutoCAD based image classifications show similar results and are consistent with each other.

The following compares canopy and rock fragment cover of the three soil erosion plots and additionally compares results from the manual and automatized analysis.

Table 4 and Table 5 show canopy and rock fragment cover derived from Arc GIS classification and manual analyse of rock fragment cover, respectively.

Table 4: Canopy and rock fragment cover derived from the Arc GIS Image Classification Tool.

	rock fragments [%]		**vegetation [%]**	
	mean	standard deviation	mean	standard deviation
Plot 1 (with SWC)	0.14	0.08	0.16	**0.15**
Plot 2 (with SWC)	0.17	0.09	**0.33**	0.12
Plot 3 (no SWC)	**0.24**	**0.11**	0.14	0.07

Table 5: Rock fragment cover derived from manual analyse.

	rock fragments [%]	
	mean	standard deviation
Plot 1 (with SWC)	0.13	0.07
Plot 2 (with SWC)	0.17	0.08
Plot 3 (no SWC)	**0.26**	**0.14**

Vegetation cover is in the same range for Plot 1 and Plot 3 and significantly higher on Plot 2. As surface cover has a high impact on surface runoff, this variation might influence the results from the soil erosion plots.

Figure 23 shows vegetation cover for each mini-plot at the three soil erosion plots. As Plot 3 is nearly double as long as Plot 1 and Plot 2, 20 mini-plots were distributed over Plot 3 while 10 mini-plots were installed at Plot 1 and Plot 2. The mini-plots of Plot 2 are in the same level as mini-plots 1 – 10 from Plot 3 and the mini-plots of Plot 1 on the other hand have the same level as the mini-plots 11 – 20 from Plot 3.

Focusing at the distribution of vegetation cover over the plot profiles, Figure 23 shows that vegetation cover increases at the bottom end of Plot 2 in front of the sediment retention basin. At the two other plots, there so no such effect noticeable. In contrary, vegetation cover at Plot 1 is highest directly behind the upper stone bund, which builds the top end of the plot. Vegetation cover has a slightly decreasing tendency from top to bottom.

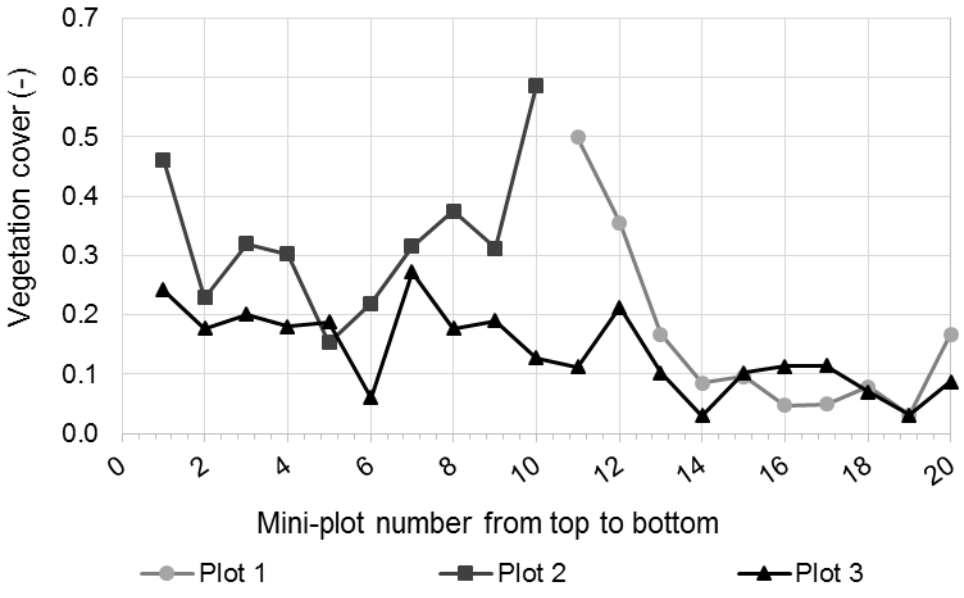

Figure 23: Vegetation cover for the mini-plots at Plot 1, 2 & 3 derived from the automatized Arc GIS analysis.

Concerning the rock fragment cover, Plot 3 shows higher values for this parameter than both treated plots. Figure 24 shows rock fragment cover for each mini-plot at the three soil erosion plots.

It is obvious, that the variation of rock fragment cover between mini-plots is high. At Plot 3 rock fragment cover varied from 7 % to 55 % (standard deviation of 0.14 %). Rock fragment cover of Plot 1 and Plot 2 ranged from 3 % - 25 % and 5 % - 28 %, respectively. Especially the long plot shows a systematic decline of rock fragment cover from top to bottom. The detailed list including rock fragment cover for all mini-plots separately is attached to the Annex.

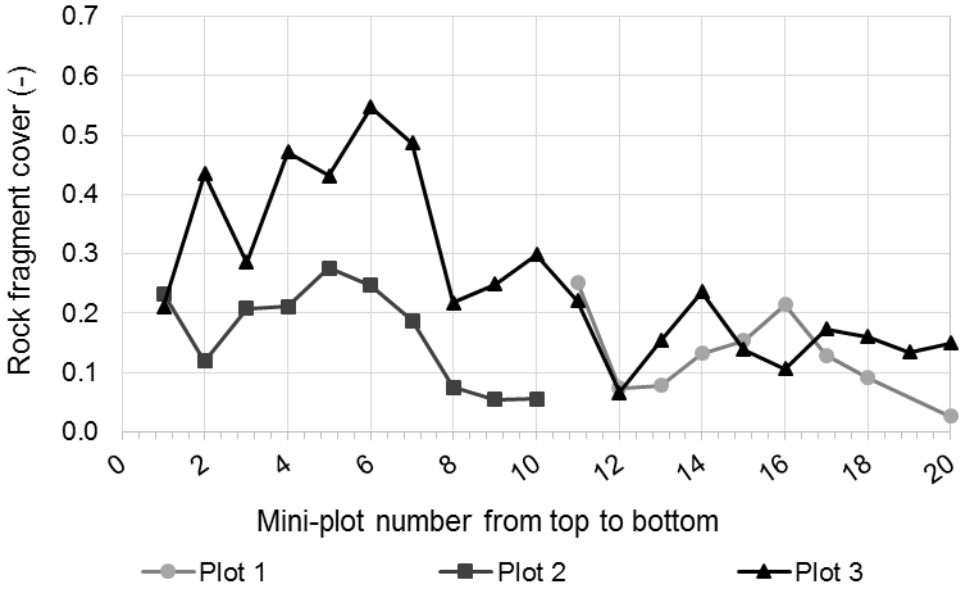

Figure 24: Rock fragment cover for the mini-plots at Plot 1, 2 & 3 derived from the manual analyse using AutoCAD.

8.4 Soil loss measurement

Sediments, which eroded during rainfall events, were collected in three retention basins located at the outlets of the plots. Next to the sediments, water accumulated in the basins. We assumed that this water results from surface runoff. As the clay content of the soil is high, the infiltration of the stored water is low and thus the water stays in the basins. The monitoring of removed water showed that this was not the case. Even if no rainfall occurred, the basins filled with water again after the removal. This indicates that the basins acted as a drainage of the fields and water infiltrated from the soil into the basins. Consequently, the amount of stored and measured water in the basins after rainfall events is not related to surface runoff and cannot be evaluated or used for the successive model calibration. A second effect, which supports this assumption, is that the basins mostly filled to the same level and never overtopped the basins. Because of this, solely information of the soil loss monitoring was used for the entire WEPP model calibration.

Figure 25 shows the amount of collected sediments per day of removal and daily rainfall during this period. It is noticeable, that the amount of accumulated sediments in the basin of Plot 2 was very low compared to the other basins. The highest amount of sediments was removed on August 1st, 2012. More than 450 kg accumulated in the sediment retention basins of Plot 1 and Plot 3.

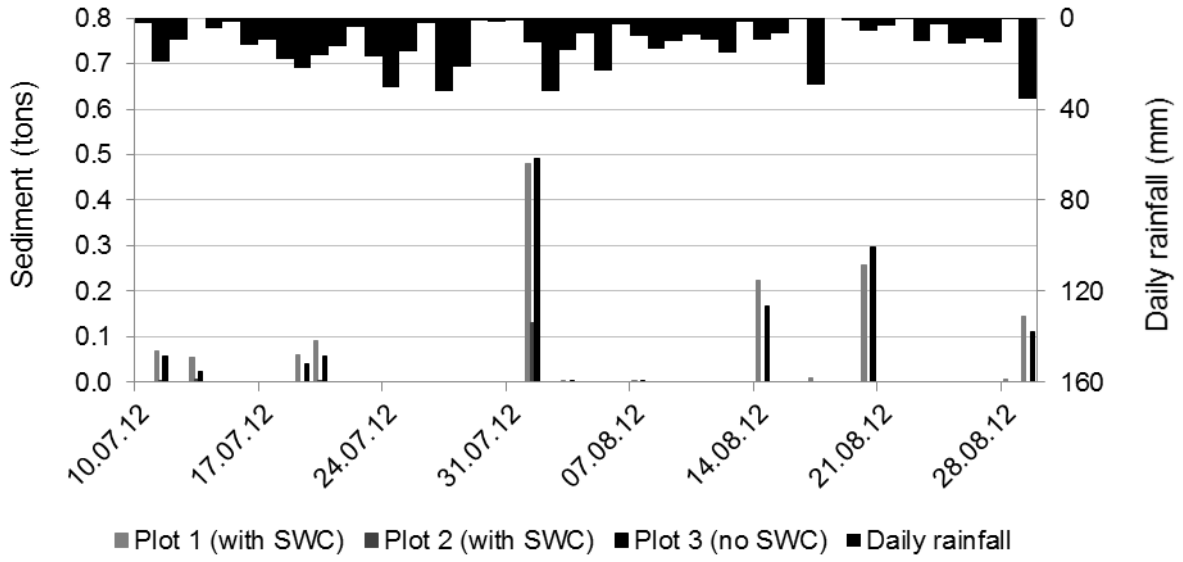

Figure 25: Mass of sediments in the retention basins for all days of monitoring

Figure 25 shows that on five days collected sediments were very low. On these five days water, which accumulated in the basins was removed and the sediment concentration of the water led to the recorded soil loss. Especially measurements on the last day of sediment removal emphasize the assumption that collected water did not result from surface runoff. Between the removal on August 29th and the following day no rainfall occurred. However, all water was removed from the basins on the first day and the basins were full with water again on August 30th; more than 2000 litres accumulated in the basins.

In the following, these five events were not considered as single events, but added to the next event with visible soil loss. Soil loss rates arise from relating the dry weight of the collected material to the contributing areas derived from the Arc GIS analysis of the surveying data (see Figure 19). Figure 26 shows soil loss rates from the three plots for the remaining eight days of soil loss monitoring.

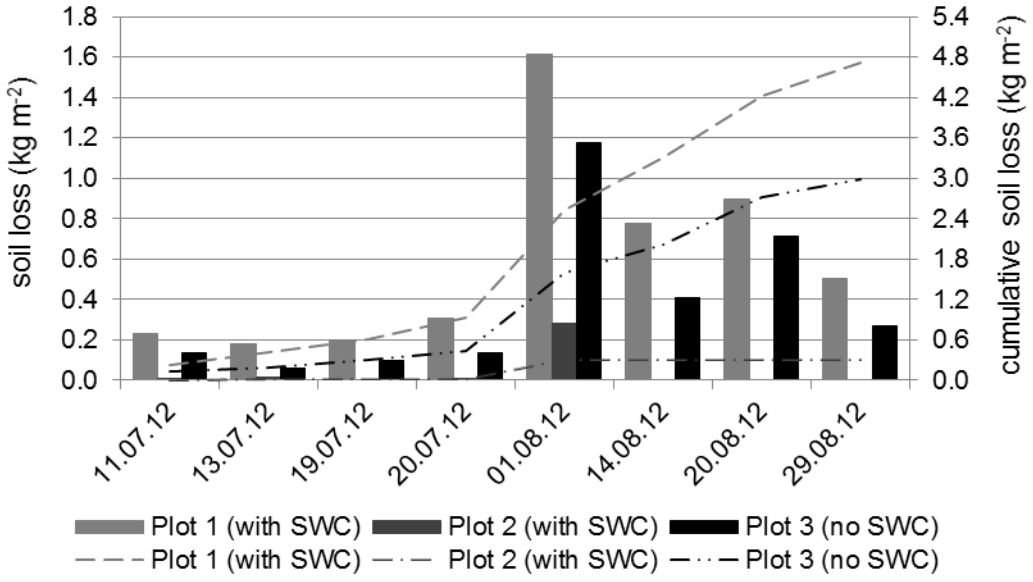

Figure 26: Comparison of soil loss rates from the three experimental plots

Figure 26 clearly shows that highest soil loss occurred at Plot 1 (with SWC). At Plot 2, the second plot with soil conservation measure, nearly no soil loss occurred. While at Plot 1 cumulative soil loss over the rainy season was 4.7 kg m^{-2}, only 0.3 kg m^{-2} sediments accumulated in the retention basin at Plot 2. Only on August 1st, 2012 considerable amount of sediments were removed from this basin (0.28 kg m^{-2}).

Soil loss from Plot 3 is lower than soil loss from the treated Plot 1, even though it is in the same range. Over the rainy period, cumulative soil loss from Plot 3 is about 3.0 kg m^{-2}.

The length of Plot 3 equals the length of Plot 1 and Plot 2 together. In this sense, Plot 3 and the combination of Plot 1 and Plot 2 can be seen as two transacts as shows Figure 27. Soil loss is in the same range for both transacts. However, most soil loss from the transact with stone bunds comes from Plot 1 (116 kg m^{-1}). Sediment delivery from Plot 2 is low (11 kg m^{-1}). Thus, this result for the weighted average soil loss has to be handled with care.

Plot 2, having the same length as Plot 1, shows much lower soil loss. The soil loss of 0.3 kg m^{-2} and 11 kg m^{-1} over the rainy season 2012 is extremely low compared to 4.7 kg m^{-2} and 116 kg m^{-1} and 3.0 kg m^{-2} and 133 kg m^{-1} for Plot 1 and Plot 3, respectively.

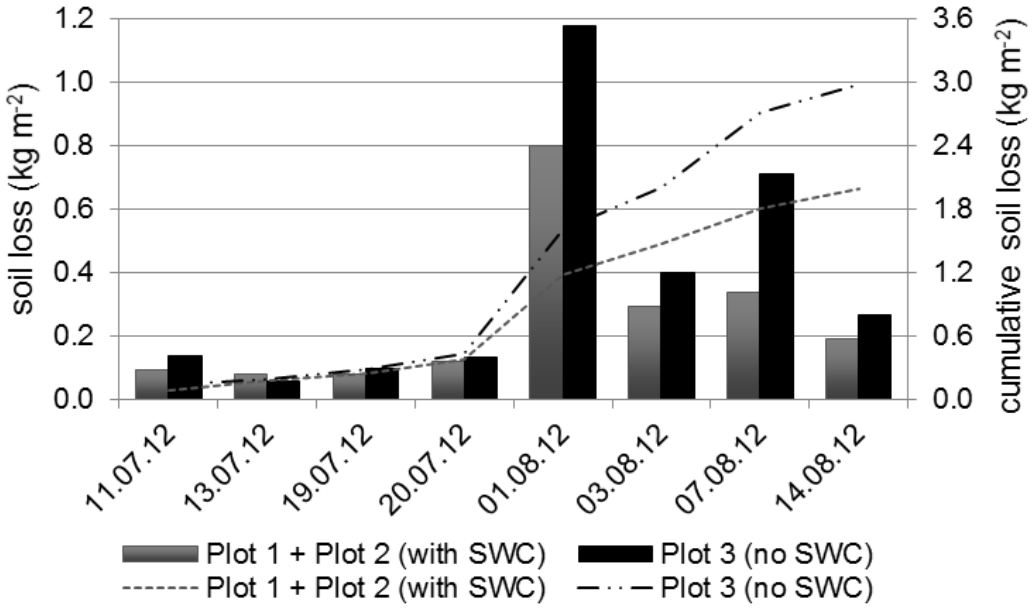

Figure 27: Weighted average soil loss of the two treated plots and Plot 3, separately.

8.5 Discussion of the field work results

Hurni (1988) estimated a mean soil loss rate from arable land of 4.2 kg m^{-2} for the Ethiopian Highlands. However, this value is an average for a bigger scale. Locally soil erosion rates might be significantly higher or lower. For Ethiopia, Gebreyesus and Kirubel (2009) defined a maximum tolerable soil loss of 1.8 kg m^{-2} per year. Thus, observed soil loss is more than twice this maximum tolerable value. However, it can be expected that parts of the eroded soil would deposit in depressions within the sub-catchment and would not leave the watershed. Concerning soil loss monitoring from 2012 it has to be mentioned that monitoring started in the end of June. Sometimes, intensive events occur in the beginning of the rainy season when soils are bare. These events were not monitored during the fieldwork. Additionally, the intensity of rainfall events was low compared to 2011 and 2013. Both facts make ongoing research necessary.

Soil loss measurements showed high variation at the three experimental plots. Comparing the two plots at fields with stone bunds, Plot 1 showed the highest and Plot 2 the lowest soil loss. Soil loss at Plot 1 was 15 times higher than at Plot 2. Plot 1 lay between two subsequent stone bunds and studied the effect of slope reduction by the bunds. An intersecting stone bund divided Plot 2 into an upper and lower part. Considering only the lower part of Plot 2 with a length of approximately 20 m, soil loss still is very low, compared to the second plot under treated conditions.

This significant difference in soil loss rates between Plot 1 and Plot 2 is only explicable by combination of several influencing parameters. One reason for this considerably smaller soil loss of Plot 2 is the higher canopy cover. As shown in 8.3 canopy cover on Plot 2 was double as high as on the other two plots. Figure 28 and Figure 29 show canopy cover at Plot 1 and Plot 2, respectively. Pictures were taken on August 14th 2012. Even though farmers cultivated sorghum and sow in the same time, the development of vegetation cover is completely different at the two plots.

Figure 28: Vegetation cover at Plot 1.

Figure 29: Vegetation cover at Plot 2.

However, the measurements imply that another reason for the low soil loss rate is the deposition of detached material from Plot 2 in the plot area in front of the retention basin. Thus, not all sediments moved downslope to the retention basin. The slope profile of this plot shows a slight elevation at the bottom end, which indicates that sediments deposited in this section. As the survey of the site was conducted only at the end of the rainy season, it is not possible to know if this deposition is due to the construction of the basins or already existed before. This aggravates the evaluation of soil loss from Plot 2.

Plot 3 was the longest plot, situated on fields without soil conservation measure. Soil loss from this plot was in the same range as for Plot 1, but still lower. In the case of Plot 3 the relatively higher rock fragment cover (mean 26 %) compared to the treated plots (mean 14 % and 17 %), might had have a positive effect on the soil erosion process. Especially the heterogeneous distribution of rock fragment cover of Plot 3 with higher fraction at the upper than at the bottom end, affects the soil erosion process. In the upper part, rock fragment cover was high with a mean value of 41 % for the first 15 m. Also for the rest of the slope length, rock fragment cover was higher (18 %) than at Plot 1 (13 %).

a) Effect of rock fragment cover

Stone fragment cover has a retardant effect on soil erosion. This positive effect is a result of several sub-processes, which are affected by rock fragment cover and lead to a reduction of soil erosion. Rock fragments protect the soil surface against raindrop impact and overland flow. Additionally, rock fragments reduce the effect of surface sealing (Poesen and Lavee 1994). Rock fragments retard ponding and slow down surface runoff and thus reduce its detachment and transport capacity (Cerdà 2001; Martínez-Zavala and Jordán 2008).

Especially at the untreated Plot 3, which is the longest soil erosion plot, rock fragment cover was high in the upper part and decreased towards the bottom. This can be reasoned by the fact that soil erodes from the upper part of the hillslope, exposing rock fragments. The selective erosion of fine particles by tillage erosion enforces this effect. While at the bottom part deposited sediments fill up the space between rock fragments and cover them. This second effect is apparent in in the slope profile (see Figure 24), as for all three soil erosion plots the lowest mini-plots showed relatively low rock fragment cover.

Another reason for the higher rock fragment cover at Plot 3 can be that farmers use rock fragments for the construction of the stone bunds from their fields. The higher rock fragment cover on the field without measure might reflect this fact. The lower rock fragment cover on the plots with stone bunds can be explained by the removal of stones for the construction of the bunds (Nyssen et al. 2001).

Nyssen et al. (2001) and Nyssen et al. (2007) showed that removal of rock fragments results in increased erosion rates and hence there exists a negative relationship between soil loss by water erosion and rock fragment cover. On the other hand, high rock fragment cover aggravates tillage and reduces the area available for plants. Hereby, farmers evaluate big stones as particularly disturbing.

b) Effect of infiltration rate

In general, Figure 26 shows that soil loss in the first half of the rainy season is low compared to the second half of the season. This is interesting, as one would expect that highest soil losses occur in the beginning when soils are bare and exposed to the erosive force of the rainfall and surface runoff.

The distribution of soil loss over the rainy season shows a heterogeneous pattern with lower soil erosion in the beginning of the rainy season and higher erosion rates towards the end (see Figure 26). This might be reasoned by the incidence of cracks in the soil. Over the dry season, shrinkage cracks develop due to very low soil moisture content. The cracks close during the first rainfall events as a consequence of swelling effects. It was assumed that these cracks cause a higher infiltration rate in the beginning of the rainy season, which will go down as the cracks start to close. Figure 30 shows cracks at the experimental site, on June 20th. After the first rainfall events, these cracks were not apparent at the soil surface. Nevertheless, these cracks might have a long-lasting effect on the subsurface structure of the soil. Nyssen et al. (2009) observed similar trends. They observed considerable surface runoff one month after the beginning of the main rainy season and not in the beginning of the rainy season when soils are bare and freshly tilled.

Figure 30: Cracks in the soil at the beginning of the rainy season

After the cracks close, infiltration should decrease drastically leading to important runoff. Due to the soil texture at the experimental site (clay 42 %, silt 36 %, sand 22 %), one would expect low hydraulic conductivity and infiltration capacity, which result in high surface runoff. Surprisingly, field measurements by Schürz (2012) showed high hydraulic conductivity at the plots (10^{-4} – 10^{-5} m s^{-1}) over the whole rainy season. Another fact, which supports the assumption of high hydraulic conductivity at the fields, is the filling of the sediment retention basins due to soil water. After rainfall events, when the soil was very wet, the sediment retention basins filled with water. The soil drained into the basins and filled them from bottom to the top.

c) Effect of slope length

As mentioned before, Plot 3 was the longest plot, with a longest distance of 55 m. In comparison, Plot 1 and Plot 2 had a length of 24.5 m and 38 m, respectively (see 8.2 c).

The length of the slope is positively correlated with soil erosion. Longer slopes lead to more accumulated runoff with increased velocity and kinetic energy. Finally, rill erosion starts and ends in the formation of gullies (Roose 1996). In the Universal Soil Loss Equation erosion increases exponentially with the length of the slope with an exponent of 0.5 (Wischmeier and Smith 1965). However, experiments showed that the influence of slope length is not consistent nor particularly strong (Roose 1996).

The theoretical basis of increased soil erosion due to longer hillslope is the ongoing accumulation of surface runoff, which leads to the initiation of rills. Rill erosion can contribute a big part to total soil erosion. Thus, the influence of slope length is linked to the soils sensitivity to rill erosion. In contrast, the increase in sheet erosion is little as the surface roughness controls the velocity of the sheet runoff and keeps it low (Roose 1996).

Surface roughness at the experimental plots was high (see 8.6.7). Signs that indicate the formation of rills at the fields were not visible over the rainy season. Additionally, the analysis of canopy and rock fragment cover (see 8.3) showed that especially in the upper part, rock fragment cover was high at Plot 3. This also might influence soil loss from this plot in the way that the high rock fragment cover in the upper part slowed down the runoff, enhanced infiltration

and reduced the erodibility in this section; hence, compensated the negative effect of the longer slope. This suggests that the impact of the slope length is not very strong at the plots.

d) Effect of the stone bunds

Even though soil loss was highest at the plot with stone bunds, the effect of stone bunds on the retention of sediments has to be stressed. Eroded soil within sections between two stone bunds accumulates behind the bunds and thus sediments are not delivered to the runoff channel and stay in the field. Gebremichael et al. (2005) conducted measurements in Tigray Region, in the Ethiopian Highlands, to assess the effectiveness of stone bunds in controlling soil erosion. He stresses that the introduction of stone bunds reduced annual soil loss by 68 %. Sediments accumulated behind the bunds until they filled up. After some years, the effect decreases if stone bunds are not maintained regularly. Additionally, stone bunds increase the number of boundaries between fields and hinder tillage erosion, which contributes a big part of the downslope movement of the soil. This effect was not measureable with the design in this work. The sediment retention basins of the plots were situated above the stone bunds. Soil loss from Plot 2, with a stone bund intersecting the plot in the middle, was 15 times smaller than soil loss from the two other plots. This cannot be attributed to the effect of the stone bunds. Considering that the intersecting stone bund hold back all sediments coming from above, soil loss at this plot was still one decade below soil loss from Plot 1. However, on-site observations showed that sediments accumulated in the area behind the stone bunds, but sediments also overtopped the bunds as show Figure 31 and Figure 32.

Figure 31: Sediments overtopping the stone bund

Figure 32: Stone bund; the area behind the bund did not fill entirely with sediments yet.

8.6 Results and Discussion of the computer-based modelling

8.6.1 Model sensitivity analysis

The sensitivity analysis describes the model's output response to variation of single parameters. Table 6 shows the sensitivity ratio (SR) for the analysed parameters. It shows that WEPP was sensitive to changes of rock fragment content, rill erodibility, random roughness and hydraulic conductivity and less sensitive to alteration of cation exchange capacity, maximum leaf area index, initial saturation level, canopy cover coefficient and interrill erodibility.

Table 6: Sensitivity analysis for selected parameters

Parameter	Unit	Tested range	Sensitivity Ratio (SR)
rock fragments	%	5 - 55	1.09
rill erodibility	s m^{-1}	0.003 - 0.009	0.82
random roughness	cm	4 - 15	0.68
effective hydraulic conductivity	mm h^{-1}	2 - 400	0.54
cation exchange capacity	meq $(100g)^{-1}$	20 - 35	0.14
maximum leaf area index	-	4 -10	0.07
initial saturation level	%	0 - 100	0.04
canopy cover coefficient	-	6 - 18	0.04
interrill erodibility	kg s m^{-4}	2500000 - 5000000	0.02

Rock fragment cover varied from 5 to 55 % in the field assessment. In these limits rock fragment cover was the most sensitive parameter of all.

If interrill and rill erodibility are known parameters the user can enter them as input parameters. In case of missing information on these parameters, the WEPP model calculates them according to dependencies from other input parameters (see 6.1, d). K_i ranged from 2500000 to 5000000 kg s m^{-4}, with the calculated value of 3740000 kg s m^{-4}. K_r varied between the limits 0.003 and 0.009 s m^{-1} with a calculated value 0.7 s m^{-1}. In this range, the sensitivity ratio was 0.82.

Concerning the random roughness of the surface, Zeleke (2001) used a value of 5 cm for the ox-drawn ard plough. Random roughness was tested in the range of 4 cm to 15 cm and showed a sensitivity ratio of 0.68.

"Baseline" hydraulic conductivity varied from 2 mm h^{-1} to 400 mm h^{-1}. The lower end of the range represents the value suggested by the WEPP model. The very high value of 400 mm h^{-1} on the other side results from measurements by Schürz (2012). Schürz conducted measurements of hydraulic conductivity at the experimental site during the period of observation and found that hydraulic conductivity is unexpectedly high for the given soil texture. He measured values of 300 mm h^{-1}. This range resulted in a sensitivity ratio of 0.54.

This information is the basis for defining the range of variation of the variable parameters rock fragment cover, rill erodibility coefficient, random roughness and "baseline" hydraulic conductivity. It was assumed that all other parameters are either known or not sensitive.

8.6.2 Analysis and definition of the model input

The objective of the modelling was to find a configuration of the model, which is calibrated to local conditions and enables simulation of various scenarios.

Soil loss was simulated for Plot 1 and Plot 3 using the WEPP model. Concerning Plot 2, soil loss was not simulated by the model. The results from the fieldwork showed that high uncertainty lies in the results of this plot. Preliminary tests to model the soil loss process at this plot showed that too little data is available to draw accurate conclusions from a simulation of this plot. In the following, this work concentrated on the configuration of a model setup, which predicts soil loss from the two other plots – without intersecting stone bund – adequately. Information from this work can contribute to the simulation of stone bunds in successive works.

a) Soil input

The soil is built from one layer with a soil depth of 1.5 m. Soil texture was determined from mixed samples for each plot. Variation in soil texture from one plot to the other was negligible and thus soil texture was set to a single value representative for all three plots. Table 7 shows fractions of clay, silt and sand. For the given composition of soil fractions, the soil is defined as a clay soil.

Table 7: Soil texture of the three plots used in the WEPP soil file

Soil texture	Clay [%]	Silt [%]	Sand [%]
Plot 1,2 & 3	42	36	22

Albedo was set to 0.3 as a function of organic matter, which is 1.5 %. According to Flanagan and Livingston (1995) cation exchange capacity (CEC) for clay soils is between 30 – 150 meq $(100g)^{-1}$. Alternatively CEC can be estimated by Equation 13 and results in 24 meq $(100g)^{-1}$.

$$CEC = 0.5 * clay + 2 * organic\ matter$$

Equation 13

Preliminary tests showed that soil loss prediction is slightly better using a CEC value of 24 meq $(100g)^{-1}$.

For soils with clay contents exceeding 40 %, WEPP estimates “baseline” hydraulic conductivity using Equation 5 (see 6.1 d).

Determined clay content at Plot 1 and Plot 2 was about 42 %. Applying Equation 5 to this soil, estimated hydraulic conductivity is 2.2 mm h^{-1}. At Plot 1 Schürz (2012) measured mean hydraulic conductivity of 296 mm h^{-1}, ranging from 204 – 419 mm h^{-1}. Mean hydraulic conductivity at Plot 2 averaged 291 mm h^{-1}, ranging from 194 – 362 mm h^{-1}. These values are high for a loamy clay soil, but measurements were stable over the rainy season. Huge cracks and the fissured structure of the soil affect the infiltration of surface water. To account for this enormous range of hydraulic conductivity and the fact that the model is sensitive to the variation of this parameter, the model ran scenarios with different K_b values. Four different scenarios accounted for the effect of “baseline” effective hydraulic conductivity.

For Plot 1 and 3 K_b was set to 2 mm h^{-1}, 100 mm h^{-1}, 200 mm h^{-1} and 300 mm h^{-1} for sets of simulations, respectively.

Another soil specific factor, which is a sensitive parameter in the model, is the rill erodibility factor. At Plot 1, one set of scenarios used the internally calculated K_r value of 0.007 s m^{-1},

while the other two scenarios used an increased value of 0.009 s m^{-1} and a reduced value of 0.005 s m^{-1}. For Plot 3, a different combination of rill erodibility coefficients was tested. The value of 0.007 s m^{-1} built the upper limit. Two other sets of scenarios included coefficients of 0.003 and 0.005 s m^{-1}.

The initial saturation level represents the saturation level of the soil on January 1st. Due to the precipitation pattern in the study area, saturation level is low in the beginning of the year. In the model, soil water stays at a constant level until the first rainfall occurs, as the model simulates no evaporation from bare soils below a residual moisture content (see 6.1 c). As mentioned before, there was no rainfall data available for the first months of 2012. The rainfall, which occurred in this period, infiltrated into the soil and increased the moisture content of the soil. Due to measurements by Schürz (2012) soil water content in the beginning of precipitation records is known. In order to compensate the lack of rainfall data from January to mid of June, the initial saturation level was adjusted to fit the field measurements and was set to 75 %.

At Plot 1, the mean of all rock fragment cover measurements (13%) was used for the whole hillslope. Due to high variation of rock fragment cover within the mini-plots at Plot 3 with a decrease from top to bottom of the hillslope, two rock fragment cover values were implemented in the model. The soil input interface allows the input of more than one Overland Flow Elements (OFE's). This means, that the hillslope can be divided into more sections with different soil properties. Thus, for the upper 15 m rock fragment cover was set to 41 % and to 18 % for the rest of the hillslope (30 m). 41 % and 18 % are the mean values for mini-plot 1 -7 and 8 – 20, respectively. Rock fragment cover is also a sensitive parameter for the model. Thus, the measured values varied in different scenarios with an increase and decrease of 3 % for each plot.

b) Management input

Over the period of one year, the management input file lists management operations chronologically. Table 8 gives an overview on the management in 2012. Starting point is the initial condition of the fields on January 1st.

Table 8: Chronology of Operation Types

MANAGEMENT
Rotation

Date	Operation Type
01.01.2012	Initial Conditions
10.02.2012	Primary Tillage
10.05.2012	Secondary Tillage
01.06.2012	Plant – Annual (Sorghum)
15.12.2012	Harvest – Annual (Sorghum)

Each operation type is specified in a separate file. The detailed list of input parameters for all management steps are given in the Annex.

The initial condition file describes the actual situation on January 1st, before the beginning of the experiment. Initial plant is tef, a traditional crop, which farmers cultivated during the

cropping season 2011. Tef was harvested in the end of November 2011. Last tillage operation was before sowing tef in June. Initial rill and interrill cover was set to zero.

Farmers tilled their fields twice before planting sorghum in 2012. Primary tillage was in February, while secondary tillage was in May. Tillage implement is a tradition ox-drawn ard plough, called *maresha*, which is used for both, primary and secondary tillage (see Figure 33 and Figure 34). Tillage depths were set to 12 cm and 10 cm for primary and secondary tillage, respectively. Ridge height (12 cm) and ridge interval (35 cm) were higher in primary tillage, which leaves 70 % of the surface area disturbed. Ridge height after secondary tillage was 10 cm. The ridge interval reduced to 25 cm. After secondary tillage, 100 % of the area is disturbed. Zeleke (2001) analysed the applicability of WEPP for runoff and soil loss prediction in the Ethiopian Highlands. In this work, similar values were used for tillage depth, ridge height and ridge interval and surface disturbance. In this work Zeleke (2001) used random roughness values for the ox-drawn ard plough between 4.5 and 5.5 cm. The simulation included four sets of scenarios with random roughness values of 5 cm, 8 cm, 11 cm and 14 cm.

Figure 33: Farmer in the study area ploughing his field using the *maresha* plough

Figure 34: wedge-shaped metal share of the *maresha* plough © (Nyssen et al. 2000)

In 2012 farmers cultivated sorghum at the plots. Sowing is in the beginning of June. WEPP contains plant files for sorghum under different fertilization levels. The file Sorghum – Low

Fertilization Level was used as draft and was adapted to local conditions. According to the farmers, maximum canopy height is 1.8 m. In the study area, sorghum is not planted in-row, but in an irregular pattern. Hence, the default row width was reduced to 15 cm, while the in-row plant spacing was slightly increased (15 cm).

The canopy cover coefficient (BBB), a crop-dependent parameter, describes the relationship between canopy cover and vegetative biomass. By increasing the parameter, the canopy cover will increase as a function of biomass. As second plant specific parameter, which influences the evolution of canopy cover over the cropping season is the maximum leaf area index (XMXLAI). It exist canopy cover records from July 25th, 2012, as described in 7.5. By running the model with different canopy cover coefficients and maximum leaf area indices, canopy cover can be altered until observed and simulated values coincide. Two ratios between canopy cover coefficient and maximum leaf area index are leading to the same canopy cover on the observation day. Preliminary tests showed that the ratio with lower BBB and higher XMXLAI leads to higher erosion rates in the end of the rainy season. This coincides better with field observations. As both parameters are not sensitive for the soil loss prediction, only one scenario with a BBB of 12 and the corresponding XMXLAI of 8 ran in the simulation of Plot 1. For Plot 3 this ratio was slightly different, with BBB 11 and XMXLAI 8.

8.6.3 Model scenarios

a) Plot 1 (plot with stone bunds at the upper and lower limits):

According to the variation of input parameters described in the previous section 8.6.2, soil loss for Plot 1 was calculated for 144 scenarios. Table 9 shows the variable input parameters in short.

Table 9: Overview of variable input parameters for Plot 1

Rill erodibility coefficient (RE)	0.005, 0.007, 0.009 s m^{-1}
Rock fragment cover (RO)	10, 13, 16 %
Random roughness (RR)	5, 8, 11, 14 cm
Baseline hydraulic conductivity (K_b)	2, 100, 200, 300 mm h^{-1}

b) Plot 3 (plot without stone bunds)

Soil loss simulation of Plot 3 included 144 scenarios. Values of the variable parameters shows Table 10.

Table 10: Overview of variable input parameters for Plot 3. * The first values stands for rock fragment cover in the upper 15 m, the second value for rock fragment cover at the rest of the plot.

Rill erodibility coefficient (RE)	0.003, 0.005, 0.007 s m^{-1}
Rock fragment cover (RO)	38/15, 41/18, 44/21* %
Random roughness (RR)	5, 8, 11, 14 cm
Baseline hydraulic conductivity (K_b)	2, 100, 200, 300 mm h^{-1}

8.6.4 WEPP soil loss prediction: Plot 1

Three objective functions, the root mean square error (RMSE), model efficiency function (NSE) and the coefficient of determination (R^2) proved the goodness of fit of each simulation scenario.

a) Objective functions

In the simulation of Plot 1, the development of all three functions was identical, which means that the ranking due to each function resulted in the same order of the scenarios. Out of all 144 scenarios, 14 had a model efficiency of zero or more. This means, that the model is the better predictor than the mean of the observed data. For the same 14 scenarios, the coefficient of determination was 0.90 or more and the mean root square error was below 0.5. Within these scenarios, 12 of 14 had a rill erodibility coefficient of 0.005 s m^{-1}, which is the lowest of the three tested values. The three other parameters occurred in more variations. Concerning random roughness, values of 8, 11 and 14 cm led to good objective functions; only the lowest value of 5 cm did not occur within the best simulation runs. Rock fragment cover existed in all its variations 10, 13 and 16 % within these 14 scenarios. Hydraulic conductivity ranged from 100 – 300 mm h^{-1}. Figure 35 shows the frequency of each parameter value graphically.

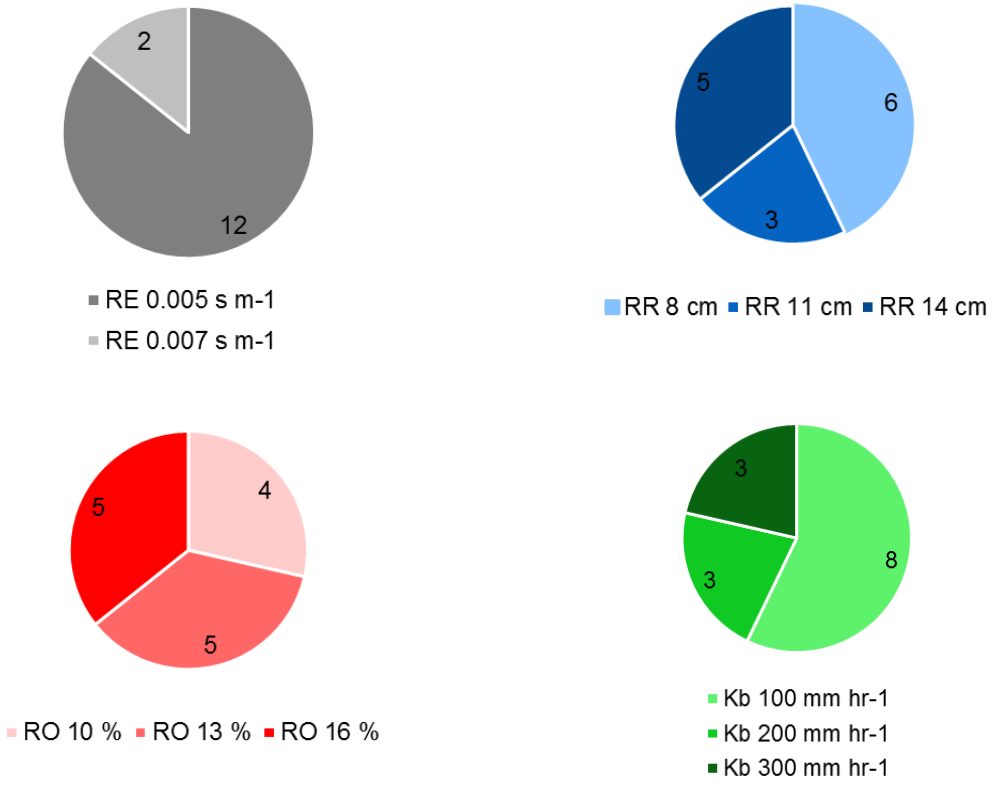

Figure 35: Frequency of each parameter value among the simulations with the best objective function results for Plot 1 (low RMSE, high NSE and R^2). RE = rill erodibility, RR = random roughness of the surface, RO = rock fragment cover, K_b = "baseline" hydraulic conductivity.

On the other hand, the scenarios with the poorest fit between observed and predicted soil loss had low hydraulic conductivity values in common. From the 14 simulation (10 %) with the worst objective function values (high RMSE, low NSE and R^2) 13 simulations ran with a hydraulic conductivity of 2 mm h^{-1}. Rock fragment cover again occurred in all combinations. While rill erodibility showed a tendency to higher values (0.007 and 0.009 s m^{-1}), random roughness

showed a reverse tendency to lower values (5 and 8 cm). This distribution of the parameters shows Figure 36.

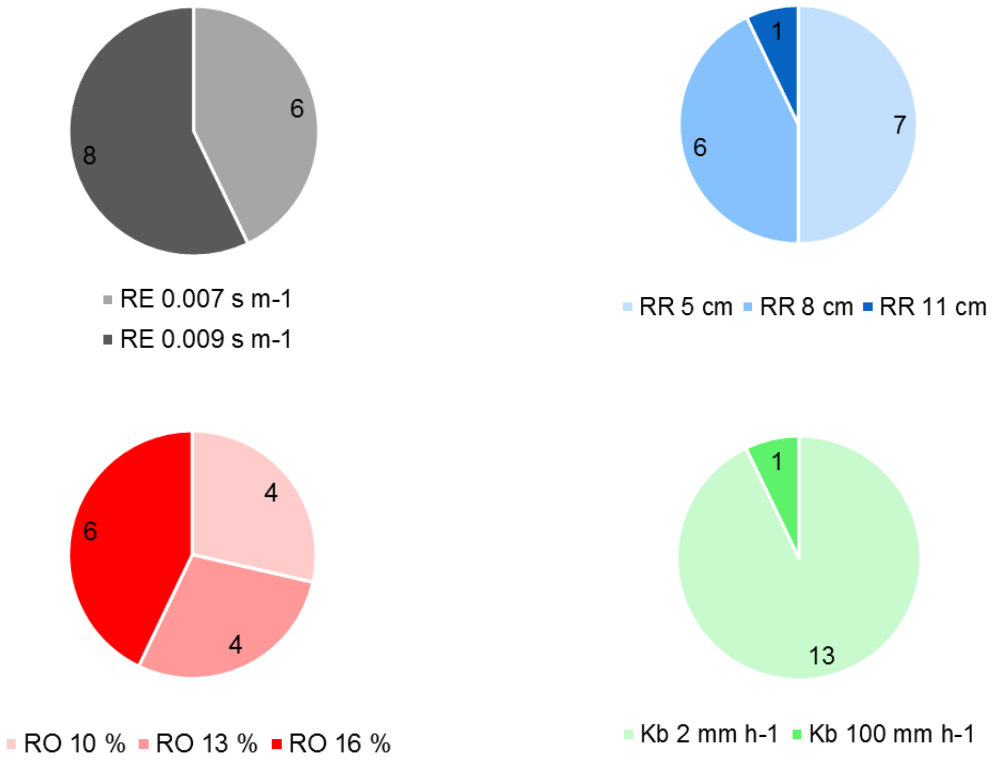

Figure 36: Frequency of each parameter values among the simulations with the worst objective function results for Plot 1 (high RMSE, low NSE and R^2). RE = rill erodibility, RR = random roughness of the surface, RO = rock fragment cover, K_b = "baseline" hydraulic conductivity.

The analysis of the objective functions shows that low values of hydraulic conductivity coincide with poor accordance of predicted and observed soil loss, while the low rill erodibility coefficient leads to the best results concerning the quality of fit between observed and predicted data.

b) Confidence interval

Predicted soil loss ranged from 2.0 kg m^{-2} to 18.6 kg m^{-2} for all simulation runs. These two boundary values result from the superposition of extreme parameter values for all variable parameters, which have the same effect on soil erosion. For the analysed parameters, all combinations were tested. Thus, scenarios with low hydraulic conductivity, rock fragment cover, and random roughness and high rill erodibility delivered very high soil loss rates. The vice versa case led to very low soil loss prediction. Histograms represent the distribution of data by showing the frequency of data classes. Using the statistic software "R", histograms showed the distribution of predicted soil loss for all observation days. Except for two days, soil loss is approximating a normal distribution, even though with pronounced skewness. The introduction of a confidence interval should help to eliminate the effect of superposition of parameter values, which lead to unlikely results as described above. The 2,5 % and 97,5 % quintile delimit the 95 % confidence interval. Figure 37 shows the area, which forms between the quintiles and observed soil loss for each day of removal.

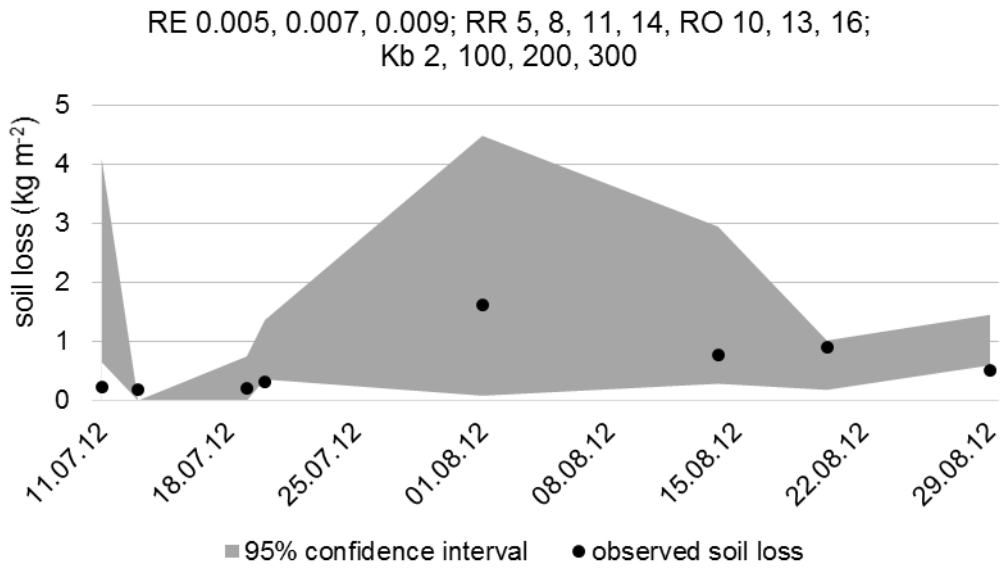

Figure 37: Simulated soil loss of Plot 1 with a 95 % confidence interval and measured values for all days of sediment removal and all combinations of parameters.

It was already clear from the analysis of the objective functions (8.6.2 a) that low agreement of measured and predicted soil loss is linked to low hydraulic conductivity and high rill erodibility coefficients. Two further bands of confidence intervals showed that the range in the confidence interval decreases by eliminating all scenarios with hydraulic conductivity of 2 mm h^{-1} and a rill erodibility coefficient of 0.009 s m^{-1}. The observed soil loss of 0.9 kg m^{-2} on 20th August 2012 left the confidence interval. For five days of removal, 13th, 19th, 20th July and 20th, 29th August 2012 the variance in the scenarios is low, which means that the confidence interval is narrow. On July 13th and 20th as well as August 29th the observed soil loss lies outside this interval but very close to it.

Still, the 95 % confidence interval built a wide band of simulation results. In further steps, the analysis of the development of the confidence interval intended to spot those parameters whose removal leads to a reduction of the area between the quintiles so that still the same amount of measurement points lies within the confidential range.

Random roughness of 5 cm did not appear in the best simulation results with positive model efficiency and a coefficient of determination above 0.9. Its removal led to a reduction of the confidential band. The elimination of the WEPP suggested value of the rill erodibility coefficient (0.007 s m^{-1}) narrowed the range of predictions even more. Then the only value of this parameter was 0.005 s m^{-1}. As all parameters, which result in too high soil loss by trend, were removed, the confidence interval shifted to lower values, as shows Figure 38.

In a last step, the removal of parameter combinations, which led to very low soil loss predictions, random roughness of 14 cm and hydraulic conductivity of 300 mm h^{-1}, led to the narrowest range of predicted soil loss for each day of removal. Even though, the area between the confidence interval decreased with every eliminated parameter value, the number of observations in this area stayed the same.

Figure 38 shows the change of the 95 % confidence interval due to a reduction of the parameter range of the four parameters rill erodibility, random roughness and hydraulic conductivity. The widest band of the confidence interval results from the analysis of all scenarios; the narrowest

band includes only those parameter values with the best accordance between observed and predicted soil loss (see Figure 39).

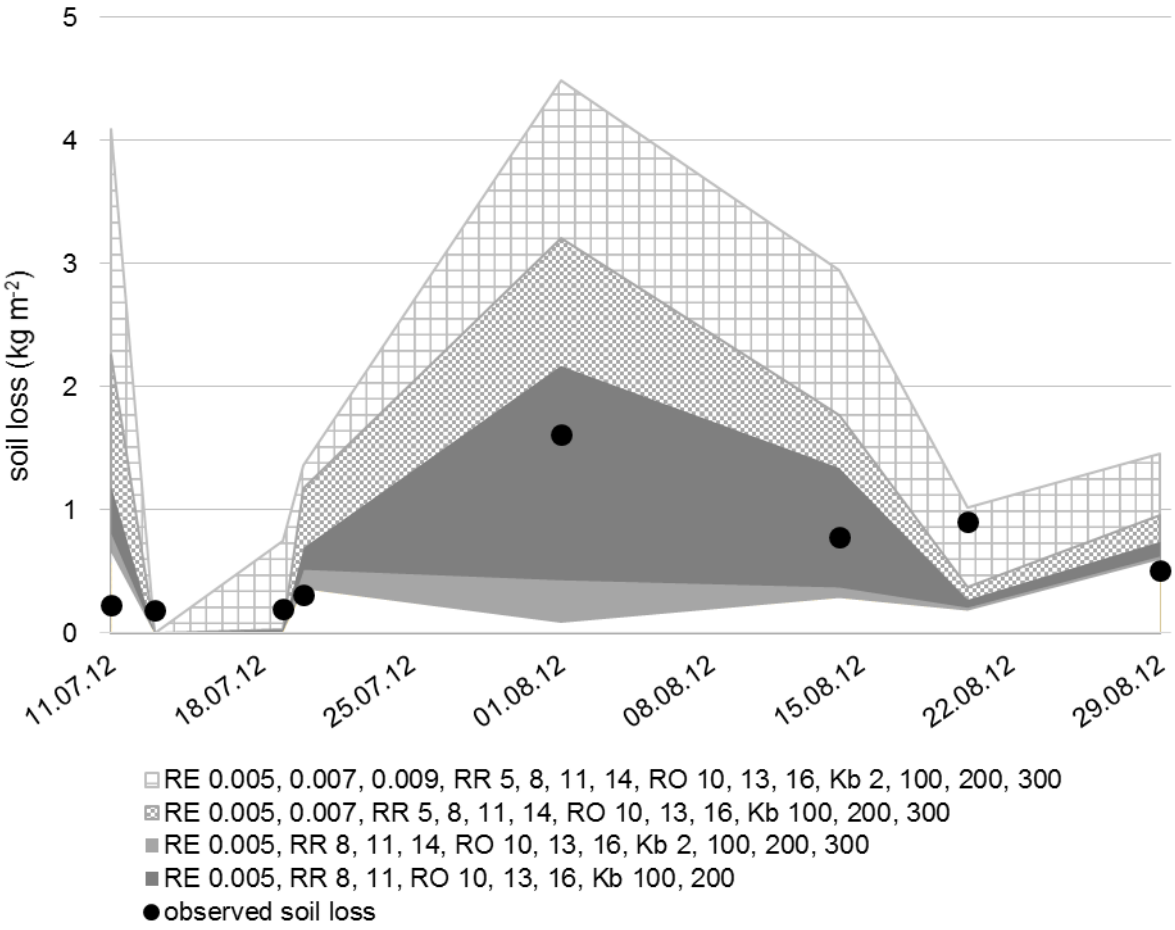

Figure 38: 95 % confidence interval of soil loss prediction and measured values for all days of sediment removal at Plot 1. Beginning from the combination of all scenarios, the interval decreases as some parameter values were eliminated from the analysis. Stepwise, scenarios that led to very high or low soil loss prediction were removed and thus the confidence interval narrowed. RE = rill erodibility, RR = random roughness of the surface, RO = rock fragment cover, K_b = "baseline" hydraulic conductivity

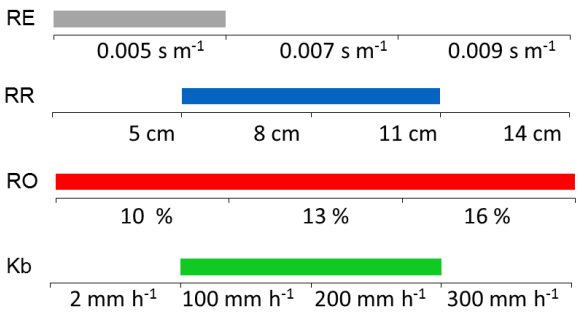

Figure 39: Range of parameter values, which remained in the set of scenarios leading to the narrowest confidence interval for Plot 1

The remaining parameter values are those, which performed best in simulating observed soil loss. The rill erodibility coefficient was lower than the value suggested by the model. Random roughness lay in the range of 8 to 11 cm. Rock fragment cover had little influence on the

simulation results; all three values led to good predictions. Hydraulic conductivity showed best results with values of 100 mm h^{-1} and 200 mm h^{-1}.

Twelve scenarios remained; six of these had positive model efficiency values. For all, the coefficient of determination ranged from 0.86 to 0.93, model efficiency from - 0.46 to 0.32 and the root mean square error from 0.38 to 0.56. Table 11 shows a list of the scenarios, which remained in the set of simulations.

Table 11: Measured and observed soil loss rates and objective functions of the remaining parameter value for the simulation of soil loss at Plot 1.

Scenario	Meas. soil loss (kg m^{-2})	obs. soil loss (kg m^{-2})	RMSE	ME	R^2
RE 0.005,RR 11,RO 16%,Kb 100	4.7	4.84	0.38	0.32	0.93
RE 0.005,RR 11,RO 13%,Kb 100	4.7	4.79	0.38	0.32	0.93
RE 0.005,RR 11,RO 10%,Kb 100	4.7	4.38	0.39	0.29	0.93
RE 0.005,RR 8,RO 10%,Kb 200	4.7	5.24	0.42	0.16	0.92
RE 0.005,RR 8,RO 13%,Kb 200	4.7	5.38	0.44	0.12	0.91
RE 0.005,RR 8,RO 16%,Kb 200	4.7	5.60	0.45	0.05	0.91
RE 0.005,RR 8,RO 10%,Kb 100	4.7	6.01	0.48	-0.08	0.89
RE 0.005,RR 8,RO 13%,Kb 100	4.7	6.25	0.51	-0.20	0.88
RE 0.005,RR 8,RO 16%,Kb 100	4.7	6.44	0.53	-0.29	0.87
RE 0.005,RR 11,RO 16%,Kb 200	4.7	3.09	0.55	-0.42	0.86
RE 0.005,RR 11,RO 13%,Kb 200	4.7	3.02	0.55	-0.43	0.86
RE 0.005,RR 11,RO 10%,Kb 200	4.7	2.95	0.56	-0.46	0.86

8.6.5 Best simulation scenario: Plot 1

Next to soil loss prediction, WEPP models additional output for each scenario. This additional information is presented for the scenario with a rill erodibility of 0.005 s m^{-1}, random roughness of 11 cm, rock fragment cover of 13 % and Kb of 100 mm h^{-1}.

a) Predicted surface runoff

In the time of observation, precipitation was 817 mm. Of this rainfall, the model calculated a surface runoff of 164 mm. This leads to a rainfall – runoff ration of 20 %, which is relatively low.

b) Predicted soil loss

Predicted soil loss is 4.8 kg m^{-2}, while measured soil loss was 4.7 kg m^{-2}. According to the simulation, there is no deposition zone along the whole hillslope profile but all net detached sediments leave the profile at the lowest point. Figure 40 shows the spatial distribution of soil loss over the profile. As shows Figure 20 in section 8.2 c, Plot 1 has a slightly undulating profile, with small local elevations and sinks. Between these two formations develop steeper slopes than the mean slope. The part with relatively high erosion rates (around 17 kg m^{-2}) is located in a transition between a high and low point and close to the end of the hillslope where runoff already gained considerable erosive forces. Besides this outlier, from a distance of about 8 m the erosion rate increases linearly with the slope length. The up and down of erosion rates in the first 8 m causes also the sequencing of sections with steeper and more gentle slope.

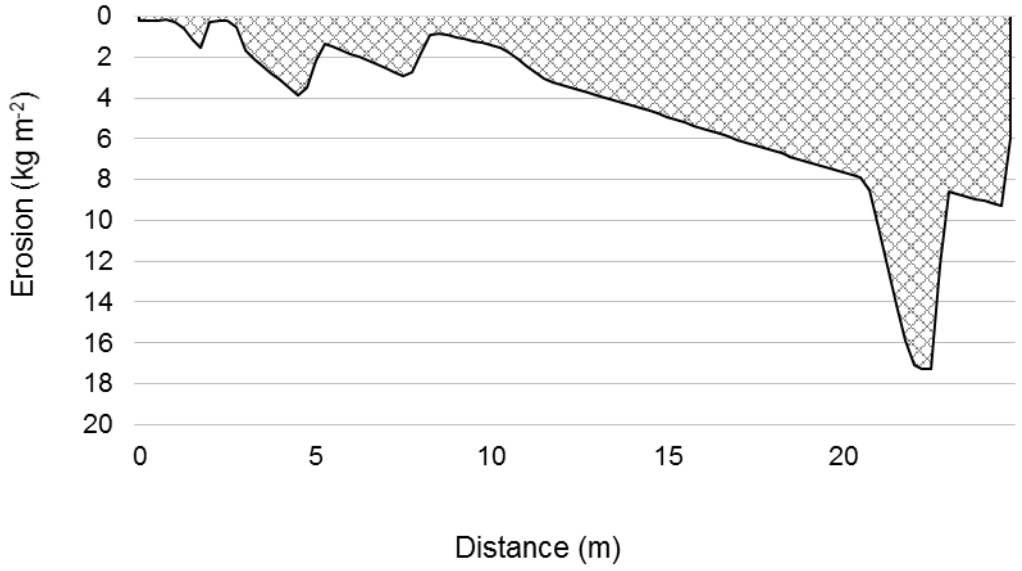

Figure 40: WEPP soil loss graph of Plot 1.

Figure 41 shows the direct comparison of measured and observed soil loss for every day of removal. No tested scenario was capable of predicting soil loss of the first event on July 11th 2012 adequately. The analysis of all events showed that there is a systematic error in the prediction of the first event. On July 13th 2012, sediments were removed for the second time. The sediments resulted from a rainfall event in the night from 11th to 12th of July. Due to a very low peak runoff rate and a rainfall duration, WEPP predicted runoff but no soil loss. The same situation occurred on July 19th. Beginning from this day, predicted and observed soil loss fit fairly well, with an exception of August 20th. The accumulated sediments eroded in a rainfall event on July 17th. WEPP under-predicted soil loss for this event.

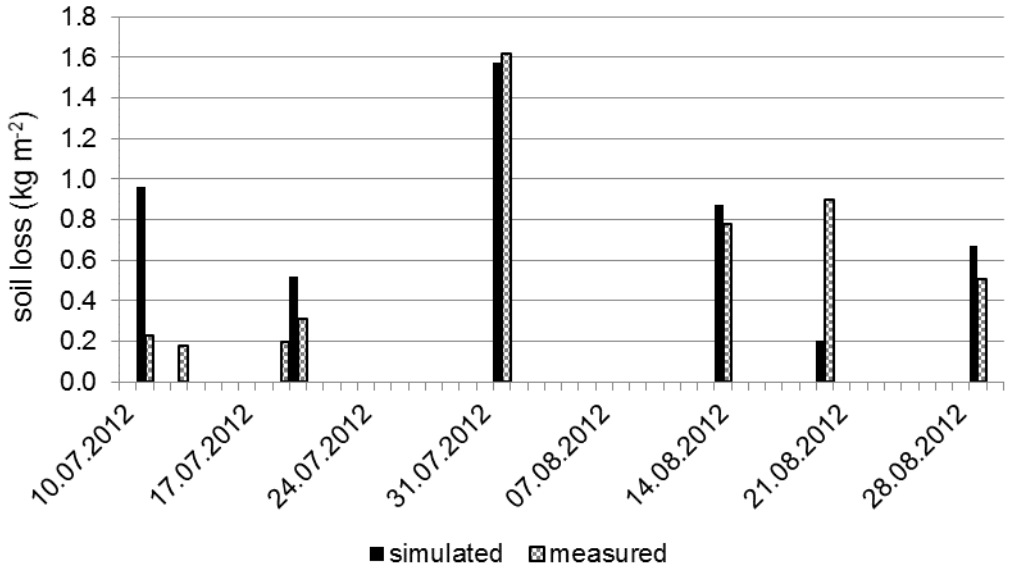

Figure 41: Comparison of observed and simulated soil loss of Plot 1 for all days of removal

c) Canopy cover and height

Sorghum seeding was on June 1st 2012. On June 28th 2012, crop height was 1 cm. Both parameters, canopy cover and height, then developed until they reached a maximum value before senescence of the plant starts and canopy cover decreases. At the end of the cropping season before harvesting at December 15th 2012, sorghum was around 1.25 m high and had a canopy cover of 0.83.

d) Predicted sorghum yield from the cropping season 2012

Predicted sorghum yield is 2.0 t ha^{-1}, which is too high in relation to the actual yield of 0.8 t ha^{-1} from 2012. Farmers reported that average sorghum yield at the experimental site reaches up to 2 t ha^{-1} but was low in the observed cropping season. The definition of the canopy cover coefficient and maximum leaf area index plays an important role for the development of the seasonal crop yield. As described in 7.7.3 d) two different ratios of these two parameters lead to the same canopy cover at the day of canopy cover determination at the field. Running the same model with all parameters as they are but changing this ratio from BBB 12 and XMXLAI 8 to BBB 17 and XMXLAI 5 the yield drops to 0.9 kg m^{-2}, while soil loss stays at a level of 4.5 kg m^{-2}. Too little information exists for these parameters at the experimental site, to exclude one of the two possible values. However, the effect on soil loss and runoff prediction is low (see 8.6.1).

e) Development of the parameters random roughness, rill erodibility, and hydraulic conductivity

The scenarios ran with four variable input parameters, of which three show a development over time – random roughness, rill erodibility coefficient, hydraulic conductivity. Rock fragment content of the soil does not change WEPP internally over time. For the other three input parameters the model uses the user input value and adapts it automatically as a function of cumulative rainfall, surface cover, roots and sealing and crusting.

As described in 6.1 d) random roughness is negatively correlated with the amount of cumulative rainfall and thus decreases while cumulative rainfall increases. This can cause problems with high rock fragment cover in the soil. Figure 42 shows this opposing trend of random roughness and rainfall accumulation.

The adjustment of the “baseline” hydraulic conductivity is a function of cumulative rainfall and of the development of canopy cover and residues. As shows Figure 43, hydraulic conductivity increased to its maximum value of 100 mm h^{-1} after the first tillage operation and stayed at this high value until July 8th 2012. At this day, hydraulic conductivity decreased drastically to only 2 mm h^{-1}. July 8th 2012 was the first day when surface runoff and soil erosion occurred. Hydraulic conductivity oscillated between 100 mm h^{-1} and 2 mm h^{-1} for the first runoff events and reached 100 mm h^{-1} at July 21st 2012 for the last time. After this, it ranged from 2 mm h^{-1} and 40 mm h^{-1} during the observation time.

Figure 44 shows the development of the rill erodibility factor, adjusted on a daily base due to ground cover, roots, incorporated residues, crusting and sealing of the surface.

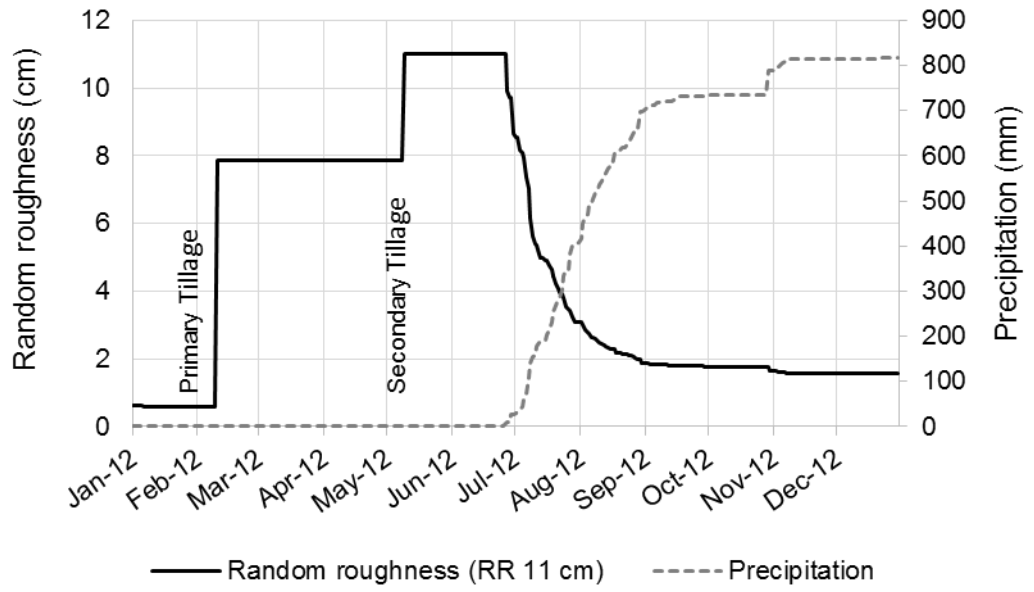

Figure 42: Development of random roughness and rainfall accumulation for Plot 1, where input random roughness is set to 11 cm.

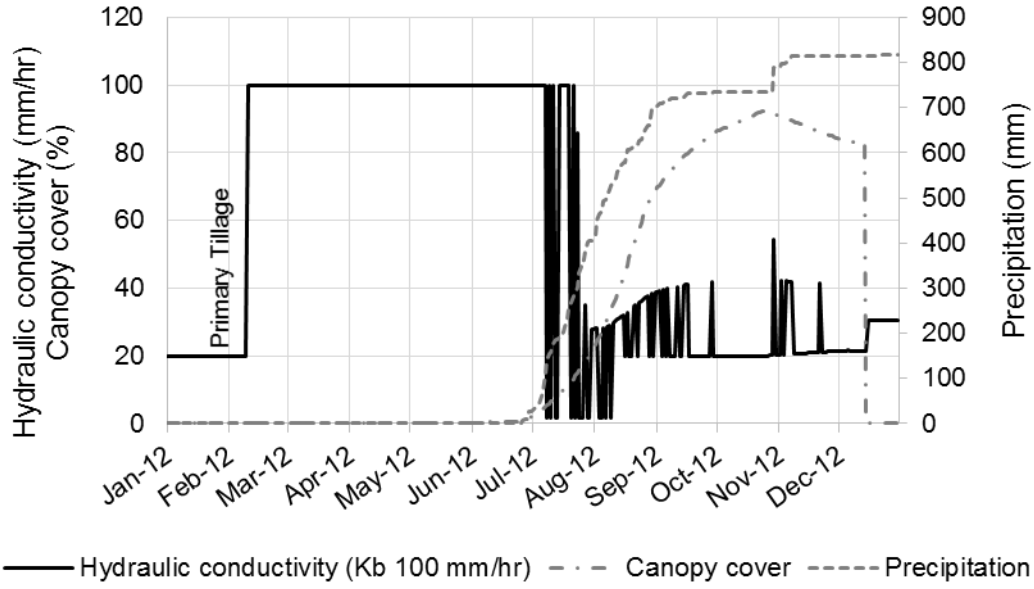

Figure 43: Development of hydraulic conductivity and opposing development of canopy cover and cumulative rainfall for Plot 1.

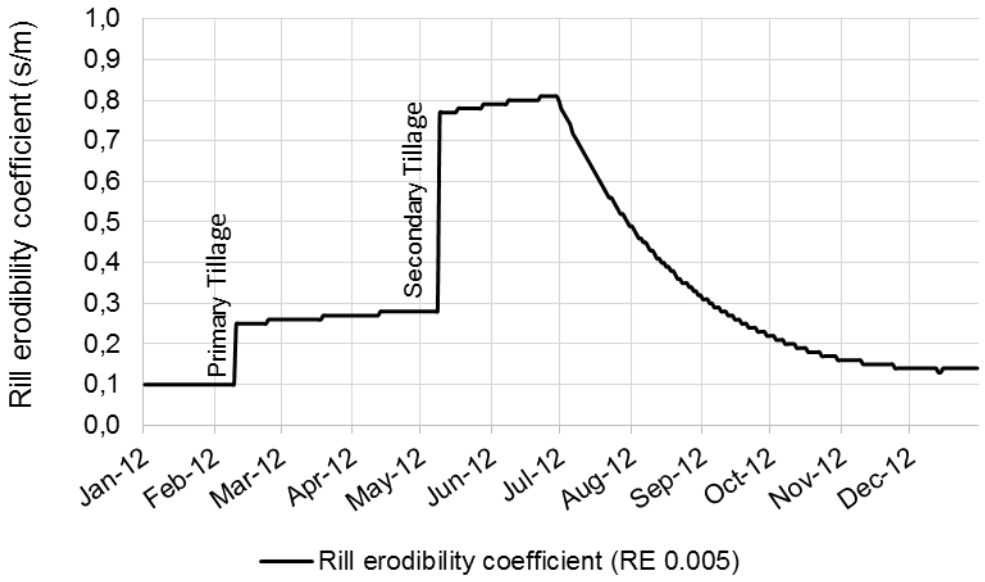

Figure 44: Development of rill erodibility coefficient over time.

8.6.6 WEPP soil loss prediction: Plot 3

In 144 scenarios the four sensitive input parameters varied within certain limits. Random roughness and hydraulic conductivity had the same range as for Plot 1 (RR 5, 8, 11, 14 cm and Kb 2, 100, 200, 300 mm h^{-1}). Rock fragment cover had two values, which represent the percentage of rock fragments in the upper and lower part of the plot separately according to field measurements (38/15, 41/18, 44/21 %). Rill erodibility had a lower range than at Plot 1 (0.003, 0.005, 0.007 s m^{-1}).

a) Objective functions

In the simulation of Plot 3 the development of all three functions was identical, which means that the ranking due to each function resulted in the same order of the scenarios. 10 of all 144 scenarios had a positive model efficiency (NSE), which means, that the model is the better predictor than the mean of the observed data. For the same 10 scenarios, the coefficient of determination ranged from 0.72 to 0.82 and the mean root square error was below 0.35. Within these scenarios, 9 of 10 had a rill erodibility coefficient of 0.003 s m^{-1}. Hydraulic conductivity values were 100 mm h^{-1} and 200 mm h^{-1}. Concerning random roughness, only the two high values, 11 cm and 14 cm, appeared in these 10 best results. Rock fragment cover occurred in all variations. Figure 45 shows the frequency of each parameter value graphically.

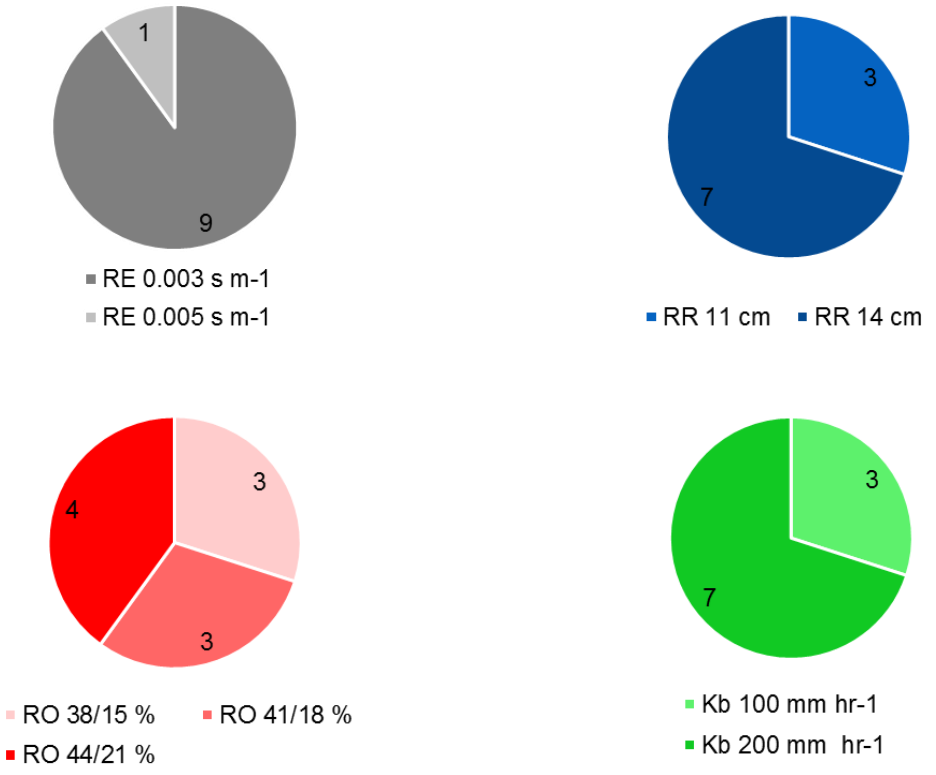

Figure 45: Frequency of each parameter value among the simulations with the best objective function results for Plot 3 (low RMSE, high NSE and R^2). RE = rill erodibility, RR = random roughness of the surface, RO = rock fragment cover, K_b = "baseline" hydraulic conductivity.

In contrast, low hydraulic conductivity had a dominant effect on the worst results of the three objective functions. All of the 14 simulation (10 % of all simulation runs) with the highest RMSE and lowest NSE and R^2 ran with a hydraulic conductivity of 2 mm h^{-1}. In trend, higher rill erodibility and lower random roughness led to less accordance of the prediction with the

observed data. Figure 46 shows for each parameter the number of parameter values occurring amongst the scenarios with the least accordance with observed soil loss.

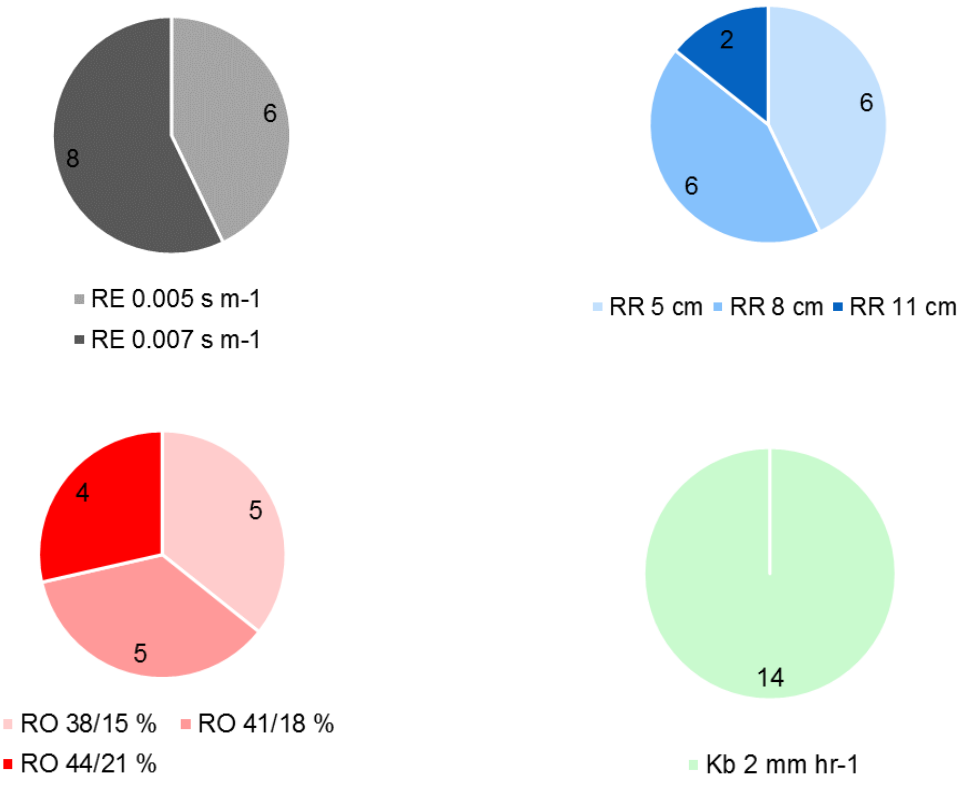

Figure 46: Frequency of each parameter value among the simulations with the worst objective function results for Plot 3 (high RMSE, low NSE and R^2). RE = rill erodibility, RR = random roughness of the surface, RO = rock fragment cover, K_b = "baseline" hydraulic conductivity.

b) Confidence interval

In general, soil loss in all simulations varied between 1.8 kg m^{-2} to 30.8 kg m^{-2}; thus, the variance in the results was high. The 95 % confidence interval shows the range of predicted soil loss for each day of removal of soil loss in the field without the influence of outliers on both sides. It shows that especially for August 1st 2012 the variation in prediction is high. This is because the time span from the previous field day, 20th July 2012, is relatively long and thus more events added up in between the two days of removal. The last observed event lies outside this confidence interval – all simulation runs over-estimated soil loss for this day. Using the statistic software "R", histograms showed the distribution of predicted soil loss for all observation days. Except for July 13th, soil loss is approximating a normal distribution. On July 13th, no scenario simulated soil loss. Figure 47 shows the 95 % confidence interval for all tested scenarios as well as observed soil loss.

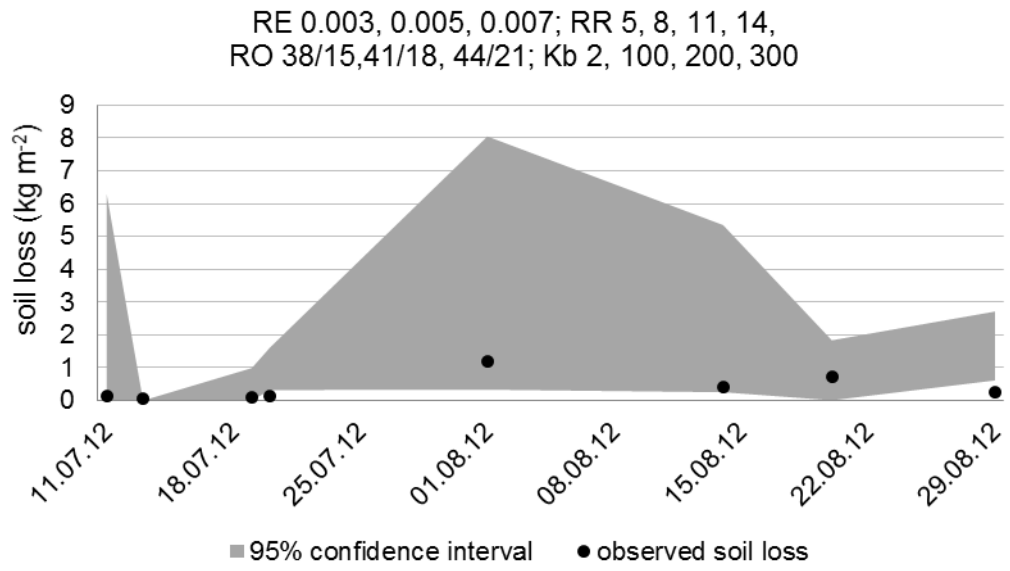

Figure 47: Simulated soil loss of Plot 3 with a 95 % confidence interval and measured values for all days of sediment removal and all combinations of parameters.

In a next step the parameter values, which did not occur in the best scenarios as described in 8.6.2 a), were removed from the simulation analysis. The confidence interval without a hydraulic conductivity of 2 mm h^{-1} and a rill erodibility coefficient of 0.007 s m^{-1} reduced drastically and narrowed the range of predicted soil loss. Removing the low random roughness values of 5 cm and 8 cm scaled down the range of the 95 % confidence interval even more. Consequently, soil loss from August 20th 2012 was under-estimated by the model and left the confidence interval. All the other days of removal stayed in the same relation to the confidence interval as for the interval considering all parameter combinations.

Hydraulic conductivity of 300 mm h^{-1} did not lead to good agreement between measured and simulated values and thus was eliminated from the input options. By removing the rill erodibility coefficient of 5 s m^{-1} the area between the 2.5 % and 97.5% quintiles further decreased. Figure 48 shows the decrease of the area between the 2.5 % and the 97.5 % quintile due to the reduction of possible input parameter values and scenarios. The narrowest band includes only those parameter value combinations (see Figure 49), which led to a good fit between observed and simulated soil loss.

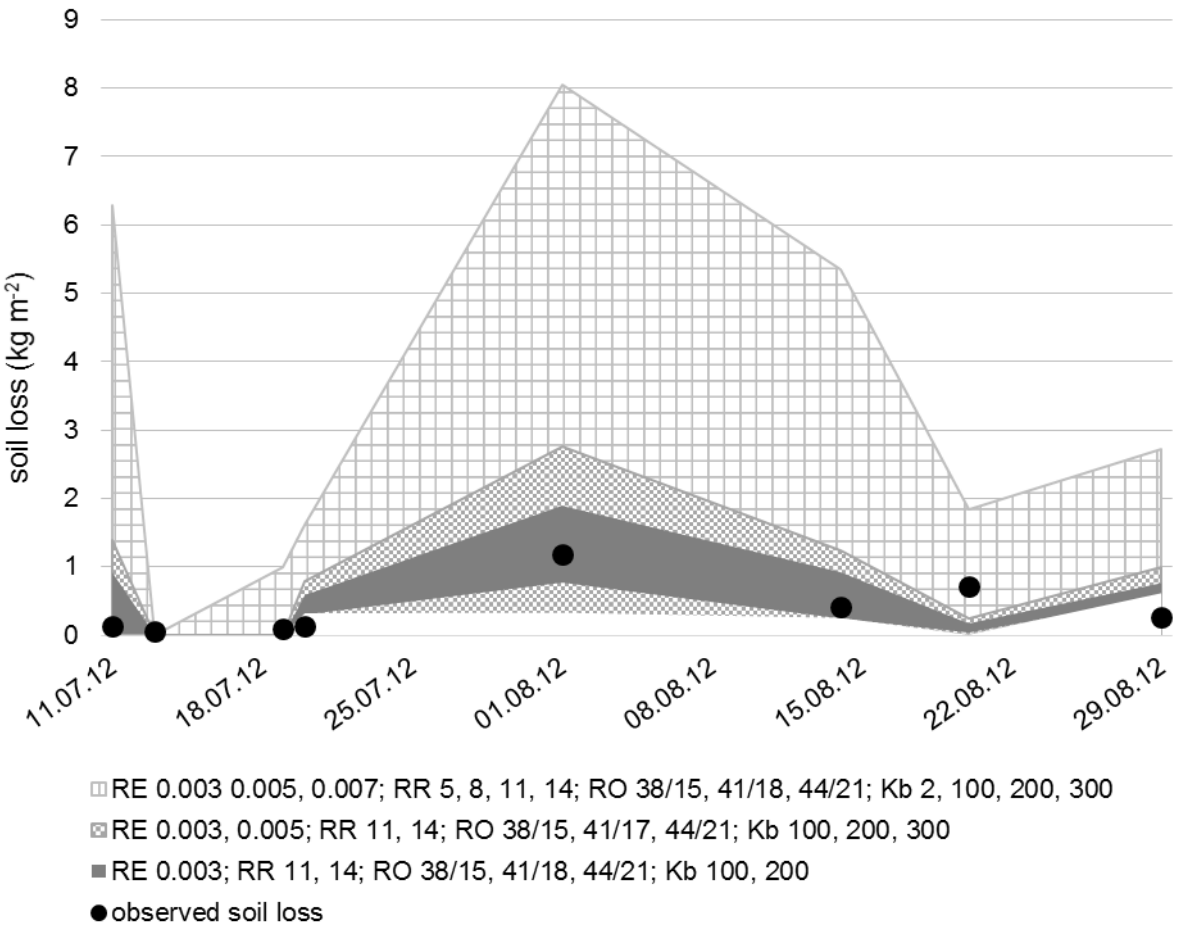

Figure 48: 95 % confidence interval of soil loss prediction and measured values for all days of sediment removal at Plot 3. Beginning from the combination of all scenarios, the interval decreases as some parameter values were eliminated from the analysis. Stepwise, scenarios that led to very high or low soil loss prediction were removed and thus the confidence interval narrowed. RE = rill erodibility, RR = random roughness of the surface, RO = rock fragment cover, K_b = "baseline" hydraulic conductivity

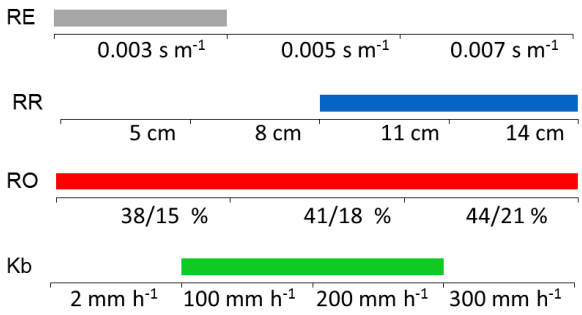

Figure 49: Range of parameter values, which remained in the set of scenarios leading to the narrowest confidence interval for Plot 3.

According to this analysis of influential parameters and their best fitting values of the tested range, best results coincide with a low rill erodibility coefficient (0.003 s m^{-1}), high random roughness (11 cm and 14 cm) and hydraulic conductivity of 100 mm h^{-1} and 200 mm h^{-1}. The effect of rock fragment cover is not significant. Table 12 shows a list of the scenarios, which remained in the set of simulations.

Table 12: Measured and observed soil loss rates and objective functions of the remaining parameter value for the simulation of soil loss at Plot 3.

Scenario	meas. soil loss (kg m^{-2})	obs. soil loss (kg m^{-2})	RMSE	ME	R^2
RE0.003,RR11,R4118,Kb200	3.0	2.86	0.28	0.40	0.82
RE0.003,RR11,R3815,Kb200	3.0	3.12	0.28	0.39	0.82
RE0.003,RR14,R4421,Kb100	3.0	2.79	0.29	0.38	0.82
RE0.003,RR14,R3815,Kb200	3.0	2.89	0.29	0.35	0.81
RE0.003,RR14,R4118,Kb100	3.0	3.03	0.29	0.35	0.81
RE0.003,RR14,R3815,Kb100	3.0	3.24	0.30	0.31	0.80
RE0.003,RR14,R4118,Kb200	3.0	2.80	0.31	0.29	0.79
RE0.003,RR11,R4421,Kb200	3.0	3.12	0.34	0.14	0.75
RE0.003,RR14,R4421,Kb200	3.0	1.76	0.35	0.06	0.72
RE0.003,RR11,R4421,Kb100	3.0	4.42	0.44	-0.46	0.57
RE0.003,RR11,R4118,Kb100	3.0	5.07	0.51	-0.94	0.43
RE0.003,RR11,R3815,Kb100	3.0	5.30	0.53	-1.10	0.39

8.6.7 Best simulation scenario: Plot 3

Next to soil loss prediction, WEPP models additional output for each scenario. This additional information is presented for the scenario with a rill erodibility of 0.003 s m^{-1}, random roughness of 11 cm, rock fragment cover of 41 % at the upper part and 18 % at the lower part. Hydraulic conductivity is 200 mm h^{-1}.

a) Predicted surface runoff

From 817 mm precipitation, the model calculates runoff of 126 mm. Thus, it results a rainfall – runoff ration of 15 %, which is most properly under-estimating actual runoff. High rock fragment mainly causes this low rainfall – runoff ratio.

b) Predicted soil loss

Predicted soil loss is 2.8 kg m^{-2}, while observed soil loss was 3.0 kg m^{-2}. As for Plot 1, no deposition zone developed. As shows Figure 50, in the upper section soil loss is relatively low as the rock fragment cover is high. At a 15 m distance from the top of the hillslope rock fragment cover drops from 41 % to only 18 % as the determination of rock fragment cover in the field showed.

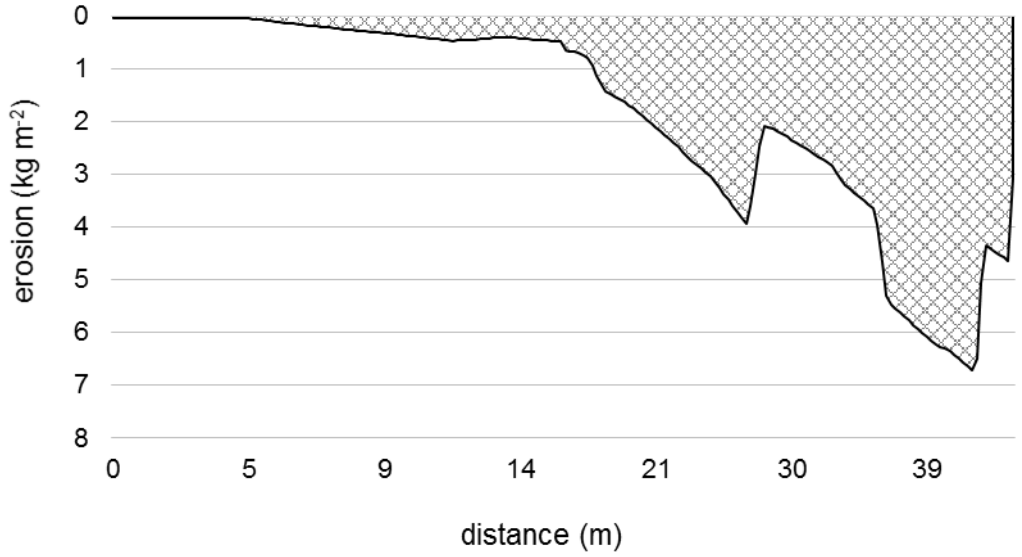

Figure 50: WEPP soil loss graph of Plot 3.

Figure 51 shows the comparison of measured and predicted soil loss for each day of sediment removal. Again, there is a systematic error in the simulation of the first event. However, with an opposing trend than at Plot 1. While all scenarios over-estimated soil loss for the first event at Plot 1, the model under-estimates soil loss at Plot 3.

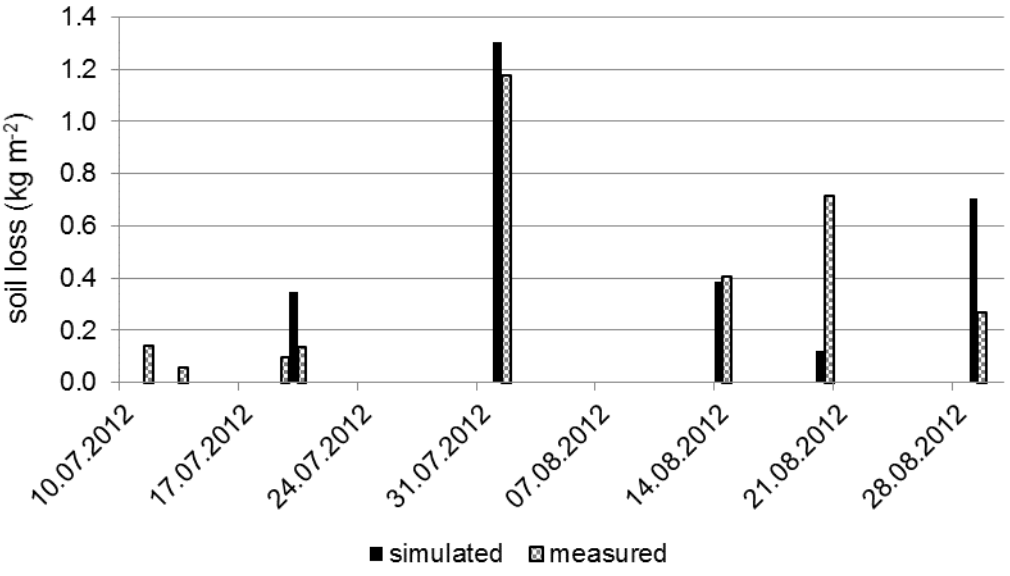

Figure 51: Comparison of observed and simulated soil loss of Plot 3 for all days of removal.

c) Canopy cover and height

Sorghum seeding was on June 1st 2012. On June 28th 2012, crop height was 1 cm. Both parameters, canopy height and cover, then developed until they reached a maximum value before senescence of the plant started and canopy cover decreased. At the end of the cropping season before harvesting at December 15th 2012, sorghum was around 1.26 m high and had a canopy cover of 0.82

d) Predicted yield from the cropping season 2012

The yield from Plot 3 reached the same value as for Plot 1 and was 2.0 t ha^{-1}. As described above this value exceeds the actual yield from 2012 with 0.8 t ha^{-1}. Again, the change of the ratio between canopy cover coefficient and maximum leaf area index leads to a predicted soil loss of 0.9 kg m^{-2}.

e) Development of the parameters random roughness, hydraulic conductivity and rill erodibility coefficient

Random roughness reached its maximum of 11 cm after second tillage and decreased as a function of cumulative rainfall. Figure 52 shows random roughness and cumulative rainfall over the year 2012.

"Baseline" hydraulic conductivity was 200 mm h^{-1} and stayed constant between first tillage operation and July 8th 2012. On this day, hydraulic conductivity dropped to 2 mm h^{-1} at the second surface runoff event – in contrary to Plot 1 at the event no soil loss occurred. Afterwards it increased again to 200 mm h^{-1} and then started decreasing on July 21st. From July 24th and the end of the period of observation it oscillated between 75 m/hr and 2 mm h^{-1}. Figure 53 shows hydraulic conductivity and cumulative rainfall and canopy cover, as those two are responsible for the WEPP internal adaption of this parameter.

The development of the rill erodibility coefficient varied for the two Overland Flow Elements (OFE) with different rock fragment content of the soil. WEPP calculates higher rill erodibility at the upper part with higher rock fragment cover. Figure 54 shows the difference in the development of the rill erodibility coefficient as a function of rock fragment cover.

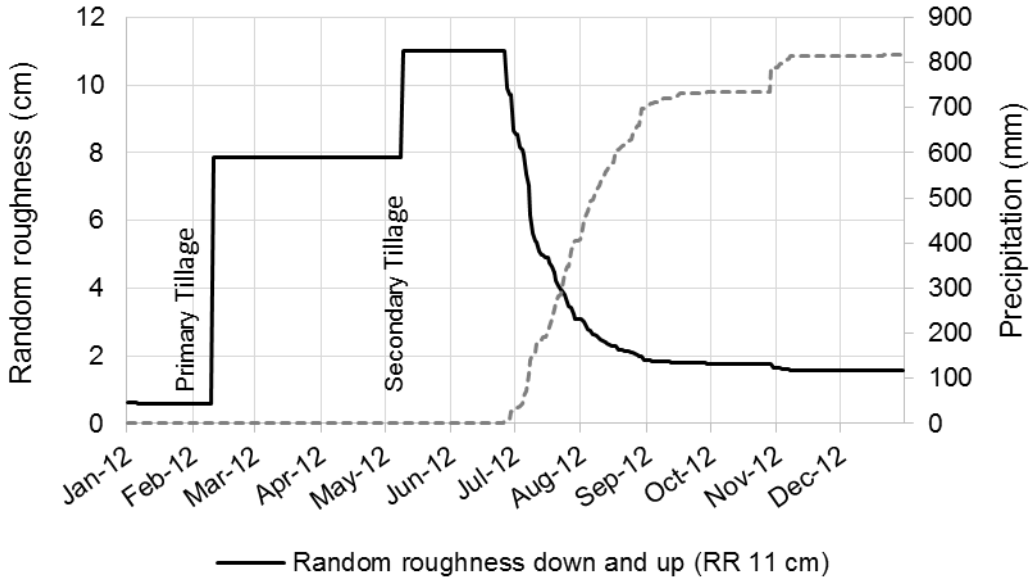

Figure 52: Development of random roughness and rainfall accumulation for Plot 3, where input random roughness is set to 11 cm

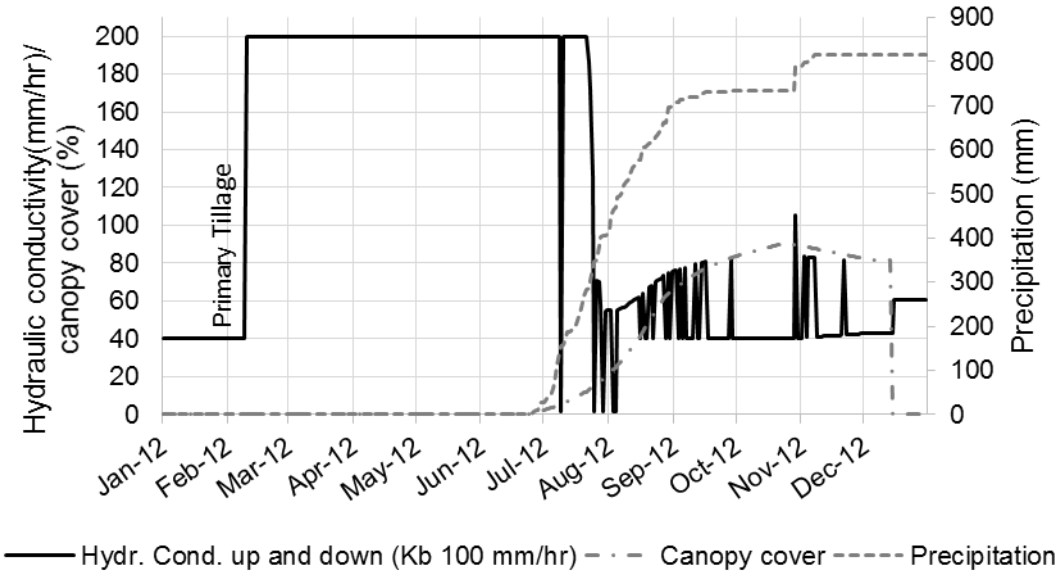

Figure 53: Development of hydraulic conductivity and opposing development of canopy cover and cumulative rainfall for Plot 3.

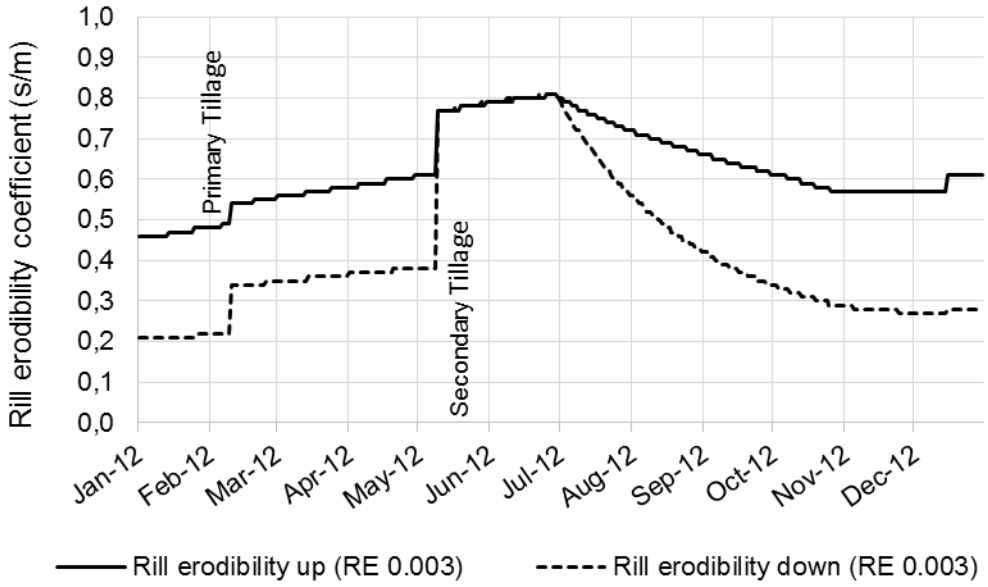

Figure 54: Development of rill erodibility coefficient at the two overland flow elements (OFE) with different rock fragment cover over time for Plot 3. Up and down stand for the OFE at the upper and lower part of the hillslope with a rock fragment content of 41 % and 18 %, respectively.

8.6.8 Discussion of the simulation results

The field experiment was the basis for the successive simulation of soil loss by the Water Erosion Prediction Project (WEPP). In this respect, the evaluation of the WEPP output depends on the results from the fieldwork. Measurement errors in the field would affect the model as well.

Field measurements are time-consuming and can monitor soil loss only under actual conditions. The simulation of the erosion process allows the evaluation of different management practices and conditions in short time.

For both plots, WEPP performed considerably well in predicting soil loss. The simulation ran 144 scenarios with varying input parameters for each plot. Best results went along with rill erodibility coefficients of 0.003 s m^{-1} and 0.005 s m^{-1}, hydraulic conductivity of 100 mm h^{-1} and 200 mm h^{-1} and random roughness of 8 cm, 11 cm, and 14 cm.

Concerning Plot 2, preliminary tests showed that soil loss simulation at this plot is difficult and involves important uncertainties. The profile of the hillslope implies that a considerable portion of detached sediments deposited within the plot. The topographic survey was too coarse to depict the irregular micro relief of this plot. As any conclusion would be difficult, the simulation process was limited to the two other plots.

a) Effect of rock fragment cover and random roughness

The scenario analysis showed that variation of rock fragment cover had little influence on the simulation result. This might be because variation of rock fragment cover was +/- 3 % of the determined cover (see 8.3). This variation might be too low to get a high response by the model.

Comparing the erosion profile of both plots (see Figure 40 and Figure 50), the reduction effect of high rock fragment cover on the soil erosion process is evident. While at Plot 1 soil loss starts from the top of the hillslope, considerable soil loss at Plot 3 starts at the transition from high (41 %) to lower (18 %) rock fragment cover. Beginning from this point, soil loss increases, with a section where the soil loss rate declines a little due to a flatter slope. This implies that the high rock fragment cover at the upper part of this plot kept soil loss from this section low. However, even though no soil detaches, surface runoff accumulates and gains flowing velocity. The sediment load of the accumulated surface flow is low and thus the capacity of the runoff to transport newly detached sediments is high. This explains the relatively strong increase of erosion beginning at 15 m from the top. Additionally, rock fragment cover also affects the development of the random roughness of the surface.

Concerning random roughness, higher values occurred at Plot 3, with high rock fragment cover especially in the upper part of the profile. Simulations performed best with random roughness of 8 cm and 11 cm at Plot 1 and random roughness values of 11 cm and 14 cm at Plot 3. Both showed bad soil loss prediction with random roughness of 5 cm.

Random roughness of the surface after tillage is an input of the tillage input file. The influence and integration of random roughness into the WEPP model is described in 6.1 d. The model assumes that random roughness is highest directly after tillage operations and decays with the amount of cumulative rainfall after tillage. Aggregates break down and sealing of the soil surface starts.

Van Wesemael et al. (1996) showed that this assumption is not valid for soils with high rock fragment cover. Random roughness of soils with small sized rock fragments decreased firstly

due to cumulative rainfall for the first 17.5 mm but then increases with cumulative rainfall. For soils with large rock fragments random roughness increased from the beginning. Van Wesemael et al. (1996) stress that rock fragments jut out of the soil and thus determine the roughness of the surface.

As stone cover at the plot was high and reached up to 55 % at the upper part of Plot 3, the model might misinterpret the evolution of random roughness. To account for the effect of the high rock fragment cover on the fields, the simulation included scenarios with higher random roughness values. This should compensate the effect of decreasing random roughness due to cumulative rainfall. Thus, even though Zeleke (2001) used random roughness values of 5 cm for the *maresha* ox-drawn ard plough in the Ethiopian Highlands, the higher random roughness value is justified by the incidence of high rock fragment cover.

From the high random roughness value after secondary tillage, the model adapts this parameter beginning from the first rainfall event. Random roughness decreases rapidly. On July 13th, it drops below 5 cm. In this sense, the high input value of random roughness might not represent this parameter correctly for the first rainfall events. However, it compensates the decrease due to cumulative rainfall. This fact might be the reason for the under-estimation of soil loss at the beginning of the rainy season for Plot 3, as high random roughness and rock fragment cover interact with each other.

Figure 55 shows the influence of rock fragment cover on soil loss as a function of random roughness. Starting from soil loss with a rock fragment cover of 0 %, the figure shows the variations of soil loss with the increase of rock fragment cover. With increasing random roughness, the effect of varying fragment cover gets more important.

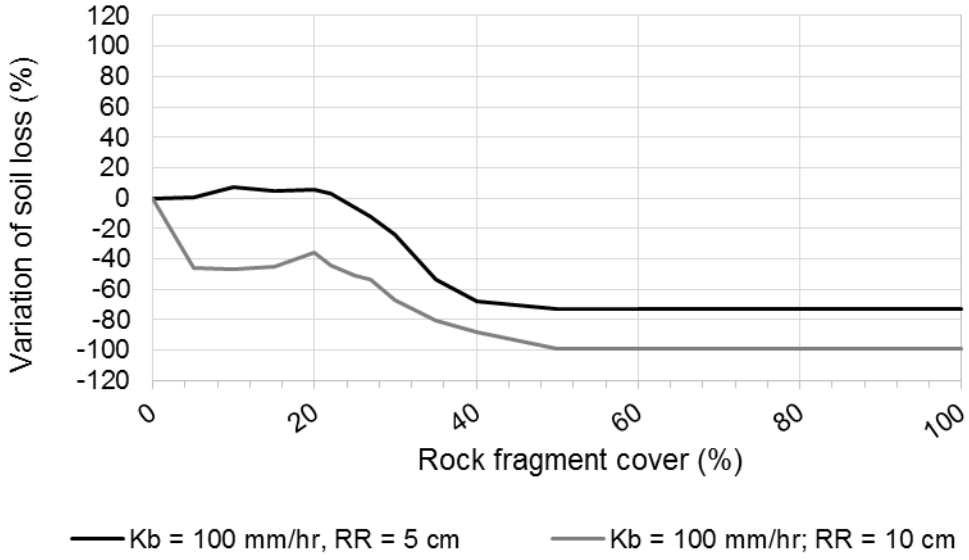

Figure 55: Variation of soil loss as function of rock fragment cover

b) Effect of hydraulic conductivity

In both simulations, the intermediate hydraulic conductivity values of 100 mm h^{-1} and 200 mm h^{-1} performed better than the lowest and highest parameter values (2 mm h^{-1} and 300 mm h^{-1}). Even if this seems high for the given soil texture, this hydraulic conductivity values give sense as firstly measurements by Schürz (2012) showed even higher values for the experimental site (300 mm h^{-1}) and secondly, the model internally reduces the high “baseline” value due to canopy cover and cumulative rainfall. Cracks in the soil lead to rapid infiltration of

surface water into the soil. Flanagan and Livingston (1995) suggest to adjust the effective hydraulic conductivity to account for the incidence of biopores, wormholes and cracks in the soil. The ratio, which is multiplied with the calculated or observed hydraulic conductivity, depends on size and abundance of biopores as well as the input hydraulic conductivity value. Thus, the high K_b input values also represents the effect of the cracks in the soil.

c) Effect of the rill erodibility coefficient

Best simulation results coincided with lower rill erodibility coefficients as the value suggested by WPP. The WEPP internal equation uses the clay fraction as only independent variable for the computation of rill erodibility. Nearing et al. (1990) found that rill erodibility is one of the most dominant factors related to the model response. According to measurements by Romero et al. (2007), the WEPP intern equations over-estimated the rill erodibility factor, while measurements by Reichert and Norton (2013) on a Vertisol soil resulted in the contrary. They showed that WEPP under-predicted the K_r factor. WEPP calculated a value of 0.007 s m^{-1} for this parameter. Best results at Plot 1 and Plot 3 came with a rill erodibility coefficient of 0.003 s m^{-1} and 0.005 s m^{-1}. It has to be mentioned that at Plot 1 no scenario ran with 0.003 s m^{-1} because information of the simulation of Plot 1 led to the adaption of the tested parameter range at Plot 3. Zeleke (2001) applied the WEPP model to an experimental site in the Ethiopian Highlands. The aim of this work was to adapt WEPP to tradition Ethiopian farming systems and site-specific factors. Amongst others, Zeleke (2001) changed the rill erodibility factor. Also from a suggested value of 0.007 s m^{-1} to 0.003 s m^{-1}. This coincides with findings in this work that lower rill erodibility values lead to better soil loss prediction.

d) Development of soil loss over the rainy season

For both plots, no tested scenario evaluated soil loss from the first event correctly. At Plot 1, the model over-predicted soil loss for the first surface runoff event. At Plot 3, the model under-predicted soil loss for the same event. This might be due to the high random roughness in combination with higher rock fragment content and lower rill erodibility. In all cases, predicted soil loss at Plot 1 was much higher than the observed value. The incidence of cracks in the soil might cause this poor accordance for the beginning of the rainy season. Even though hydraulic conductivity is high over the whole rainy season, the cracks in the soil might act as channels of preferential flow in the first rainfall events and reduce even more the development of the surface runoff.

Another reason for the poor quality of prediction in the first event might be the fact, that rainfall data was not available for the whole year but rainfall records started on June 26th, 2012. A high initial saturation level should compensate the missing data of rainfall from January to June.

In general, the fieldwork showed low soil loss rates in the beginning and higher rates in the end of the rainy season. In contrary, the simulation showed no such trend. Soil loss prediction gained accordance with measured soil loss as the rainy season advanced. As discussed in 8.5 b), various studies in the Ethiopian Highlands showed this similar trend of low soil loss in the beginning of the rainy season due to shrinking cracks in the soil. Hence, there is an inverse trend in the modelling and observation: While hydraulic conductivity declines in the WEPP model over time, observation shows increasing or at least constant hydraulic conductivity values. This emphasizes the assumption of a systematic error in soil loss prediction in the beginning of the rainy season.

The 95 % confidence interval of soil loss prediction of the simulation scenarios spans an area of possible model output with assumed parameter combinations. The analysis of this

confidence intervals showed that the range of predicted soil loss is little for several events; meaning that all scenarios lead to similar results. Observed soil loss lies outside this band for some events, but very close to it. In general, it has to be stressed that the use of more observed data points would strengthen the informative value of the model configuration. Thus ongoing research is necessary.

In soil erosion measurements in the Ethiopian Highlands Zeleke (2001) found that WEPP over-predicted runoff and slightly under-predicted soil loss and that prediction of soil loss is better than of runoff. However, he evaluated the WEPP model to perform fairly well under local conditions. This study did not include measurements of surface runoff, but only soil loss. With the found best fitting soil loss simulation, the model simulated rainfall – runoff ratios of 0.20 and 0.15 for Plot 1 and Plot 3, respectively. This implies that the model presumably under-estimated surface runoff. However, measurements in the study area from the following rainy season 2013 also indicate that the rainfall – runoff ratio is around 0.3. Considering that daily rainfall amount and intensities lay below those of 2013 and the average of long-term observations (see 8.1), this ratio is in a realistic range.

Information on the rainfall – runoff ration can improve the calibration of the WEPP model to observations at this site.

9. Summary and Conclusion

During the rainy season 2012 soil erosion measurements were carried out at three soil erosion plots. Additionally, canopy and rock fragment cover, hydraulic conductivity and soil texture were determined

Soil loss from these experimental plots was variable. Two plots showed comparable soil loss rates of 4.7 kg m^{-2} and 3.0 kg m^{-2}. Soil loss from the third plot was considerably lower (0.3 kg m^{-2}). For this plot, it is assumed that sediments deposited before entering the sediment retention basins. From the two other plots, one was situated on fields with stone bunds while the fields at the other plot were not treated with soil and water conservation measures.

Even if stone bunds reduce the effective length of the slope, highest soil loss occurred at the plot with stone bunds. The measurements imply that rock fragment cover determined the development of soil loss to a great extent. The untreated plot showed high rock fragment cover especially in the upper part. The high rock fragment cover and resulting high random roughness of the surface might have superposed the effect of the longer slope.

The distribution of soil loss over the rainy season showed a heterogeneous pattern with increasing soil loss rates from the beginning to the end of the rainy season. This might be attributed to the incidence of shrinkage cracks in the soil, which form during the dry period and close during the first rainfall events. Even though the cracks are invisible after the first days of rainfall, the constant high hydraulic conductivity (measured values from 200 to 400 mm h^{-1}) implies that the cracks affect the subsurface structure of the soil over the whole rainy season.

For the WEPP simulation of soil loss, the model's response to variation of several parameters was tested. The sensitivity analysis showed that the variation of random roughness, rock fragment cover, rill erodibility and hydraulic conductivity decisively affects the soil erosion prediction.

Good accordance between observed and simulated soil loss coincided with relatively high random roughness (8 – 14 cm), high hydraulic conductivity (100 – 200 mm h^{-1}) and a rill erodibility coefficient, which was lower than the value suggested by the model (0.003 – 0.005 s m^{-1}).

The hydraulic conductivity values are justified by the incidence of cracks in the soil, which act as paths of preferential flow and lead to rapid infiltration of surface water. According to Flanagan and Livingston (1995), the incidence of biopores or cracks can be accounted for by increasing the "baseline" hydraulic conductivity of the soil.

The high values of random roughness should compensate the effect of the WEPP internal adjustment of random roughness due to cumulative rainfall since last tillage. This decay of random roughness might lead to misinterpretation of this parameter in combination with high rock fragment cover. However, surface runoff with little sediment load accumulates in sections with high rock fragment cover and leads to increased soil erosion rates when rock fragments decline.

For the two simulated plots, soil loss prediction showed poor agreement with measurements at the beginning of the rainy season and improved as rainy season advanced.

Ongoing research and field measurements are necessary in order to validate the WEPP model in its presumed configuration. The implementation of data from soil erosion measurements of following years can help to further calibrate the model.

10. Outlook

For the WEPP model, little of the required input is known certainly for the experimental site. WEPP uses input databases for experimental sites in other regions, which hold long-term information on climate, cropping conditions etc. Thus, the validation of the model with the adapted parameter input needs on-site measurements to prove the goodness of simulation under different boundary conditions. During the rainy season 2013, again soil loss measurements were conducted at the same site. Comparison of soil loss prediction and observed soil loss can lead to further calibration of the model.

Additional measurements of the sensitive parameters in the WEPP model can help to prove if assumed parameters lie in a realistic range. Measurements of hydraulic conductivity, random roughness and rock fragment cover and content over depth contribute to the improvement of the model's prediction efficiency.

Further research is needed to assess the influence of stone bunds on the soil erosion process in the study area. Measurements behind the bunds might reveal the fraction of sediments depositing behind the bunds and lead to a quantitative assessment of the retention capacity of the stone bunds.

Improvements in the set-up of the experimental plots might be considered in ongoing research:

As mentioned before the setup in this work did not allow monitoring of surface runoff. The idea was to keep the material input in the field low and conduct soil loss measurements without the installation of dividers and storage tanks. Due to the same reason, plots were naturally delineated without the installation of artificial borders. Even though this setup has the advantage that there are no additional obstacles for the farmers managing the fields (e.g. tillage), this aggravated the delineation of the contributing areas and holds uncertainty in the soil erosion measurement.

During the design of the setup, much attention was paid to the fact that little material has to be left in the field. The perception was, that especially metal might be removed during the run-time of the project. After the first year of monitoring, this perception changed. Agreements with local farmers work fine. In return to some expenses, farmers oversee the installed equipment. The introduction of metal borders to the plots in future soil erosion monitoring plots could ease the delineation of the contributing areas and reduce uncertainty in the soil loss monitoring.

The collection of surface runoff can contribute to further validate the soil loss measurement. The installation of rain collectors distributed above the sub-catchment can validate if precipitation of the neighbouring Aba-Kaloye sub-catchment describes the rainfall pattern in the experimental site correctly.

Bibliography

Albert, E.E., M.A. Nearing, M.A. Weltz, L.M. Risse, F.B. Pierson, X.C. Zhang, J.M. Laflen, and J.R. Simanton. 1995. “Chapter 7. Soil Component.” NSERL Report. West Lafayette, Indiana: USDA-ARS National Soil Erosion Research Laboratory.

Amore, Elena, Carlo Modica, Mark A Nearing, and Vincenza C Santoro. 2004. “Scale Effect in USLE and WEPP Application for Soil Erosion Computation from Three Sicilian Basins.” *Journal of Hydrology* 293 (1–4) (June): 100–114. doi:10.1016/j.jhydrol.2004.01.018.

aquastat. 2005. “Country Fact Sheet Ethiopia”. 29. FAO Water Report. aquastat.

Blanco-Canqui, Humberto, and Rattan Lal. 2008. *Principles of Soil Conservation and Management*. Springer.

Bosshart, U. 1997. “Catchment Discharge and Suspended Sediment Transport as Indicators of Physical Soil and Water Conservation in the Michet Catchment, Anjeni Research Unit.” 40. Soil Conservation Research Project. Research Report. Schwitzerland: Centre for Development and Environment University of Berne.

Braimoh, Ademola K., and Paul L.G. Vlek. 2008. *Land Use and Soil Resources*. Springer.

Cerdà, A. 2001. “Effects of Rock Fragment Cover on Soil Infiltration, Interrill Runoff and Erosion.” *European Journal of Soil Science* 52 (1): 59–68. doi:10.1046/j.1365-2389.2001.00354.x.

Dejene, Alemneh. 2003. *Integrated Natural Resources Management to Enhance Food Security*. Organisation des Nations Unies pour l’alimentation et l’agriculture. ftp://ftp.fao.org/docrep../FAO/005/Y4818E/Y4818E00.pdf.

“European Commission.” 2013. Accessed July 15. http://ec.europa.eu/environment/soil/index_en.htm.

FAO. 2013. “Country Pasture/ Forage Resource Profiles, Ethiopia.” Accessed July 15. http://www.fao.org/ag/AGP/AGPC/doc/Counprof/Ethiopia/Ethiopia.htm#3.%20CLIMATE%20AND%20AGRO%20ECOLOGICAL.

Flanagan, D.C., and Stanley J. Livingston. 1995. “WEPP User Summary.” *NSERL Report* 11 (July). http://www.ars.usda.gov/SP2UserFiles/ad_hoc/36021500WEPP/usersum.pdf.

Flanagan, D.C., and M.A. Nearing. 1995. “USDA-Water Erosion Prediction Project - Hillslope Profile and Watershed Model Documentation.” NSERL Report. West Lafayette, Indiana: USDA-ARS National Soil Erosion Research Laboratory.

GARC. 2010. “Socio-economic Survey of Gumara-Maksegnit Watershed”. Gonder, Ethiopia: ICARDA, ARARI, EIAR, BOKU, SASAKAWA.

Gebremichael, D., J. Nyssen, J. Poesen, J. Deckers, M. Haile, G. Govers, and J. Moeyersons. 2005. “Effectiveness of Stone Bunds in Controlling Soil Erosion on Cropland in the Tigray Highlands, Northern Ethiopia.” *Soil Use and Management* 21 (3): 287–297. doi:10.1079/SUM2005321.

Gebreyesus, B, and M Kirubel. 2009. “Estimating Soil Loss Using Universal Soil Loss Equation (USLE) for Soil Conservation Planning at Medego Watershed, Northern Ethiopia.” *Journal of AMerican Science* 5 (1): 58–69.

Gentile, Anna Rita, and Robert JA Jones. 2013. “REPORTS OF THE TECHNICAL WORKING GROUPS.” Accessed July 15. http://citeseerx.ist.psu.edu/viewdoc/download?doi=10.1.1.130.5966&rep=rep1&type=pdf.

Global Environment Outlook 4: Environment for Development. 2007. Nairobi, Kenya: United Nations Environment Programme.

"Guide to Texture by Feel | NRCS Soils." 2013. Accessed July 21. http://soils.usda.gov/education/resources/lessons/texture/.

Hengsdijk, H., G.W. Meijerink, and M.E. Mosugu. 2005. "Modeling the Effect of Three Soil and Water Conservation Practices in Tigray, Ethiopia." *Agriculture, Ecosystems & Environment* 105 (1-2) (January): 29–40. doi:10.1016/j.agee.2004.06.002.

Herweg, Karl, and Eva Ludi. 1999. "The Performance of Selected Soil and Water Conservation Measures—case Studies from Ethiopia and Eritrea." *Catena* 36 (1): 99–114.

Hurni, H. 1988. "Degradation and Conservation of the Resources in the Ethiopian Highlands." *Mountain Research & Development* 8 (2-3): 123–130.

Jones, A., H Breuning-Madsen, M Brossard, and A Dampha. 2013. *Soil Atlas of Africa*. http://eusoils.jrc.ec.europa.eu/library/maps/Africa_Atlas/Documents/JRC_africa_soil_atlas_part1.pdf.

Jones, A., P. Panagos, S. Barcelo, F. Bourani, C. Bosco, O. Dewitte, C. Gardi, et al. 2012. "The State of Soil in Europe JRC Reference Report." http://ec.europa.eu/dgs/jrc/downloads/jrc_reference_report_2012_02_soil.pdf.

Kasperson, Roger E., and Emma RM Archer. 2005. "Vulnerable Peoples and Places." *Ecosystems and Human Well-Being: Current State and Trends: Findings of the Condition and Trends Working Group* 1: 143.

Kendie Addis, H., St. Strohmeier, R. Srinivasan, F. Ziadat, and A. Klik. 2013. "Using SWAT Model to Evaluate the Impact of Community-based Soil and Water Conservation Interventions for an Ethiopian Watershed." In *Proceedings of the 2013 International SWAT Conference, Paul Sabatier University, Toulouse, France July 17-19th, 2012*. Toulouse.

Kendie Addis, Hailu. unpublished. "Assessment of the Impact of Rainwater Harvesting and Soil Conservation Structures on Surface Runoff and Sediment Yield From an Agricultural Watershed in Ethiopia.pdf."

Krüger, H. J., Berhanu Fantew Yohannes Gebremichael, and Kefeni Kejela. 1997. "Inventory of Indigenious Soil and Water Conservation Measures on Selected Sites in the Ethiopia Highlands". 34. Soil Conservation Research Project. Research Report. Centre for Development and Environment University of Berne.

Liniger, H. P., Dennis Cahill, D. B. Thomas, G. W. J. van Lynden, and Gudrun Schwilch. 2002. "Categorization of SWC Technologies and Approaches–a Global Need." In *Proceedings of ISCO Conference 2002*, 3:6–12. http://www.wocat.net/fileadmin/user_upload/documents/Articles/ISCOSWC2002.PDF.

Mahmoodabadi, Majid, and Artemi Cerdà. 2013. "WEPP Calibration for Improved Predictions of Interrill Erosion in Semi-arid to Arid Environments." *Geoderma* 204–205 (August): 75–83. doi:10.1016/j.geoderma.2013.04.013.

Martínez-Zavala, L., and A. Jordán. 2008. "Effect of Rock Fragment Cover on Interrill Soil Erosion from Bare Soils in Western Andalusia, Spain." *Soil Use and Management* 24 (1): 108–117. doi:10.1111/j.1475-2743.2007.00139.x.

McKay, M.D., R.J. Beckman, and W.J. Conover. 1979. "A Comparison of Three Methods for Selecting Values of Input Variables in the Analysis of Output from a Computer Code." *Technometrics* 21 (2) (May).

Merritt, W.S., R.A. Letcher, and A.J. Jakeman. 2003. "A Review of Erosion and Sediment Transport Models." *Environmental Modelling & Software* 18 (8-9) (October): 761–799. doi:10.1016/S1364-8152(03)00078-1.

Morgan, R. P. C. 1995. *Soil Erosion and Conservation*. London and New York: Longman.

Nash, J.E., and J.V. Sutcliffe. 1970. “River Flow Forecasting through Conceptual Mmodels. Part 1. A Discussion of Principles.” *Journal of Hydrology* 10: 282 – 290.

“Natural Resources and Environment: Land Degradation Assessment.” 2013. Accessed July 15. http://www.fao.org/nr/land/degradation/en/.

Nearing, M.A., L. Deer-Ascough, and J.M. Laflen. 1990. “Sensitivity Analysis of the WEPP Hillslope Profile Erosion Model.” *Transactions of the ASAE* 33 (3): 839–849.

Nyssen, J, Jean Poesen, Desta Gebremichael, Karen Vancampenhout, Margo D’aes, Gebremedhin Yihdego, Gerard Govers, et al. 2007. “Interdisciplinary On-site Evaluation of Stone Bunds to Control Soil Erosion on Cropland in Northern Ethiopia.” *Soil and Tillage Research* 94 (1) (May): 151–163. doi:10.1016/j.still.2006.07.011.

Nyssen, J., J. Nyssen, Mitiku Haile, J. Poesen, J. Deckers, and J. Moeyersons. 2001. “Removal of Rock Fragments and Its Effect on Soil Loss and Crop Yield, Tigray, Ethiopia.” *Soil Use and Management* 17 (3) (September 1): 179–187. doi:10.1079/SUM200173.

Nyssen, J., J. Poesen, M. Haile, J. Moeyersons, and J. Deckers. 2000. “Tillage Erosion on Slopes with Soil Conservation Structures in the Ethiopian Highlands.” *Soil and Tillage Research* 57 (3): 115–127.

Nyssen, J., J. Poesen, M. Haile, J. Moeyersons, and H. Hurni. 2009. “Effects of Land Use and Land Cover on Sheet and Rill Erosion Rates in the Tigray Highlands, Ethiopia.” *Zeitschrift Für GEomorphologie* 53 (2) (June): 171–197.

Oldeman, L.R., R.T.A. Hakkeling, and W.G. Sombroek. 1991. *Global Assessment of Soil Degradation (GLASOD). World Map of the Status of Human-Induced Soil Degradation*. Wageningen: Internation Soil Reference and Information Centre, United Nations Environment Programme.

Oldeman, LR. 1991. “The Global Extent of Soil Degradation.” ISRIC Bi-Annuan Rport. Wageningen, Netherlands.

Poesen, J., and H Lavee. 1994. “Rock Fragments in Top Soils: Significance and Processes” 23 (1-2) (September): 1–28. doi:10.1016/0341-8162(94)90050-7.

Reichert, José Miguel, and L. Darrell Norton. 2013. “Rill and Interrill Erodibility and Sediment Characteristics of Clayey Australian Vertosols and a Ferrosol.” *Soil Research* 51 (1): 1. doi:10.1071/SR12243.

Romero, Consuelo C., Leo Stroosnijder, and Guillermo A. Baigorria. 2007. “Interrill and Rill Erodibility in the Northern Andean Highlands.” *CATENA* 70 (2) (July): 105–113. doi:10.1016/j.catena.2006.07.005.

Roose, Eric. 1996. *Land Husbandry: Components and Strategy*. Vol. 70. FAO Rome. http://www.betuco.be/CA/Land%20husbandry%20-%20Components%20and%20strategy%20erosion%20FAO.pdf.

Schürz, Christoph. 2012. “Field Measurements in the Framework of Data Acquisition for the Master Thesis.”

“The World Factbook.” 2013. Accessed July 15. https://www.cia.gov/library/publications/the-world-factbook/geos/et.html.

Thomann, R.V. 1982. “Verification of Water Quality Models.” *Journal of the Environmental Enineering Division* 108 (5): 923 – 940.

Toy, T. J., G. R. Foster, and K. G. Renard. 2002. *Soil Erosion: Processes, Prediction, Measurement, and Control*. 1st ed. John Wiley & Sons.

USDA-ARS. 1989. *Water Erosion Prediction Project (WEPP)*. Fortran. West Lafayette, Indiana: USDA-ARS, United States Department of Agriculture - Agricultural Research Service.

Van Lynden, G. W. J., H. P. Liniger, and Gudrun Schwilch. 2002. “The WOCAT Map Methodology, a Standardized Tool for Mapping Degradation and Conservation.” In *Proceedings of ISCO Conference*, 4:11–16. http://www.tucson.ars.ag.gov/isco/isco12/VolumeIV/TheWOCATMap.pdf.

Van Wesemael, Bas, Jean Poesen, Tomás de Figueiredo, and Gérard Govers. 1996. “Surface Roughness Evolution of Soils Containing Rock Fragments.” http://bibliotecadigital.ipb.pt/handle/10198/6480.

Wischmeier, W.H. 1966. “Surface Runoff in Relation to Physical and Management Factors.” In , 237–244. San Paulo, Brazil.

Wischmeier, W.H., and D.D. Smith. 1965. “Predicting Rainfall-erosion Losses from Cropland East of the Rocky Mountains: Guide for Selection of Practices for Soil and Water Conservation.”

“World Atlas of Desertification.” 1997. UNEP, International Soil Reference and Information Centre (ISRIC).

Wyss, G.D., and K.H. Jorgensen. 1998. “A User’s Guide to LHS: Sandia’s Latin Hypercube Sampling Software”. Albuquerque: Risk Assessment and Systems Modeling Department, Sandia National Laboratories.

Zeleke, Gete. 2001. “Application and Adaptation of WEPP to Traditional Farming Systems of the Ethiopian Highlands.” In *Sustaining the Global Farm. Selected Papers from the 10th International Soil Conservation Organization Meeting Held May 24-29, 1999*, edited by D.E. Stott, R.H Mohtar, and G.C. Steinhardt, 903–912. Purdue University and USDA-ARS National Soil Erosion Research Laboratory.

Zhang, X.C., M.A. Nearing, L.M. Risse, and K.C. McGregor. 1996. “Evaluation of WEPP Runoff and Soil Loss Predictions Using Natural Runoff Plot Data.” *Transactions of ASAE* 39 (3): 855–863.

12. Tables

12.1 Table of figures

12.2 Table directory

13. Annex

13.1 Survey: Delimiting watersheds with Arc GIS 10

Arc GIS 10 was used for post-processing of the survey data.

1)	Insert XYZ measurement points from spreadsheet	Add XY Data	
2)	Create TIN (Triangulated Irregular Network)	Create TIN	3D Analyst Tool
3)	Create DEM (Digital Elevation Model)	TIN to Raster Resolution: 0.1 x 0.1 m	3D Analyst Tool
4)	Insert retention basins 1,2,3	Draw polygon Convert Graphics to Features - Insert field "Elevation = 1"	Draw Tool
		Polygon to raster - Resolution: 0.1 x 0.1 m - Extent same as layer DEM	Conversion Tool
5)	Insert downhill stone bund	Draw polygon Convert Graphics to Features - Insert field "Elevation = 1"	Draw Tool
		Polygon to raster - Resolution: 0.1 x 0.1 m - Extent same as layer DEM	Conversion Tool
6)	Define basins and vertical stone bund as areas with no elevation information	Reclassify - basins 1,2,3: Elevation noData --> 1 Elevation 1 --> 0 - vertical stone bund: Elevation NoData --> 1 Elevation 1 --> 2	3D Analyst Tool
7)	Modify DEM	Raster Calculator - DEM * reclassified basins * vertical stone bund	Spatial Analyst Tool
8)	Eliminate sinks from DEM	Fill	Spatial Analyst Tool
9)	Compute flow direction	Flow Direction	Spatial Analyst Tool
10)	Compute flow accumulation	Flow Accumulation	Spatial Analyst Tool
11)	Compute watersheds for the three basins	Watershed	Spatial Analyst Tool
		Raster to Polygon	Conversion Tool

The first column refers to the purpose of each step, the second and third columns refer to the Arc GIS tool name and Arc GIS toolbox name, respectively.

The downhill-orientated stone bund, which builds the border between treated and untreated fields, influences the direction of the surface runoff and the area which drainages to each basin. To account for this effect, the digital elevation model was modified by inserting a linear structure with raised elevation along the vertical stone bund. Thus, the vertical stone bund acts as drainage divide.

13.2 Canopy and rock fragment cover

13.2.1 Automatized assessment of canopy and rock fragment cover

a) Plot 1 (treated):

Vegetation (-)	Rock fragments (-)	Soil (-)
0.50	0.18	0.32
0.36	0.05	0.60
0.17	0.10	0.70
0.08	0.19	0.71
0.10	0.19	0.71
0.05	0.21	0.74
0.05	0.14	0.80
0.08	0.10	0.82
0.03	0.00	0.95
0.17	0.24	0.59
0.16 (mean)	**0.14 (mean)**	**0.69 (mean)**
0.15 (standard deviation)	**0.08 (standard deviation)**	**0.17 (standard deviation)**

b) Plot 2 (treated)

Vegetation (-)	Rock fragments (-)	Soil (-)
0.50	0.18	0.32
0.36	0.05	0.60
0.17	0.10	0.70
0.08	0.19	0.71
0.10	0.19	0.71
0.05	0.21	0.74
0.05	0.14	0.80
0.08	0.10	0.82
0.03	0.00	0.95
0.17	0.24	0.59
0.16 (mean)	**0.14 (mean)**	**0.69 (mean)**
0.15 (standard deviation)	**0.08 (standard deviation)**	**0.17 (standard deviation)**

c) Plot 3 (untreated)

Vegetation (-)	Rock fragments (-)	Soil (-)
0.24	0.14	0.62
0.18	0.37	0.45
0.20	0.41	0.38
0.18	0.44	0.38
0.19	0.32	0.49

0.06	0.43	0.51
0.27	0.38	0.34
0.18	0.18	0.64
0.19	0.18	0.63
0.13	0.26	0.61
0.11	0.18	0.71
0.21	0.09	0.70
0.10	0.13	0.77
0.03	0.22	0.75
0.10	0.16	0.74
0.11	0.17	0.72
0.11	0.20	0.69
0.07	0.19	0.74
0.03	0.21	0.76
0.09	0.18	0.73
0.07	0.17	0.74
0.07	0.11	0.81
0.06	0.15	0.80
0.14	0.18	0.67
0.08	0.09	0.83
0.10	0.10	0.79
0.08	0.14	0.77
0.13	0.12	0.75
0.10	0.15	0.74
0.14 (mean)	**0.24 (mean)**	**0.62 (mean)**
0.07 (standard deviation)	**0.11 (standard deviation)**	**0.14 (standard deviation)**

13.2.2 Manual assessment of rock fragment cover

rock fragment cover (-)		
Plot 1 (treated)	Plot 2 (treated)	Plot 3 (untreated)
0.23	0.25	0.21
0.12	0.07	0.43
0.21	0.08	0.29
0.21	0.13	0.47
0.28	0.15	0.43
0.25	0.21	0.55
0.19	0.13	0.49
0.08	0.09	0.22
0.05	-	0.25

0.06	0.03	0.30
-	-	0.22
-	-	0.07
-	-	0.15
-	-	0.24
-	-	0.14
-	-	0.11
-	-	0.17
-	-	0.16
-	-	0.13
-	-	0.15
0.13 (mean)	**0.17 (mean)**	**0.26 (mean)**
0.07 (standard deviation)	**0.08 (standard deviation)**	**0.14 (standard deviation)**

13.3 Sediment amounts

Date	Precipitation	Plot 1 (treated) A = 297 m²		Plot 2 (treated) A = 482 m²		Plot 3 (treated) A = 418 m²	
	between days of removal	sediment	water	sediment	water	sediment	water
	(mm)	(kg)	(l)	(kg)	(l)	(kg)	(l)
11.07.12	-	68	-	1	-	58	250
13.07.12	28.8	54	1946	8	-	24	563
19.07.12	67.2	60	2827	-	-	41	1504
20.07.12	16.4	92	2085	1	-	57	862
01.08.12	148	480	1759	129	-	491	491
03.08.12	46.2	4	3095	-	-	1	2570
07.08.12	40.6	4	2250	-	-	3	1260
14.08.12	57	224	2441	-	-	256	1440
17.08.12	16.6	9	3065	-	-	-	-
20.08.12	36.0	258	2439	-	-	298	1305
28.08.12	47.6	5	2640	-	-	-	-
29.08.12	35.2	145	1965	-	-	111	2160
30.08.12	0	7	2355	-	-	7	2370

13.4 WEPP model input

13.4.1 Slope input file

Plot 1		Plot 3	
Length (m)	Slope (%)	Length (m)	Slope (%)
0.999	18.3	12.62	11.8
0.998	39.66	4.5	9.3
0.799	14.04	5.7	11.9
2.097	24.08	4.7	12.2
3.095	12.67	5.5	7.8
2.396	6.96	2.6	8.2
11.183	8.69	4.2	10
0.799	15.04	2.3	9.9
2.19	8.39	2.3	7.3
Mean	10.84	mean	10.78

13.4.2 Soil input file

SOIL Plot 1			
Number	Parameter	Value	Unit
1	Soil File Name	Maksegnit Plot 1 Soil	-
2	Soil Texture	Clay	-
3	Albedo	0.3	-
4	Initial Saturation Level	75	%
5	Interrill erodibility		kg s m^{-4}
6	Rill erodibility*	0.005, 0.007, 0.009*	s m^{-1}
7	Critical Shear		Pa
8	Eff. Hydr. Conductivity*	2, 100, 200, 300*	mm h^{-1}
9	Layer	1	-
10	Depth	1500	mm
11	Sand	22	%
12	Clay	42	%
13	Organic matter	1.5	%
14	CEC	24	meq $(100g)^{-1}$
15	Rock*	10, 13, 16*	%
* Variable parameters; changed in the scenarios			

SOIL Plot 3			
Number	Parameter	Value	Unit
1	Soil File Name	Maksegnit Plot 3 Soil	-
2	Soil Texture	Clay	-
3	Albedo	0.3	-
4	Initial Saturation Level	75	%
5	Interrill erodibility		kg s m^{-4}
6	Rill erodibility*	0.003, 0.005, 0.007*	s m^{-1}
7	Critical Shear		Pa
8	Eff. Hydr. Conductivity*	2, 100, 200, 300*	mm h^{-1}
9	Layer	1	-
10	Depth	1500	mm
11	Sand	22	%
12	Clay	42	%
13	Organic matter	1.5	%
14	CEC	24	meq $(100g)^{-1}$
15	Rock*	38/15, 41/18, 44/21*	%
* Variable parameters; changed in the scenarios			

13.4.3 Management input file

MANAGEMENT
Initial Condition

Number	Parameter	Value	Units
1	Initial Plant	Teff	-
2	Bulk density after last tillage	1.1	(g/cub. cm)
3	Initial canopy cover (0-100%)	0	%
4	Days since last tillage	180	days
5	Days since last harvest	35	days
6	Initial frost depth	0	cm
7	Initial interrill cover (0-100%)	0	%
8	Initial residue cropping system	Annual	-
9	Cumulative rainfall since last tillage	1000	mm
10	Initial ridge height after last tillage	4	cm
11	Initial rill cover (0-100%)	0	%
12	Initial roughness after last tillage	4	cm
13	Rill spacing	0	cm
14	Rill width type	Temporary	-
15	Initial snow depth	0	cm

16	Initial depth of thaw	0	cm
17	Depth of secondary tillage layer	10	cm
18	Depth of primary tillage layer	15	cm
19	Initial rill width	2.54	cm
20	Initial total dead root mass	0.2	kg/sq.m
21	Initial total submerged residue mass	0.1	kg/sq.m

MANAGEMENT
Tillage

Number	Parameter	Value	Value	Units
1	Percent residue buried on interrill areas for fragile crops	98		%
2	Percent residue buried on interrill areas for non-fragile crops	95		%
3	Number of rows of tillage implement	1		-
4	Implement Code	Other		-
5	Cultivator Position	Rear mounted		-
6	Ridge height value after tillage	12	6	cm
7	Ridge interval	35	20	cm
8	Percent residue buried on rill areas for fragile crops	98		%
9	Percent residue buried on rill areas for non-fragile crops	95		%
10	Random roughness value after tillage*	5/8/11/14*	5/8/11/14*	cm
11	Surface area disturbed (0-100%)	70	100	%
12	Mean tillage depth	12.5	10	cm
	Tillage Depth:	15	10	cm
	Tillage Type:	Primary	Secondary	
	* Variable parameters; changed in the scenarios			

MANAGEMENT
Plant - Annual
Sorghum, Plot 1

Number	Parameter	Value	Units
1	**Plant Growth and Harvest Parameters**		
2	Biomass energy ratio	12	kg/MJ
3	Growing degree days to emergence	60	Degrees C.days
4	Growing degree days for growing season	1450	Degrees C.days
5	In-row plant spacing	15	cm
6	Plant stem diameter at maturity	3.2	cm
7	Height of post-harvest standing residue; cutting height	60.9	cm
8	Harvest index (dry crop yield/total above ground dry biomass)	50	%
9	**Temperature and Radiation Parameters**		
10	Base daily air temperature	10	Degrees C
11	Optimal temperature for plant growth	27.5	Degrees C
12	Maximum temperature that stops the growth of a perennial crop	0	Degrees C
13	Critical freezing temperature for a perennial crop	0	Degrees C
14	Radiation extinction coefficient	0.6	
15	**Canopy, LAI and Root Parameters**		
16	Canopy cover coefficient	12	
17	Parameter value for canopy height equation	3	
18	Maximum canopy height	180	cm
19	Maximum leaf area index	8	
20	Maximum root depth	150	cm
21	Root to shoot ratio (% root growth/% above ground growth)	25	%
22	Maximum root mass for a perennial crop	0	kg/sq.m
23	**Senescence Parameters**		
24	Percent of growing season when leaf area index starts to decline (0-100%)	85	%
25	Period over which senescence occurs	40	days
26	Percent canopy remaining after senescence (0-100%)	90	%
27	Percent of biomass remaining after senescence (0-100%)	90	%
28	**Residue Parameters**		
29	Parameter for flat residue cover equation	2.9	sq.m/kg

30	Standing to flat residue adjustment factor (wind, snow, etc.)	99	%
31	Decomposition constant to calculate mass change of above-ground biomass	0.0074	
32	Decomposition constant to calculate mass change of root-biomass	0.0074	
33	Use fragile or non-fragile mfo values	Non-Fragile	
34	**Other Parameters**		
35	Plant specific drought tolerance (% of soil porosity)	0	%
36	Critical live biomass value below which grazing is not allowed	0	kg/sq.m
37	Maximum Darcy Weisbach friction factor for living plant	0	
38	Harvest Units	WeppWillSet	
39	Optimum yield under no stress conditions	0	kg/sq.m
	Row Width	20	cm

MANAGEMENT
Plant - Annual
Sorghum, Plot 3

Number	Parameter	Value	Units
1	**Plant Growth and Harvest Parameters**		
2	Biomass energy ratio	12	kg/MJ
3	Growing degree days to emergence	60	Degrees C.days
4	Growing degree days for growing season	1450	Degrees C.days
5	In-row plant spacing	15	cm
6	Plant stem diameter at maturity	3.2	cm
7	Height of post-harvest standing residue; cutting height	60.9	cm
8	Harvest index (dry crop yield/total above ground dry biomass)	50	%
9	**Temperature and Radiation Parameters**		
10	Base daily air temperature	10	Degrees C
11	Optimal temperature for plant growth	27.5	Degrees C
12	Maximum temperature that stops the growth of a perennial crop	0	Degrees C
13	Critical freezing temperature for a perennial crop	0	Degrees C
14	Radiation extinction coefficient	0.6	
15	**Canopy, LAI and Root Parameters**		
16	Canopy cover coefficient	11	

17	Parameter value for canopy height equation	3	
18	Maximum canopy height	180	Cm
19	Maximum leaf area index	8	
20	Maximum root depth	150	cm
21	Root to shoot ratio (% root growth/% above ground growth)	25	%
22	Maximum root mass for a perennial crop	0	kg/sq.m
23	**Senescence Parameters**		
24	Percent of growing season when leaf area index starts to decline (0-100%)	85	%
25	Period over which senescence occurs	40	days
26	Percent canopy remaining after senescence (0-100%)	90	%
27	Percent of biomass remaining after senescence (0-100%)	90	%
28	**Residue Parameters**		
29	Parameter for flat residue cover equation	2.9	sq.m/kg
30	Standing to flat residue adjustment factor (wind, snow, etc.)	99	%
31	Decomposition constant to calculate mass change of above-ground biomass	0.0074	
32	Decomposition constant to calculate mass change of root-biomass	0.0074	
33	Use fragile or non-fragile mfo values	Non-Fragile	
34	**Other Parameters**		
35	Plant specific drought tolerance (% of soil porosity)	0	%
36	Critical live biomass value below which grazing is not allowed	0	kg/sq.m
37	Maximum Darcy Weisbach friction factor for living plant	0	
38	Harvest Units	WeppWillSet	
39	Optimum yield under no stress conditions	0	kg/sq.m
	Row Width	20	cm

13.5 Simulation results: soil loss and objective functions for all scenarios

a) Plot 1 (treated)

Scenario	Soil loss (kg/m²)	RMSE	ME	R²
RE 0.003,RR 8,RO 10%,Kb 100	4.06	0.34	0.47	0.95
RE 0.003,RR 8,RO 10%,Kb 200	3.54	0.38	0.33	0.93
RE 0.005,RR 11,RO 16%,Kb 100	4.84	0.38	0.32	0.93
RE 0.005,RR 11,RO 13%,Kb 100	4.79	0.38	0.32	0.93
RE 0.005,RR 11,RO 10%,Kb 100	4.38	0.39	0.29	0.93
RE 0.005,RR 8,RO 10%,Kb 200	5.24	0.42	0.16	0.92
RE 0.005,RR 14,RO 16%,Kb 100	3.48	0.43	0.15	0.92
RE 0.005,RR 14,RO 13%,Kb 100	3.42	0.43	0.14	0.91
RE 0.005,RR 8,RO 13%,Kb 200	5.38	0.44	0.12	0.91
RE 0.005,RR 14,RO 10%,Kb 100	3.35	0.44	0.11	0.91
RE 0.007,RR 14,RO 16%,Kb 100	4.56	0.44	0.10	0.91
RE 0.007,RR 14,RO 13%,Kb 100	4.51	0.44	0.08	0.91
RE 0.005,RR 8,RO 10%,Kb 300	4.52	0.45	0.07	0.91
RE 0.003,RR 8,RO 10%,Kb 300	3.07	0.45	0.06	0.91
RE 0.005,RR 8,RO 13%,Kb 300	4.67	0.45	0.05	0.91
RE 0.005,RR 8,RO 16%,Kb 200	5.60	0.45	0.05	0.91
RE 0.005,RR 8,RO 16%,Kb 300	4.83	0.46	0.02	0.90
RE 0.005,RR 8,RO 10%,Kb 100	6.01	0.48	-0.08	0.89
RE 0.007,RR 11,RO 10%,Kb 200	5.79	0.51	-0.19	0.88
RE 0.007,RR 11,RO 10%,Kb 100	5.79	0.51	-0.19	0.88
RE 0.005,RR 8,RO 13%,Kb 100	6.25	0.51	-0.20	0.88
RE 0.009,RR 14,RO 16%,Kb 100	5.60	0.51	-0.22	0.88
RE 0.009,RR 14,RO 13%,Kb 100	5.56	0.51	-0.23	0.88
RE 0.009,RR 14,RO 10%,Kb 100	5.50	0.52	-0.25	0.88
RE 0.007,RR 11,RO 16%,Kb 100	6.31	0.52	-0.27	0.87
RE 0.007,RR 11,RO 13%,Kb 200	6.29	0.52	-0.28	0.87
RE 0.007,RR 11,RO 13%,Kb 100	6.29	0.52	-0.28	0.87
RE 0.005,RR 8,RO 16%,Kb 100	6.44	0.53	-0.29	0.87
RE 0.003,RR 8,RO 10%,Kb 2	6.37	0.55	-0.39	0.86
RE 0.007,RR 8,RO 10%,Kb 300	5.90	0.55	-0.40	0.86
RE 0.005,RR 5,RO 10%,Kb 300	5.80	0.55	-0.41	0.86
RE 0.005,RR 11,RO 16%,Kb 200	3.09	0.55	-0.42	0.86
RE 0.005,RR 11,RO 13%,Kb 200	3.02	0.55	-0.43	0.86
RE 0.005,RR 11,RO 10%,Kb 200	2.95	0.56	-0.46	0.86
RE 0.005,RR 5,RO 13%,Kb 300	5.92	0.56	-0.47	0.86
RE 0.007,RR 8,RO 13%,Kb 300	6.06	0.56	-0.47	0.85

RE 0.007,RR 11,RO 16%,Kb 200	4.02	0.56	-0.48	0.85
RE 0.005,RR 14,RO 10%,Kb 2	6.67	0.57	-0.49	0.85
RE 0.005,RR 5,RO 16%,Kb 300	6.09	0.58	-0.56	0.85
RE 0.005,RR 14,RO 13%,Kb 2	6.83	0.58	-0.57	0.85
RE 0.007,RR 8,RO 16%,Kb 300	6.23	0.58	-0.57	0.85
RE 0.005,RR 14,RO 16%,Kb 2	6.95	0.59	-0.60	0.84
RE 0.005,RR 11,RO 10%,Kb 2	7.20	0.59	-0.63	0.84
RE 0.007,RR 8,RO 10%,Kb 200	6.86	0.60	-0.68	0.83
RE 0.009,RR 11,RO 13%,Kb 200	4.85	0.60	-0.69	0.83
RE 0.009,RR 11,RO 16%,Kb 200	4.92	0.60	-0.70	0.83
RE 0.009,RR 11,RO 10%,Kb 200	4.79	0.61	-0.72	0.83
RE 0.005,RR 11,RO 13%,Kb 2	7.37	0.61	-0.73	0.83
RE 0.007,RR 8,RO 13%,Kb 200	7.01	0.62	-0.79	0.82
RE 0.005,RR 14,RO 16%,Kb 200	2.32	0.63	-0.87	0.82
RE 0.005,RR 14,RO 13%,Kb 200	2.28	0.63	-0.87	0.82
RE 0.005,RR 14,RO 10%,Kb 200	2.25	0.64	-0.88	0.81
RE 0.005,RR 5,RO 10%,Kb 200	6.62	0.64	-0.89	0.81
RE 0.005,RR 11,RO 16%,Kb 300	2.78	0.64	-0.90	0.81
RE 0.007,RR 14,RO 16%,Kb 200	3.03	0.64	-0.92	0.81
RE 0.007,RR 14,RO 13%,Kb 200	3.00	0.64	-0.92	0.81
RE 0.007,RR 14,RO 10%,Kb 200	2.97	0.64	-0.93	0.81
RE 0.005,RR 14,RO 16%,Kb 300	2.10	0.64	-0.93	0.81
RE 0.005,RR 11,RO 13%,Kb 300	2.65	0.64	-0.93	0.81
RE 0.007,RR 14,RO 13%,Kb 2	2.06	0.65	-0.94	0.81
RE 0.005,RR 14,RO 13%,Kb 300	2.06	0.65	-0.94	0.81
RE 0.005,RR 11,RO 10%,Kb 300	2.55	0.65	-0.95	0.81
RE 0.007,RR 8,RO 16%,Kb 200	7.25	0.65	-0.95	0.81
RE 0.007,RR 14,RO 16%,Kb 300	2.73	0.65	-0.95	0.81
RE 0.005,RR 14,RO 10%,Kb 300	2.01	0.65	-0.96	0.81
RE 0.007,RR 14,RO 13%,Kb 300	2.70	0.65	-0.96	0.81
RE 0.007,RR 14,RO 10%,Kb 300	2.66	0.65	-0.97	0.81
RE 0.005,RR 11,RO 16%,Kb 2	7.71	0.65	-0.99	0.80
RE 0.009,RR 14,RO 16%,Kb 300	3.34	0.66	-1.06	0.80
RE 0.009,RR 14,RO 13%,Kb 300	3.31	0.67	-1.07	0.80
RE 0.007,RR 11,RO 16%,Kb 300	3.61	0.67	-1.07	0.80
RE 0.009,RR 14,RO 10%,Kb 300	3.28	0.67	-1.07	0.80
RE 0.009,RR 14,RO 13%,Kb 200	3.69	0.67	-1.08	0.80
RE 0.009,RR 14,RO 16%,Kb 200	3.71	0.67	-1.08	0.80
RE 0.007,RR 11,RO 10%,Kb 300	3.34	0.67	-1.08	0.80

RE 0.009,RR 14,RO 10%,Kb 200	3.67	0.67	-1.09	0.79
RE 0.007,RR 11,RO 13%,Kb 300	3.47	0.67	-1.09	0.79
RE 0.005,RR 5,RO 16%,Kb 200	7.02	0.68	-1.13	0.79
RE 0.009,RR 8,RO 10%,Kb 300	7.20	0.70	-1.26	0.78
RE 0.005,RR 5,RO 10%,Kb 100	7.29	0.70	-1.31	0.77
RE 0.009,RR 11,RO 16%,Kb 100	7.72	0.71	-1.35	0.77
RE 0.009,RR 11,RO 10%,Kb 300	4.11	0.71	-1.35	0.77
RE 0.009,RR 11,RO 13%,Kb 100	7.70	0.71	-1.37	0.77
RE 0.009,RR 11,RO 13%,Kb 300	4.24	0.72	-1.39	0.77
RE 0.009,RR 11,RO 16%,Kb 300	4.41	0.72	-1.39	0.77
RE 0.005,RR 5,RO 13%,Kb 200	7.51	0.72	-1.44	0.76
RE 0.005,RR 5,RO 13%,Kb 100	7.51	0.72	-1.44	0.76
RE 0.007,RR 8,RO 10%,Kb 100	7.86	0.74	-1.56	0.75
RE 0.007,RR 5,RO 10%,Kb 300	7.43	0.74	-1.57	0.75
RE 0.009,RR 8,RO 16%,Kb 300	7.56	0.74	-1.58	0.75
RE 0.005,RR 5,RO 16%,Kb 100	7.71	0.75	-1.59	0.75
RE 0.007,RR 5,RO 13%,Kb 300	7.57	0.76	-1.69	0.73
RE 0.007,RR 8,RO 13%,Kb 100	8.14	0.78	-1.81	0.72
RE 0.007,RR 5,RO 16%,Kb 300	7.75	0.78	-1.86	0.72
RE 0.007,RR 8,RO 16%,Kb 100	8.34	0.80	-1.96	0.71
RE 0.009,RR 8,RO 10%,Kb 200	8.39	0.82	-2.09	0.70
RE 0.009,RR 8,RO 13%,Kb 300	8.55	0.84	-2.26	0.68
RE 0.009,RR 8,RO 13%,Kb 200	8.55	0.84	-2.26	0.68
RE 0.009,RR 8,RO 16%,Kb 200	8.82	0.87	-2.52	0.65
RE 0.007,RR 5,RO 10%,Kb 200	8.52	0.90	-2.80	0.63
RE 0.007,RR 14,RO 10%,Kb 100	8.84	0.91	-2.89	0.62
RE 0.007,RR 14,RO 10%,Kb 2	8.84	0.91	-2.89	0.62
RE 0.007,RR 5,RO 13%,Kb 200	8.67	0.92	-2.94	0.61
RE 0.007,RR 14,RO 16%,Kb 2	9.10	0.94	-3.07	0.60
RE 0.007,RR 11,RO 10%,Kb 2	9.47	0.95	-3.24	0.58
RE 0.007,RR 5,RO 16%,Kb 200	8.95	0.96	-3.25	0.58
RE 0.009,RR 5,RO 10%,Kb 300	8.97	0.96	-3.26	0.58
RE 0.005,RR 8,RO 10%,Kb 2	9.40	0.98	-3.44	0.56
RE 0.007,RR 11,RO 13%,Kb 2	9.65	0.98	-3.44	0.56
RE 0.009,RR 5,RO 13%,Kb 300	9.12	0.98	-3.45	0.56
RE 0.005,RR 8,RO 16%,Kb 2	9.72	0.99	-3.54	0.55
RE 0.005,RR 8,RO 13%,Kb 2	9.60	0.99	-3.54	0.55
RE 0.009,RR 5,RO 16%,Kb 300	9.30	1.00	-3.70	0.54
RE 0.009,RR 8,RO 10%,Kb 100	9.63	1.02	-3.83	0.52

RE 0.007,RR 11,RO 16%,Kb 2	10.05	1.02	-3.84	0.52
RE 0.007,RR 5,RO 10%,Kb 100	9.38	1.02	-3.85	0.52
RE 0.007,RR 5,RO 13%,Kb 100	9.64	1.05	-4.09	0.50
RE 0.009,RR 8,RO 13%,Kb 100	9.93	1.06	-4.22	0.49
RE 0.007,RR 5,RO 16%,Kb 100	9.83	1.07	-4.31	0.48
RE 0.009,RR 8,RO 16%,Kb 100	10.15	1.08	-4.43	0.47
RE 0.009,RR 5,RO 10%,Kb 200	10.32	1.18	-5.44	0.37
RE 0.009,RR 5,RO 16%,Kb 200	10.78	1.24	-6.13	0.30
RE 0.009,RR 14,RO 10%,Kb 2	10.91	1.27	-6.46	0.27
RE 0.005,RR 5,RO 10%,Kb 2	11.44	1.28	-6.61	0.25
RE 0.009,RR 14,RO 13%,Kb 2	11.06	1.28	-6.63	0.25
RE 0.009,RR 14,RO 16%,Kb 2	11.16	1.28	-6.67	0.24
RE 0.005,RR 5,RO 13%,Kb 2	11.70	1.30	-6.91	0.22
RE 0.009,RR 11,RO 10%,Kb 100	11.65	1.31	-7.04	0.21
RE 0.009,RR 11,RO 10%,Kb 2	11.65	1.31	-7.04	0.21
RE 0.009,RR 5,RO 10%,Kb 100	11.36	1.34	-7.31	0.18
RE 0.009,RR 11,RO 13%,Kb 2	11.82	1.34	-7.34	0.18
RE 0.005,RR 5,RO 16%,Kb 2	12.05	1.35	-7.48	0.17
RE 0.009,RR 5,RO 13%,Kb 200	11.64	1.37	-7.68	0.15
RE 0.009,RR 5,RO 13%,Kb 100	11.64	1.37	-7.68	0.15
RE 0.009,RR 11,RO 16%,Kb 2	12.28	1.38	-7.88	0.13
RE 0.009,RR 5,RO 16%,Kb 100	11.85	1.39	-7.96	0.12
RE 0.007,RR 8,RO 10%,Kb 2	12.27	1.43	-8.48	0.07
RE 0.007,RR 8,RO 16%,Kb 2	12.58	1.44	-8.60	0.06
RE 0.007,RR 8,RO 13%,Kb 2	12.47	1.44	-8.63	0.05
RE 0.007,RR 5,RO 10%,Kb 2	14.72	1.80	-14.07	-0.48
RE 0.007,RR 5,RO 13%,Kb 2	14.99	1.83	-14.53	-0.53
RE 0.009,RR 8,RO 10%,Kb 2	15.00	1.86	-15.18	-0.59
RE 0.009,RR 8,RO 16%,Kb 2	15.29	1.87	-15.28	-0.60
RE 0.009,RR 8,RO 13%,Kb 2	15.20	1.88	-15.38	-0.61
RE 0.007,RR 5,RO 16%,Kb 2	15.39	1.88	-15.48	-0.62
RE 0.009,RR 5,RO 10%,Kb 2	17.81	2.30	-23.54	-1.41
RE 0.009,RR 5,RO 13%,Kb 2	18.11	2.33	-24.17	-1.48
RE 0.009,RR 5,RO 16%,Kb 2	18.55	2.39	-25.54	-1.61

b) Plot 3 (untreated)

Scenario	Soil loss (kg/m²)	RMSE	ME	R²
RE0.003,RR11,R4118,Kb200	2.857	0.28	0.40	0.82
RE0.003,RR11,R3815,Kb200	3.115	0.28	0.39	0.82
RE0.003,RR14,R4421,Kb100	2.788	0.29	0.38	0.82
RE0.003,RR14,R3815,Kb200	2.89	0.29	0.35	0.81
RE0.003,RR14,R4118,Kb100	3.031	0.29	0.35	0.81
RE0.003,RR14,R3815,Kb100	3.24	0.30	0.31	0.80
RE0.003,RR14,R4118,Kb200	2.804	0.31	0.29	0.79
RE0.003,RR11,R4421,Kb200	3.12	0.34	0.14	0.75
RE0.005,RR14,R4421,Kb200	2.479	0.34	0.13	0.75
RE0.003,RR14,R4421,Kb200	1.761	0.35	0.06	0.72
RE0.007,RR14,R4421,Kb200	3.153	0.37	-0.03	0.70
RE0.003,RR11,R4118,Kb300	3.059	0.39	-0.18	0.65
RE0.003,RR11,R3815,Kb300	3.054	0.40	-0.22	0.64
RE0.003,RR8,R4421,Kb300	3.84	0.40	-0.24	0.64
RE0.003,RR14,R4118,Kb300	2.619	0.41	-0.27	0.63
RE0.003,RR8,R3815,Kb200	4.45	0.42	-0.33	0.61
RE0.005,RR11,R4118,Kb200	4.08	0.43	-0.42	0.58
RE0.005,RR14,R4421,Kb100	3.961	0.43	-0.43	0.58
RE0.003,RR11,R4421,Kb100	4.419	0.44	-0.46	0.57
RE0.003,RR8,R4421,Kb200	4.305	0.45	-0.52	0.55
RE0.003,RR14,R3815,Kb300	2.44	0.46	-0.60	0.53
RE0.003,RR8,R4118,Kb300	4.64	0.48	-0.74	0.49
RE0.005,RR11,R3815,Kb200	4.493	0.48	-0.74	0.49
RE0.003,RR14,R4421,Kb300	2.024	0.48	-0.77	0.48
RE0.005,RR14,R3815,Kb200	4.20	0.49	-0.82	0.47
RE0.005,RR14,R4118,Kb100	4.344	0.49	-0.83	0.47
RE0.003,RR8,R3815,Kb300	4.91	0.49	-0.84	0.46
RE0.005,RR14,R4118,Kb300	3.81	0.49	-0.84	0.46
RE0.005,RR14,R4118,Kb200	4.04	0.50	-0.91	0.44
RE0.003,RR11,R4118,Kb100	5.068	0.51	-0.94	0.43
RE0.003,RR11,R4421,Kb300	2.286	0.51	-0.96	0.43
RE0.005,RR11,R4118,Kb300	4.426	0.52	-1.02	0.41
RE0.005,RR11,R3815,Kb300	4.47	0.52	-1.06	0.40
RE0.005,RR14,R3815,Kb100	4.68	0.52	-1.06	0.40
RE0.003,RR11,R3815,Kb100	5.303	0.53	-1.10	0.39
RE0.003,RR8,R4118,Kb200	4.715	0.53	-1.15	0.37
RE0.005,RR14,R3815,Kb300	3.58	0.55	-1.25	0.34

RE0.005,RR14,R4421,Kb300	2.931	0.55	-1.27	0.33
RE0.005,RR11,R4421,Kb200	4.433	0.57	-1.42	0.29
RE0.005,RR11,R4421,Kb300	3.286	0.60	-1.74	0.20
RE0.005,RR8,R4421,Kb300	5.434	0.61	-1.78	0.19
RE0.007,RR14,R4118,Kb300	4.918	0.62	-1.89	0.15
RE0.007,RR14,R4421,Kb100	5.046	0.63	-1.96	0.13
RE0.007,RR11,R4118,Kb200	5.223	0.63	-2.03	0.11
RE0.007,RR14,R4421,Kb300	3.78	0.64	-2.09	0.10
RE0.007,RR14,R3815,Kb300	4.66	0.67	-2.36	0.02
RE0.007,RR11,R4118,Kb300	5.69	0.68	-2.47	-0.02
RE0.003,RR5,R4421,Kb200	6.008	0.68	-2.52	-0.03
RE0.003,RR8,R4421,Kb100	5.966	0.69	-2.55	-0.04
RE0.007,RR11,R3815,Kb300	5.792	0.69	-2.55	-0.04
RE0.007,RR11,R3815,Kb200	5.773	0.71	-2.85	-0.13
RE0.003,RR5,R4118,Kb300	6.344	0.71	-2.86	-0.13
RE0.007,RR14,R4118,Kb100	5.55	0.72	-2.89	-0.14
RE0.007,RR11,R4421,Kb300	4.216	0.72	-2.89	-0.14
RE0.005,RR11,R4421,Kb100	6.321	0.72	-2.93	-0.15
RE0.007,RR14,R3815,Kb200	5.40	0.72	-2.95	-0.16
RE0.003,RR5,R3815,Kb300	6.513	0.73	-3.02	-0.18
RE0.007,RR14,R4118,Kb200	5.188	0.73	-3.05	-0.19
RE0.005,RR8,R3815,Kb200	6.359	0.74	-3.12	-0.21
RE0.005,RR8,R4421,Kb200	6.057	0.76	-3.34	-0.27
RE0.007,RR14,R3815,Kb100	6.01	0.77	-3.45	-0.30
RE0.003,RR8,R4118,Kb100	6.654	0.78	-3.65	-0.36
RE0.003,RR5,R4118,Kb200	7.082	0.80	-3.83	-0.41
RE0.007,RR11,R4421,Kb200	5.651	0.81	-4.01	-0.47
RE0.005,RR8,R4118,Kb300	6.635	0.82	-4.09	-0.49
RE0.007,RR8,R4421,Kb300	6.889	0.83	-4.18	-0.52
RE0.003,RR8,R3815,Kb100	6.896	0.83	-4.20	-0.52
RE0.003,RR5,R4421,Kb300	6.953	0.84	-4.39	-0.58
RE0.003,RR5,R3815,Kb200	7.194	0.85	-4.45	-0.60
RE0.005,RR8,R3815,Kb300	7.073	0.86	-4.54	-0.62
RE0.005,RR11,R4118,Kb100	7.296	0.86	-4.61	-0.64
RE0.005,RR11,R3815,Kb100	7.703	0.91	-5.20	-0.82
RE0.005,RR8,R4118,Kb200	6.696	0.92	-5.38	-0.87
RE0.003,RR5,R3815,Kb100	7.62	0.95	-5.85	-1.01
RE0.007,RR11,R4421,Kb100	8.049	1.00	-6.63	-1.23
RE0.003,RR14,R4421,Kb2	9.129	1.04	-7.24	-1.42

RE0.007,RR8,R3815,Kb200	8.087	1.05	-7.34	-1.44
RE0.007,RR8,R4421,Kb200	7.648	1.06	-7.51	-1.49
RE0.003,RR5,R4421,Kb100	8.223	1.06	-7.53	-1.50
RE0.005,RR5,R4421,Kb200	8.325	1.07	-7.60	-1.52
RE0.005,RR8,R4421,Kb100	8.449	1.11	-8.36	-1.74
RE0.003,RR14,R3815,Kb2	9.317	1.12	-8.53	-1.79
RE0.003,RR14,R4118,Kb2	9.465	1.13	-8.62	-1.82
RE0.007,RR8,R4118,Kb300	8.455	1.15	-8.98	-1.92
RE0.005,RR5,R4118,Kb300	8.942	1.16	-9.17	-1.98
RE0.003,RR5,R4118,Kb100	8.797	1.17	-9.41	-2.05
RE0.005,RR5,R4421,Kb300	9.191	1.20	-9.87	-2.18
RE0.007,RR11,R4118,Kb100	9.316	1.20	-9.95	-2.21
RE0.005,RR5,R3815,Kb300	9.266	1.20	-9.95	-2.21
RE0.007,RR8,R3815,Kb300	9.043	1.20	-9.95	-2.21
RE0.005,RR5,R4118,Kb200	9.877	1.26	-11.04	-2.53
RE0.007,RR11,R3815,Kb100	9.881	1.27	-11.17	-2.56
RE0.005,RR8,R4118,Kb100	9.517	1.28	-11.36	-2.62
RE0.007,RR8,R4118,Kb200	8.498	1.28	-11.48	-2.66
RE0.003,RR11,R3815,Kb2	10.609	1.32	-12.21	-2.87
RE0.003,RR11,R4118,Kb2	10.803	1.34	-12.52	-2.96
RE0.003,RR11,R4421,Kb2	11.021	1.35	-12.83	-3.05
RE0.005,RR8,R3815,Kb100	9.93	1.36	-12.96	-3.09
RE0.005,RR5,R3815,Kb200	10.166	1.36	-12.98	-3.10
RE0.007,RR5,R4421,Kb200	10.406	1.42	-14.31	-3.49
RE0.005,RR5,R3815,Kb100	10.69	1.50	-16.04	-3.99
RE0.007,RR8,R4421,Kb100	10.685	1.51	-16.26	-4.06
RE0.005,RR5,R4421,Kb100	11.022	1.52	-16.54	-4.14
RE0.007,RR5,R4421,Kb300	11.201	1.54	-16.92	-4.25
RE0.007,RR5,R4118,Kb300	11.281	1.57	-17.58	-4.44
RE0.007,RR5,R3815,Kb300	11.756	1.64	-19.31	-4.95
RE0.005,RR14,R4421,Kb2	12.831	1.65	-19.56	-5.02
RE0.005,RR5,R4118,Kb100	11.732	1.66	-19.89	-5.12
RE0.007,RR5,R4118,Kb200	12.389	1.68	-20.42	-5.28
RE0.007,RR8,R4118,Kb100	12.088	1.73	-21.72	-5.66
RE0.005,RR14,R4118,Kb2	13.476	1.80	-23.49	-6.17
RE0.003,RR8,R3815,Kb2	14.113	1.81	-23.89	-6.29
RE0.005,RR14,R3815,Kb2	13.43	1.82	-24.17	-6.37
RE0.007,RR5,R3815,Kb200	12.843	1.83	-24.21	-6.39
RE0.007,RR8,R3815,Kb100	12.647	1.85	-24.74	-6.54

RE0.003,RR8,R4118,Kb2	14.521	1.87	-25.39	-6.73
RE0.003,RR8,R4421,Kb2	14.524	1.88	-25.72	-6.83
RE0.007,RR5,R4421,Kb100	13.514	1.95	-27.65	-7.39
RE0.007,RR5,R3815,Kb100	13.427	2.00	-29.26	-7.87
RE0.005,RR11,R4421,Kb2	15.436	2.08	-31.69	-8.58
RE0.005,RR11,R4118,Kb2	15.293	2.09	-32.05	-8.68
RE0.005,RR11,R3815,Kb2	15.198	2.10	-32.29	-8.75
RE0.007,RR5,R4118,Kb100	14.355	2.12	-32.97	-8.95
RE0.007,RR14,R4421,Kb2	16.175	2.20	-35.70	-9.75
RE0.003,RR5,R3815,Kb2	16.883	2.28	-38.21	-10.49
RE0.003,RR5,R4118,Kb2	17.545	2.37	-41.58	-11.48
RE0.007,RR14,R4118,Kb2	17.095	2.41	-43.00	-11.89
RE0.003,RR5,R4421,Kb2	17.919	2.42	-43.26	-11.97
RE0.007,RR14,R3815,Kb2	17.14	2.46	-44.82	-12.42
RE0.007,RR11,R4421,Kb2	19.405	2.74	-55.72	-15.62
RE0.007,RR11,R4118,Kb2	19.323	2.77	-57.15	-16.04
RE0.005,RR8,R3815,Kb2	20.163	2.80	-58.07	-16.31
RE0.007,RR11,R3815,Kb2	19.316	2.80	-58.33	-16.38
RE0.005,RR8,R4421,Kb2	20.308	2.83	-59.36	-16.68
RE0.005,RR8,R4118,Kb2	20.537	2.84	-60.07	-16.89
RE0.005,RR5,R3815,Kb2	23.767	3.41	-86.79	-24.72
RE0.005,RR5,R4118,Kb2	24.488	3.51	-92.34	-26.35
RE0.005,RR5,R4421,Kb2	24.771	3.54	-93.93	-26.81
RE0.007,RR8,R3815,Kb2	25.533	3.67	-100.53	-28.75
RE0.007,RR8,R4421,Kb2	25.453	3.67	-100.64	-28.78
RE0.007,RR8,R4118,Kb2	25.886	3.71	-102.89	-29.44
RE0.007,RR5,R3815,Kb2	29.806	4.39	-144.94	-41.76
RE0.007,RR5,R4118,Kb2	30.578	4.51	-152.68	-44.02
RE0.007,RR5,R4421,Kb2	30.782	4.52	-153.74	-44.34